Exploring nickel catalysis in carbonyl and alcohol addition reactions

By

Amrah Nasim

A thesis submitted in partial fulfillment of the requirements for
a Master's degree in Chemistry

Department of Chemistry and Biomolecular Sciences
University of Ottawa

Thesis Supervisor: Dr. Stephen G. Newman

Abstract

The nucleophilic addition of organomagnesium/lithium reagents to aldehydes and ketones has long enabled the synthesis of valuable alcohol derivatives; however, these types of transformations are often plagued by poor functional group tolerance and require harsh reaction conditions. The direct coupling of carbonyls and alcohols with aryl halides is an appealing alternative to access secondary alcohol products. However, this necessitates a formal C-H bond activation which is not well established in the literature.

Chapter 1 provides a detailed literature background of the transition metal-catalyzed functionalization of carbonyls and alcohols. The work discussed in **Chapter 2** of this thesis demonstrates the addition of aryl halides to aryl and aliphatic aldehydes and alcohols providing secondary alcohol products in moderate to high yields. Key to the success of this transformation was the implementation of underexplored and readily synthesized 1,5-diaza-3,7-diphosphacyclooctane (P_2N_2) ligands.

Chapter 3 extends the methodology established in chapter 2 and aims to get a preliminary understanding of the application and mechanism of the reaction described above. For this purpose, pharmaceutically relevant isatin substrates are derivatized, providing access to substitution at the 3-position. Coupling isatins with aryl halides yields 3-aryl-3-hydroxy-2-oxindole products which are scaffolds for many natural product derivatives. Through high-throughput experimentation (HTE), we were able to

discover that 1,2-addition at the carbonyl position of isatins is highly compatible with our established system and led us to develop a modest scope as well as gain useful mechanistic insights for this coupling.

Acknowledgements

I would like to begin by extending a huge thank you to my supervisor Dr. Stephen Newman for giving me the opportunity to work in his lab and for guiding me through every step of the way. Your constant encouragement and valuable feedback are truly unmatched, and I could not have asked for a better graduate school experience. The lessons I have learned in the past few years will stick with me through life, both professionally and personally. Your meticulousness, knowledge in chemistry and attention to detail are truly inspirational and encourage me to strive to be a better chemist everyday.

I would like to thank my co-workers and friends for being a big part of my life the past two years and for making them truly memorable. I have learned a lot from each and every one of you and I am so glad I was able to have meaningful scientific discussions in the office everyday. I want to extend a special thank you to Eric Isbrandt for being an amazing co-worker, collaborator, and trainer and for always entertaining my ideas however pointless they may be and for answering my endless questions. I wish you best of luck for all your future endeavours- you will surely do great things! Thank you to all the graduate students, past and present, Eric Skrotzki, Garrett, August, Piers, Adam and Omid for being a part of this journey and making it wonderful. A huge thank you to our post-doc and my dear friend, Victoria for being an integral part of the final year of my master's and for teaching me so much within a short span of time. I will forever be in awe of your wisdom and ingenuity.

Thank you to the amazing undergraduate students who joined the lab and who I had the pleasure of working with. Katie, Karen, Shajia, Casey, JD and Jonathan, your hard-work, determination, and work ethic is very inspiring, and you were all an invaluable resource in the lab.

Thank you to my parents for always believing in me and for always supporting me and my dreams. You are truly amazing parents. Last but certainly not the least, thank you to my wonderful husband for always being there for me and for standing by my side during all the challenges encountered in the past few years.

Table of Contents

List of Tables:

List of Figures:

List of Schemes:

List of Abbreviations:

1°	primary
2°	secondary
Ac	acetyl
aq.	aqueous
Ar	aryl
BDE	bond dissociation energy
Bn	benzyl
BOC	tert-butyloxycarbonyl
calcd	calculated
cat.	catalytic or catalyst
Cp	cyclopentadienyl
C-C	carbon-carbon bond
C-H	carbon-hydrogen bond
C=O	carbon-oxygen double bond
Cod	1,5-Cyclooctadiene
Cy	cyclohexyl
Cyp	cyclopentyl
d	doublet
DMF	dimethylformamide
DMA	dimethyl acetamide
DMSO	dimethylsulfoxide
dppp	1,3-bis(diphenylphosphino)propane
dppf	1,1′-Ferrocenediyl-bis(diphenylphosphine)
dcype	1,2-Bis(dicyclohexylphosphino)ethane
IPr•HCl	1,3-Bis-(2,4,6-Tribenzhydrylphenyl)-1*H*-imidazol-3-ium chloride
E or E^+	electrophile

e.e.	enantiomeric excess
e.r.	enantiomeric ratio
EDG	electron-donating group
EI	electron impact
equiv	equivalent
ESI	electrospray ionization
Et	ethyl
EWG	electron-withdrawing group
FID	flame ionization detector
g	gram(s)
GC	gas chromatography
h	hour(s)
HPLC	high performance liquid chromatography
HAT	hydrogen atom transfer
HTE	high throughput experimentation
Hz	hertz
IR	infrared
J	coupling constant
KO^{t}Bu	potassium tert-butoxide
L	neutral ligand
LA	Lewis acid
LED	light emitting diode
M	generic metal, or molecular ion, or molar
m	meta or multiplet
m/z	mass over charge
m-CPBA	meta-chloroperbenzoic acid
Me	methyl

MeCN	acetonitrile
mg	milligram(s)
min	minute(s)
mL	milliliter(s)
mol	mole(s)
mp	melting point
MS	mass spectrometry
NHC	N-heterocyclic carbene
Ni	nickel
NMR	nuclear magnetic resonance
Nu	nucleophile
o	ortho
π	pi
p	para
Pd	palladium
Pent	pentyl
Ph	phenyl
PhMe	toluene
P_2N_2	1,5-diaza-3,7-diphosphacyclooctane
ppm	parts per million
q	quartet
quin	quintet
R	generic chemical group
Rh	rhodium
r. t.	room temperature
SET	single electron transfer
t	triplet

T. or temp.	temperature
^{t}Bu or *t*-Bu	tert-butyl
THF	tetrahydrofuran
TLC	thin layer chromatography
TMS	trimethylsilyl
Ts	tosyl
UV	ultraviolet
X	generic halogen/heteroatom

Statement of Contributions:

In Chapter 2, the initial conditions for the α-arylation of alcohols and the successful application of P_2N_2 ligands was discovered by a senior PhD student in the lab, Eric Isbrandt. The project was therefore done in collaboration with Eric, and we simultaneously worked on optimizing conditions and broadening the scope for the 1,2-addition of aldehydes and α-arylation of alcohols. The majority of the initial optimization results were generated by him. Compounds **2.17, 2.18, 2.20** from the aldehyde scope and compounds **2.26, 2.27** and **2.28** from the alcohol scope were synthesized and isolated by Eric and were part of a larger scope which can be found in our published manuscript.[1] Unless otherwise stated, all other results discussed in Chapter 2 and Chapter 3 were obtained by me.

[1] Isbrandt, E. S.; Nasim, A.; Zhao, K.; Newman, S. G. *J. Am. Chem. Soc*. **2021**, *143*, 14646.

Chapter 1: An Introduction to Coupling with Carbonyls and Alcohols.

Introduction:

The formation of carbon-carbon (C-C) bonds has been a key tool in synthetic organic chemistry throughout history. Since their discovery in the 19th Century, C-C bond forming reactions have played an enormously important role in shaping chemical synthesis.[2] A breakthrough in traditional organic chemistry came with the use of transition metal catalysis for C-C cross-coupling reactions, allowing challenging transformations to occur with high selectivity and large turnover numbers.[3] The pharmaceutical industry heavily relies on C-C coupling reactions using transition metal catalysis for the production of active pharmaceutical ingredients.

For this reason, the functionalization of simple, small molecules to synthesize substituted compounds containing attractive functionalities such as alcohols, carbonyls and olefins is highly desired. **Chapter 1** aims to take a deep dive into classical and modern literature focusing predominantly on coupling aryl halides, pseudohalides or boronic acids with carbonyls and alcohols. The discussion of coupling sp^2 hybridized carbons to give rise to a new sp^2-carbon center would be incomplete without talking about the Heck

[2] Budarin, V.L.; Shuttleworth, P.S.; Clark, J.H.; Luque, R. *Curr. Org. Syn.* **2010**, 7, 614.
[3] Tasker, S.Z.; Standley, E.A.; Jamison, T.F. *Nature*. **2014**, *509*, 299.

reaction. A brief history of the Heck reaction and how variations of it have led to the discovery of exciting reactivity can be found in this chapter.

1.1.1: Traditional Mizoroki-Heck coupling

The Mizoroki-Heck reaction, also often referred to as the Heck reaction was discovered in the early 1970's by Tsutomu Mizoroki and Richard F. Heck and was the topic of the Nobel Prize in Chemistry in 2010.[4] This palladium catalyzed cross-coupling between alkenes and aryl or vinyl halides (or pseudohalides) enables new carbon-carbon bond formation and remains one of the most widely studied and used strategies to synthesise substituted olefins (**Scheme 1**). The extensive research and optimization performed on the Heck reaction has resulted in it proceeding under mild reaction conditions and tolerating sensitive functionalities in moderate to high yields.

Scheme 1: A general scheme of the palladium-catalyzed Mizoroki-Heck reaction

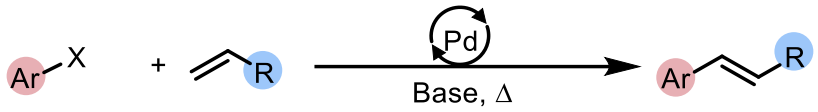

Scheme 2 describes a general, widely accepted mechanism for the Heck reaction.[5] The mechanism begins with the oxidative addition of Pd(0) into the C–X bond of an aryl (pseudo)halide, followed by coordination to the π system of the olefin. The olefin then

[4] Drahl, C. *Chem. Eng. News.* **2010**, *88*, 31.
[5] Varnado, C. D.; Bielawski, C. W. *Polymer Science: A Comprehensive Reference.* **2012**, *5*, 175.

inserts into the palladium–carbon bond, forming a new carbon–carbon bond and simultaneously an alkyl-palladium bond. Syn β-hydride elimination then takes place resulting in the generation of a trans olefin. Pd(II) is then reduced to restore the active catalyst by base-facilitated removal of the coordinated HX.

Scheme 2: A general mechanism for the palladium catalyzed Mizoroki-Heck reaction

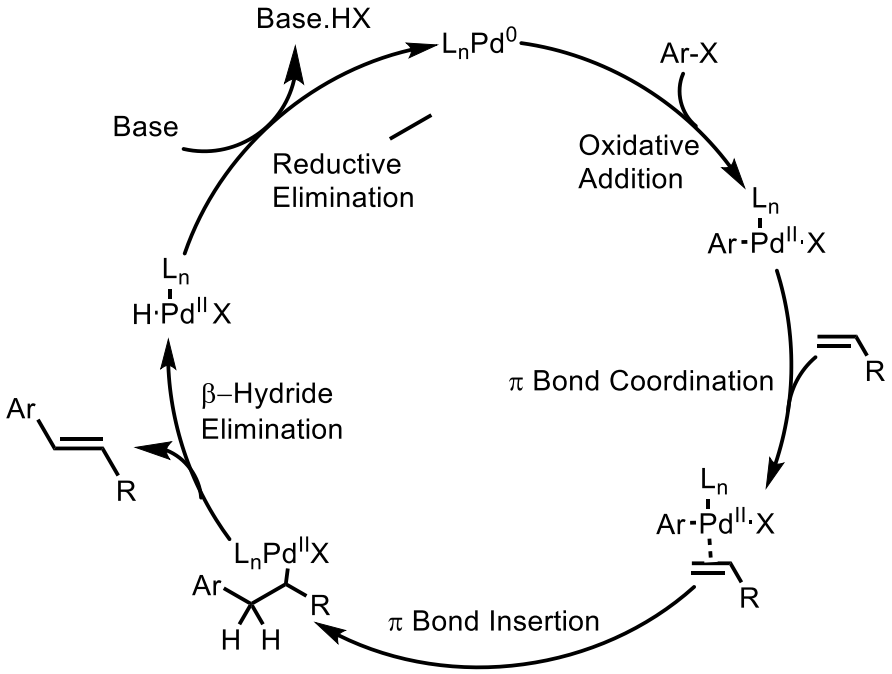

The olefin can be mono or disubstituted and can be electron rich, poor, or neutral. The Heck reaction can be regioselective and a single isomer may be preferred depending on the polarization of the π system of the olefin.[6] Due to the reaction being quite

[6] Clayden, J.; Greeves, N.; Warren, S. G. *Organic Chemistry*; Oxford University Press: Oxford, **2012**; pp 1079–1081.

accommodating, strong bases are usually not required and Et_3N, NaOAc or Na_2CO_3 can be used.

The ability of palladium to readily perform β-hydride elimination to provide the desired trans alkene product makes it an attractive choice over other transition metals that have been studied in Heck coupling. One of the main drawbacks, however, is that using alkyl halides in Heck coupling can be particularly tricky due to the difficulty in oxidative addition the presence of labile β-hydrogens which can undergo elimination giving rise to undesired side products (**Scheme 3**).[7]

Scheme 3: Challenges in Pd-catalyzed Heck coupling with alkyl halides

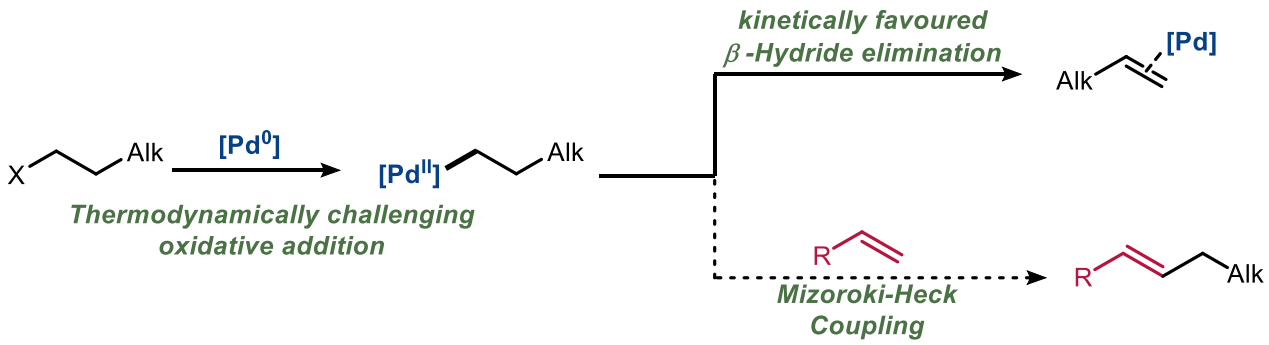

1.1.2: Transition metal-catalyzed synthesis of ketones from carbonyls

In the mid-to-late 20th century, researchers started exploring different strategies to functionalize various sp^2-hybridized carbon centers. Broadly speaking, utilizing an

[7] Lee, G.S., Kim, D. & Hong, S.H. *Nat. Commun.* **2021**, *12*, 991.

aldehyde or a carbonyl derivative to synthesise a ketone, is in many ways analogous to Heck coupling because both involve π-bond insertion to form a new bond and ultimately give a substituted sp^2-hybridized carbon, retaining the original π–system (**Scheme 4**).[8]

Scheme 4: Analogy between traditional Mizoroki-Heck coupling and coupling with carbonyls

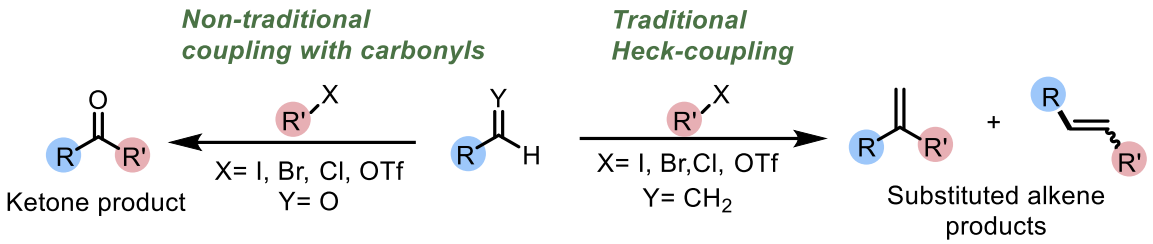

Nucleophilic addition:

Early reports of this transformation typically involved nucleophilic addition using stoichiometric organometallic additives such as Grignard reagents[9] and organolithium reagents.[10] These reagents, however, made the overall process less atom-economical due to significant by-product formation and were plagued by functional group intolerance. **Scheme 5** highlights the works of Mukaiyama *et al.* as well as Nahm and Weinreb who made noteworthy contributions to the synthesis of ketones from carbonyls containing labile, heteroatom leaving groups that also serve to stabilize the tetrahedral intermediate that forms.

---

[8] Vandavasi, J. K.; Hua, X.; Ben Halima, H.; Newman, S. G. *Angew. Chem. Int. Ed.* **2017**, *56*, 15441.
[9] T. Mukaiyama, M. Araki, and H. Takei, *J. Am. Chem. Soc.* **1973**, *95*, 4763.
[10] Nahm, S.; Weinreb, S. M. *Tet. Lett.* **1981**, *22*, 3815.

Scheme 5: Past approaches for synthesizing ketones from carbonyls

Mukaiyama, *et al.*, 1973

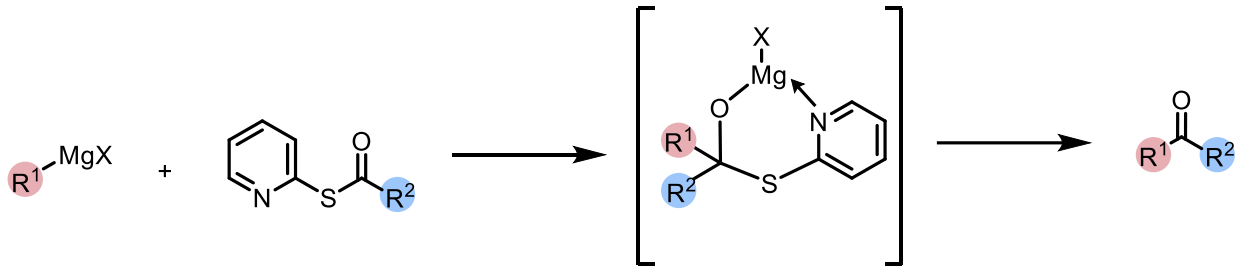

Nahm and Weinreb, 1981

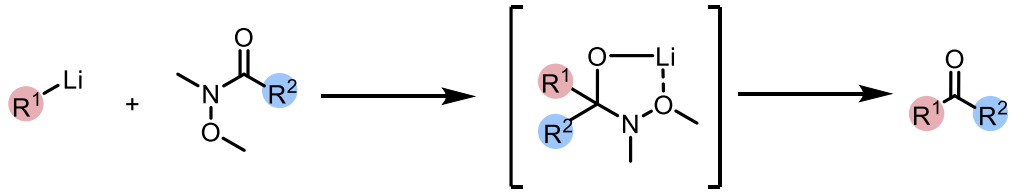

Coupling with aryl boronic acids:

Alongside the development of these strategies, there were also significant advancements in transition metal-catalyzed methods to synthesize ketones from carbonyls using aryl boronic acids or esters as nucleophiles. Arylboron reagents are generally a more attractive choice compared to organomagnesium or lithium reagents due to their commercial availability and stability. **Scheme 6** demonstrates some key contributions to the transition metal-catalyzed coupling of carbonyls and aryl boronic acids to form ketones by the groups of McCarthy, Gooßen and Genet in the late 1990's and early 2000's.

Scheme 6: Transition metal-catalyzed coupling of aryl boronic acids/esters and carbonyls

Haddach and McCarthy, 1999.[11]

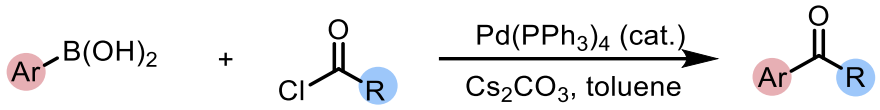

Gooßen *et al.*, 2001.[12]

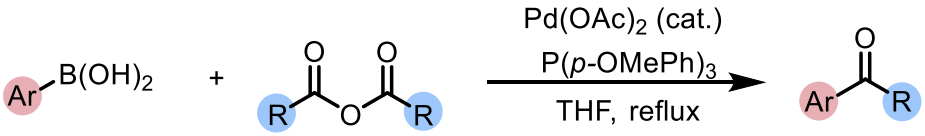

Genet *et al.*, 2004.[13]

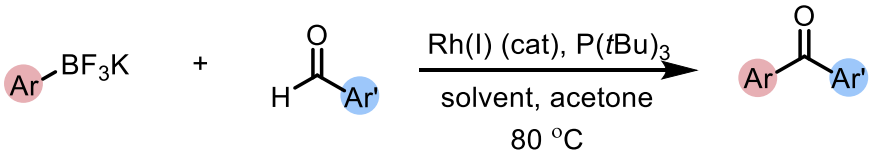

Coupling with aryl halides and pseudohalides:

In modern literature, there has a been a surge of reports discussing the coupling of aryl (pseudo)halides with aldehydes to generate ketones. Cheng and coworkers showed in 2002 that nickel could be used for this transformation in the presence of zinc to turnover the catalyst.[14] From our own group, the successful coupling of aryl triflates

[11] Haddach, M.; McCarthy, J. R. *Tet. Lett.* **1999**, *40*, 3109.
[12] Gooßen, L.J.; Ghosh, K. *Angew. Chem. Int. Ed*. **2001**, *40*, 3458.
[13] Pucheault, M.; Darses, S.; Genet, J-P. *J. Am. Chem. Soc.* **2004**, *126*, 15356.
[14] Huang, Y.-C.; Majumdar, K. K.; Cheng, C.-H. *J. Org. Chem.* **2002**, *67*, 1682.

and aldehydes in the presence of a nickel catalyst was reported in 2017.[8] In 2018, Kanai and coworkers demonstrated a useful palladium-catalyzed coupling of aryl bromides and aldehydes to synthesise highly desired ketones, albeit requiring even higher temperatures.[15]

Scheme 7: Transition metal-catalyzed coupling of aryl halides or pseudohalides and aldehydes to form ketones

Cheng and coworkers, 2002

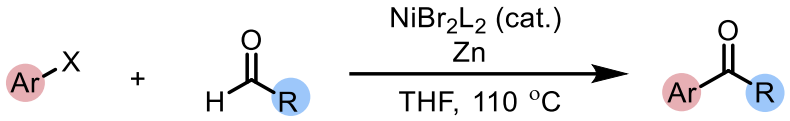

Newman and coworkers, 2017

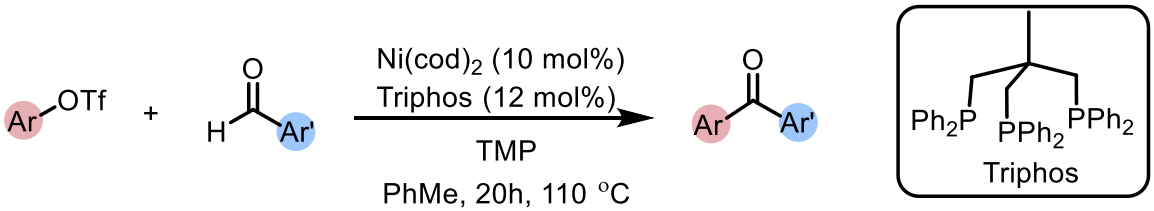

Kanai and coworkers, 2018

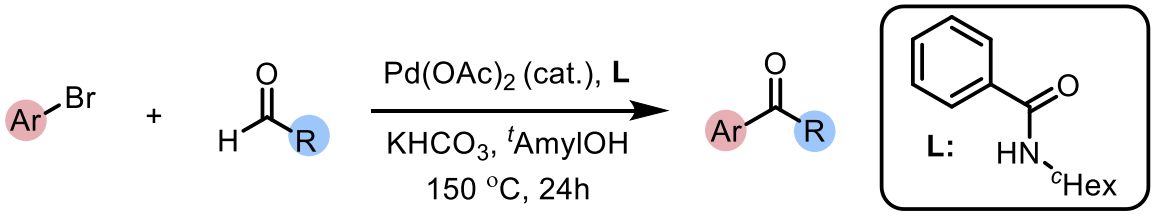

[15] Wakaki, T.; Togo, T.; Yoshidome, D.; Kuninobu, Y.; Kanai, M. *ACS Catal.* **2018**, *8*, 3123.

1.1.3: Reductive 1,2-addition of organo(pseudo)halides to carbonyls to form alcohols

Past approaches using stoichiometric organometallic reagents:

In parallel with the functionalization of carbonyls to synthesize ketones, a reductive process can also take place whereby the final product is an alcohol and H_2 is formally added across the C=O double bond. Discovered in the early 1900's, the Grignard reaction utilizes a stoichiometric organomagnesium reagent to reductively functionalize a ketone to form the corresponding substituted alcohol. This reaction, although still widely used to date, is often low yielding and requires cryogenic conditions (**Scheme 8**).

Scheme 8: The Grignard Reaction, 1900

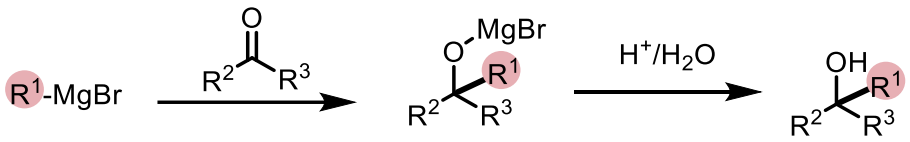

A shift towards employing transition metal-catalysis for the 1,2-addition of aldehydes and ketones led to the development of the Nozaki-Hiyama-Kishi (NHK) reaction in late 1970's, which was a pioneering discovery sparking much subsequent research in this area (**Scheme 9**).[16]

[16] Gil, A.; Albericio, F.; Álvarez, M. *Chem. Rev.* **2017**, *117*, 8420.

Scheme 9: The Nozaki-Hiyama-Kishi Reaction, 1977

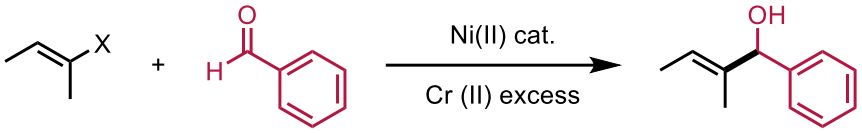

Scheme 10 summarizes the commonly proposed mechanism of this reaction. In a traditional NHK reaction, Ni(II) is first reduced to Ni(0) using two equivalents of chromium(II) chloride, a sacrificial reductant, leaving chromium(III) chloride as a by-product of the reaction. The next step is the oxidative addition of nickel into the carbon-halogen bond, forming an alkenyl nickel R–Ni(II)–X intermediate followed by a transmetallation step with Cr(III) to generate an alkenyl chromium R–Cr(III)–X intermediate and regenerating Ni(II). This species then reacts with the carbonyl group in a nucleophilic addition reaction. A key disadvantage of this approach, however, was the use of stoichiometric quantities of toxic chromium salts.[17]

[17] Fürstner, A.; Shi, N. *J. Am. Chem. Soc.* **1996**, *118*, 12349.

Scheme 10: A mechanism for the Nozaki-Hiyama-Kishi reaction

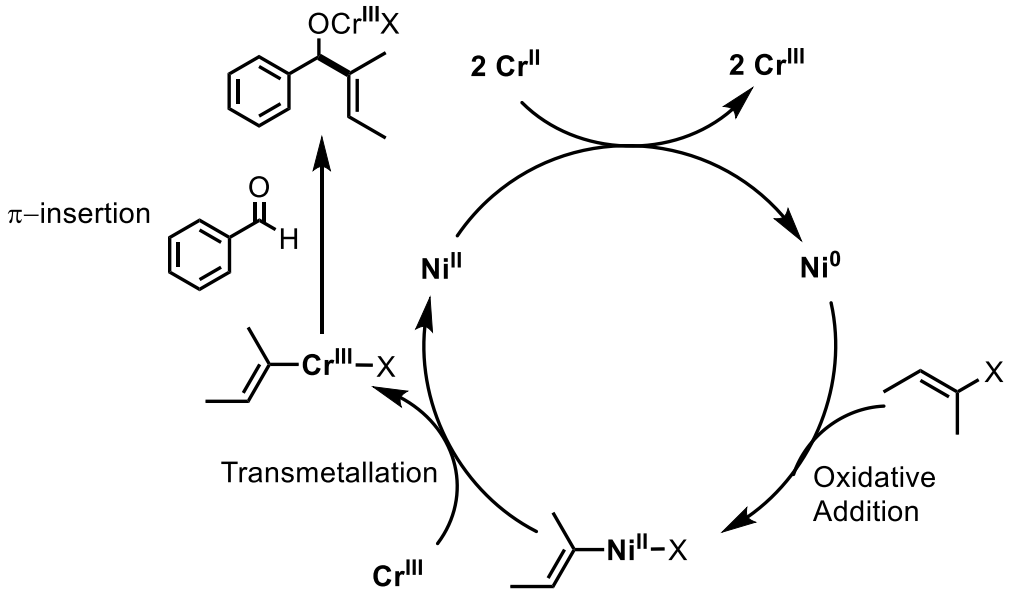

Coupling with aryl boronic acids:

Strategies involving the use of aryl boronic acids and esters to reductively add to an aldehyde gained popularity following the initial work of Miyaura,[18] who reported the first rhodium-catalyzed addition of aryl boronic acids to aldehydes, Kawakami,[19] who reported the first nickel-catalyzed variant, and Yamamoto *et al.*,[20] who used palladium as a catalyst.

[18] Sakai, M.; Euda, M.; Miyaura, N. *Angew. Chem. Int. Ed.* **1998**, 37, 3279.
[19] Takahashi, G.; Shirakawa, E.; Tsuchimoto, T.; Kawakami, Y. *Chem. Commun.* **2005**, *11*, 1459.
[20] Yamamoto, T.; Ohta, T.; Ito, Y. *Org. Lett.* **2005**, 7, 4153.

Scheme 11: Transition metal-catalyzed addition of aryl boronic acids/esters to aldehydes

Miyaura and coworkers, 1998

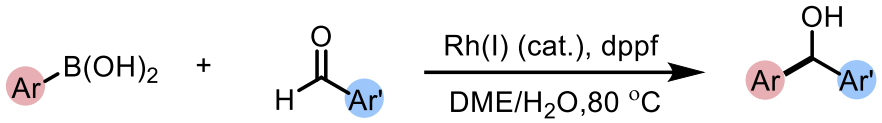

Kawakami and coworkers, 2005

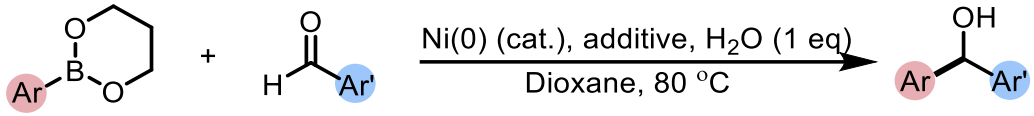

Yamamoto *et al.*, 2005

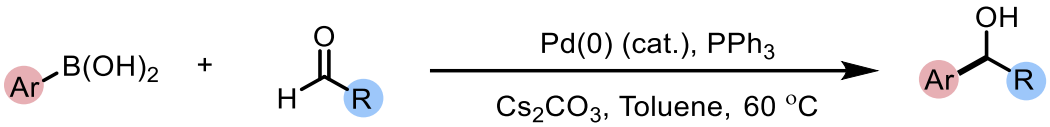

Current approaches of reductive 1,2-addition of aldehydes:

In recent years, the Weix and Krische groups have made significant progress in the addition of aryl halides to benzylic or aliphatic aldehydes. In 2019, the Krische group demonstrated the intermolecular carbonyl-aryl halide reductive coupling via rhodium catalyzed transfer hydrogenation (**Scheme 12**).[21]

[21] Swyka, R. A.; Zhang, W.; Richardson, J.; Ruble, J. C.; Krische, M. J. *J. Am. Chem. Soc.* **2019**, *141*, 1828.

Scheme 12: Rhodium catalyzed reductive 1,2-addition of aldehydes

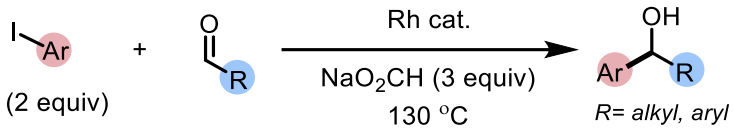

This work depicted an alternative strategy to access secondary alcohol products by completely avoiding the need to use a stoichiometric metal reductant such as chromium, zinc, or manganese. The reductant of choice for the Krische group was sodium formate, which was one of the first examples of successfully employing an organic salt reductant in this transformation. Moreover, sensitive alcohol, carbamate, and sulfonamide functional groups as well as acidic OH and NH groups, were well-tolerated in their scope. Some heterocyclic functionality, ortho hindrance and electron-rich aldehydes also seem to be compatible with their strategy. It should also be noted that the oxidative insertion was selective for aryl iodides, and chlorides or bromides elsewhere on the aromatic ring were unaffected.

Scheme 13: Proposed catalytic cycle for Rh-catalyzed reductive 1,2-addition onto aldehydes

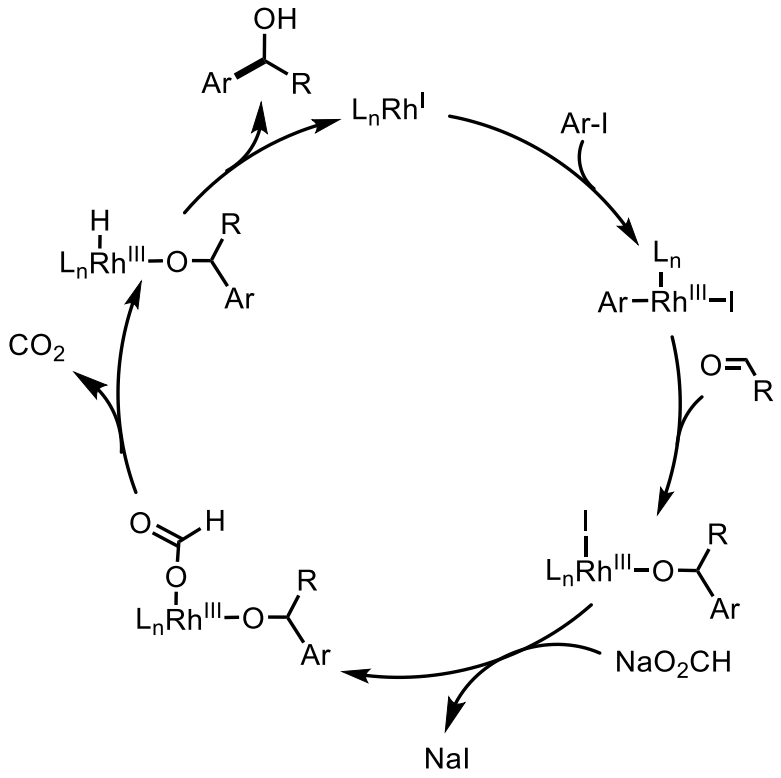

The Weix group subjected aryl bromides and aliphatic or aryl aldehydes to a nickel-catalyzed reductive arylation procedure using stoichiometric zinc as a reductant **(Scheme 14)**.[22] Zinc dibromide generated in-situ is also proposed to coordinate to the aldehyde and facilitate insertion by the nickel catalyst.

[22] Garcia, K. J.; Gilbert, M. M.; Weix, D. J. *J. Am. Chem. Soc.* **2019**, *141*, 1823.

Scheme 14: Ni(II) catalyzed reductive coupling of aldehydes and aryl bromides

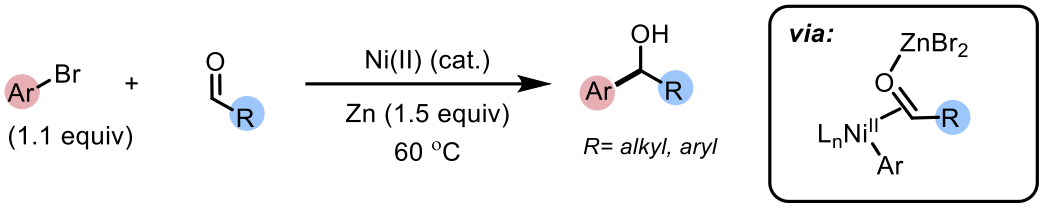

The scope reported by the Weix group incorporated diverse functional groups with ortho hindrance and alcohol functionality on both the aryl halide and aldehyde, as well as heterocycle-containing compounds, being well-tolerated. Moderate to high yields of linear, branched, and cyclic aliphatic aldehydes provided an edge to Weix's approach over Krische's that lacked any unactivated aliphatic functionality.

Recently, related work from Montgomery and Cruz presented an alternative nickel-catalyzed strategy to activate alkyl halides and promote a reductive sp^3-sp^3 coupling with aliphatic aldehydes (**Scheme 15**).[23] In their strategy, a cross-electrophile coupling is proposed between the alkyl bromide starting material and the sp^3-hybridized α-silyloxy(alkyl)nickel intermediate that forms in-situ.

[23] Cruz, C. L.; Montgomery, J. *Chem. Sci.* **2021**, *12*, 11995.

Scheme 15: Nickel-catalyzed reductive sp^3-sp^3 cross-coupling

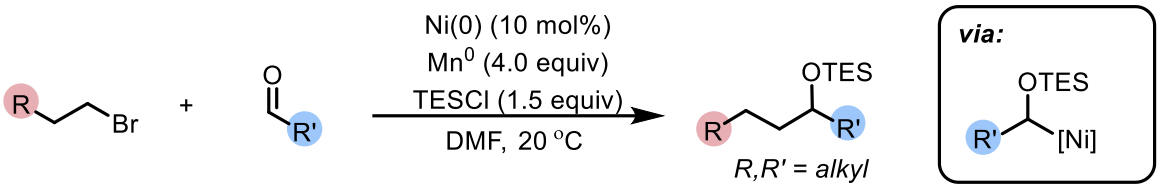

This was particularly attractive because of the selective activation of unactivated alkyl halides, which are known to either undergo β-hydride elimination or homocoupling under catalytic conditions.[24] Therefore, they proposed that alkyl bromides and aliphatic aldehydes can be coupled to give rise to silyl-protected secondary alcohols in the presence of Ni(I)/(II)/(III), a manganese reductant, and triethylsilyl chloride (**Scheme 16**).

[24] D. J. Weix, *Acc. Chem. Res*. **2015**, *48*, 1767.

Scheme 16: Proposed catalytic cycle for Ni-catalyzed reductive sp^3-sp^3 cross-coupling

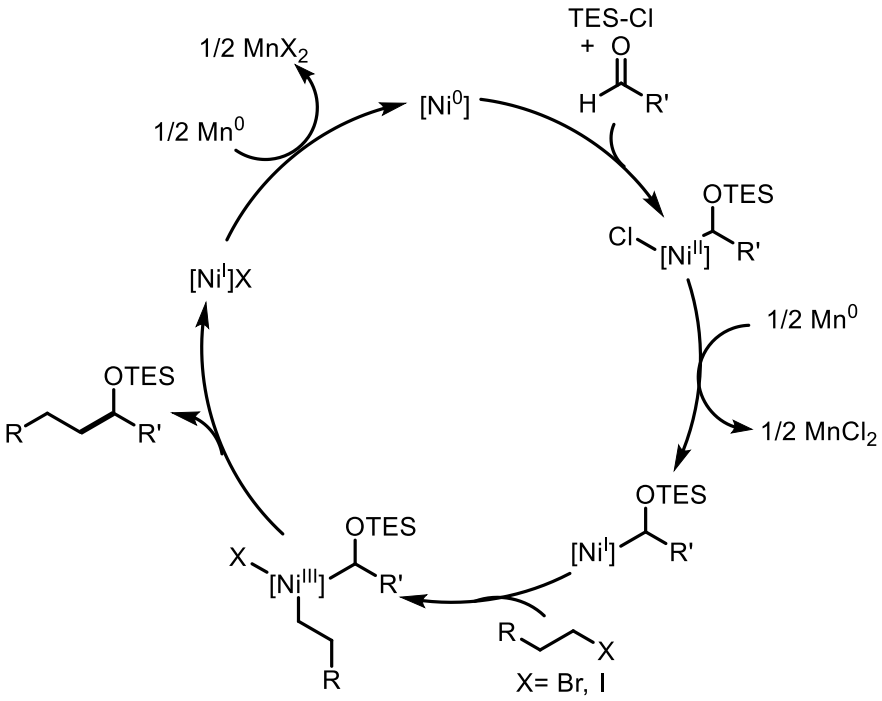

Their scope highlighted that esters, nitriles, ethers, acetates and protected amine functional groups were tolerated reasonably well. Unfortunately, aryl halides and benzaldehyde derivatives were incompatible with their optimized conditions which eliminates the possibility of forming useful secondary benzylic alcohol and diaryl methanol derivatives. Furthermore, the use of manganese as a reductant to turnover the active Ni(0) catalyst brings to surface the previously encountered issue of generating stoichiometric metal waste.

1.1.4: Transition-metal catalyzed α-arylation of alcohols

Alcohols are amongst the most abundant functional groups in naturally occurring compounds, present in sugars, steroids, proteins, and more. Their bioactive

characteristics and the ability to be readily engaged in functional group interconversion makes them a suitable choice in a broad range of pharmaceutical agents. The lone pair on the oxygen enables them to act as a nucleophile and the ionizable O-H bond can also render them as a source of protons. The lack of diverse methodologies that exist in the literature to carry out the direct α-arylation of alcohols makes it an area worth exploring.[25] This is formally a redox-neutral process due to no net gain or loss of hydrogen atoms.

In 2011, the Itami group demonstrated a Ni^0/IPr-catalyzed strategy to couple aryl boronic esters with primary or secondary alcohols (**Scheme 17**).[26] Interestingly, they proposed the use of chlorobenzene (PhCl) to facilitate the formation of a nickel-alkoxide intermediate and to turnover the active Ni^0-IPr catalyst. Their method, however, only included simple alcohols and aryl boronic acids as substrates whereas heterocyclic groups and sensitive functionalities were not well-tolerated.

[25] Santana, C. G.; Krische, M. J. *ACS Catal.* **2021**, *11*, 5572.
[26] Maekawa, T.; Sekizawa, H.; Itami, K. *Angew. Chem. Int. Ed.* **2011**, *50*, 7022.

Scheme 17: Nickel-catalyzed direct arylation of primary or secondary alcohols

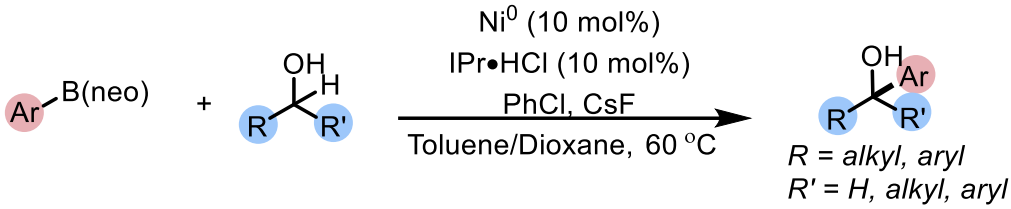

It is not surprising that direct, redox-neutral arylation of alcohols to yield alcohol products is an attractive transformation. If starting from aldehydes such as that in reductive 1,2-addition, a reductant is required. Furthermore, aldehydes are difficult to work with since they are often prone to decomposition, most commonly by aerobic oxidation. [27] It should also be noted that many aldehydes are non-naturally occurring and are in fact synthesised by oxidizing their primary alcohol counterparts, introducing an additional step in the overall process. The MacMillan group, in 2018, published a nickel metallophotoredox catalyzed approach combining HAT (hydrogen atom transfer) catalysis and Lewis acid activation (**Scheme 18**).[28]

Scheme 18: Photoredox coupling of 1° alcohols and aryl bromides

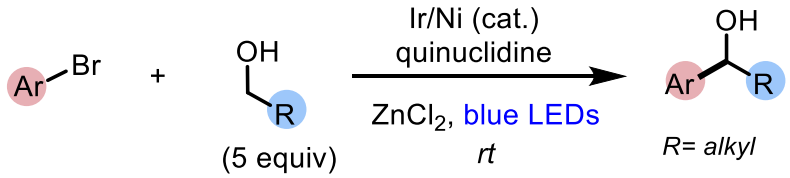

[27] Vanoye, L.; Favre-Réguillon, A.; Aloui, A.; Philippe, R.; de Bellefon, C. *RSC Adv.* **2013**, *3*, 18931.
[28] Twilton, J.; Christensen, M.; DiRocco, D. A.; Ruck, R. T.; Davies, I. W.; MacMillan, D. W. C. *Angew. Chem. Int. Ed.* **2018**, *57*, 5369.

The use of zinc dichloride as a Lewis acid is proposed to facilitate the alcohol deprotonation to activate the α-hydroxy C-H bond and suppress C-O bond formation by preventing nickel alkoxide formation. The mechanistic proposal provided by the authors begins with the photoexcitation of the Ir(III) photocatalyst followed by single electron transfer (SET) from the quinuclidine HAT catalyst which reduces the excited Ir(III)* to Ir(II) and gives an oxidized quinuclidine radical cation. The secondary alcohol in the presence of a base and the Lewis acid, $ZnCl_2$, gets deprotonated and forms zinc alkoxide in-situ. The quinuclidine radical cation abstracts a hydrogen atom at the α carbon providing a secondary alkyl radical which can then add to the Ar-Ni^{II}-Br oxidative addition complex and further undergo reductive elimination to give the final product (**Scheme 19**).

Scheme 19: Mechanism for the α-arylation of primary alcohols through photoredox, HAT and nickel catalysis.

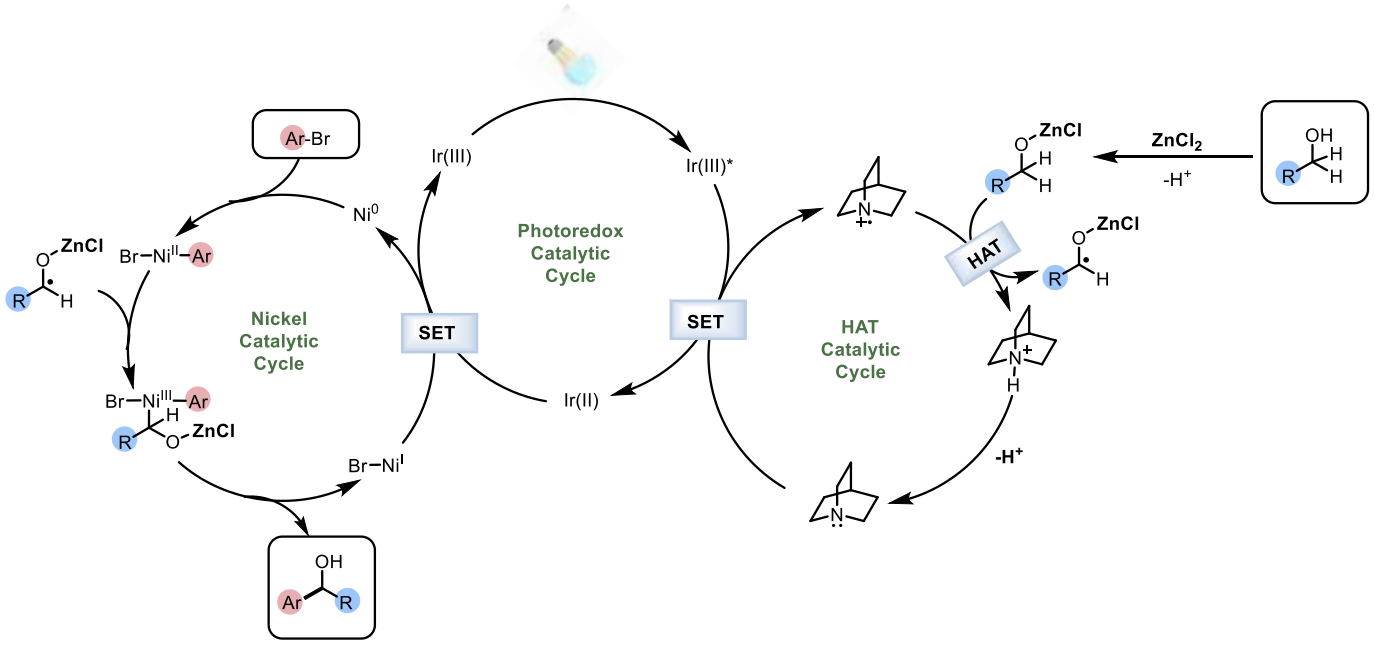

Their approach led them to establish a diverse scope containing simple aliphatic alcohol and heterocyclic aryl bromide coupling partners as well as tolerating sensitive functional groups on the alcohol and the aryl halide. They demonstrated their work in the synthesis of active pharmaceutical ingredients, with moderate to high yields obtained. A major drawback of this approach, however, was the use of stoichiometric $ZnCl_2$ which leads to stoichiometric zinc waste making the overall process less atom economical.

1.1.5: Reductive 1,2-addition with isatins

Isatins or indolin-2,3-diones, essentially cyclic analogs of α-keto amides, are naturally occurring and pharmaceutically relevant structural motifs. Nucleophilic addition to the 3-position of isatins leads to the formation of 3-substituted-3-hydroxy-2-oxindoles which are of particular importance both due to the challenge involved in accessing heterocyclic tertiary alcohols cleanly and due to the wide range of bioactive natural products that contain this functionality (**Figure 1**).[29]

[29] Yu, B.; Xing, H.; Yu, D.-Q.; Liu, H.-M. *Beilstein. J. Org. Chem.* **2016**, *12*, 1000.

Figure 1: Bioactive natural products and small-molecules with a 3-substituted-3-hydroxy-2-oxindole backbone.

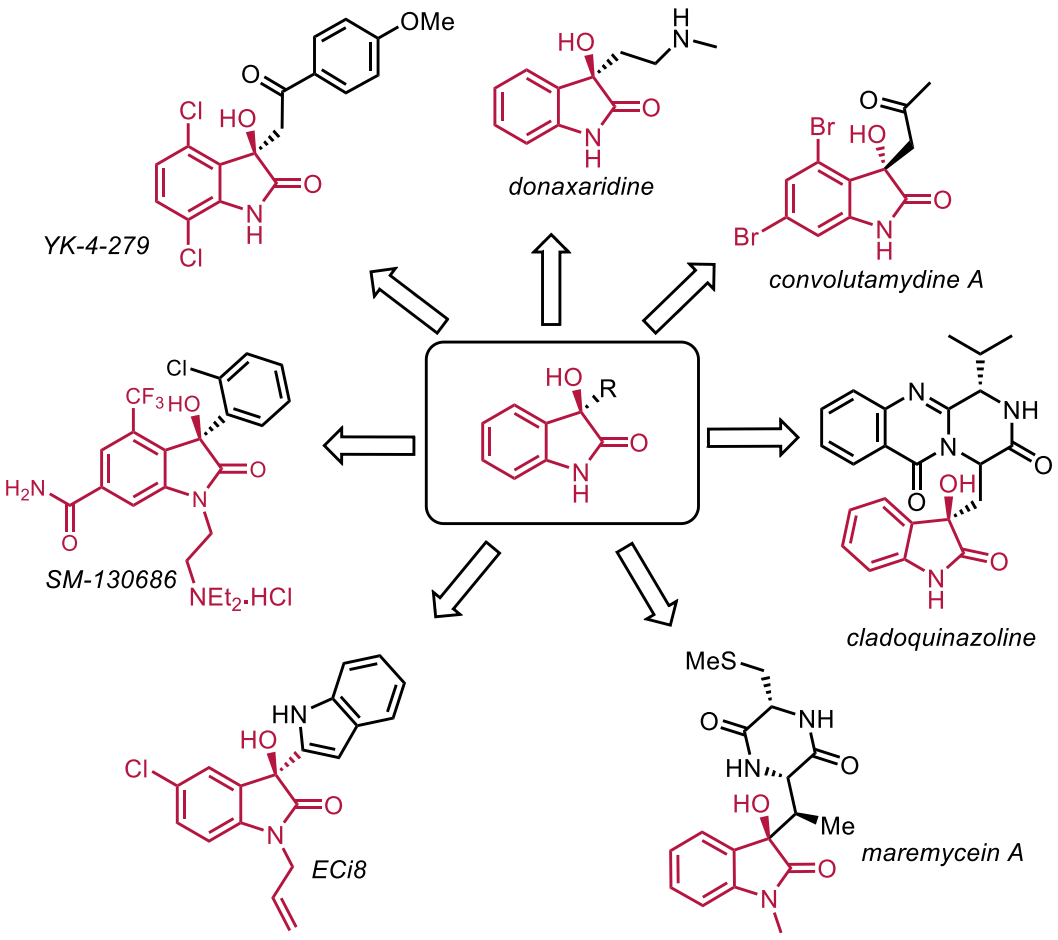

The reactive nature of an unprotected amide within close proximity to the ketone adds another level of complexity to the 1,2-functionalization of this position.[30] The formation of a quaternary carbon centre via nucleophilic attack onto ketone derivatives remains a challenge in synthetic chemistry, where many strategies still involve the use of

[30] Muthukumar, A.; Sangeetha, S.; Sekar, G. *Org. Biomol. Chem.* **2018**, *16*, 7068.

a stoichiometric organometallic reagents or additives for the key C-C bond forming reaction.[31] For several years, reports on substitution at the carbonyl group of α-keto esters and α-keto amides were limited to zinc mediated alkynation and alkylation reactions while reports on alkenylations and arylations were scarce.[32]

In 2006, Minnaard and coworkers were the first to publish the Rh(I)/(III) catalyzed arylation of unprotected isatins using aryl boronic acids as coupling partners, and phosphites as ligands (**Scheme 20**).[33] They were able to couple simple isatin derivatives with electron rich and electron poor arylboronic acids with yields ranging from 45-99%. In an isolated example, isatin and phenylboronic acid in the presence of Rh(I) and a phosphoramidite ligand gave the desired product enantioselectively in quantitative yield and 55% ee. Although quiet a modest enantioselectivity, this strategy paved the way for further exploration into 1,2 additions of isatins.

Scheme 20: Rhodium catalyzed coupling between isatins and aryl boronic acids

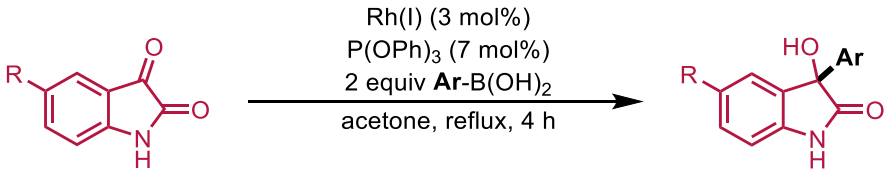

[31] Liu, Y.-L.; Lin, X.-T. *Adv. Synth. Catal.* **2018**, *361*, 876.
[32] a) Jiang, B.; Chen, Z.; Tang, X. *Org. Lett.* **2002**, *4*, 3451.
b) Wieland, L. C.; Deng, H.; Snapper, M. L.; Hoveyda, A. H. *J. Am. Chem. Soc.* **2005**, *127*, 15453.
[33] Toullec, P. Y.; Jagt, R. B.; de Vries, J. G.; Feringa, B. L.; Minnaard, A. J. *Org. Lett.* **2006**, *8*, 2715.

Following this initial report, other transition metal complexes were also employed in the addition of arylboronic acids to isatins including nickel,[34] copper,[35] and palladium.[36] The Krische group in 2015 proposed an alternative strategy to access 3-substituted-3-hydroxy-2-oxindoles via the intramolecular reductive cyclization of halo-ketones.[37] Their method involved a hydrogen gas-mediated palladium-catalyzed Grignard-type addition to α-keto amides (**Scheme 21**). A limited scope, competing hydrogenolysis of the aryl halide and failure to generate enantioenriched products when employing chiral ligands made this strategy only moderately successful. Furthermore, since the substrates were subjected to intramolecular cyclization, there was little opportunity for diversity and the starting materials were quite contrived. Therefore, this method was viewed predominantly as proof-of-concept that could drive further research in the area.

Scheme 21: Pd-catalyzed reductive cyclization of halo ketones

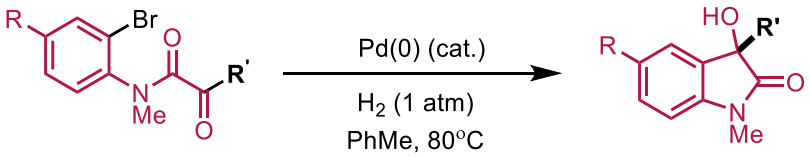

Many groups have attempted slight variations of the aforementioned strategies with the hope of expanding the scope of isatins and nucleophilic coupling partners as

[34] Zhang, Y.-Y.; Chen, H.; Jiang, X.; Liang, H.; He, X.; Zhang, Y.; Chen, X.; He, W.; Li, Y.; Qiu, L. *Tetrahedron.* **2018**, *74*, 2245.
[35] Shintani, R.; Takatsu, K.; Hayashi, T. *Chem. Commun.* **2010**, *46*, 6822.
[36] Liu, Z.; Gu, P.; Shi, M.; McDowell, P.; Li, G. *Org. Lett.* **2011**, *13*, 2314.
[37] Shin, I.; Ramgren, S. D.; Krische, M. J. *Tetrahedron.* **2015**, *71*, 5776.

well as generating enantioenriched products.[38] However, there is a lack of methods which use commercially available and stable aryl or heteroaryl halides and mild reductants as well as those that could tolerate a wide range of functional groups on both the electrophile as well as at the isatin.

1.1.6: Diazadiphosphacyclooctane ligands

This thesis describes efforts made towards expanding upon the catalytic arylation reactions described in **Chapters 2** and **3**. A key discovery that enabled this work was the recognition of 1,5-diaza-3,7-diphosphacyclooctane ligands (P_2N_2) as a unique class of bidentate bis-phosphine ligands for achieving such chemistry. Due to their pendant amine groups, these ligands have garnered interest in recent years. A key feature of these ligands is that they can adopt various conformations which in turn governs accessibility of the reactants to the metal core (**Figure 2**).[39]

---

[38] **a)** Jia, Y.-X.; Katayev, D.; Kündig, E. P. *Chem. Commun.* **2010**, *46*, 130.
b) Hu, J. X.; Wu, H.; Li, C. Y.; Sheng, W. J.; Jia, Y. X.; Gao, J. R. *Chem. Eur. J.* **2011**, *17*, 5234.
c) He, J.-Q.; Chen, C.; Yu, W.-B.; Liu, R.-R.; Xu, M.; Li, Y.-J.; Gao, J.-R.; Jia, Y.-X. *Tet. Lett.* **2014**, *55*, 2805.
d) Zhang, J.; Chen, J.; Ding, J.; Liu, M.; Wu, H. *Tetrahedron.* **2011**, *67*, 9347.
e) Gui, J.; Chen, G.; Cao, P.; Liao, J. *Tetrahedron: Asymmetry*. **2012**, *23*, 554.
f) Ganci, G. R.; Chisholm, J. D. *Tet. Lett.* **2007**, *48*, 8266.
g) Zhuang, Y.; He, Y.; Zhou, Z.; Xia, W.; Cheng, C.; Wang, M.; Chen, B.; Zhou, Z.; Pang, J.; Qiu, L. *J. Org. Chem.* **2015**, *80*, 6968.
h) Zhang, Y.-Y.; Chen, H.; Jiang, X.; Liang, H.; He, X.; Zhang, Y.; Chen, X.; He, W.; Li, Y.; Qiu, L. *Tetrahedron.* **2018**, *74*, 2245.
[39] Karasik, A. A.; Musina, E. I.; Balueva, A. S.; Strelnik, I. D.; Sinyashin, O. G. *Pure Appl. Chem.* **2017**, *89*, 293.

Figure 2: Various conformations of the 1,5-diaza-3,7-diphosphacyclooctane ligands

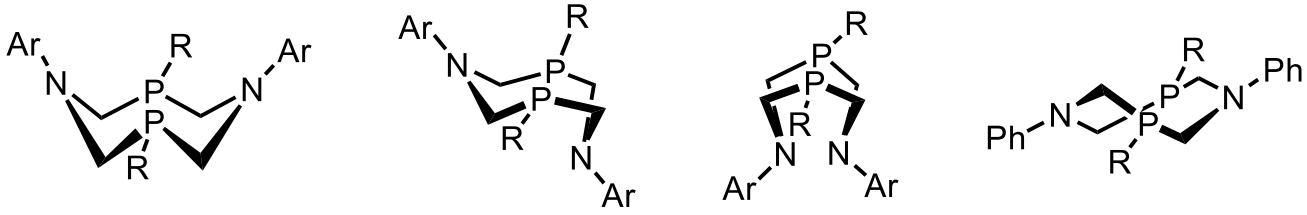

Changing the R groups at the phosphorus and nitrogen atoms can alter the electrondensity and steric bulk at the metal center, which affects the overall reactivity of the complex. Some commonly reported applications for these ligands in the literature are in electrocatalytic processes for fuel generation, hydrogen splitting reactions, reduction of carbon dioxide and oxidation of alcohols and formate.[40] These ligands have been employed in these kinds of electrocatalysis reactions with several transition metals, including but not limited to, platinum,[41] ruthenium,[42] palladium,[43] cobalt,[44] and nickel.[45]

In order to demonstrate the usefulness of these ligands in π-bond activation reactions and carbon-heteroatom bond formation, a noteworthy example came out of the Blacquiere lab in 2020 in which they reported that a Fe-P_2N_2 complex can be used to

[40] Galan, B. R.; Schöffel, J.; Linehan, J. C.; Seu, C.; Appel, A. M.; Roberts, J. A.; Helm, M. L.; Kilgore, U. J.; Yang, J. Y.; DuBois, D. L.; Kubiak, C. P. *J. Am. Chem. Soc.* **2011**, *133*, 12767.
[41] Curtis, C. J.; Miedaner, A.; Ellis, W. W.; DuBois, D. L. *J. Am. Chem. Soc.* **2002**, 124, 1918.
[42] Liu, T.; DuBois, M. R.; DuBois, D. L.; Bullock, R. M. *Energy Environ. Sci.* **2014**, *7*, 3630.
[43] DuBois, D. L.; Berning, D. E. *Appl. Org. Met. Chem*. **2000**, *14*, 860.
[44] Roy, S.; Sharma, B.; Pécaut, J.; Simon, P.; Fontecave, M.; Tran, P. D.; Derat, E.; Artero, V. *J. Am. Chem. Soc.*, **2017**, *139*, 3685.
[45] Yang, J. Y.; Bullock, R. M.; Dougherty, W. G.; Kassel, W. S.; Twamley, B.; DuBois, D. L.; DuBois, M. R. *Dalton Trans.* **2010**, *39*, 3001.

promote the hydrofunctionalization of alkynes facilitated by the formation of a metal vinylidene intermediate (**Scheme 22**).[46] This was one of the first few reports of these ligands showing promise in organic synthesis. The authors believed that the ligands play a role in the endo-selectivity of the intramolecular hydrofunctionalization reaction as well as the metal vinylidene formation, owing to their proton shuttling activity.

Scheme 22: Fe-P_2N_2 catalyzed intramolecular hydrofunctionalization of alkynes

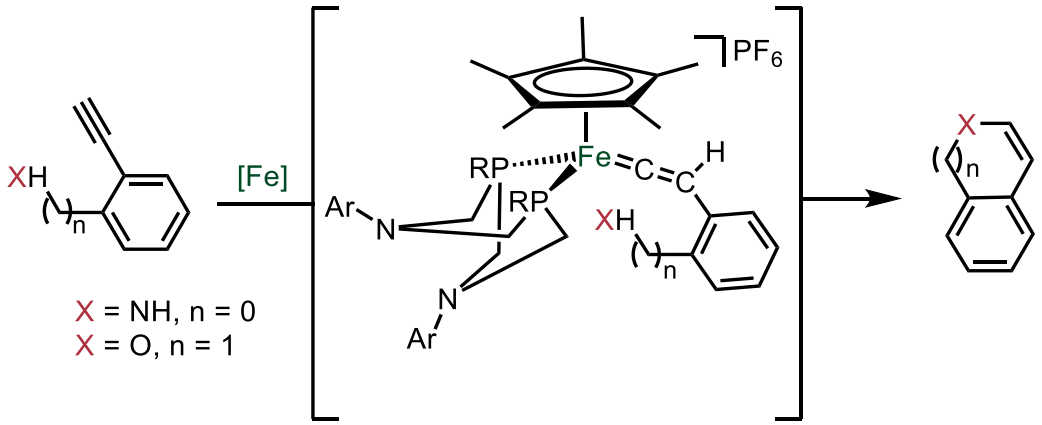

Bullock and coworkers from the Pacific Northwest National Laboratory (PNNL) reported in 2011 that the nitrogen arm of the P_2N_2 ligands can act as a proton shuttle to and from the metal center, which would explain why these ligands have been studied extensively in certain oxidation and reduction reactions (**Figure 3**).[47] The group tested Ni-$(P_2N_2)_2$ complexes in these reactions and found that the proton shuttling activity of the

[46] Bridge, B. J.; Boyle, P. D.; Blacquiere, J. M. *Organometallics.*, **2020**, *39*, 2570.
[47] Kilgore, U. J.; Stewart, M. P.; Helm, M. L.; Dougherty, W. G.; Kassel, W. S.; DuBois, M. R.; DuBois, D. L.; Bullock, R. M. *Inorg. Chem.*, **2011**, *50*, 10908.

nitrogen arm enables high turnover numbers and gives rise to a Ni-H species making this an efficient strategy for proton reduction and H_2 oxidation.

Figure 3: Ni-P_2N_2 catalyzed H_2 formation facilitated via pendant amine groups

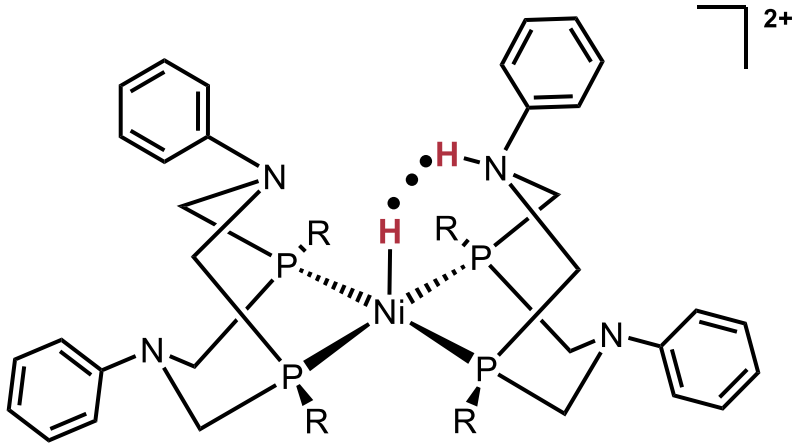

In 2015, Kubiak and coworkers explored the possibility of employing various $[Rh(P_2N_2)_2]^+$ complexes for the catalytic hydrogenation of CO_2 into formate.[48] The primary motivation for using rhodium complexes was the fact that rhodium has been well-studied for the hydrogenation of a wide range of substrates including alkenes, nitriles, and *N*-heterocycles; along with a variety of rhodium bis-diphosphine complexes being used for hydrogenation of CO_2.[49] The group hypothesized that the pendant amine groups of P_2N_2 ligands would lead to rate enhancement by increasing electron density at the metal center and can contribute to splitting of H_2 by accepting protons.

[48] Lilio, A. M.; Reineke, M. H.; Moore, C. E.; Rheingold, A. L.; Takase, M. K.; Kubiak, C. P. *J. Am. Chem. Soc.*, **2015**, *137*, 8251.
[49] Jessop, P. G.; Joó, F.; Tai, C.C. *Coord. Chem. Rev.*, **2004**, *248*, 2425

The main stages of hydrogenation described by the authors involved the addition of rhodium into H_2 in the presence of a base to form a Rh(I)-H intermediate which then transfers the hydride to CO_2 to carry out hydrogenation and lead to the production of formate (**Scheme 23**). After testing the reactivity of various $[Rh(P_2N_2)_2]^+$ complexes in this transformation, the group concluded that the additional steric bulk provided by the P_2N_2 ligands hinders access to the Rh center and slows down catalysis. Therefore, contrary to their initial hypothesis, the effect of the steric bulk contradicts any benefit provided by the basicity of the ligands, and the pendant amine groups were unable to additionally contribute to the formation of the catalytically active Rh(I)-H species.

Scheme 23: $Rh(P_2N_2)_2$ mediated CO_2 reduction to formate

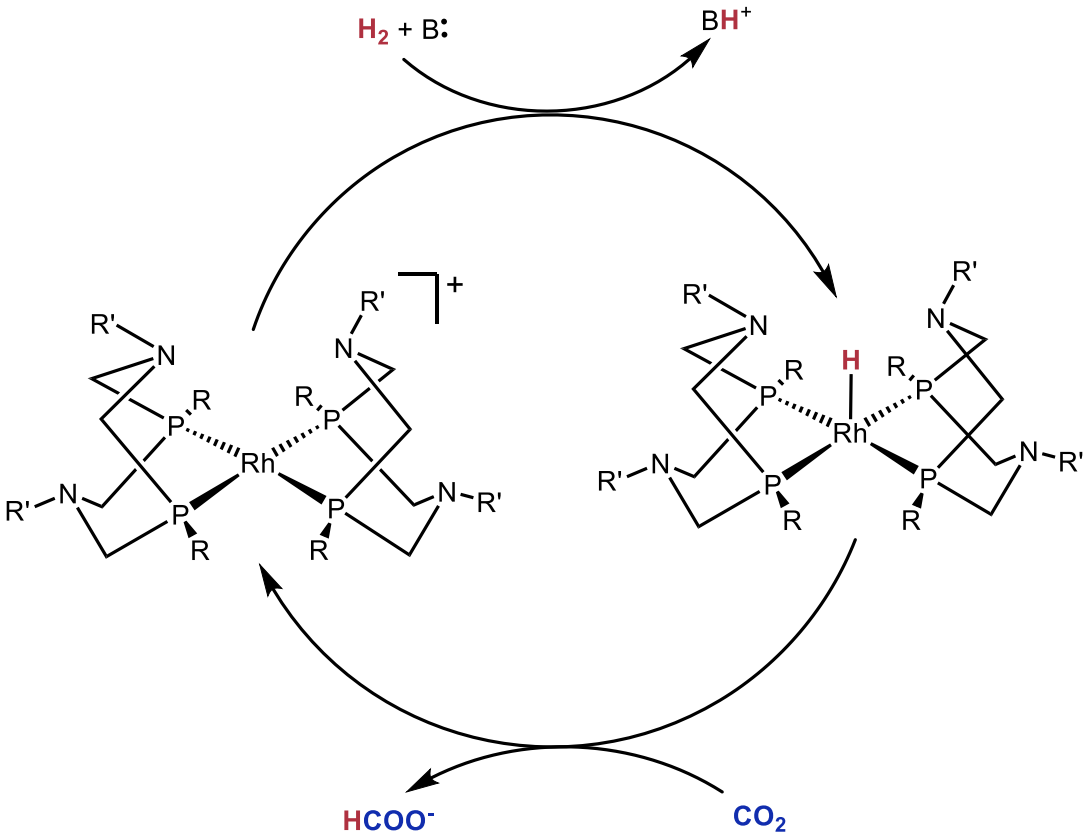

The interactions between different transition metals and this unique class of ligands are quite intriguing and there is indeed much left to be explored about their applications and their reactivity in carbon-carbon bond forming and C-H activation reactions.

1.1.7: Research Goals

The successful work done previously in the Newman group to couple aldehydes with aryl triflates for the synthesis of ketones (**Scheme 7**) led to a renewed research goal where the synthesis of secondary alcohols was to be prioritized. Synthetically useful

secondary alcohol products can be accessed via a reductive pathway starting from the corresponding aldehyde or a redox-neutral pathway from the corresponding primary alcohol and previous work in this area has been discussed in the sections above. We set out to explore the use of Nickel and P_2N_2 ligands, which are unprecedented in these types of cross-coupling reactions. Nickel was an attractive choice of catalyst due to its availability and affordability compared to metals like palladium or rhodium and its known cooperative reactivity in these types of coupling reactions.

Scheme 24: General Scheme for the research projects

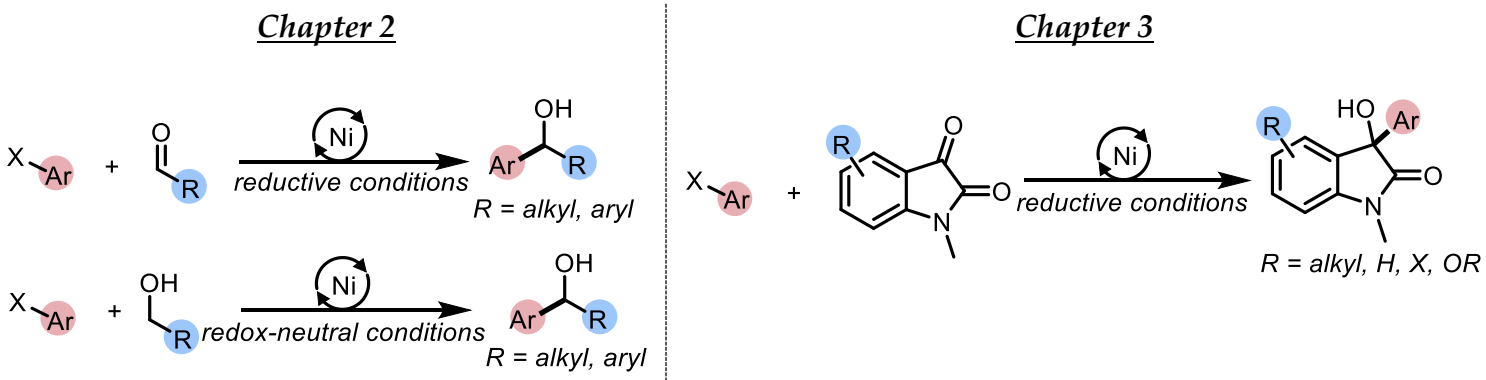

Chapter 2 will describe the nickel-catalyzed direct α-arylation of primary alcohols and reductive 1,2-addition of aldehydes will be described using aryl halides and a metal-free reductant, while employing P_2N_2 ligands and mild reaction conditions. Our goal was to design conditions that would be robust enough to carry out both transformations without the need to significantly alter reaction conditions, which would eventually make our strategy a useful synthetic tool to form secondary alcohols. We were determined to tackle the drawbacks noticed in previously reported methods in which the use of a

stoichiometric metal reductant such as zinc, high temperatures and harsh reaction conditions were common. In **Chapter 3**, we will further build upon the methodology developed and attempt a reductive coupling between aryl halides and isatins.

One of the primary goals of our research was to interrogate and understand a potential mechanism of this transformation, which would eventually help us develop the most favourable system. We believed that this coupling was quite possible because a plausible mechanism could be envisioned composed of previously established elementary steps (**Scheme 25**).

Scheme 25: Proposed mechanism of the reductive 1,2-addition of aldehydes and the redox-neutral *α*-arylation of alcohols

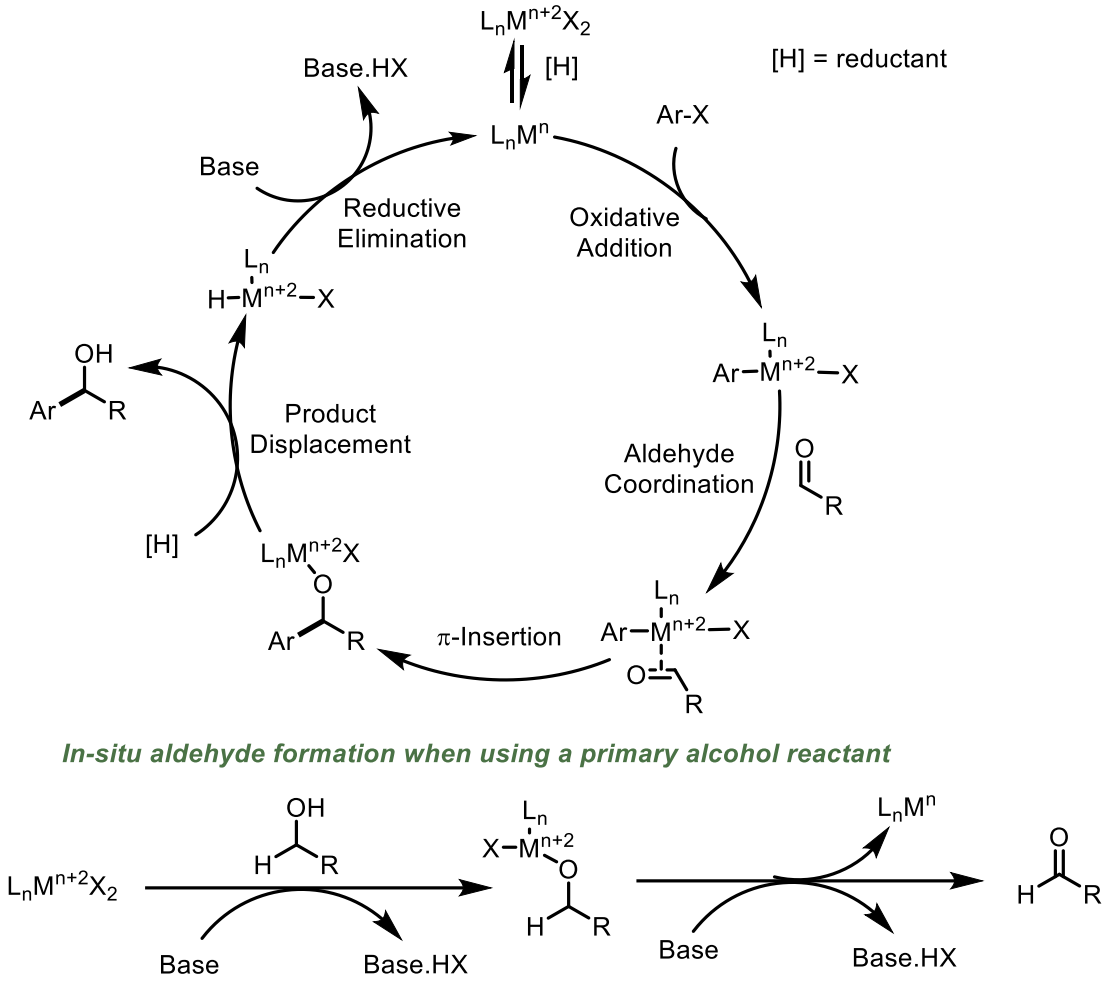

Literature precedence[21] and previous studies from our group[50] suggested that a transition metal precatalyst (M) in the presence of a reductant can be reduced down to a low oxidation state, allowing it to oxidatively insert into the Ar-X bond of an aryl halide. For the reductive 1,2-addition, coordination of the aldehyde starting material followed

[50] Verheyen, T.; Turnhout, L. V.; Vandavasi, J. K.; De Borggraeve, W. M.; Isbrandt, E. S.; Newman, S. G. *J. Am. Chem. Soc.* **2019**, *141*, 6869.

by insertion into its π-system would lead formation of a new C-C bond, with metal bound to the oxygen atom forming a metal-alkoxide. A stoichiometric, non-metallic reductant added in the reaction mixture can displace the final product from the metal center and lead to the formation of a metal hydride intermediate which can consequently undergo reductive elimination to turnover the active catalyst. When using a primary alcohol starting material such as that for the redox-neutral variant of this coupling, a similar catalytic cycle could be envisioned. An in-situ aldehyde can form via a metal-alkoxide intermediate, and this aldehyde can then proceed to product formation via steps similar to the ones described above.

Chapter 2: Addition to Aldehydes and Primary Alcohols[51]

The remarkable efforts of previous members of the Newman group led them to fully optimize and report the Ni(0) catalyzed redox-neutral transformation of aldehydes to ketones in the presence of aryl triflates (**Scheme 26**), discussed earlier in Chapter 1.[Error! Bookmark not defined.]

Scheme 26: Ni-catalyzed coupling of aryl triflates and aldehydes to synthesize ketones

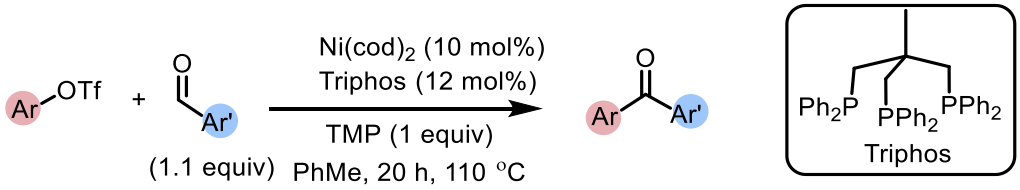

Expanding onto this work, our group also demonstrated in 2019, that the dehydrogenative arylation of primary alcohols to ketones was possible under similar conditions, in the presence of acetone as a sacrificial oxidant (**Scheme 27**).[50]

[51] Much of the work described in this chapter was done in collaboration with Eric Isbrandt and the results presented herein have been published in a peer-reviewed journal: Isbrandt, E. S.; Nasim, A.; Zhao, K.; Newman, S. G. *J. Am. Chem. Soc*. **2021**, *143*, 14646. The following compounds were isolated and characterized by Mr. Isbrandt: **2.17, 2.18, 2.20, 2.26, 2.27 and 2.28.**

Scheme 27: Ni-catalyzed dehydrogenative coupling of primary alcohols to form ketones

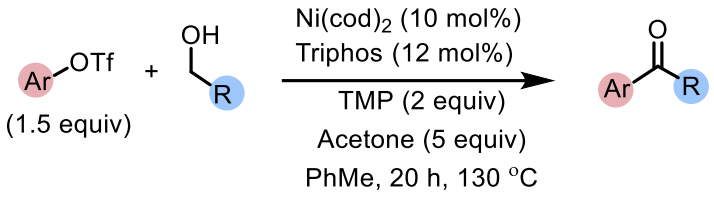

For this thesis chapter, the goal was to instead access secondary alcohols rather than ketones, either by reductive coupling with aldehydes or via direct addition of primary alcohols (**Scheme 28**).

Scheme 28: The desired transformations to access secondary alcohols

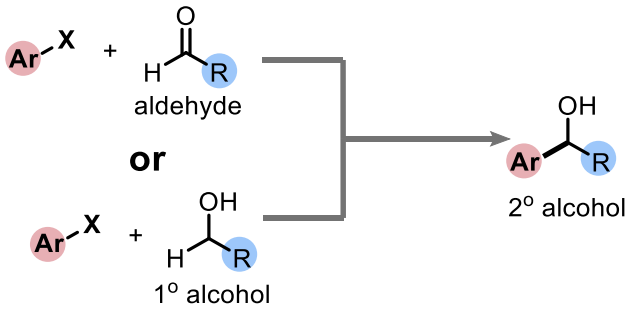

Initial testing, however, quickly led to the realization that the same approach of utilizing $Ni(cod)_2$ as a catalyst and Triphos as a ligand could not be extended to the synthesis of secondary alcohols. This confirmed that we needed to modify our approach and discover new conditions that could be applied to both, 1,2-addition of aldehydes and α-arylation of primary alcohols.

2.1.1: Optimization for the reductive 1,2-arylation of aryl aldehydes

The results of initial screening experiments conducted by PhD student Eric Isbrandt led to the identification of P_2N_2 ligands as a promising ligand choice for this transformation. A library of P_2N_2 ligands was synthesized, varying the substitutions and consequently the sterics and electronics on the phosphorus and nitrogen atoms. This allowed us to compare the reactivity of a diverse range of P_2N_2 ligands in this coupling. Initial screening of several Ni(0) and Ni(II) sources revealed $NiBr_2$•diglyme to work best. Amongst all aryl halides and pseudohalides pre-screened, aryl iodides gave the most favourable reactivity. **Table 1** shows an excerpt of the P_2N_2 screen performed on the coupling between 6-iodoquinoline and benzaldehyde as our model substrates at 75 °C for 16 h.

Table 1: Screening of P_2N_2 ligands for the reductive 1,2-arylation of aldehydes

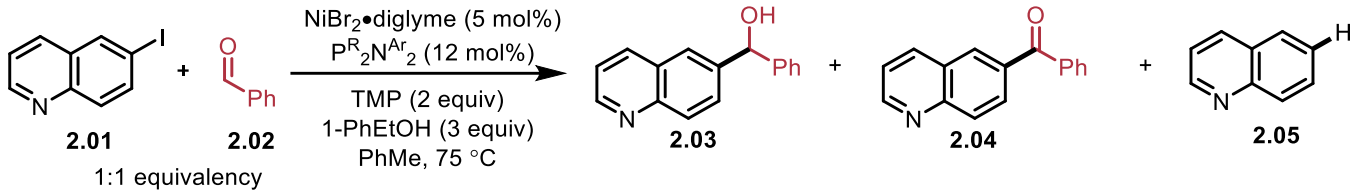

Entry	P_2N_2	Yield 2.03[a]	Yield 2.04[a]	Yield 2.05[a]
1	$P^{iBu}{}_2N^{ArCF3}{}_2$	13%	0%	59%
2	$P^{tBu}{}_2N^{ArCF3}{}_2$	0%	0%	91%
3	$P^{Ph}{}_2N^{ArCF3}{}_2$	35%	0%	10%
4	$P^{Cy}{}_2N^{ArCF3}{}_2$	78%	Trace	0%
5	$P^{Cy}{}_2N^{ArOMe}{}_2$	13%	0%	63%
6	$P^{Cy}{}_2N^{Ar(CF3)2}{}_2$	0%	0%	80%

General conditions: aryl iodide (0.30 mmol), aldehyde (0.30 mmol), TMP (0.6 mmol), 1-phenylethanol (0.90 mmol), $NiBr_2$•diglyme (5 mol%), P_2N_2 (12 mol%) in PhMe (0.40 M), 75 °C for 16 h, under inert atmosphere (set-up inside of the glovebox). [a]Yields are calculated by ^1H NMR with 1,3,5-trimethoxybenzene as the internal standard.

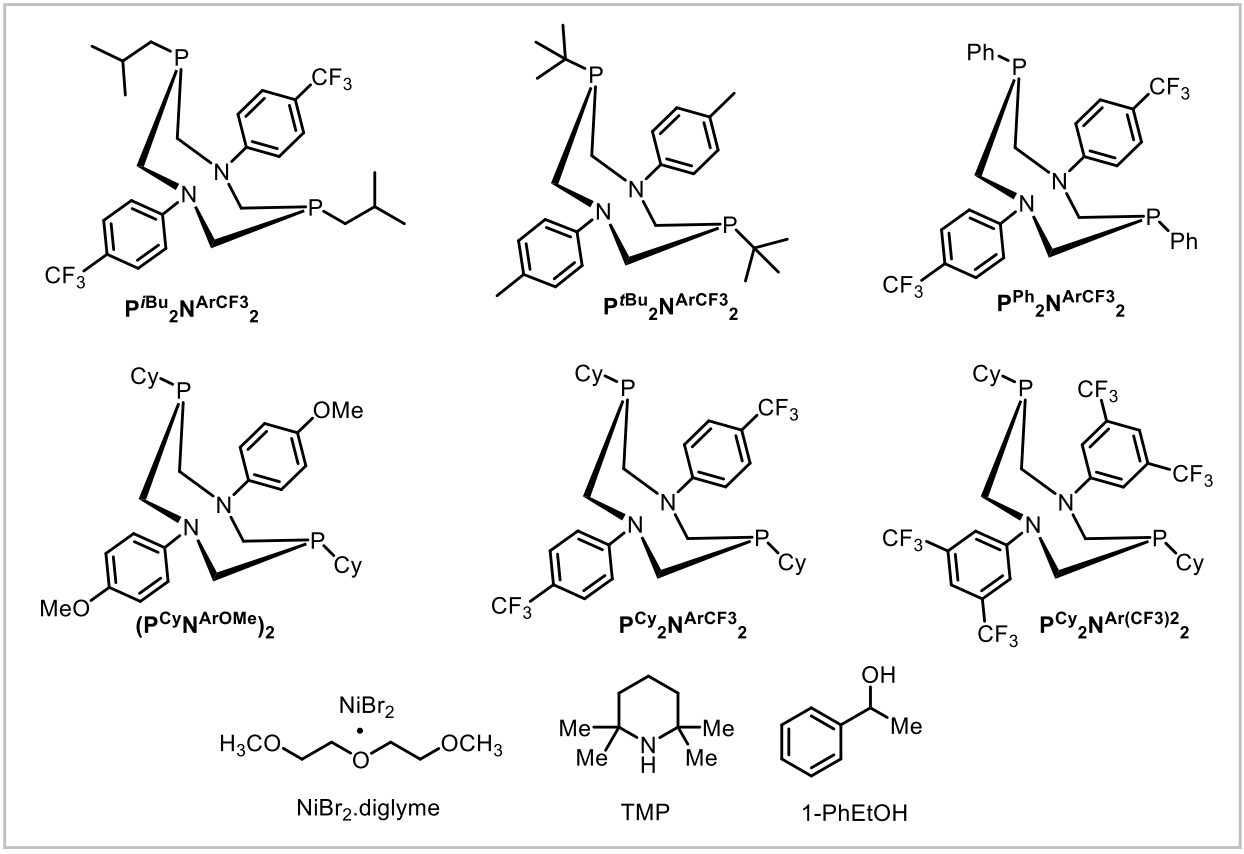

P_2N_2 ligands bearing P^{iBu}, P^{tBu}, P^{Ph} and P^{Cy} substituents (**entries 1-4**) were evaluated and based on the results obtained above, it was evident that the P^{Cy} containing ligand gave us the highest yield (78%) and selectivity for the desired alcohol **2.03**. Substitution on the aniline fragment was also altered to make the nitrogen either more basic by the addition of an electron-donating group (**entry 5**) or less basic by addition of highly electron-withdrawing groups (**entry 6**), both of which were detrimental to the reaction outcome, providing predominantly unwanted by-products. Consequently, we identified $P^{Cy}{}_2N^{ArCF3}{}_2$ (**entry 4**) to be the optimal ligand for subsequent optimization and scope experiments. It was indeed interesting to observe that this ligand possessed moderate

steric bulk compared to some of the bulkier analogs tested and had intermediate electron-withdrawing properties relative to the more electron-rich or electron-poor ligands used.

For reactions that did not lead to significant product formation, the majority of the mass balance was attributed to unreacted started material, the undesired redox-neutral ketone product (**2.04**) and the dehalogenated aryl iodide (**2.05**). Reductive cross-couplings featuring aryl halide or pseudohalide starting materials often suffer from side reactivity primarily due to dehalogenation[52] and formation of homocoupled dimers (**Scheme 29**).[53] Fortunately, this dimerization was rarely observed.

[52] Weidauer, M.; Irran, E.; Someya, C. I.; Haberberger, M.; Enthaler, S. *J. Org. Met. Chem.* **2013**, 729, 53.
[53] Jhaveri, S. B.; Carter, K. R. *Chem. Eur. J.* **2008**, *14*, 6845.

Scheme 29: Common fates of aryl halides in cross-coupling in the presence of reductant

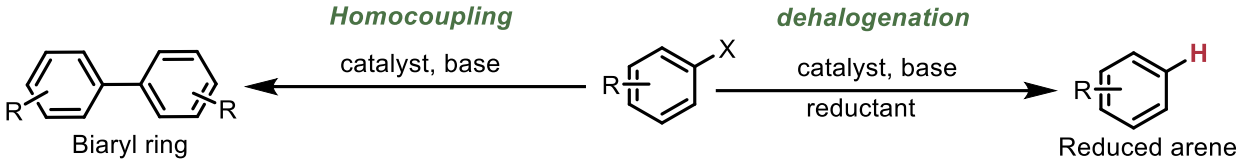

Part of our efforts were also focused on finding a reducing agent that would efficiently displace the final arylated alcohol product from the metal center and turnover the active catalyst while suppressing side reactivity and only serve as a hydride source. We were determined to avoid the use of harsh metal reductants seen previously in these types of cross-coupling reactions, which led us to screen several potential reductants. Because of this, secondary alcohols emerged as promising, clean alternatives to typically employed hydride sources, consequently getting oxidized over the course of the reaction. There was a possibility, however, that these reductants in the presence of nickel and organohalides could lead to the previously reported O-arylation ether products which were never observed under our optimal conditions, discussed in this chapter.[54]

Amongst the reducing agents that we screened, 1-phenylethanol was found to be one of the very few that facilitated the reaction, providing a 78% yield of the desired alcohol **2.03** (**Table 2, entry 1**). Other secondary alcohols, including *sec*-butanol (**entry 2**)

[54] MacQueen, P. M.; Tassone, J. P.; Diaz, C.; Stradiotto, M. *J. Am. Chem. Soc*. **2018**, *140*, 5023.

and isopropyl alcohol (**entry 3**) gave moderate yields of the 1,2-addition product **2.03** along with substantial reduction of the starting material to provide quinoline **2.05**. Either of these (*sec*-butanol or *i*-PrOH) would have been attractive reductant choices because the low boiling ketone by-products resulting from their oxidation could simply be evaporated off and contribute to ease of purification. Zinc (**entry 4**), which is a relatively commonly used metal reductant, sodium formate (**entry 5**), which was the organic reductant of choice for the Krische group,[21] and hydrogen gas (**entry 6**) all provided trace yields of the desired product giving predominantly the dehalogenated by-product. **Scheme 30** demonstrates how a secondary alcohol reductant such as 1-phenylethanol would fit into the proposed catalytic cycle, shown earlier.

Table 2: Screening of reducing agents

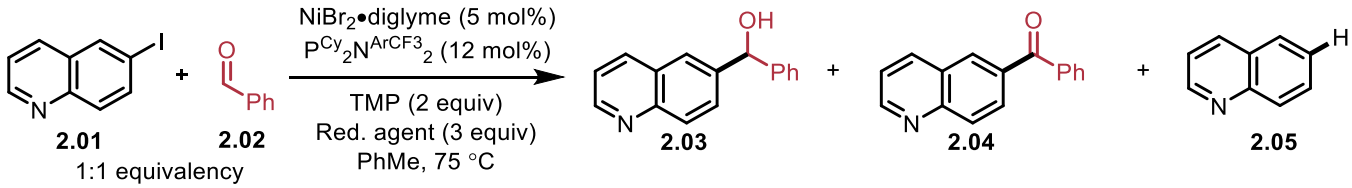

Entry	Reducing Agent	Yield 2.03[a]	Yield 2.04[a]	Yield 2.05[a]
1	1-phenylethanol	78%	Trace	0%
2	*sec*-butanol	52%	Trace	46%
3	2-PrOH	34%	Trace	47%
4	zinc	0%	14%	58%
5	HCO_2Na	Trace	8%	68%
6	H_2	0%	0%	86%

General conditions: aryl iodide (0.30 mmol), aldehyde (0.30 mmol), TMP (0.6 mmol), reducing agent (0.90 mmol), $NiBr_2$•diglyme (5 mol%), $P^{Cy_2}N^{ArCF_3{}_2}$ (12 mol%) in PhMe (0.40 M), 75 °C for 16 h, under inert atmosphere (set-up inside of the glovebox). [a]Yields are calculated by ^1H NMR with 1,3,5-trimethoxybenzene as the internal standard.

Scheme 30: Role of a secondary alcohol reductant in the 1,2-addition of aldehydes

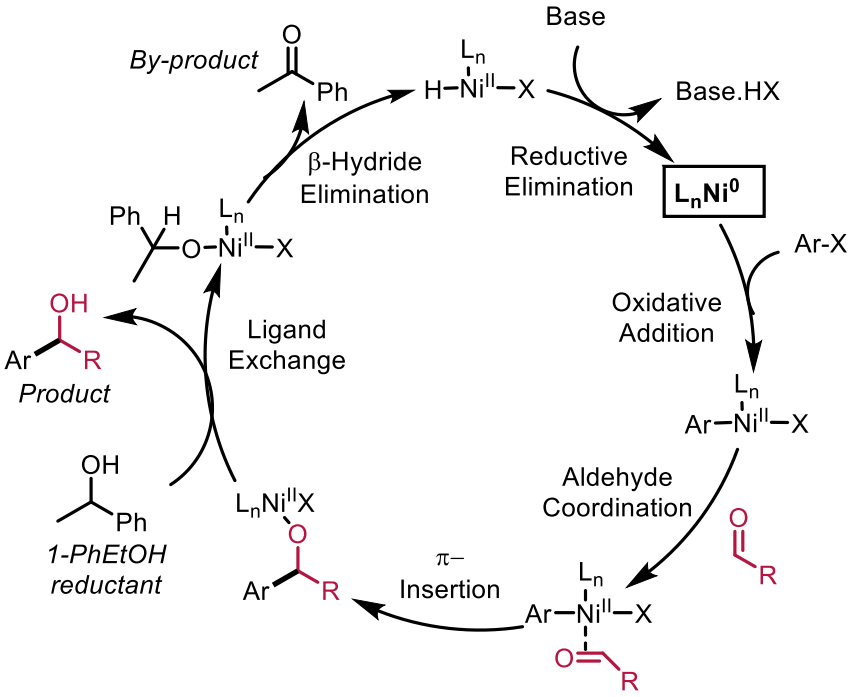

In order to further confirm the hypothesis that the ligand $P^{Cy_2}N^{ArCF3_2}$, is better than other commonly employed ligands in cross-coupling reactions, we also performed a screen comparing those ligands to $P^{Cy_2}N^{ArCF3_2}$ and $P^{Cy_2}N^{ArOMe_2}$, which represented the two P_2N_2 ligands possessing distinct electronic properties at the aniline fragment. **Table 3** summarizes this screen and clearly shows that the model ligand $P^{Cy_2}N^{ArCF3_2}$ (**entry 1**) gives the highest yield, while $P^{Cy_2}N^{ArOMe_2}$ (**entry 2**) gives a 13% yield of the desired alcohol **2.03**. Other ligands such as dppp, dppf, dcype, PCy_3 and IPr•HCl (**entries 3-7**) all only gave trace amounts of the product and majority of the mass balance was attributed to the dehalogenated quinoline side product **2.05**. In some cases, such as that for dppf (**entry 4**), we observed quantitative recovery of the starting material suggesting that this ligand

potentially prevents the oxidative-addition complex from reacting with benzaldehyde or the reducing agent.

Table 3: Comparison of P_2N_2 ligands with other ligands

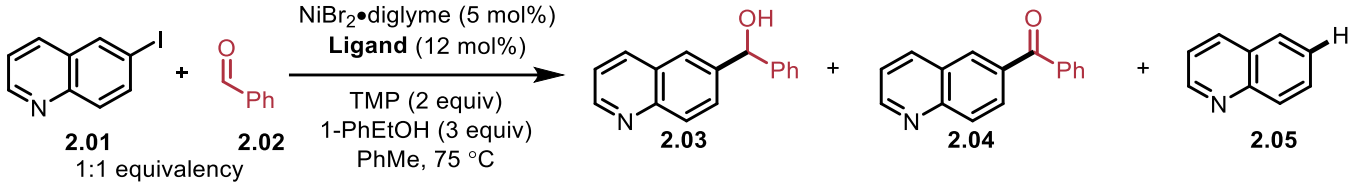

Entry	Ligand	Yield 2.03[a]	Yield 2.04[a]	Yield 2.05[a]
1	$P^{Cy}{}_2N^{ArCF3}{}_2$	78%	Trace	0%
2	$P^{Cy}{}_2N^{ArOMe}{}_2$	13%	0%	63%
3	dppp	5%	0%	53%
4	dppf	0%	0%	0%
5	dcype	0%	0%	85%
6	PCy_3 [b]	0%	Trace	88%
7	IPr•HCl	Trace	0%	81%

General conditions: aryl iodide (0.30 mmol), aldehyde (0.30 mmol), TMP (0.6 mmol), 1-phenylethanol (0.90 mmol), $NiBr_2$•diglyme (5 mol%), Ligand (12 mol%) in PhMe (0.40 M), 75 °C for 16 h, under inert atmosphere (set-up inside of the glovebox). [a]Yields are calculated by ^1H NMR with 1,3,5-trimethoxybenzene as the internal standard. [b]24 mol% of PCy_3 was added.

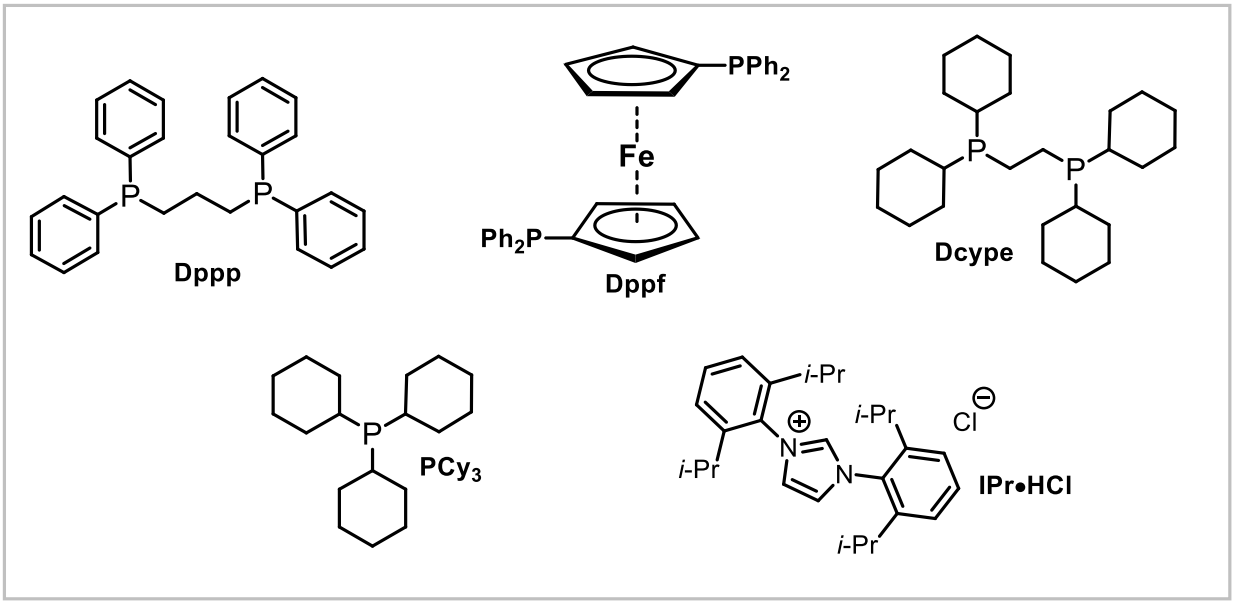

During the initial stages of optimization, prior to developing the conditions already described above, we identified 75 ºC to be the ideal temperature for this coupling. This was tested on 1-iodo-4-methoxy benzene (**2.06**) and 4-pyridine carboxaldehyde (**2.07**) as coupling partners under suboptimal conditions. However, soon after, we selected 6-iodoquinoline (**2.01**) and benzaldehyde (**2.02**) to be our model substrates because of data suggesting better reproducibility and slightly higher yields with these starting materials.

Although we screened temperatures under unoptimized conditions, the results later translated well to our optimized conditions and model substrates. It was interesting to note that the yields practically remained within a 10% range when the reaction was done at 65 ºC, 75 ºC and 85 ºC, giving the desired product **2.08** in 58%, 65% and 56% yield,

respectively (**entries 1-3**). This suggested that our yields were approximately within a ±5% error margin for these temperatures (**Table 4**).

Table 4: Temperature screen for coupling with 4-pyridine carboxaldehyde

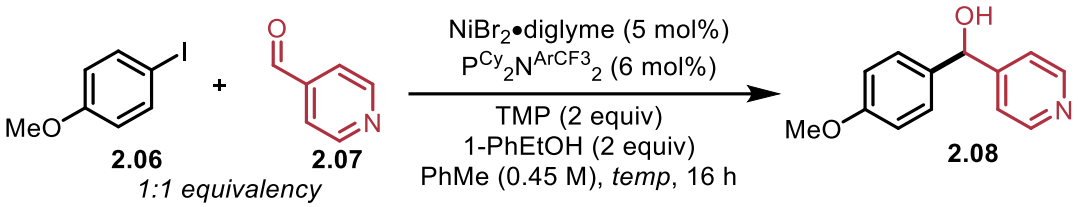

Entry	Temperature	Yield 2.08[a]
1	65 °C	58%
2	75 °C	65%
3	85 °C	56%

General reaction conditions: aryl iodide (0.15 mmol), aldehyde (0.15 mmol), TMP (0.30 mmol), 1-phenylethanol (0.30 mmol), $NiBr_2$•diglyme (5 mol%), $P^{Cy}{}_2N^{ArCF3}{}_2$ (6 mol%) in PhMe (0.45 M) at listed temperature for 16 h. [a]Crude NMR yield determined using 0.05 mmol 1,3,5-trimethoxybenzene as internal standard.

When we began exploring the 1,2-arylation of aldehydes and α-arylation of alcohols, TMP was chosen as the default base for screening but was not yet thoroughly validated as optimal. Base plays a very important role in these reactions, facilitating both formation of the metal-alkoxide in the first step of the catalytic cycle as well as reductive elimination of the H-[Ni^{II}]-X intermediate to provide nickel in its lowest oxidation state so it can oxidatively insert into the Ar-X bond. Therefore, to evaluate the effect of base, a targeted screen was carried out (**Table 5).**

Table 5: Screening of bases

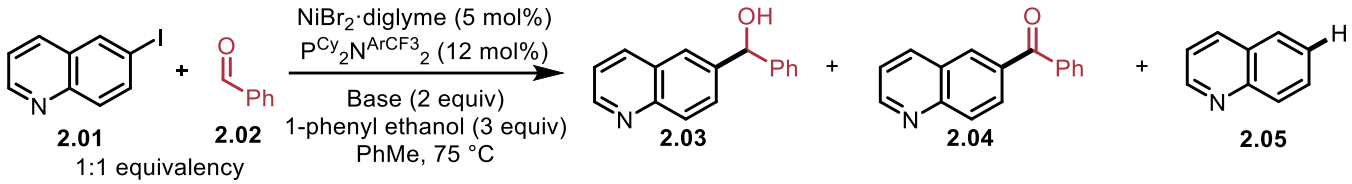

Entry	Base	Yield 2.03[a]	Yield 2.04[a]	Yield 2.05[a]
1	TMP	78%	Trace	0%
2	PMP	21%	20%	37%
3	DIPEA	Trace	29%	44%
4	Pyridine	0%	12%	50%
5	Triethylamine	Trace	10%	50%
6	K_3PO_4	0%	0%	0%

General conditions: aryl iodide (0.30 mmol), aldehyde (0.30 mmol), Base (0.6 mmol), 1-phenylethanol (0.90 mmol), $NiBr_2$•diglyme (5 mol%), $P^{Cy}{}_2N^{ArCF3}{}_2$ (12 mol%) in PhMe (0.40 M), 75 °C for 16 h, under inert atmosphere (set-up inside of the glovebox). [a]Yields are calculated by ^1H NMR with 1,3,5-trimethoxybenzene as the internal standard.

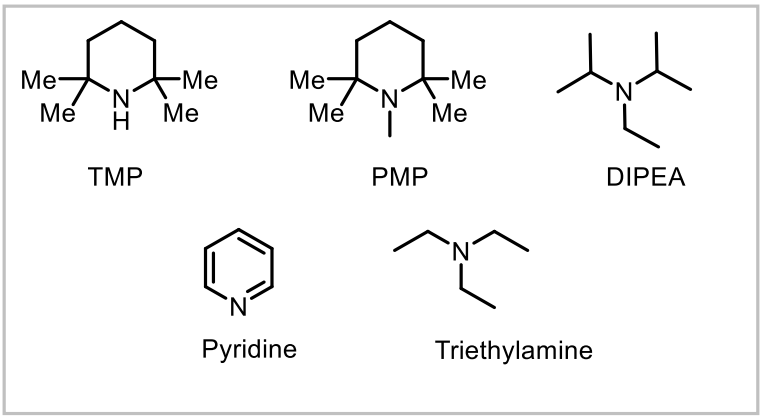

The table above demonstrates the base screen and clearly shows that under the optimized conditions, TMP (**entry 1**) gave exclusively the desired product whereas other amine bases such as PMP, DIPEA, pyridine and triethylamine (**entries 3-5**) gave very low yields or no product at all, providing up to a 50% yield of quinoline **2.05**. Inorganic bases

such as K_3PO_4 (**entry 6**) were also detrimental to the reaction outcome, allowing quantitative recovery of the starting material.

The base screen was essentially the last piece of the puzzle needed to convince us that we had reached a ceiling in our optimization efforts for the 1,2-arylation of aryl aldehydes. With the optimized conditions in hand (**Scheme 31**) we sought to determine if the reaction was also applicable to the 1,2-arylation of aliphatic aldehydes. However, this proved to be a lot more challenging, as will be discussed in Section 2.1.2.

Scheme 31: Optimized conditions for the 1,2-arylation of benzaldehyde derivatives

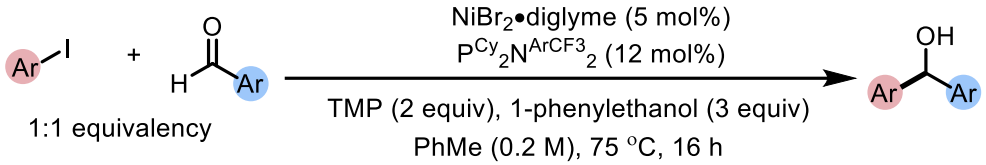

2.1.2: Coupling with aliphatic aldehydes

Section 2.1.1 disclosed our optimization efforts with benzaldehyde derivatives to obtain diaryl secondary alcohol products. Our attempts to access secondary benzylic alcohols via coupling between aryl iodides and linear, aliphatic aldehydes posed several challenges. One possible reason for this could be the presence of enolizable hydrogen

atoms α to the carbonyl which can often lead to the formation of side products via aldol condensation (**Scheme 32**).[55]

Scheme 32: Challenges in coupling with linear, aliphatic aldehydes

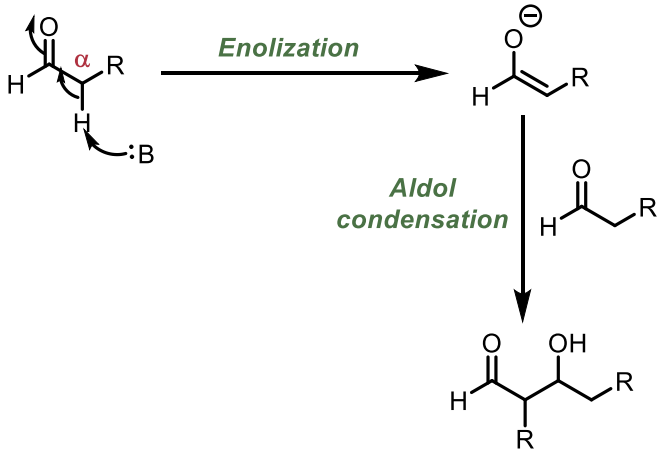

Unfortunately, the reaction conditions optimized for coupling with aryl aldehydes did not translate well to the aliphatic aldehydes. A preliminary scope exploration quickly revealed that these substrates were heavily dependent on the nature and electronics of the aryl iodide and seemed to give appreciable amounts of the redox-neutral ketone product and generally lower yields of the desired alcohol product (**Table 6**).

[55] Xiao, J.; Li, Z.; Montgomery, J. *J. Am. Chem. Soc.* **2021**, *142*, 21234.

Table 6: Alcohol:ketone ratio distribution with different aryl iodides

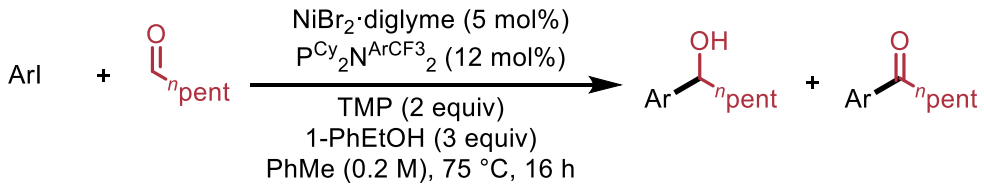

Entry	ArI	Yield alcohol[a]	Yield ketone[a]
1	1-iodonaphthalene	85%	trace
2	4-iodomethylbenzoate	63%	trace
3	2-methoxy-5-iodopyridine	53%	8%
4	1-iodo-3,4-methylenedioxy benzene	41%	8%
5	6-iodoquinoline	21%	4%

General reaction conditions: aryl iodide (0.30 mmol), aldehyde (0.30 mmol), TMP (0.6 mmol), 1-phenylethanol (0.90 mmol, $NiBr_2$•diglyme (5 mol%), $P^{Cy_2}N^{ArCF3_2}$ (12 mol%) in PhMe (0.20 M), 75 °C for 16 h. [a] Crude NMR yield determined using 0.05 mmol 1,3,5-trimethoxybenzene as internal standard.

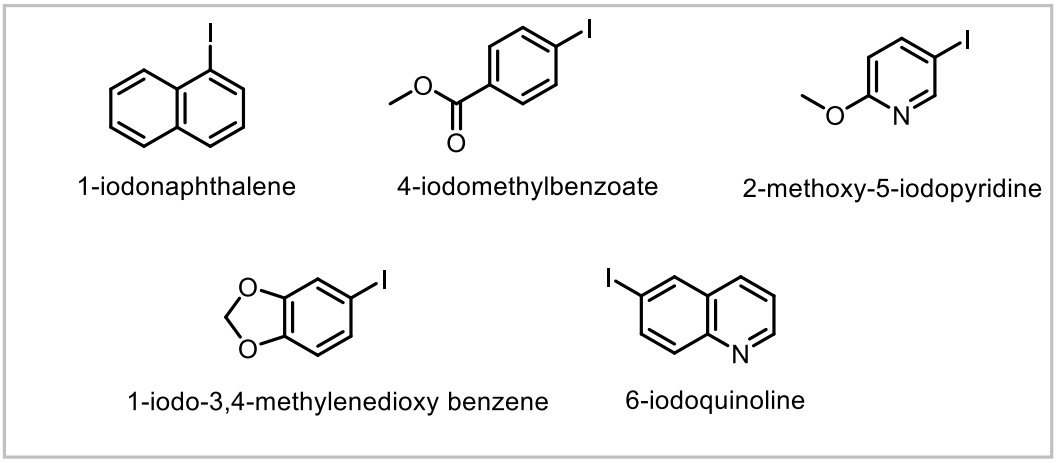

Hexanal was coupled with different aryl iodides that represented diverse electronics and was subjected to the reaction conditions optimized for aryl aldehydes. 1-

iodonapthalene gave the highest yield and trace amounts of the ketone product (**entry 1**). We quickly established that this was a biased aryl iodide and typically gave considerably higher yields and phenomenal selectivity with aliphatic aldehydes. The electron-deficient aryl iodide, 4-iodomethyl benzoate provided good selectivity and moderate yield of 63% (**entry 2**). It was generally seen that electron-rich aryl iodides gave lower yields and diminished selectivity for the alcohol product (**entries 3 and 4**).

Unexpectedly, 6-iodoquinoline, which was the model substrate used in the optimization experiments for aryl aldehydes, provided only a 21% yield of the desired alcohol and a 5:1 ratio of the alcohol to ketone product (**entry 5**). The results from this screen and several attempts made to expand the scope of aliphatic aldehydes were unsuccessful and we concluded that the scope for coupling with these aldehydes would be fairly limited. Therefore, it was recognized that these products may be better accessed via the redox-neutral pathway starting from a primary aliphatic alcohol (vide infra).

2.1.3: Selected optimization for the redox neutral α-arylation of primary aliphatic alcohols

With the conditions for the reductive 1,2-addition of aldehydes in hand, we next explored the redox-neutral α-arylation of primary alcohols (**Scheme 33**).

Scheme 33: General reaction for the redox-neutral α-arylation of primary alcohols

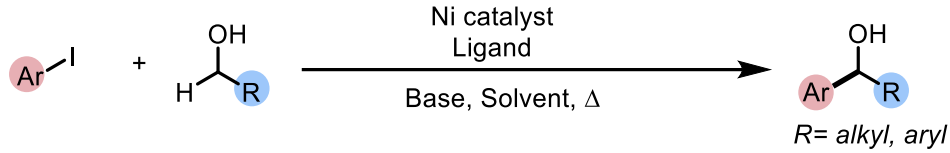

It was quite intriguing to discover that for this coupling we needed to have an excess of the primary alcohol starting material relative to the aryl iodide to ensure selectivity for the secondary alcohol product. Although extensive mechanistic experiments would be required to back this hypothesis, the dependence of the reaction on the stoichiometry of the alcohol could be related to proposed mechanism discussed in Section 2.1.1. Since an external reducing agent, such as the addition of 1-phenylethanol for the reductive 1,2-arylation of aldehydes, is not added in the redox-neutral coupling, we speculated that the primary alcohol reactant could serve as an "internal reductant". It could displace the functionalized secondary alcohol product (ligand exchange) from the Ni(II) center, and consequently turnover over the Ni(0) catalyst (**Scheme 34**). Thus, excess starting material would be required to generate the final product and to regenerate the active catalyst.

Scheme 34: Part of the proposed mechanism displaying the role of the primary alcohol reactant as an internal reductant

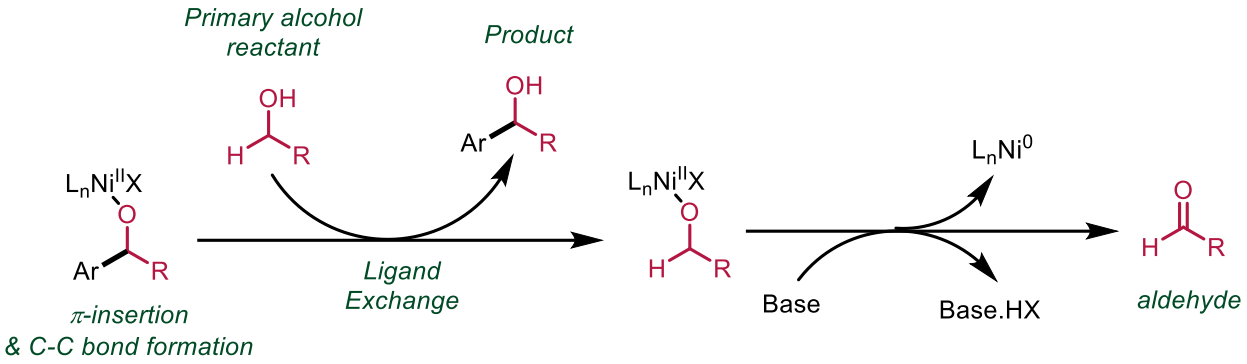

For this transformation, we adopted a combination approach, simultaneously optimizing for both primary benzylic and aliphatic alcohols, to avoid running into similar selectivity and transferability issues as we did for the aliphatic aldehyde coupling in Section 2.1.2. We first tested out the effect of the catalyst and ligand loading on the coupling between 1-iodo-3-trifluoromethyl benzene (**2.09**) and 1-octanol (**2.10**) while keeping all other parameters consistent with the aldehyde coupling conditions (**Table 7**). It should be noted that we later realized that these substrates gave considerably lower yields compared to the substrates that eventually became a part of our scope.

We found that 5 mol% of Ni and 12% of $P^{Cy_2}N^{ArCF3_2}$ resulted in a diminished yield of 33% for the desired product **2.11** and provided the ketone side product **2.12** in an 11% yield (**entry 1**). Doubling the catalyst loading to 10 mol% plummets the yield significantly because the ratio of catalyst to ligand is about 1:1.2 and we have previously found an

excess of the ligand to be highly beneficial (**entry 2**). When we added 3 times the amount of ligand relative to the nickel catalyst, we saw about a 30% jump in our yield providing alcohol **2.11** in a 50% yield (**entry 3**). We acknowledge that further investigation would be required to justify the large excess of the ligand required and we currently lack a solid hypothesis as to why this is the case.

Table 7: Catalyst and ligand loading for the redox-neutral α-arylation of primary aliphatic alcohols

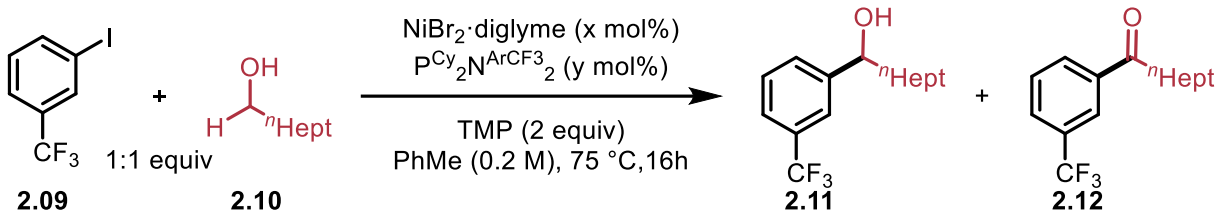

Entry	Catalyst loading (x mol%)	Ligand loading (y mol%)	Yield 2.11[a]	Yield 2.12[a]
1	5 mol%	12 mol%	33%	11%
2	10 mol%	12 mol%	20%	9%
3	10 mol%	30 mol%	50%	9%

General reaction conditions: aryl iodide (0.30 mmol), alcohol (0.30 mmol), TMP (0.6 mmol), $NiBr_2$•diglyme (x mol%), $P^{Cy}{}_2N^{ArCF3}{}_2$ (y mol%) in PhMe (0.20 M), 75 °C for 16 h. [a]Crude NMR yield determined using 0.05 mmol 1,3,5-trimethoxybenzene as internal standard.

We decided to carry on with 10 mol% loading of Ni(II) and 30 mol% loading of the $P^{Cy}{}_2N^{ArCF3}{}_2$ ligand for the primary alcohol arylation for subsequent experiments. Most of our optimization experiments featured 2.5 equivalents of the primary alcohol relative to the aryl iodide due to preliminary data that suggested it to be beneficial for the reaction yield and selectivity (**Table 8**). Increasing the equivalency of the alcohol from 1 equivalent

relative to the aryl iodide to 2.5 equivalents caused a significant increase in the yield for the desired alcohol **2.11** from 50% to 70% (**entries 1-3**) and <10% yield of the ketone side product **2.12**. Increasing the stoichiometry to 3 equivalents did not cause a large difference in the yield of the product (**entry 4**).

Table 8: Stoichiometry of alcohol

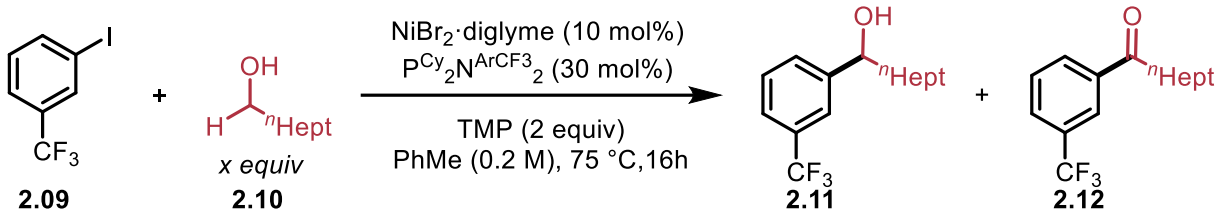

2.09 **2.10** **2.11** **2.12**

Entry	Stoichiometry of alcohol	Yield 2.11[a]	Yield 2.12[a]
1	1.0 equiv	50%	9%
2	2.0 equiv	61%	8%
3	2.5 equiv	70%	8%
4	3.0 equiv	73%	7%

General reaction conditions: aryl iodide (0.30 mmol), alcohol (x mmol), TMP (0.6 mmol), $NiBr_2$•diglyme (5 mol), $P^{Cy}{}_2N^{ArCF3}{}_2$ (12 mol%) in PhMe (0.20 M), 75 °C for 16 h. [a]Crude NMR yield determined using 0.05 mmol 1,3,5-trimethoxybenzene as internal standard.

We were satisfied with the yield and selectivity for coupling with primary aliphatic alcohols and were pleased to observe that significant modifications were not required from the conditions established in Section 2.1.1. Ultimately, the conditions described below (**Scheme 35**) were found to be optimal for the arylation of primary aliphatic and benzylic alcohols.

Scheme 35: Standard conditions for coupling between aryl iodides and primary alcohols

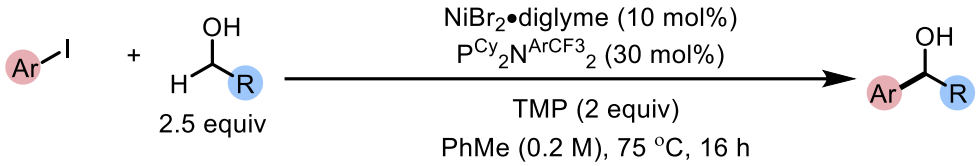

2.1.4: Selected optimization experiments for coupling with primary benzylic alcohols

The findings from the optimization experiments for aliphatic alcohols were further employed to primary benzylic alcohols. It was quickly realized that extensive optimization was not required for the α-arylation of primary benzylic alcohols, and we conducted a series of test experiments to further confirm this. **Table 9** summarizes some key deviations from the standard conditions that were subjected to the coupling between 1-iodo-3,4-methylenedioxybenzne (**2.13**) and benzyl alcohol (**2.14**).

Table 9: Optimization of the α-arylation of primary benzylic alcohols

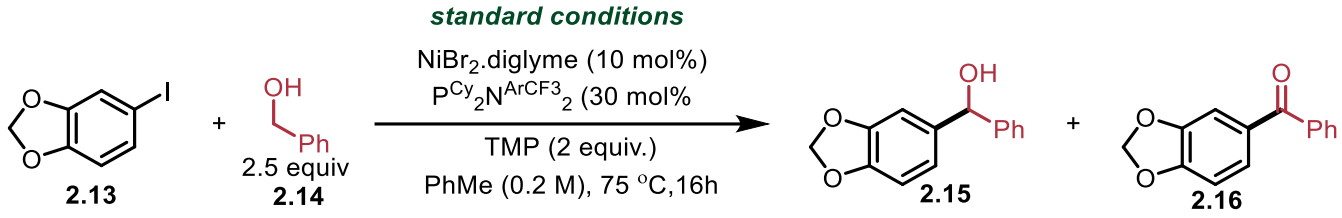

Entry	Deviation from standard conditions	Yield 2.15[a]	Yield 2.16[a]
1	None	75%	Trace
2	1.0 equivalent of **2.14**	74%	10%
3	2.0 equivalents of **2.13**	61%	25%
4	12 mol % $P^{Cy_2}N^{ArCF_3{}_2}$ instead of 30 mol %	8%	Trace
5	$P^{Cy_2}N^{ArOMe_2}$	30%	Trace
6	$P^{tBu_2}N^{ArCF_3{}_2}$	0%	0%
7	$P^{Ph_2}N^{ArCF_3{}_2}$	Trace	0%
8	NEt_3 as base	58%	Trace
9	Pyridine as base	0%	0%
10	5 mol % catalyst loading	64%	Trace

General reaction conditions: aryl iodide (0.30 mmol), alcohol (0.75 mmol), TMP (0.6 mmol), $NiBr_2$•diglyme (10 mol%), $P^{Cy_2}N^{ArCF_3{}_2}$ (30 mol%) in PhMe (0.20 M), 75 °C for 16 h. [a]Crude NMR yield determined using 0.05 mmol 1,3,5-trimethoxybenzene as internal standard.

Under the standard conditions, the yield for the desired secondary alcohol product **2.15** was 75% with only trace amounts of the ketone product **2.16** observed (**entry 1).** Although using 1 equivalent of the alcohol starting material (**2.14**) did not change the

yield of the desired product, a significant reduction in selectivity was observed, affording ketone **2.16** in a 10% yield (**entry 2**). Furthermore, using an excess of the aryl iodide depreciated the yield and selectivity for alcohol **2.15** even more, giving a ratio of about 2.5:1 for the alcohol to ketone product, **2.16** (**entry 3**). Other deviations from the base conditions such as using 12 mol % of the ligand $P^{Cy_2}N^{ArCF3_2}$ instead of 30 mol % (**entry 4**) or using a P_2N_2 ligand that is electron-rich at the nitrogen atom $P^{Cy_2}N^{ArOMe_2}$ (**entry 5**), resulted in drastic reductions of yield for alcohol **2.15**. When $P^{tBu_2}N^{ArCF3_2}$ and $P^{Ph_2}N^{ArCF3_2}$ were employed as ligands, little to no product was observed (**entries 6** and **7**).

This was quite an interesting observation and further supported the hypothesis that the substitution at the phosphorus atom had a vital role to play in the success of this transformation. As was observed in all our previous optimization experiments, TMP seemed to work best when compared to other nitrogen bases (**entries 8** and **9**). It was also reassuring to observe only a slight reduction in the yield to 64% of the desired product when using 5 mol % of the Ni catalyst (**entry 10**). Therefore, in the future, scalability of this method could be tested efficiently while keeping the metal loading lower, without detrimental effects on the yield.

2.2: Scope of arylation of aldehydes and primary alcohols

After we had confidently established our optimized conditions, our next course of action was to explore the scope and application of these methods to the synthesis of small

molecules. We simultaneously investigated the scope of both transformations, the 1,2-addition of aldehydes and α-arylation of primary alcohols and were pleased to see that conditions were well-tolerated for a wide range of electron neutral, electronic-rich, electron-deficient, and heterocyclic aryl iodide, aldehyde, and primary alcohol substrates. (**Tables 10** and **11**).

We were also able to extend our method to the synthesis of biologically relevant compounds such as cloridarol (**2.21**) which is a vasodilator and is often used as an experimental medication in the treatment of heart disease.[56] It was also interesting to observe that the coupling of quinoline and 4-bromobenzaldehyde gave us a 92% yield of the desired product **2.19**, without oxidative insertion into the C-Br bond. Coupling with aldehydes containing a highly strained cyclopropane ring (**2.24**), or labile benzylic hydrogens that could potentially undergo β-hydrogen elimination (**2.25**), also proceeded successfully.

[56] National Center for Biotechnology Information (2021). PubChem Compound Summary for CID 71132, *Cloridarol.* Retrieved November 1, 2021 from https://pubchem.ncbi.nlm.nih.gov/compound/Cloridarol.

Table 10: Scope and isolated yields for the reductive 1,2-addition of aldehydes

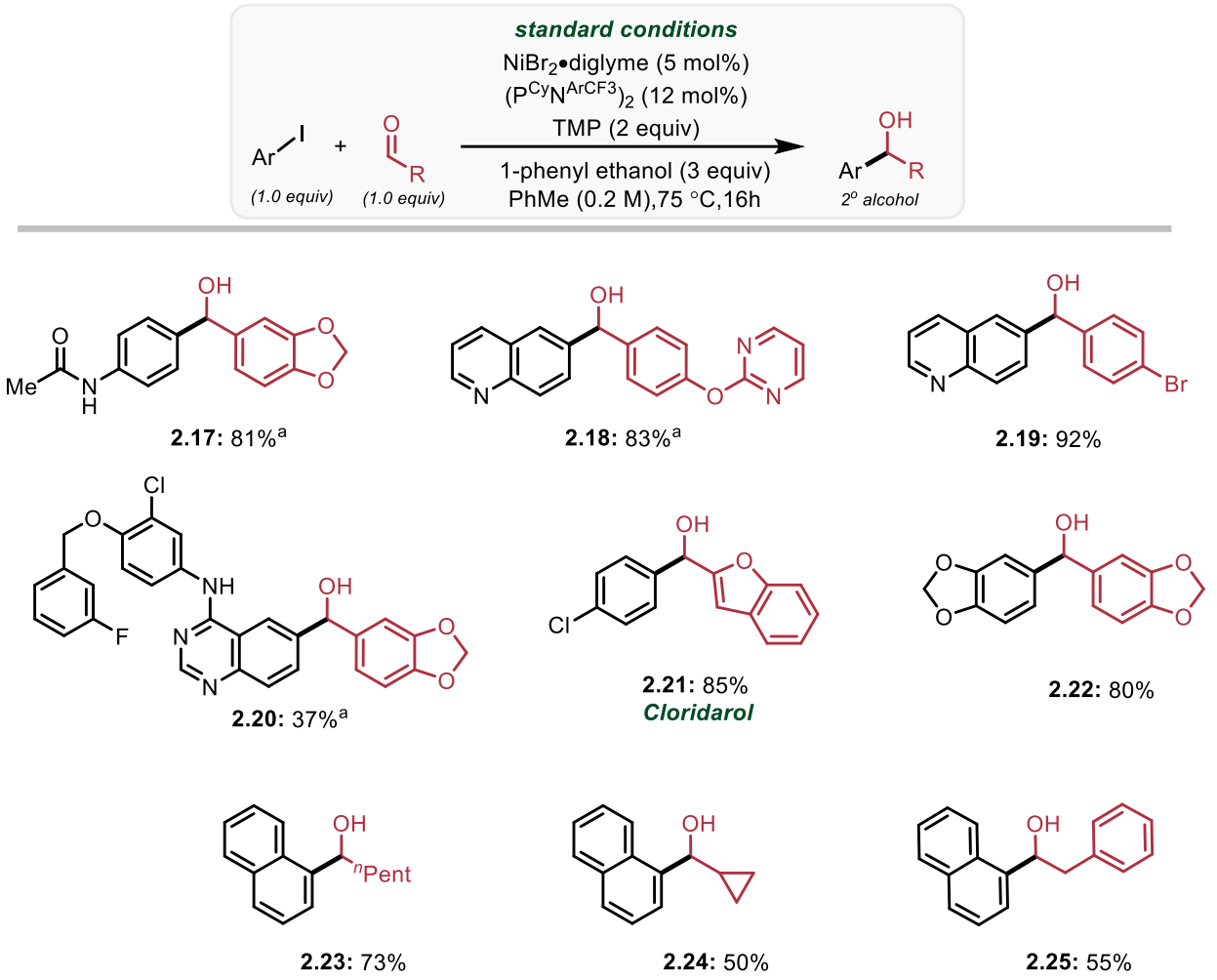

General reaction conditions: aryl iodide (0.30 mmol), aldehyde (0.30 mmol), TMP (0.6 mmol), 1-phenylethanol (0.90 mmol), $NiBr_2$•diglyme (5 mol%), $(P^{Cy}N^{ArCF3})_2$ (12 mol%) in PhMe (0.20 M), 75 °C for 16 h. [a] Compounds **2.17**, **2.18** and **2.20** were synthesised and isolated by Eric Isbrandt.

We were able to develop a very diverse scope when coupling aryl iodides and alcohols. Heteroaryl groups were incorporated effectively and gave up to a 75% yield (**2.26, 2.27, 2.28**) Generally, aliphatic alcohols were a lot more cooperative compared to aliphatic aldehydes. Strained 1-boc-azetidine-methanol (**2.35**) and cyclobutanemethanol (**2.36**) were tolerated exceptionally well, and the latter ended up being the model

substrate for coupling with various aryl iodides. Noteworthy examples from our alcohol scope also include coupling between 1-iodonapthalene and Tryptophol, which is a natural product derivative containing an unprotected indole functionality (**2.41**). In our attempt to synthesize compounds that could potentially be used as a handle for further modifications, we subjected 1-boc-azetidine-methanol and iodoloratidine, a derivative of an antihistamine medication, to our reaction conditions and were pleased to obtain the desired product in 52% isolated yield (**2.42**).

Table 11: Scope and isolated yields for the redox-neutral α-arylation of alcohol

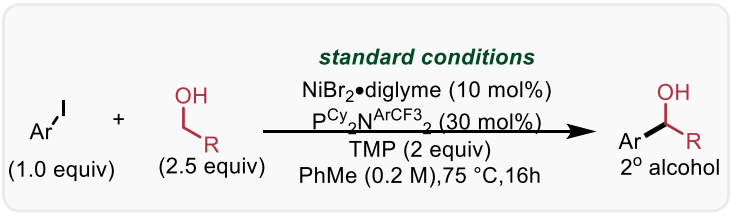

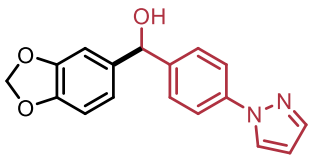

2.26: 66%[a]

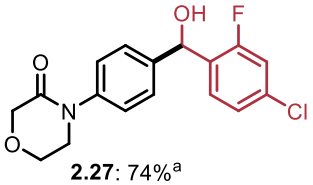

2.27: 74%[a]

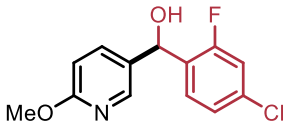

2.28: 66%[a]

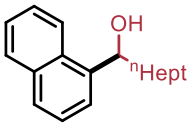

2.29: 68%

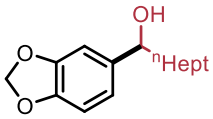

2.30: 75%

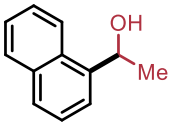

2.31: 68%

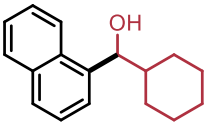

2.32: 78%

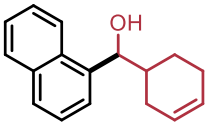

2.33: 42%
1.3:1 *dr*

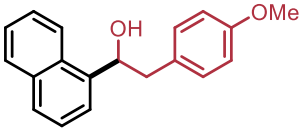

2.34: 85%

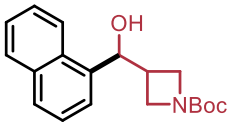

2.35: 73%

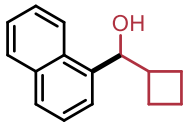

2.36: 83%

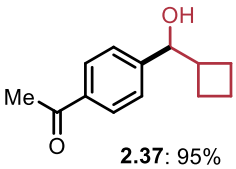

2.37: 95%

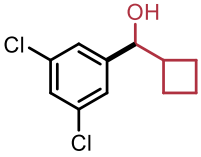

2.38: 86%

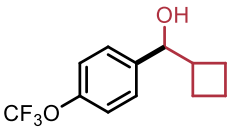

2.39: 70%

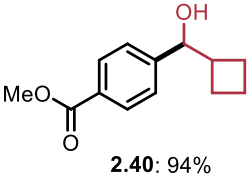

2.40: 94%

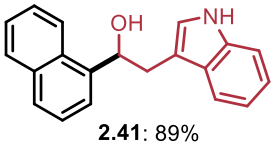

2.41: 89%
from *Tryptophol*

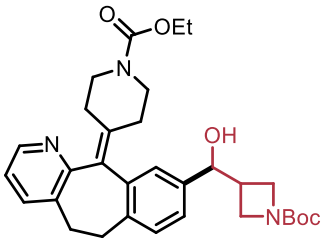

2.42: 52%
from *iodoloratidine*

General reaction conditions: aryl iodide (0.30 mmol), alcohol (0.75 mmol), TMP (0.6 mmol), $NiBr_2$•diglyme (10 mol%), ($P^{Cy}N^{ArCF3}$)$_2$ (30 mol%) in PhMe (0.20 M), 75 °C for 16 h. [a] Compounds 2.26, 2.27 and 2.28 were synthesised and isolated by colleague Eric Isbrandt

Along with our successful scope examples giving us moderate to high yields, we also experienced some scope limitations due to which many challenging substrates were not compatible with our optimized conditions (**Tables 12** and **13**). For coupling with aldehydes, we found that highly electron-deficient iodides (**2.43, 2.46, 2.49**) had detrimental effects on the yield. Ortho-hindered substrates such as 2-ethyliodo benzene (**2.45**) or 1,3,5-trimethyl benzaldehyde (**2.53**) were often less tolerated. Furthermore, potentially chelating substrates such as 2,6-dimethoxy iodobenzene (**2.52**) provided only trace products presumably due to catalyst deactivation.

Some products such as the one resulting from coupling between 4-pyridine carboxaldehyde and *N*-Boc-5-iodoindole (**2.48**), although obtained in a moderate yield, were excluded from our final scope due to rapid decomposition and challenging purification. Coupling with 4-iodobenzyl alcohol is also quite notable and chemo selectivity was observed towards the aldehyde starting material, albeit in a low yield. However, C-C coupling at the benzyl alcohol was not observed.

Table 12: Selected low-yielding couplings between aryl iodides and aldehydes

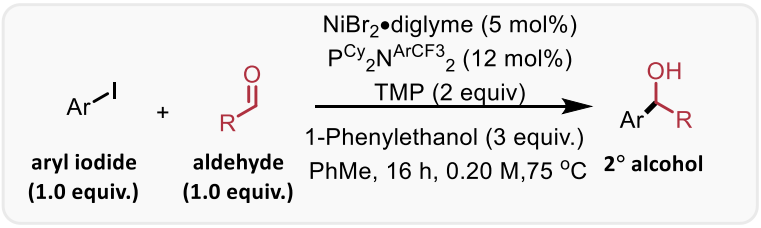

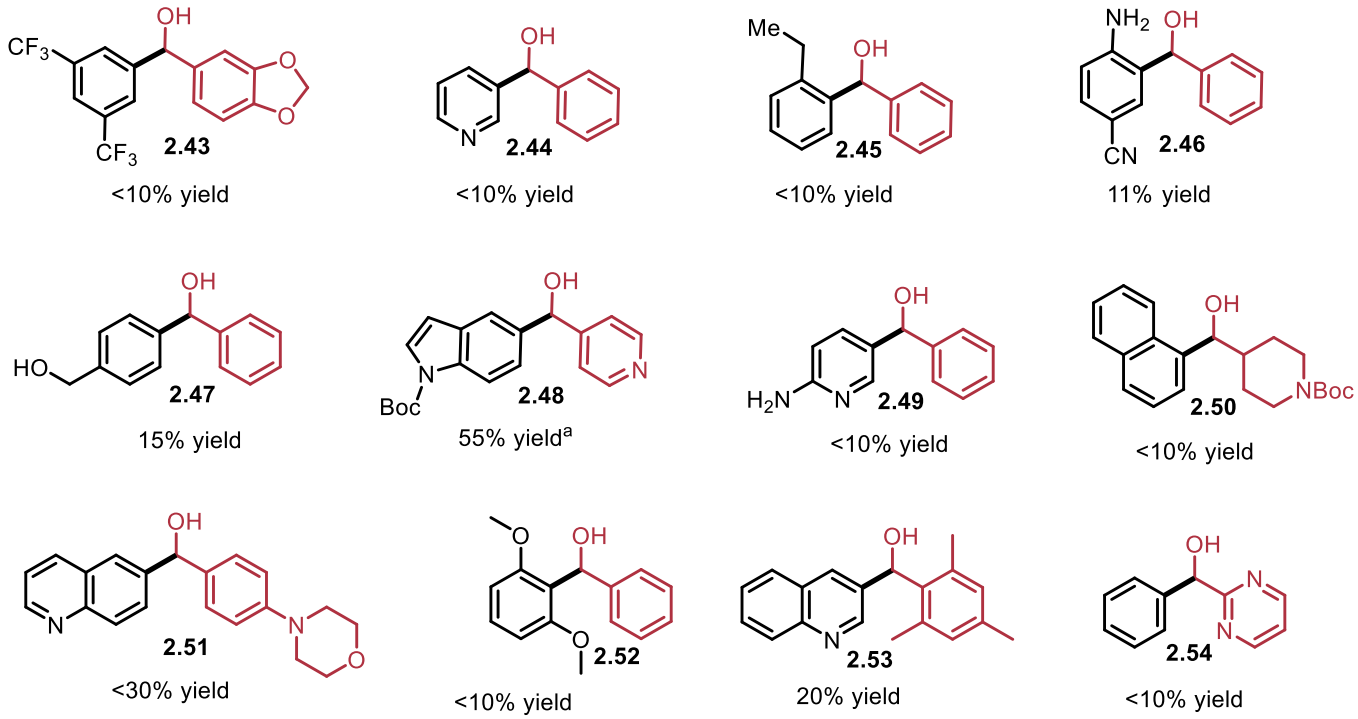

General reaction conditions: aryl iodide (0.30 mmol), aldehyde (0.30 mmol), TMP (0.6 mmol), 1-phenyl ethanol (0.90 mmol), $NiBr_2$•diglyme (5 mol%), $(P^{Cy}N^{ArCF3})_2$ (12 mol%) in PhMe (0.20 M), 75 °C for 16 h in an inert atmosphere. [a] Decomposes readily.

Coupling with aliphatic alcohols also posed significant challenges for some tough substrates. As was seen when coupling with aldehydes, highly electron-deficient aryl iodides such as 1,3-bistrifluoromethyl iodobenzene (**2.55**), N-(4-Iodophenyl) benzamide (**2.58**) or 4-iodoaniline (**2.59**) were incompatible with our standard conditions. Furthermore, aliphatic alcohols containing a distal heteroatom (**2.60, 2.61**) also proved

detrimental to the reaction outcome potentially due to the stable transition states that can be obtained via chelation with the metal, consequently occupying its coordination sites and making it unavailable for further catalysis. Difficult to oxidize aliphatic alcohols such as those containing C-F bonds (**2.63**, **2.64**, **2.65**) only gave the desired product in trace yields.

Table 13: Selected unsuccessful coupling between aryl iodides and aliphatic alcohols

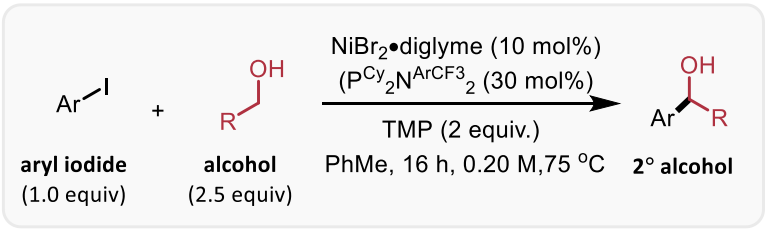

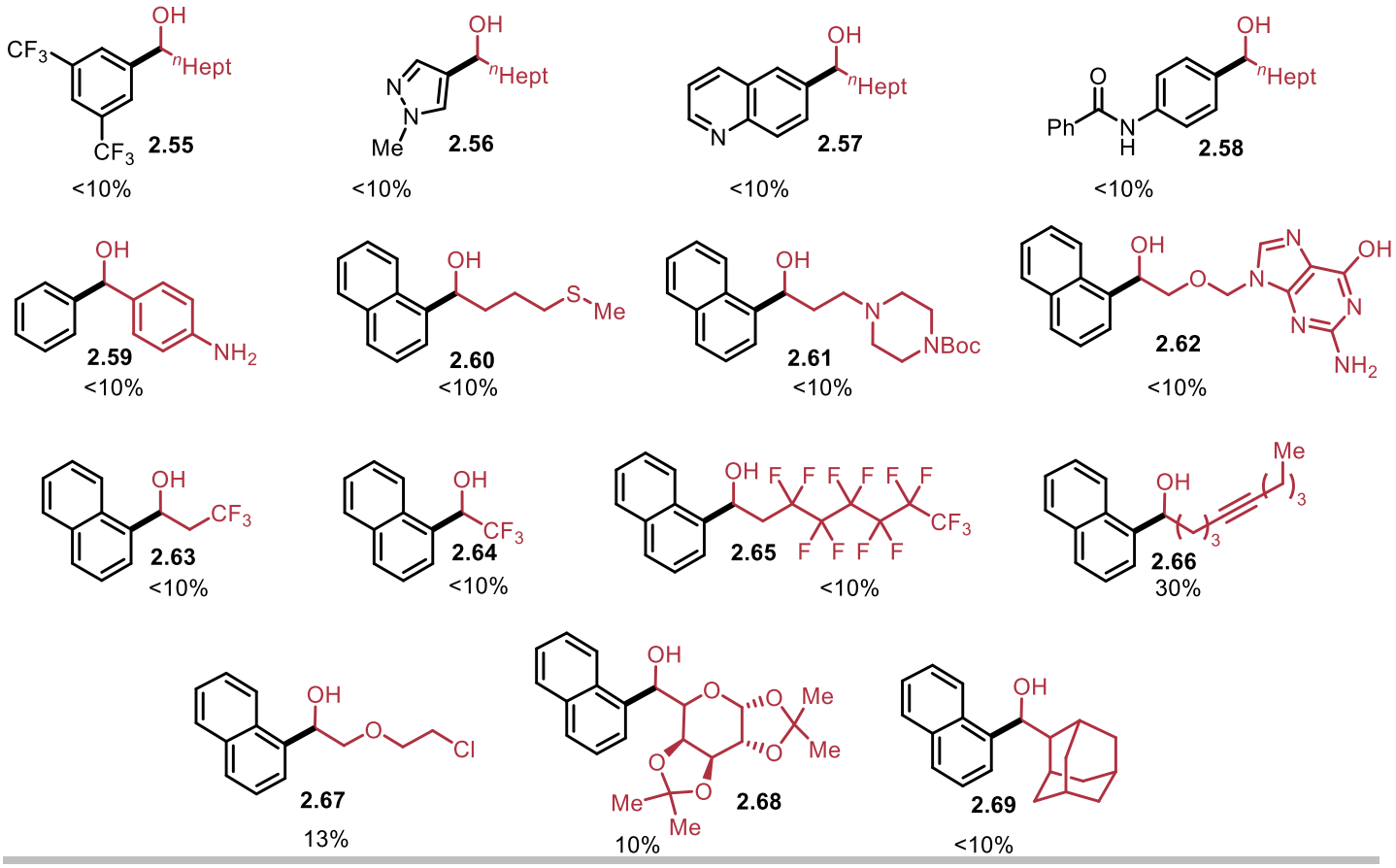

General reaction conditions: aryl iodide (0.30 mmol), alcohol (0.75 mmol), TMP (0.6 mmol), $NiBr_2$•diglyme (10 mol%), $P^{Cy}{}_2N^{ArCF3}{}_2$ (30 mol%) in PhMe (0.20 M), 75 °C for 16 h in an inert atmosphere

2.3: Summary and future work

Secondary benzylic alcohols are amongst the most desired and useful functional groups in organic synthesis. Alongside recent literature discussed in Chapter 1, our own work has demonstrated promise for a widely used method for addition onto carbonyls or direct addition onto alcohols to generate substituted alcohols. Although the research done in this area has been quite impactful, there is still much left to discover, and many questions remain unanswered. For instance, coupling with ketones and secondary alcohols to make tertiary alcohols is quite challenging and many methods that work for aldehydes and primary alcohols do not work for ketones and secondary alcohols (**Scheme 36**).

Scheme 36: Coupling with ketones and secondary alcohols

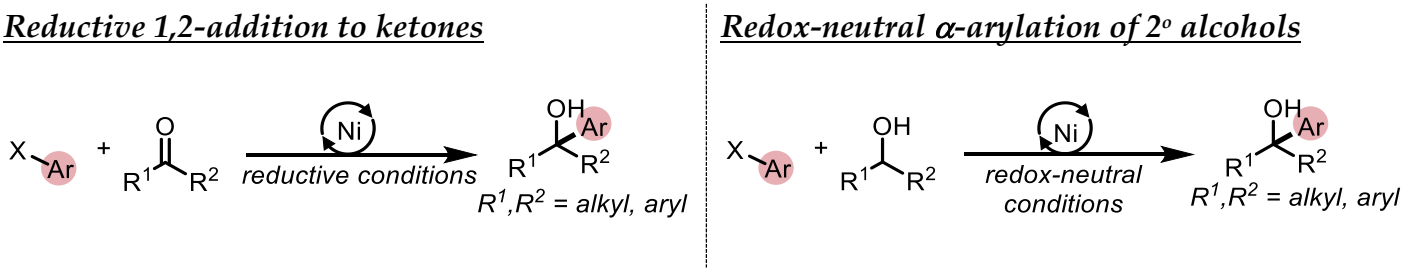

We briefly attempted to seek reactivity with ketones and secondary alcohols in a preliminary screen but soon realized that the hits we observed were specific to the substrate used and were not widespread (discussed briefly in Chapter 3). Initial testing revealed significant reproducibility issues, low yields, and functional group incompatibility. Therefore, the goal of future research projects will be to find a system

that would allow coupling with these challenging, sterically incumbered substrates to generate highly substituted and difficult to access tertiary alcohols.

Due to the importance of enantioselective synthesis in medicinal chemistry and drug discovery, asymmetric catalysis is always of interest to organic chemists. Some research groups have demonstrated success in synthesizing enantioselective secondary and tertiary alcohols via functionalization of carbonyls and alcohols.[57,58,59] However, it should be noted that most of these methods employ aryl boronic acids as nucleophiles and enantioselective arylation using aryl halides is still quite underexplored. It would be interesting to delve into the possibility of using nickel in enantioselective coupling to generate highly useful alcohol products from carbonyls or racemic alcohols (**Scheme 37**).

[57] Lainer, B.; Lichosyt, D.; Aleksandrova, M.; Dydio, P. *J. Org. Chem.* **2021**, *86*, 9253.
[58] Molander, G.A., Wisniewski, S.R. *J. Am. Chem. Soc.* **2012**, 134, 16856.
[59] Cai, Y.; Shi, S.-L. *J. Am. Chem. Soc.,* **2021**, *143*, 11963.

Scheme 37: Enantioselective coupling with carbonyls and alcohols to generate enantiopure substituted alcohols

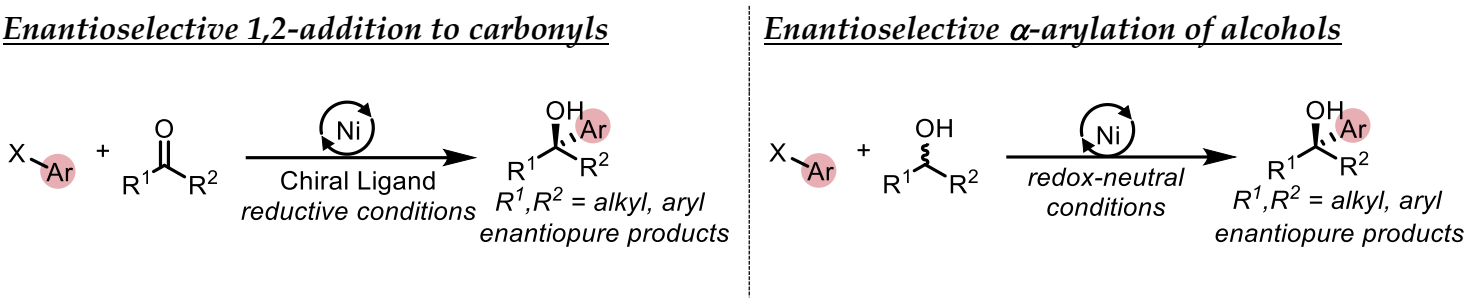

In our group, we have yet to explore chiral P_2N_2 ligands and how they might behave in this transformation. This could also be a potential future area to take a closer look at. Although reports of using these ligands in cross-coupling reactions are non-existent, Karasik *et al.* demonstrated their use in transition-metal catalyzed co-polymerization reactions. They modulated the chirality of the ligand at the amine fragment of the diazadiphosphacyclooctane ring (**Scheme 38**).[60]

Scheme 38: Synthesis of a chiral P_2N_2 ligand

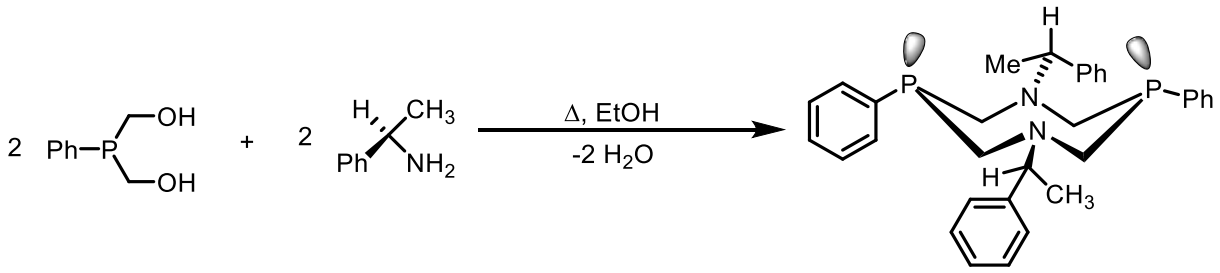

[60] Karasik, A. A.; Naumov, R. N.; Sinyashin, O. G.; Belov, G. P.; Novikova, H. V.; Lönnecke, P.; Hey-Hawkins, E. *Dalton Trans.* **2003**, No. 11, 2209–2214.

Through our optimization efforts and extensive scope exploration, we successfully designed a nickel-catalyzed strategy for the reductive coupling of aryl halides with aldehydes and redox-neutral coupling with primary alcohols. A striking feature of this research endeavour, and one that the group had been working to establish for a while, was that the mild conditions could be applied to couple with both, an aldehyde, and an alcohol without significant modifications to the standard conditions. All in all, we demonstrated an efficient strategy to access synthetically useful small molecules which can be further extended to functionalize biologically relevant compounds.

2.4: Experimental

2.4.1: General experimental details

Unless otherwise indicated, reactions were conducted under an atmosphere of nitrogen in 8 mL screw-capped vials that were oven dried (120 °C) or flame dried and shipped into a glovebox. Column chromatography was performed manually using Silicycle F60 40−63 μm silica gel. Analytical thin layer chromatography (TLC) was conducted with aluminum backed EMD Millipore Silica Gel 60 F_{254} pre-coated plates. Visualization of developed plates was performed under UV light (254 nm). For certain purifications, cerium ammonium molybdate (CAM) or potassium permanganate ($KMnO_4$) stains were used to better visualize the compounds on the TLC plates.

2.4.2: Instrumentation

^{1}H NMR and ^{13}C NMR were recorded on a Bruker AVANCEII 300 MHz spectrometer, a Bruker AVANCEII 400 MHz spectrometer, or a Bruker AVANCEIII 500 MHz spectrometer. ^{1}H NMR spectra were internally referenced to the residual solvent signal (e.g., $CDCl_3$ = 7.27 ppm). ^{13}C NMR spectra were internally referenced to the residual solvent signal (e.g., $CDCl_3$ = 77.00 ppm). Data for ^{1}H NMR are reported as follows: chemical shift (δ ppm), multiplicity (s = singlet, d = doublet, t = triplet, q = quartet, m = multiplet), coupling constant (Hz), integration. NMR yields for optimization studies were obtained by ^{1}H NMR analysis of the crude reaction mixture using 1,3,5-trimethoxybenzene as an internal standard. IR spectra were obtained using a Cary 630 FTIR (Agilent Technologies) and are reported in terms of frequency of absorption (cm^{-1}). Melting point ranges were determined on a Canlab Gallen Kamp Melting Point Apparatus. Accurate mass data (EI) was obtained from an Agilent 5977A GC/MSD using MassWorks 4.0 from CERNO Bioscience. HRMS data was obtained from a Micromass Q-TOF 2 quadrupole – time-of-flight mass spectrometer with ESI source.

Note: After completion and publication of some of the data described below, it was noticed that the error (in ppm) of several of the Accurate Mass measurements was too large to allow conclusive confirmation of the proposed molecular formula. We regret this mistake. We are still confident in the conclusions made in the data for the following reasons:

1) the fact that all molecules previously reported matched the literature.
2) Some functional groups are not amenable to MS accurate analysis and have lower than normal spectral accuracy (aliphatic compounds, boron containing compounds and polyhalogenated groups).
3) The instrument might not have been tuned when the samples were run, or they might have been too dilute for accurate analysis.

2.4.3: Materials

Organic solvents were purified by rigorous degassing with nitrogen before passing through a PureSolv solvent purification system. Low water content was confirmed by Karl Fischer titration (<25 ppm for all solvents). Unless otherwise noted, reagents were used as received. $NiBr_2$•diglyme was purchased from Sigma Aldrich. Phenylphosphine was obtained as a 10% wt. solution in hexanes from Sigma Aldrich. Cyclohexylphosphine, isobutylphosphine and tertbutylphosphine were generously donated from Cytec-Solvay as neat liquids. Monophosphines were stored and used in the glovebox to avoid any reaction with oxygen. Commercial ligands were purchased from Sigma Aldrich, Combi-Blocks, and Strem Chemicals. 2,2,6,6-Tetramethylpiperidine (TMP) (99%) was obtained from Combi-Blocks. 1-Phenylethanol was purchased Sigma-Aldrich (98%) or Acros Organics (97%) with no discernable difference between suppliers. Unless otherwise noted, all other commercially available starting materials were obtained from Sigma-Aldrich, TCI America, Fisher Scientific, Acros Organics, Alfa Aesar, Combi-Blocks, or Oakwood Chemicals and used as received.

Initial diazadiphosphacyclooctane (P_2N_2) tests were performed from generous donations of ligand from Pacific Northwest National Laboratory (PNNL) and the Blacquière research group (Western University). Subsequently, all P_2N_2 ligands were synthesized in-house using the procedure disclosed below. Anhydrous reagent alcohol (90% ethanol, 5% methanol and 5% isopropyl alcohol), obtained from Sigma-Aldrich (≤0.005% water), was found to be an inexpensive alternative to anhydrous absolute ethanol for ligand synthesis.

2.4.4: General Procedure for the Synthesis of P_2N_2 ligands

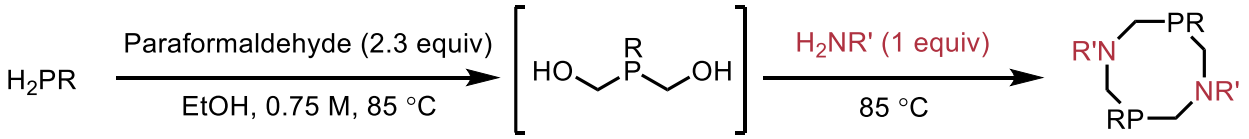

General procedure for the synthesis of P_2N_2 ligands with $(P^{Cy}N^{ArCF3})_2$ as a representative example: A 200 mL Chemglass heavy wall round bottom pressure vessel (CG-1880-R) and stir bar were oven dried (120 °C) and immediately shipped into the glovebox. In the glovebox, paraformaldehyde (powder, 95%, Sigma Aldrich; 4.61 g, 152 mmol) was added to the flask followed by cyclohexylphosphine (8.8 mL, 66 mmol). The reaction slurry was diluted with ~40 mL of anhydrous reagent alcohol (Sigma Aldrich), sealed and shipped out of the glovebox. The reaction was heated at 85 °C overnight, during which the viscous slurry turned into a clear, homogeneous, liquid. The reaction flask was allowed to cool and then shipped back into the glovebox. 4-Aminobenzotrifluoride (8.3 mL, 66 mmol) was added to the stirring solution portionwise (~1 mL per portion). The reaction was again removed from the glovebox and heated at 85 °C for 24 hours, during which a creamy white solid precipitated out of the solution. The flask was shipped back into the glovebox and diluted with acetonitrile (40 mL). The mixture was stored overnight in the glovebox freezer (-20 °C) to induce further crystallization and subsequently filtered using a fritted funnel in the glovebox. Crude solid was washed with HPLC-grade hexanes (15

mL) followed by large volumes of acetonitrile (total volume ~100 mL). The remaining white solid was removed from the glovebox and residual solvent was removed *in vacuo*. The purity of the resulting powder was assessed by NMR spectroscopy for all relevant nuclei (e.g. ^{1}H,^{13}C, ^{19}F, ^{31}P) by dissolving the sample ($CDCl_3$) with a screw-capped NMR tube under inert atmosphere. 18.8 g of white solid was obtained (94% isolated yield based on theoretical yield of 33 mmol).

Safety note: Monophosphines are highly flammable, pyrophoric, pungent, and toxic compounds that are readily oxidized. They should *always* be handled under inert atmosphere. All glassware and equipment that comes in contact with the monophosphine should be sealed in an air-tight container and subsequently quenched with a bleach bath. After sitting overnight, the glassware is rinsed with water a few times to remove any residual bleach. Afterwards, organic solvent can be used to finish the cleaning process. Monophosphines also tend to have a powerful lasting stench – any spills should be quickly cleaned up and disposed of safely. If the glassware is properly quenched and cleaned, there should be no stench.

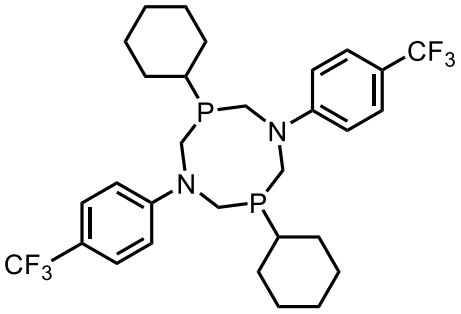

1,5-bis(*p*-benzotrifluoride)-3,7-bis(cyclohexyl)-1,5,3,7-diazadiphosphacyclooctane **$(P^{Cy}N^{ArCF3})_2$** was prepared according to the general procedure on a 33 mmol scale (66 mmol of starting materials). **$(P^{Cy}N^{ArCF3})_2$** was isolated as a creamy off-white solid (18.8 g, 94% yield). **^{1}H NMR** ($CDCl_3$, 500 MHz) δ 7.45 (d, J = 8.7 Hz, 2.95H), 7.41 (d, J = 8.7 Hz, 3.84H), 6.91 (d, J = 8.7 Hz, 2.98H), 6.67 (d, J = 8.8 Hz, 3.99H), 4.35 (t, J = 13.9 Hz, 4.11H), 3.99 (dq, J = 14.4 Hz, 1.68Hz, 3.01H), 3.74 (t, J = 14.4 Hz, 3.04H), 3.60 (dd, J = 15.1 Hz, 4.85Hz, 4H), 2.02-1.68 (m, 20.17H), 1.67-1.60 (m, 2.14H), 1.52-1.27 (m, 18.67H). **^{13}C NMR** ($CDCl_3$, 126 MHz) δ 151.4, 147.8, 126.3-126.2 (m), 125.1 (q, J = 270.3 Hz), 124.9 (q, J = 270.3 Hz), 118.8

(q, *J* = 32.7 Hz), 117.9(q, *J* = 32.7 Hz), 112.7 (t, *J* = 2.2 Hz), 111.7 (t, *J* = 3.1 Hz), 55.4, 55.2, 49.2 (d, *J* = 6.7 Hz), 49.1 (d, *J* = 6.7 Hz), 29.8 (d, *J* = 12.2 Hz), 29.2 (d, *J* = 10.5 Hz), 27.0 (d, *J* = 8.6 Hz), 26.7 (d, *J* = 9.7 Hz), 26.3-26.2 (m). **^{19}F NMR** ($CDCl_3$, 470 MHz) δ -60.9, -61.1. **^{31}P{^{1}H} NMR** ($CDCl_3$, 202 MHz) δ –27.9, -39.3. **Note**: This compound was previously reported in the primary literature as two conformers in the ^{31}P spectra but one conformer in the ^{1}H.[61] Our NMR sample displayed two conformers (major previously reported and minor unreported) in approximately 3:2 ratio with some overlapping peaks in the aliphatic region of the ^{1}H spectrum.

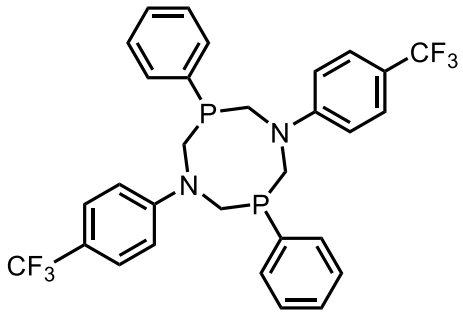

1,5-bis(*p*-benzotrifluoride)-3,7-bis(phenyl)-1,5,3,7-diazadiphosphacyclooctane ($P^{Ph}N^{ArCF3})_2$ was prepared according to the general procedure on a 2.5 mmol scale (5 mmol of starting materials). Crude solid was filtered and subsequently purified by rinsing impurities away with hexanes and MeCN. **($P^{Ph}N^{ArCF3})_2$** was isolated as a white solid (0.594 g, 40% yield). **^{1}H NMR** (C_6D_6, 300 MHz) δ 7.66-7.65 (m, 4H), 7.56-7.55 (m, 6H), 7.48 (d, *J* = 8.8 Hz, 4H), 6.78 (d, *J* = 8.8 Hz, 4H), 4.51 (t, *J* =, 13.9 Hz, 4H), 4.10 (dd, *J* = 14.9 Hz, 4.8 Hz, 4H). **^{19}F NMR** (C_6D_6, 282 MHz) δ -61.1. **^{31}P{^{1}H} NMR** (C_6D_6, 121 MHz) δ -48.9. Spectral data matches previous reported characterization of **($P^{Ph}N^{ArCF3})_2$**.[62]

[61] Seu, C. S.; Appel, A. M.; Doud, M. D.; DuBois, D. L.; Kubiak, C. P. *Energy Environ. Sci.* **2012**, *5*, 6480-6490.
[62] Kilgore, U.J.; Roberts, J. A. S.; Pool, D. H.; Appel, A. M.; Stewart, M. P.; DuBois, M. R.; Dougherty, W. G.; Kassel, W. S.; Bullock, R. M.; DuBois, D. L. *J. Am. Chem. Soc.* **2011**, *133*, 5861-5872.

2.4.5: General Procedure for the reductive coupling of aryl iodides with aldehydes

Inside the glovebox, to a dry 8 mL screw-capped reaction vial equipped with a magnetic stir bar, Ni source (0.05 equiv, 0.015 mmol) and ligand (0.12 equiv, 0.036 mmol) were added and dissolved in the reaction solvent (1.5 mL). Base (2 equiv, 0.6 mmol), aryl halide (1 equiv, 0.3 mmol), and aldehyde (1 equiv, 0.3 mmol) were added to the stirring solution followed by the reducing agent (3 equiv, 0.9 mmol). The vial was capped, removed from the glovebox, and placed in a stirring (350 rpm) pre-heated mineral oil bath at 75 °C. After stirring for 16 hours, the reaction vial was removed from the oil bath and cooled down to room temperature. For optimization experiments, 1,3,5-Trimethoxybenzene (0.05 mmol) was added as an internal standard and the mixture was diluted with ethyl acetate. The reaction was filtered through a plug of silica gel with thin layers of sodium sulfate and celite at the bottom of the frit. For very polar products, a mixture of ethyl acetate and acetone was used to flush the compound off the silica gel. The filtrate was diluted to an appropriate concentration and analyzed by GC-MS. Solvent was removed *in vacuo* and the crude sample was analyzed with NMR spectroscopy. For scope examples, the sample was dry loaded onto silica by diluting with DCM, drying *in vacuo*, and then purifying by column chromatography.

2.4.6: General Procedure for the redox-neutral coupling of aryl iodides with primary alcohols

Inside the glovebox, to a dry 8 mL screw-capped reaction vial equipped with a magnetic stir bar, Ni source (0.10 equiv, 0.030 mmol) and ligand (0.30 equiv, 0.090 mmol) were added and dissolved in the reaction (1.5 mL). Base (2 equiv, 0.6 mmol), aryl halide (1 equiv, 0.3 mmol), and alcohol (2.5 equiv, 0.75 mmol) were added to the stirring solution. The vial was capped, removed from the glovebox, and placed in a stirring (350 rpm) pre-heated mineral oil bath at 75 °C. After stirring for 16 hours, the reaction vial was removed from the oil bath and cooled down to room temperature. For optimization experiments, 1,3,5-Trimethoxybenzene (0.05 mmol) was added as an internal standard and the mixture

was diluted with ethyl acetate. The reaction was filtered through a plug of silica gel with thin layers of sodium sulfate and celite at the bottom of the frit. For very polar products, a mixture of ethyl acetate and acetone was used to flush the compound off the silica gel. The filtrate was diluted to an appropriate concentration and analyzed by GC-MS. Solvent was removed *in vacuo* and the crude sample was analyzed with NMR spectroscopy. For scope examples, the sample was dry loaded onto silica by diluting with DCM, drying *in vacuo*, and then purifying by column chromatography.

2.4.7: Characterization for the reductive coupling of aryl iodides and aldehydes

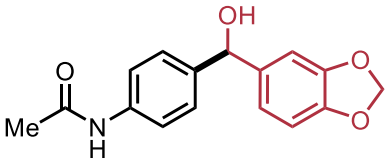

N-[4-[Hydroxy(1,3-Benzodioxol-5-yl)methyl]phenyl]acetamide (2.17) was prepared according to the general procedure. The product was purified by column chromatography with 15% to 75% EtOAc in hexanes to afford **2.17** as a white solid (69.2 mg, 81% yield). **^{1}H NMR** (CD_3OD, 400 MHz) δ 7.49 (d, J = 8.5 Hz, 2H), 7.28 (d, J = 8.5 Hz, 2H), 6.84-6.75 (m, 2H), 5.87 (d, J = 1.3 Hz, 1H), 5.65 (s, 1H), 2.09 (s, 3H). **^{13}C NMR** (CD_3OD, 100 MHz) δ 171.6, 149.2, 148.3, 139.4, 139.0, 137.5, 128.2, 121.6, 121.0, 108.8, 108.2, 102.3, 85.7, 23.8. **FT-IR ν (cm^{-1})** 3264, 3195, 3124, 3060, 2888, 1664, 1600, 1529, 1501, 1484, 1439, 1405, 1369, 1313, 1234, 1175, 1118, 1091, 1032, 965, 923, 844, 799, 777, 714, 678. **Melting point** 75 °C (dec.) **HRMS (ESI-TOF)** m/z calc'd for $C_{16}H_{15}NO_4Na$ $[M+Na]^+$ Theoretical: 308.0899. Found: 308.1414.

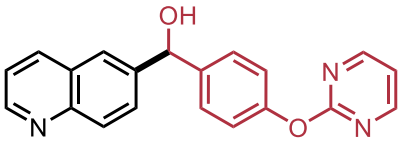

(4-(2-pyrimidinyloxy)phenyl)(6-quinolinyl)methanol (2.18) was prepared according to a modified general procedure. Prior to purification by column chromatography, the crude product in DCM was washed with NH_4Cl (aq). The product was purified by column chromatography with 25% to 50% acetone in PhMe to afford **2.18** as an off-white solid (81.3 mg, 83% yield). **^{1}H NMR** ($(CD_3)_2SO$, 400 MHz) δ 8.86 (dd, J =

4.2 Hz, 1.6 Hz, 1H), 8.60 (d, *J* = 4.8 Hz, 2H), 8.37 (dd, *J* = 8.4 Hz, 1.0 Hz, 1H), 8.06 (d, *J* = 1.4 Hz, 1H), 7.97 (d, *J* = 8.7 Hz, 2H), 7.77 (dd, *J* = 8.8 Hz, 1.8 Hz, 1H), 7.53-7.47 (m, 3H), 7.22 (t, *J* = 8.8 Hz, 1H), 7.16 -7.12 (m, 2H), 6.22 (d, *J* = 3.2 Hz, 1H), 5.97 (d, *J* = 3.6 Hz, 1H). **^{13}C NMR** ($(CD_3)_2SO$, 100 MHz) δ 164.8, 159.9, 151.6, 150.2, 147.1, 143.7, 142.2, 136.0, 128.9, 128.4, 127.7, 127.6, 124.2, 121.6, 121.4, 116.8, 73.6. **FT-IR ν (cm^{-1})** 3241, 3046, 1568, 1499, 1411, 1399, 1353, 1316, 1288, 1228, 1197, 1152, 1111, 1048, 1020, 992, 923, 902, 865, 809, 787, 749, 729, 662. **Melting point** 167 °C. **Accurate Mass (EI)** $C_{20}H_{15}N_3O_2$ Theoretical: 329.1159. Found: 329.1213. Spectral Accuracy: 97.0%

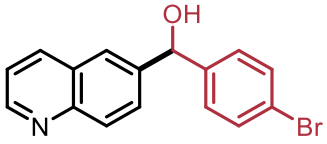

(4-bromophenyl)-quinolin-6-ylmethanol (2.19), was prepared according to the general procedure. The fractions were collected using a solvent system of 50% Acetone in Toluene to afford **2.19** as a white solid (87 mg, 92% yield). **^{1}H NMR** ($(CD_3)_2SO$, 400 MHz) δ 8.85 (dd, *J* = 5.8 Hz, 2.6 Hz, 1H), 8.35 (d, *J* = 7.7 Hz, 1H), 7.98 (broad s, 1H), 7.93 (d, *J* = 8.7 Hz, 1H), 7.68 (dd, *J* = 8.7 Hz, 1.8 Hz, 1H), 7.52 – 7.29 (m, 3H), 7.38 (d, *J* = 8.4 Hz, 1H), 6.21 (d, *J* = 3.9 Hz, 1H), 5.90 (d, *J* = 3.8 Hz, 1H). **^{13}C NMR** ($(CD_3)_2SO$, 100 MHz) δ 150.7, 147.6, 145.1, 143.7, 136.5, 131.6, 129.4, 128.8, 128.1, 124.9, 122.1, 73.8. **Melting point** 169 – 171 ^{0}C **FT-IR**: ν (cm^{-1}) 3080, 2924, 1579, 1502, 1323, 1147, 1118, 1069, 1012, 891, 809, 771, 736. **Accurate mass (EI):** $H_{12}C_{16}NOBr$ Theoretical: 313.0102. Found: 313.0097. Spectral Accuracy: 98.0%.

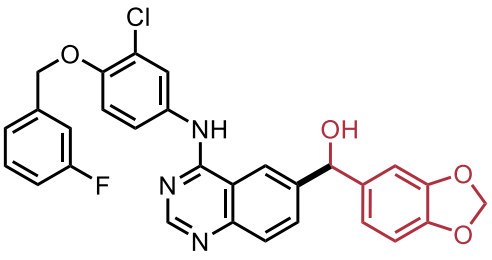

N-[3-Chloro-4-(3-fluorobenzyloxy)phenyl]-6-[Hydroxy(1,3-Benzodioxol-5-yl)methyl]quinazolin-4-amine (2.20) was prepared according to the general procedure. The product was purified by column chromatography with 0.5% to 2.5% of MeOH in 0.5% trimethylamine and DCM to afford a brown solid (containing amine impurities).

Compound was further purified with a second column of 50% EtOAc in Hexanes to 100% EtOAc to afford **2.20** as a white solid (60.2 mg, 37% yield). **^{1}H NMR** ($(CD_3)_2SO$, 400 MHz) δ 9.85 (s, 1H), 8.60 (d, J = 1.1 Hz, 1H), 8.54 (s, 1H), 8.02 (d, J = 2.6 Hz, 1H), 7.78-7.74 (m, 2H), 7.69 (d, J = 8.6 Hz, 1H), 7.47(td, J = 8.0 Hz, 6.0 Hz, 1H), 7.35-7.30 (m, 2H), 7.27 (d, J = 9.0 Hz, 1H), 7.21-7.15 (m, 1H), 7.00 (d, J = 1.6 Hz, 1H), 6.92 (dd, J = 8.1 Hz, 1.6 Hz, 1H), 6.84 (d, J = 8.0 Hz, 1H), 6.14 (d, J = 3.6 Hz, 1H), 5.96 (dd, J = 5.9 Hz, 0.9 Hz, 2H), 5.81 (J = 3.6 Hz, 1H), 5.26 (s, 2H). **^{13}C NMR** ($(CD_3)_2SO$, 100 MHz) δ 162.2 (d, J = 243.6 Hz), 157.6, 154.1, 149.2, 148.8, 147.2, 146.1, 144.0, 139.7 (d, J = 7.4 Hz), 139.4, 133.2, 131.5, 130.5 (d, J = 8.2 Hz), 127.6, 124.2, 123.3 (d, J = 2.7 Hz), 122.4, 121.0, 119.6, 119.2, 114.7 (d, J = 20.9 Hz), 114.6, 114.2, 114.0 (d, J = 21.9 Hz), 107.9, 106.8, 100.8, 74.1, 69.4 (d, J = 1.6 Hz). **^{19}F NMR** ($(CD_3)_2SO$, 325 MHz) -113.06. **FT-IR ν (cm^{-1})** 3318, 3061, 2886, 2692, 1603, 1571, 1536, 1497, 1424, 1391, 1364, 1331, 1309, 1282, 1252, 1234, 1215, 1145, 1092, 1057, 1040, 1003, 954, 947, 889, 861, 844, 818, 779, 749, 708, 686. **Melting point** 191 °C **HRMS (ESI-TOF)** m/z calc'd for $C_{29}H_{22}N_3O_4ClF$ $[M+H]^+$ Theoretical: 530.1283 Found: 530.1270.

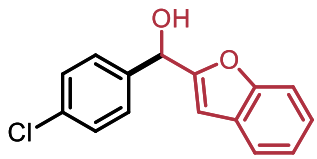

α-(4-Chlorophenyl)-2-benzofuranmethanol (2.21) was prepared according to the general procedure. The product was purified by column chromatography with 9% ether in PhMe to afford **2.21** as a yellow oil (66.0 mg, 85% yield). **^{1}H NMR** ($CDCl_3$, 400 MHz) δ 7.51-7.49 (m, 1H), 7.43-7.39 (m, 3H), 7.36-7.33 (m, 2H), 7.28-7.18 (m, 2H), 6.50 (s, 1H), 5.90 (s, 1H), 2.63 (br s, 1H). **^{13}C NMR** ($CDCl_3$, 100 MHz) δ 158.0, 155.1, 138.7, 128.8, 128.2, 127.9, 124.6, 122.9 121.3, 111.4, 104.2, 69.9. Characterization of **2.21** matched previously reported spectra.[63]

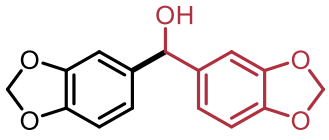

(1,3-benzodioxol-5-yl)-1,3-benzodioxole-5-methanol (2.22) was prepared according to the general procedure.

[63] Mongin, F.; Bucher, A.; Bazureau, J. P.; Bayh, O.; Awad, H.; Trécourt, F. *Tet. Lett.* **2005**, *46*, 7989-7992.

The product was purified by column chromatography with 5% to 10% acetone in PhMe to afford **2.22** as a colorless oil (65.3 mg, 80% yield). **^{1}H NMR** ($CDCl_3$, 400 MHz) δ 6.85-6.81 (m, 4H), 6.78-6.75 (m, 2H), 5.94 (s, 4H), 5.68 (s, 1H), 2.15 (br s, 1H). **^{13}C NMR** ($CDCl_3$, 100 MHz) δ 147.8, 146.9, 138.0, 119.8, 108.1, 107.0, 101.1, 75.8. Characterization of **2.22** matched previously reported spectra.[64]

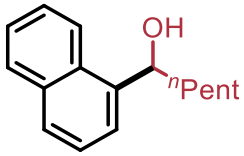

1-(naphthalen-1-yl)hexan-1-ol (2.23) was prepared according to the general procedure. The product was purified by column chromatography with 9% EtOAc in hexanes to afford **2.23** as a colourless oil (40 mg, 85% yield). **^{1}H NMR** ($CDCl_3$, 400 MHz) δ 8.10 (d, J = 8.1 Hz, 1H), 7.87 (d, J = 7.7 Hz, 1H), 7.76 (d, J = 8.2 Hz, 1H), 7.63 (d, J = 7.0 Hz, 1H), 7.53-7.44 (m, 3H), 5.45 (dd, J = 8.1 Hz, 3.0 Hz, 1H), 1.99-1.83 (m, 3H), 1.59-1.48 (m, 1H), 1.47-1.39 (m, 1H), 1.35-1.28 (m, 4H), 0.88 (t, J = 6.8 Hz, 3H). **^{13}C NMR** ($CDCl_3$, 100 MHz) δ 140.7, 133.9, 130.5, 128.9, 127.9, 125.9, 125.5, 125.4, 123.2, 122.8, 71.4, 38.4, 31.8, 25.9, 22.7, 14.1. Characterization of **2.23** matched previously reported spectra.[65]

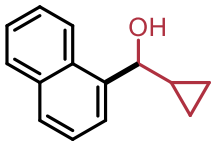

Cyclopropyl(naphthalen-1-yl)methanol (2.24) was prepared according to the general procedure. The product was purified by column chromatography with 10% to 20% EtOAc in hexanes to afford **2.24** as a colorless oil (30 mg, 50% yield). **^{1}H NMR** ($CDCl_3$, 400 MHz) δ 8.27 (d, J = 8.2 Hz, 1H), 7.89-7.87 (m, 1H), 7.82 (d, J = 8.2 Hz, 1H), 7.70 (d, J = 7.0 Hz, 1H), 7.56-7.47 (m, 3H), 4.88 (d, J = 7.8 Hz, 1H), 1.61-1.52 (m, 1H), 0.75-0.68 (m, 1H), 0.61-0.49 (m, 2H), 0.43-0.37 (m, 1H). **^{13}C NMR** ($CDCl_3$, 100 MHz) δ 138.9, 133.9, 131.1, 128.8, 128.2, 126.0, 125.6, 125.4, 124.0, 123.9, 75.1, 17.7, 3.99, 2.84. Characterization of **2.24** matched previously reported spectra.[66]

---

[64] Betschmann, P.; Sahli, S.; Diederich, F.; Obst, U.; Gramlich, V. *Helv. Chim. Acta.* **2002**, *85*, 1210-1245.
[65] Tanaka, K.; Thomihama, M.; Yamamoto, K.; Matsubara, N.; Harada, T. *J. Org. Chem.* **2018**, *83*, 6127-6132.
[66] Shibata, T.; Tabira, H.; Soai, K. *J. Org. Chem.* **2018**, *83*, 6127-6132.

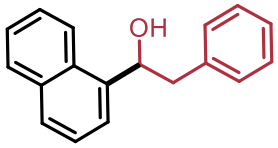

1-(α-naphthyl)-2-phenylethanol (2.25) was prepared according to the general procedure. Title compound was sensitive to acid, so the silica was neutralized with NEt_3 and dried. Compound was dry-loaded with celite. The product was purified by column chromatography with 0% to 15% EtOAc in hexanes to afford **2.25** as a white solid (41.3 mg, 55% yield). **^{1}H NMR** ($CDCl_3$, 400 MHz) δ 8.18 (d, J = 6.7 Hz, 1H), 7.91 (d, J = 6.5 Hz, 1H), 7.81 (d, J = 6.8 Hz, 1H), 7.69 (d, J = 5.1 Hz, 1H), 7.59-7.46 (m, 3H), 7.39-7.25 (m, 5H), 5.70 (d, J = 5.9 Hz, 1H), 3.31 (d, J = 12.9 Hz, 1H), 3.08 (t, J = 10.6 Hz, 1H), 1.90 (br s, 1H). **^{13}C NMR** ($CDCl_3$, 100 MHz) δ 139.4, 138.5, 133.8, 130.2, 129.5, 129.0, 128.6, 128.1, 126.7, 126.1, 125.5, 125.4, 123.0, 122.9, 72.1, 45.1. Characterization of **2.25** matched previously reported spectra.[67]

2.4.8: Characterization for the redox-neutral coupling of aryl iodides and primary alcohols

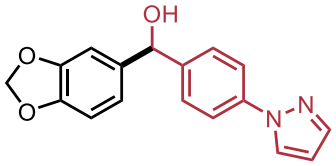

2H-1,3-benzodioxol-5-yl(4-(1H-Pyrazol-1-yl)phenyl)methanol (2.26) was prepared according to the general procedure. The product was purified by column chromatography with 5% to 7.5% acetone in PhMe to afford **2.26** as a clear oil (57.9 mg, 66% yield).**^{1}H NMR** ($CDCl_3$, 400 MHz) δ 7.88 (d, J = 2.4 Hz, 1H), 7.70 (d, J = 1.6 Hz, 1H), 7.61 (d, J = 8.4 Hz, 2H), 7.40 (d, J = 8.6 Hz, 2H), 6.85-6.81 (m, 2H), 6.77-6.74 (m, 1H), 6.45 (t, J = 2.1 Hz, 1H), 5.92 (q, J = 1.3 Hz, 2H), 5.76 (s, 1H), 2.91 (br, s, 1H). **^{13}C NMR** ($CDCl_3$, 100 MHz) δ 147.8, 147.0, 142.2, 141.0, 139.3, 137.8, 127.4, 126.8, 120.0, 119.2, 108.1, 107.5, 107.1, 101.0, 75.3. **FT-IR ν (cm^{-1})** 3344, 2893, 1607, 1500, 1473, 1413, 1329, 1228, 1204, 1150, 1105, 1072, 1031, 930, 854, 828, 775, 688. **Accurate mass (EI)**: $H_{14}C_{17}N_2O_3$ Theoretical: 294.0999. Found: 294.0961. Spectral Accuracy: 98.4%.

---

[67] Kišić, A.; Michel, S.; Mohar, B. *Org. Lett.* **2013**, *15*, 1614-1617.

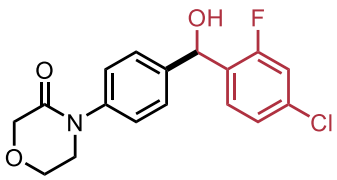

4-[4-(hydroxymethyl(α-(4-chloro-2-fluorophenyl))phenyl]-3-Morpholinone (2.27) was prepared according to the general procedure. The product was purified by column chromatography with 20% acetone in PhMe to afford an orange oil. A second column was run with 50% to 100% EtOAc in Hexanes to afford **2.27** as a colourless oil (74.5 mg, 74% yield).**^{1}H NMR** ($CDCl_3$, 400 MHz) δ 7.45 (t, J = 8.2 Hz, 1H), 7.38 (d, J = 8.5 Hz, 2H), 7.26 (d, J = 8.5 Hz, 2H), 7.13 (dd, J = 1.8 Hz, 8.5 Hz, 1H), 7.04 (dd, J = 2.0 Hz, 10.0 Hz, 1H), 5.99 (s, 1H), 4.28 (s, 2H), 4.01-3.97 (m, 2H), 3.73-3.69 (m, 2H), 3.22 (br, s, 1H). **^{13}C NMR** ($CDCl_3$, 100 MHz) δ 166.8, 159.3 (d, J = 250.0 Hz), 141.5, 140.5, 133.9 (d, J = 10.3 Hz), 129.6 (d, J = 13.4 Hz), 128.4 (d, J = 5.0 Hz), 127.2, 125.4, 124.7 (d, J = 3.5 Hz), 166.0 (d, J = 25.2 Hz), 68.7 (d, J = 2.8 Hz), 68.4, 64.0, 49.5. **^{19}F NMR** ($CDCl_3$, 100 MHz) δ -115.9. **FT-IR ν (cm^{-1})** 3370, 2869, 2246, 1646, 1607, 1579, 1508, 1482, 1409, 1325, 1237, 1219, 1178, 1124, 1070, 1040, 1016, 995, 921, 897, 856, 820, 794, 727, 680. **Accurate mass (EI)** $H_{15}C_{17}ClFNO_3$ Theoretical: 335.0719. Found: 335.0690. Spectral Accuracy: 96.7%.

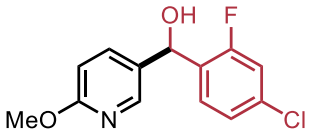

α-(4-chloro-2-fluorophenyl)-6-methoxy-3-Pyridinemethanol (2.28) was prepared according to the general procedure. The product was purified by column chromatography with 2.5% to 8.5% acetone in PhMe to afford **2.28** as a dark oil (52.7 mg, 66% yield).**^{1}H NMR** ($CDCl_3$, 400 MHz) δ 8.13 (d, J = 1.9 Hz, 1 H), 7.57-7.49 (m, 2H), 7.17 (dd, J = 1.4 Hz, 8.3 Hz, 1H), 7.05 (dd, J = 2.0 Hz, 10.0 Hz, 1H), 6.71 (d, J = 8.6 Hz, 1H), 6.04 (s, 1H), 3.91 (s, 3H), 2.60 (br, s, 1H). **^{13}C NMR** ($CDCl_3$, 100 MHz) δ 163.8, 159.3 (d, J = 250.0 Hz), 145.0, 137.2, 134.2 (d, J = 10.4 Hz), 130.7, 129.2 (d, J = 13.1 Hz), 128.0 (d, J = 4.8 Hz), 124.8 (d, J = 3.6 Hz), 116.2 (d, J = 24.9 Hz), 111.0, 67.3 (d, J = 3.0 Hz), 53.6. **^{19}F NMR** δ -115.8. **FT-IR ν (cm^{-1})** 3335, 2947, 2037, 1708, 1607, 1579, 1484, 1393, 1316, 1281, 1221, 1126, 1074, 1022, 897, 857, 824, 805, 785, 733, 675. **Accurate mass (EI)** $H_{11}C_{13}ClFNO_2$ Theoretical: 267.0457. Found: 267.0437. Spectral Accuracy: 98.8%

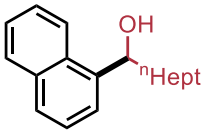

1-(naphthalen-5-yl)octan-1-ol (2.29) was prepared according to the general procedure. The product was purified by column chromatography with 10% EtOAc in hexanes to afford **2.29** as a colourless oil (52.3 mg, 68% yield). **^{1}H NMR** ($CDCl_3$, 400 MHz) δ 8.14 (m, 1H), 7.89 (m, 1H), 7.79 (m, 1H), 7.65 (m, 1H), 7.56-7.47 (m, 3H), 5.46 (dd, J = 7.9, 3.0 Hz, 1H), 2.07 (br s, 1H), 1.99-1.86 (m, 2H), 1.62-1.45 (m, 1H), 1.49-1.41 (m, 1H), 1.39-1.24 (m, 1H), 1.39-1.24 (m, 1H), 0.90 (t, J = 6.9 Hz, 3H). **^{13}C NMR** ($CDCl_3$, 100 MHz) δ 140.7, 133.9, 130.5, 128.9, 127.9, 125.9, 125.5, 125.4, 123.2, 122.8, 71.4, 38.4, 31.9, 29.6, 29.3, 26.3, 22.7, 14.1. Characterization of **2.29** matched previously reported spectra.[68]

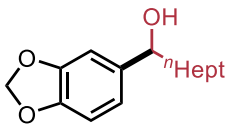

1-benzo[1,3]dioxol-5-yl-octan-1-ol (2.30) was prepared according a modified procedure. The crude reaction mixture was reduced with $NaBH_4$ and worked up as described in the literature.[69] The mixture was purified using column chromatography and the fractions were collected using a solvent system of 15% EtOAc in Hexanes to afford **2.30** as a colourless oil (56.3 mg, 75% yield). **^{1}H NMR** (($CDCl_3$, 400 MHz) δ 6.86 (s, 1H), 6.79-6.74 (m, 2H), 4.57 (t, J = 7.0 Hz, 1H), 1.94 (br s, 1H), 1.82-1.73 (m, 1H), 1.69-1.62 (m, 1H), 1.42-1.19 (m, 10H), 0.89 (t, J = 7.1 Hz, 3H). **^{13}C NMR** ($CDCl_3$, 100 MHz) δ 147.8, 146.8, 139.1, 119.3, 108.0, 106.4, 100.9, 74.6, 39.1, 31.8, 29.5, 29.2, 25.9, 22.6, 14.1. **FT-IR**: ν (cm^{-1}) 3351, 2924, 2854, 1486, 1441, 1241, 1039, 936, 862, 809, 726, 635.**Accurate mass (EI):** $H_{15}C_{22}O_3$ Theoretical: 250.1563. Found: 250.1561. Spectral Accuracy: 95.0%.

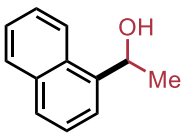

1-(naphthalen-1-yl)ethan-1-ol (2.31) was prepared according to the general procedure. The product was purified by column chromatography with 10% to 20% EtOAc in Hexanes to afford **2.31** as a

[68] Da, C.-S.; Wang, J.-R.; Ying, X.-G.; Fan, X.-Y.; Liu, Y.; Yu, S.-L. *Org. Lett.* **2009**, *11*, 5578-5581.
[69] Twilton, J.; Christensen, M.; DiRocco, D. A.; Ruck, R. T.; Davies, I. W.; MacMillan, D. W. C. *Angew. Chem., Int. Ed.*, **2018**, 57, 5369–5373.

colourless oil (35.1 mg, 68% yield). **^{1}H NMR** ($CDCl_3$, 400 MHz) δ 8.14 (d, J = 7.6 Hz, 1H), 7.89 (m, 1H), 7.79 (d, J = 7.6 Hz, 1H), 7.69 (d, J = 6.9 Hz, 1H), 7.56-7.47 (m, 3H), 5.68 (q, J = 13.1, 6.6 Hz, 1H), 1.99 (br s, 1H), 1.68 (d, J = 6.6 Hz, 3H). **^{13}C NMR** ($CDCl_3$, 100 MHz) δ 141.4, 133.8, 130.3, 128.9, 128.0, 126.1, 125.6, 125.5, 123.2, 122.0, 67.1, 24.4. Characterization of **2.31** matched previously reported spectra.[70]

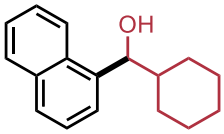

Cyclohexyl(naphthalen-1-yl)methanol (2.32) was prepared according to the general procedure. The product was purified by column chromatography with 10% EtOAc in hexanes to afford **2.32** as a colourless oil (56.2 mg, 78% yield). **^{1}H NMR** ($CDCl_3$, 400 MHz) δ 8.16 (d, J = 7.4 Hz, 1H), 7.89 (d, J = 7.2 Hz, 1H), 7.79 (d, J = 8.1 Hz, 1H), 7.55-7.46 (m, 3H), 5.20 (d, J = 6.4 Hz, 1H), 2.01-1.89 (m, 3H), 1.78-1.64 (m, 3H), 1.44 (br s, 1H), 1.29-1.15 (m, 5H). **^{13}C NMR** ($CDCl_3$, 100 MHz) δ 139.5, 133.9, 130.9, 128.9, 127.8, 125.8, 125.4, 125.3, 124.2, 123.7, 76.1, 44.4, 30.3, 28.3, 26.5, 26.3, 26.1. Characterization of **2.32** matched previously reported spectra.[Error! Bookmark not defined.]

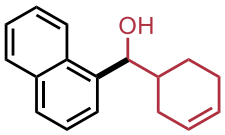

Cyclohex-3-en-1-yl(naphthalen-1-yl)methanol (2.33) was prepared according to the general procedure. The product was purified by column chromatography with 10% to 20% EtOAc in hexanes to afford **2.33** as a colourless oil (30.0 mg, 42% yield). **^{1}H NMR** ($CDCl_3$, 400 MHz) δ (1.3:1 mixture of diastereomers): 8.19-8.14 (m, 1H), 7.86 (d, J = 8.2 Hz, 1H), 7.78 (d, J = 8.1 Hz, 1H), 7.61-7.57 (m, 1H), 7.51-7.44 (m, 3H), 5.66-5.53 (m, 2H), 5.29 (minor diastereomer, d, J = 6.4 Hz, 0.42 H), 5.22 (major diastereomer, d, J = 6.5 Hz, 0.53 H), 2.23 – 1.40 (m, 8H). **^{13}C NMR** ($CDCl_3$, 100 MHz) δ 139.3, 133.9, 130.9, 130.8, 128.9, 128.1, 127.9, 127.2, 126.7, 126.4, 126.1, 125.9, 125.5, 125.4, 125.3, 124.4, 124.1, 123.7, 123.6, 75.7, 75.2, 40.32, 40.29, 28.8, 27.2, 26.2, 25.4, 25.0, 24.2. **FT-IR**: ν (cm^{-1}) 3405, 3020, 2913, 1702, 1596,

[70] Balakrishnan, V.; Murugesan, V.; Chindan, B.; Rasappan, R. *Org. Lett.* **2021**, *23*, 1333-1338.

1509, 1435, 1208, 1043, 910, 777, 730. **Accurate mass (EI):** $H_{18}C_{17}O$ Theoretical: 238.3300. Found: 238.1352. Spectral Accuracy: 98.1%.

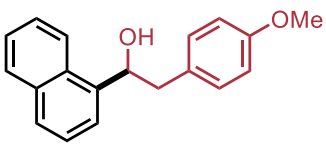

2-(4′-methoxyphenyl)-1-naphthalen-1-yl ethanol (2.34) was prepared according to the general procedure. The product was purified by column chromatography with 10% EtOAc in hexanes to afford **2.34** as a yellow semi-solid (70.9 mg, 85% yield). **^{1}H NMR** ($CDCl_3$, 400 MHz) δ 8.15 (d, J = 8.3 Hz, 1H), 7.89 (d, J = 7.7 Hz, 1H), 7.79 (d, J = 8.2 Hz, 1H), 7.65 (d, J = 7.1 Hz, 1H), 7.57-7.46 (m, 3H), 7.19 (d, J = 8.5 Hz, 2H), 6.87 (d, J = 8.5 Hz, 2H), 5.62 (dd, J = 9.0 Hz, 3.5 Hz, 1H), 3.79 (s, 3H) 3.23 (dd, J = 14.1 Hz, 3.5 Hz, 1H), 3.00 (dd, J = 14.1 Hz, 9.0 Hz, 1H), 2.24 (br s, 1H). **^{13}C NMR** ($CDCl_3$, 100 MHz) δ 158.5, 139.6, 133.9, 130.5, 130.4, 130.3, 129.0, 128.0, 126.1, 125.5, 123.1, 123.0, 114.1, 114.0, 72.2, 55.3, 44.2. **FT-IR**: ν (cm^{-1}) 3310, 2920, 1610, 1510, 1301, 1241, 1178, 1074, 1039, 985, 803, 783, 769, 734. **Accurate mass (ESI$^+$):** m/z calc'd for [$H_{18}C_{19}O_2$+ Na^+] Theoretical: 301.1205. Found: 301.1816. Spectral Accuracy: 99.9%

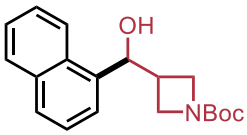

3-(hydroxy-1-naphthalenylmethyl)-1,1-dimethylethyl ester-1-Azetidinecarboxylic acid (2.35) was prepared according to the general procedure. The product was purified by column chromatography with 50% EtOAc in hexanes to afford **2.35** as a colourless oil (68.5 mg, 73% yield). **^{1}H NMR** ($CDCl_3$, 400 MHz) δ 8.17 (d, J = 8.2 Hz, 1H), 7.88 (dd, J = 7.6 Hz, 1.7 Hz, 1H), 7.80 (d, J = 8.1 Hz, 1H), 7.56 -7.26 (m, 4H), 5.21 (d, J = 7.0 Hz, 1H), 4.10 (dd, J = 8.7 Hz, 5.5 Hz, 1H), 3.96 (t, J = 8.7 Hz, 1H), 3.87 (t, J = 8.6 Hz, 1H), 3.72 (dd, J = 8.7 Hz, 5.7 Hz, 1H), 3.19 – 3.10 (m, 1H), 2.65 (br s, 1H), 1.43 (s, 9H). **^{13}C NMR** ($CDCl_3$, 100 MHz) δ 156.5, 137.3, 134.0, 130.7, 128.9, 128.7, 126.3, 125.8, 125.3, 123.5, 123.3, 79.4, 72.0, 51.2, 34.3, 28.4. **FT-IR**: ν (cm^{-1}) 3450, 2969, 2888, 1738, 1698, 1479, 1249, 1134, 1069, 804, 771. **Accurate mass (EI):** $H_{23}C_{19}NO_3$ Theoretical: 313.3970. Found: 313.1672. Spectral Accuracy: 96.1%.

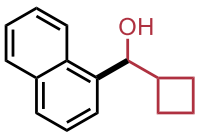

Cyclobutyl(naphthalen-1-yl)methanol (2.36) was prepared according to the general procedure. The product was purified by column chromatography with 10% EtOAc in hexanes to afford **2.36** as a colourless oil (52.9 mg, 83% yield). **^{1}H NMR** ($CDCl_3$, 400 MHz) δ 8.24 (d, J = 8.3 Hz, 1H), 7.88 (d, J = 7.7 Hz, 1H), 7.79 (d, J = 8.1 Hz, 1H), 7.56-7.47 (m, 4H), 5.37 (d, J = 7.15 Hz, 1H), 3.04-2.94 (m, 1H), 2.19-2.02 (m, 2H), 2.00 (br s, 1H), 1.94-1.83 (m, 4H). **^{13}C NMR** ($CDCl_3$, 100 MHz) δ 138.5, 133.9, 131.1, 128.8, 128.1, 126.4, 125.9, 125.5, 125.3, 123.7, 123.5, 74.3, 41.3, 24.6, 24.5, 17.8. **FT-IR**: ν (cm^{-1}) 3396, 2935, 1723, 1510, 1373, 1240, 1044, 988, 775, 619. **Accurate mass (EI):** $H_{15}C_{16}O$ Theoretical: 212.1196. Found: 212.1319. Spectral Accuracy: 98.4%.

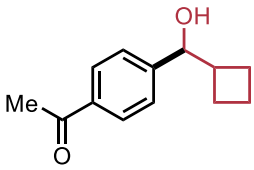

1-[4-[cyclobutyl(hydroxy)methyl]phenyl]ethanone (2.37) was prepared according to the general procedure. The product was purified by column chromatography with 10% EtOAc in hexanes to afford **2.37** as a yellow oil (58 mg, 95% yield). **^{1}H NMR** ($CDCl_3$, 400 MHz) δ 7.88 (d, J = 8.3 Hz, 2H), 7.37 (d, J = 8.2 Hz, 2H), 4.61 (d, J = 7.7 Hz, 1H), 2.55 (s, 3H), 2.17 (br s, 1H), 2.02-1.96 (m, 2H), 1.85-1.76 (m, 4H). **^{13}C NMR** ($CDCl_3$, 100 MHz) δ 197.9, 148.6, 136.3, 128.4, 126.2, 77.7, 42.5, 26.6, 24.5, 24.3, 17.7. **FT-IR**: ν (cm^{-1}) 3420, 2937, 2861, 1664, 1605, 1568, 1408, 1364, 1274, 1195, 1014, 961, 832, 715. **Accurate mass (EI):** $H_{16}C_{13}O_2$ Theoretical: 204.2690. Found: 204.1145. Spectral Accuracy: 97.1%.

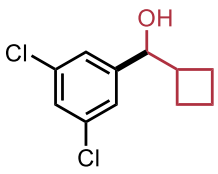

Cyclobutyl-(3,5-dichlorophenyl)methanol (2.38) was prepared according to the general procedure. The product was purified by column chromatography with 10% EtOAc in hexanes to afford **2.38** as a pale yellow semi-solid (59 mg, 86% yield). **^{1}H NMR** ($CDCl_3$, 400 MHz) δ 7.25 (t, J = 1.9 Hz, 1H), 7.20 (d, J = 1.9 Hz, 2H), 4.50 (d, J = 7.7 Hz, 1H), 2.60-2.50 (m, 1H), 2.08-1.79 (m, 7H). **^{13}C NMR** ($CDCl_3$, 100 MHz) δ 146.6, 134.9, 127.5, 124.6, 77.2, 42.3, 24.4, 24.2, 17.7. **FT-IR**: ν (cm^{-1}) 3214, 2919, 2854, 1620, 1567, 1427, 1383, 1318, 1204, 1096, 1059, 1018, 856, 795, 685.

Accurate mass (EI): $H_{12}C_{11}Cl_2O$ Theoretical: 230.0265. Found: 230.0260. Spectral Accuracy: 98.3%.

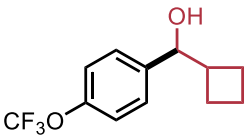

Cyclobutyl-[4-(trifluoromethoxy)phenyl]methanol (2.39) was prepared according to the general procedure. The product was purified by column chromatography with 12.5% to 16.5% EtOAc in hexanes to afford **2.39** as a colourless oil (51.7 mg, 70% yield). **^{1}H NMR** ($CDCl_3$, 400 MHz) δ 7.34 (d, J = 8.6 Hz, 2H), 7.18 (d, J = 8.0 Hz, 2H), 4.58 (d, J = 7.9 Hz, 1H), 2.64-2.54 (m, 1H), 2.12-1.77 (m, 7H). **^{13}C NMR** ($CDCl_3$, 100 MHz) δ 148.5, 141.8, 127.5, 123.0 (q, J = 257.0 Hz), 120.8, 77.6, 42.5, 24.6, 24.3, 17.7. **^{19}F NMR** δ -57.9. **FT-IR**: ν (cm^{-1}) 3416, 2939, 1725, 1508, 1375, 1253, 1156, 1045, 1011, 840, 678. **Accurate mass (EI):** $H_{13}C_{12}F_3O_2$ Theoretical: 246.2292. Found: 246.0862. Spectral Accuracy: 98.3%.

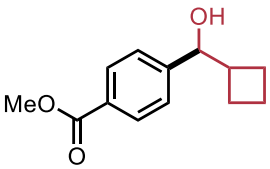

4-(cyclobutylhydroxymethyl)-benzoic acid methyl ester (2.40) was prepared according to the general procedure. The product was purified by column chromatography with 2.5% to 10% acetone in PhMe to afford **2.40** as a yellow oil (62 mg, 94% yield).**^{1}H NMR** ($CDCl_3$, 400 MHz) δ 7.98 (d, J = 8.3 Hz, 2H), 7.37 (d, J = 8.25 Hz, 2H), 4.62 (d, J = 7.73 Hz, 1H), 3.90 (s, 3H), 2.63-2.53 (m, 1H), 2.18 (br, s, 1H), 2.07-1.97 (m, 2H), 1.89-1.74 (m, 4H). **^{13}C NMR** ($CDCl_3$, 100 MHz) δ 167.0, 148.3, 129.6, 129.2, 126.0, 77.7, 52.0, 42.4, 24.5, 24.2, 17.7. **FT-IR ν (cm^{-1})** 3510, 2930, 2852, 1696, 1607, 1573, 1430, 1309, 1277, 1191, 1174, 1117, 1094, 1012, 960, 917, 852, 809, 766, 705. **Accurate mass (EI):** $H_{16}C_{13}O_3$ Theoretical: 220.1094. Found: 220.1165. Spectral Accuracy: 95%

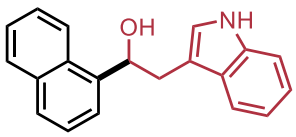

2-(1H-indol-3-yl)-1-(naphthalen-1-yl)ethanol (2.41), was prepared according to the general procedure. The fractions were collected using a gradient solvent system of 1% to 4% acetone in DCM to afford **2.41** as a white solid (77.0 mg, 89% yield). **^{1}H NMR** (($CDCl_3$, 400 MHz)

δ 8.26 (d, J = 8.5 Hz, 1H), 8.10 (br s, 1H), 7.94-7.92 (m, 1H), 7.83 (d, J = 8.2 Hz, 1H), 7.75 (d, J = 7.1 Hz, 1H), 7.69 (d, J = 7.8 Hz, 1H), 7.61-7.49 (m, 3H), 7.40 (d, J = 8.1 Hz, 1H), 7.26 (dt, J = 8.0 Hz, 1.1 Hz, 1H), 7.19 (dt, J = 7.9 Hz, 1.1 Hz, 1H), 7.11 (br s, 1H),), 5.78 (dd, J = 9.0 Hz, 3.6 Hz, 1H), 3.51 (dd, J = 14.7 Hz, 3.5 Hz, 1H), 3.24 (dd, J = 14.8 Hz, 9.0 Hz, 1H), 1.61 (br s, 1H). **^{13}C NMR** ((CDCl$_3$, 100 MHz) δ 139.8, 136.4, 133.9, 130.5, 129.0, 127.9, 127.6, 126.1, 125.6, 125.5, 123.2, 123.0, 122.3, 119.7, 119.0, 112.4, 111.4, 70.7, 35.0. Characterization of **2.41** matched previously reported spectra.[71]

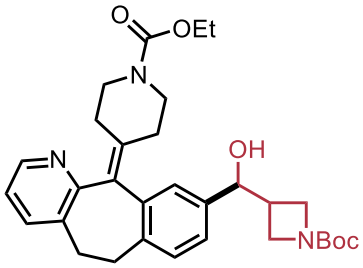

3-(hydroxy-[1-(11-(1-(Ethoxycarbonyl)piperidin-4-ylidene)-6,11-dihydro-5H-benzo[5,6]cyclohepta[1,2-b]pyridin-8-yl])-1,1-dimethylethyl ester-1-Azetidinecarboxylic acid (2.42) was prepared according to the general procedure. The product was purified by column chromatography with 20% to 40% acetone in DCM to afford **2.42** as a purple solid (83.4 mg, 52% yield). **^{1}H NMR** (CDCl$_3$, 400 MHz) δ 8.35 (d, J = 4.4 Hz, 1H), 7.47 (d, J = 7.5 Hz, 1H), 7.15-7.08 (m, 4H), 4.70 (d, J = 6.6 Hz, 1H), 4.11 (q, J = 7.1 Hz, 2H), 4.00-3.93 (m, 2H), 3.81-3.77 (m, 3H), 3.64-3.62 (m, 1H), 3.44-3.32 (m, 2H), 3.15-3.09 (m, 2H), 2.87-2.76 (m, 4H), 2.49-2.14 (m, 1H), 2.39-2.24 (m, 3H), 1.41 (s, 9H), 1.23 (t, J = 7.1 Hz, 3H). **^{13}C NMR** (CDCl$_3$, 100 MHz) δ 157.1, 156.4, 155.5, 146.0, 141.5, 138.7, 138.0, 137.9, 137.5, 134.2, 134.0, 129.7, 127.1, 127.0, 124.0, 122.4, 79.4, 75.6, 75.5, 61.3, 58.5, 51.6, 44.8, 44.7, 35.4, 31.9, 31.6, 29.7, 28.4, 27.5, 14.6. **Melting point** Decomposition upon heating **FT-IR**: ν (cm^{-1}) 3350, 2972, 1691, 1421, 1365, 1326, 1225, 1112, 995, 767, 728.**Accurate mass (ESI$^+$):** m/z calc'd for [$H_{39}C_{31}N_3O_5$] Theoretical: 556.2787. Found: 556.3256

[71] Wang, P.; Zhao, J.-Z.; Li, H.-F.; Liang, X.-M.; Zhang, Y.-L.; Da, C.-S. *Tet. Lett.* **2017**, *58*, 129-133.

Chapter 3: Reductive 1,2-Addition to *N*-Methyl Isatins

3.1: High-throughput experimentation and optimization

The conditions successfully developed in **Chapter 2** for the reductive 1,2-addition of aldehydes motivated us to seek whether a similar strategy could be applied to coupling of aryl halides with other carbonyls. For this endeavour, we employed high-throughput experimentation (HTE) to test out various conditions with the hope of discovering new reactivity with more challenging carbonyls. In our group, HTE is viewed as a valuable tool to carry out reaction discovery and to search for optimal reaction conditions.

The ability to perform a wide array of reactions in series through a fully automated process allows us to test multiple reaction parameters simultaneously. This often leads to the discovery of new and unexplored reaction conditions which might have been overlooked otherwise. In a typical HTE experiment, up to 96 reactions can be set up in parallel allowing many variables to be explored. Furthermore, since these reactions are usually set up on a small scale, they utilize less resources and materials compared to a typical benchtop experiment. **Figure 4** shows the details of the HTE screen performed on different ketone derivatives in search for a hit with the chosen substrates. For this plate, we screened different P_2N_2 ligands and bases. The coloured sections represent each carbonyl that was run while the rows and columns demonstrate each ligand and base combination that was subjected to our reaction conditions for the reductive arylation.

Figure 4: Screening P_2N_2 ligands and bases for coupling between PhI and selected carbonyls using HTE

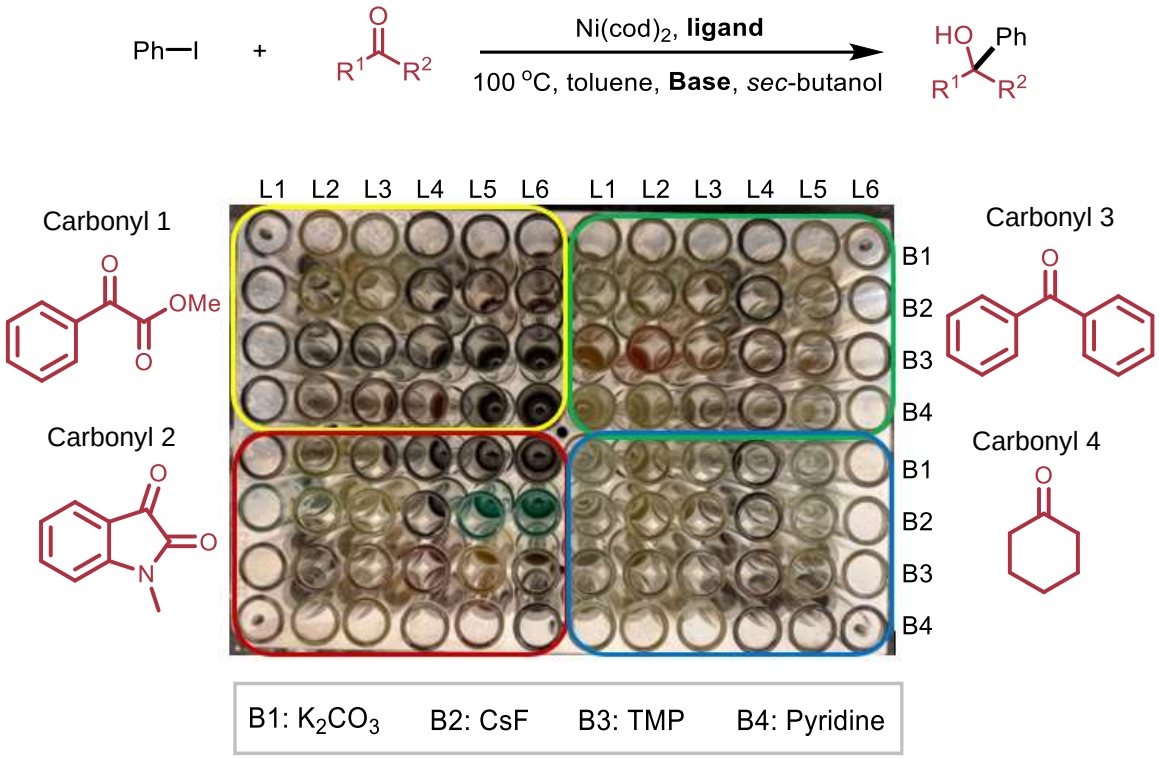

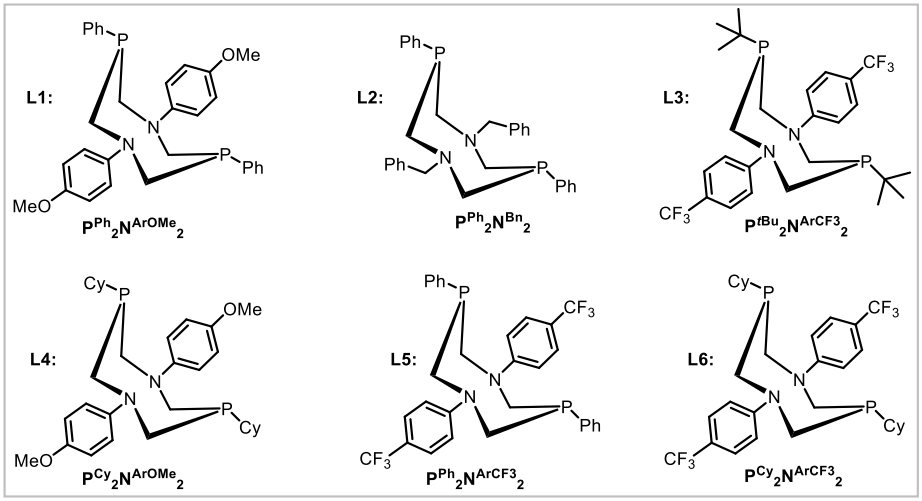

For this screen, we employed *sec*-butanol as a reducing agent because our previous tests in Chapter 2 revealed that it displays satisfactory performance when compared with

1-phenylethanol. The volatility of this secondary alcohol was beneficial during analysis compared to 1-phenylethanol, which often eluted along with the desired product when performing TLC and column chromatography and led to purification challenges. We chose 100 °C as the reaction temperature for HTE, hoping to see new reactivity that would otherwise not take place at lower temperatures while also ensuring that we were below the boiling point of toluene. We employed $Ni(cod)_2$ instead of other available Ni(II) precursors simply because it was readily soluble in toluene and stock solutions could be made. We were pleased to see some promising results emerge from this plate and the hits that were observed for cyclohexanone (carbonyl 4) and *N*-methyl isatin (carbonyl 2) are summarized in **Tables 14 and 15.**

For coupling between iodobenzene (**3.01**) and cyclohexanone (**3.02**), the desired tertiary alcohol **3.03** was only observed in three reactions amongst the ones that were screened (**Table 14**). $P^{tBu}{}_2N^{ArCF3}{}_2$, $P^{Cy}{}_2N^{ArOMe}{}_2$ and $P^{Cy}{}_2N^{ArCF3}{}_2$ were the only 3 ligands that showed product formation (**entries 1-3**). $P^{Cy}{}_2N^{ArCF3}{}_2$ and TMP, which were the optimal ligand and base for us for reductive addition of aldehydes, provided a moderate yield of 30% for coupling with cyclohexanone (**entry 3**).

Table 14: Hits for coupling with cyclohexanone from the HTE screen

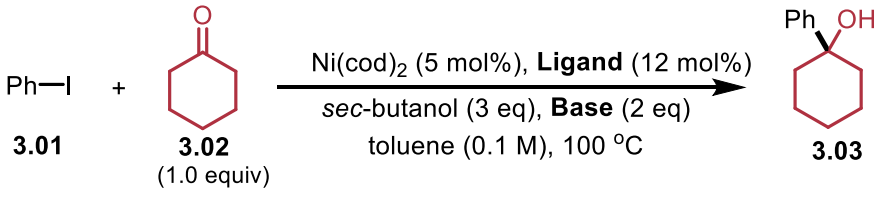

Entry	Ligand	Base	Yield 3.03[a]
1	$P^{tBu}{}_2N^{ArCF3}{}_2$	TMP	12%
2	$P^{Cy}{}_2N^{ArOMe}{}_2$	CsF	<10%
3	$P^{Cy}{}_2N^{ArCF3}{}_2$	TMP	30%

General conditions: aryl iodide (0.07 mmol), cyclohexanone (0.07 mmol), Base (0.14 mmol), *sec*-butanol (0.21 mmol), $Ni(cod)_2$ (5 mol%), Ligand (12 mol%) in PhMe (0.10 M), 100 °C for 16 h, under inert atmosphere (set-up in a HTE well plate inside the glovebox). Reactions were scaled down for HTE. [a]Yields are calculated by ^1H NMR with 1,3,5-trimethoxybenzene as the internal standard.

The results of this plate also demonstrated that when iodobenzene (**3.01**) was coupled with *N*-methyl isatin (**3.04**), the desired alcohol (**3.05**) was obtained for majority of the P_2N_2 ligands employed (**Table 15**). Not too surprisingly, TMP, which has consistently shown to be the optimal base for us for similar transformations, continued to fare better than other bases used. This was indeed good news for us because our goal was to demonstrate the generality of the strategy developed in Chapter 2. P_2N_2 ligands bearing electron-neutral or electron-rich anilines such as $P^{Ph}{}_2N^{Bn}{}_2$ and $P^{Cy}{}_2N^{ArOMe}{}_2$ (**entry 1,2**) provided a considerably lower yield of the desired product compared to those bearing the electron-withdrawing trifluoromethyl functionality on the aniline, such as $P^{tBu}{}_2N^{ArCF3}{}_2$, $P^{Ph}{}_2N^{ArCF3}{}_2$ and $P^{Cy}{}_2N^{ArCF3}{}_2$ (**entries 3-5**). This observation was not far off from what we saw in Chapter 2.

Table 15: Hits for coupling with *N*-methyl isatin from the HTE screen

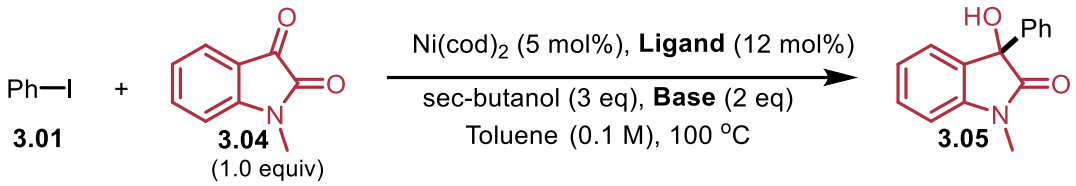

Entry	Ligand	Base	Yield 3.05[a]
1	$P^{Ph}{}_2N^{Bn}{}_2$	TMP	16%
2	$P^{Cy}{}_2N^{ArOMe}{}_2$	TMP	23%
3	$P^{tBu}{}_2N^{ArCF3}{}_2$	TMP	40%
4	$P^{Ph}{}_2N^{ArCF3}{}_2$	TMP	37%
5	$P^{Cy}{}_2N^{ArCF3}{}_2$	TMP	36%

General conditions: aryl iodide (0.07 mmol), *N*-methyl isatin (0.07 mmol), Base (0.14 mmol), *sec*-butanol (0.21 mmol), $Ni(cod)_2$ (5 mol%), Ligand (12 mol%) in PhMe (0.10 M), 100 °C for 16 h, under inert atmosphere (set-up in a HTE well plate inside the glovebox). Reactions were scaled down for HTE. [a]Yields are calculated by ^1H NMR with 1,3,5-trimethoxybenzene as the internal standard.

Following these initial hits, we were pleased to identify cyclohexanone and isatins as potential candidates for further exploration. As is good practice before proceeding forward with any project, we wanted to confirm the reproducibility of the hits that we got. It is not uncommon to observe a hit in an HTE experiment and fail to reproduce it on the benchtop, potentially due to differences in heat distribution, stirring, reaction concentration and scale.[72]

[72] Cook, A.; Clément, R.; Newman, S. G. *Nat. Prot.* **2021**, *16*, 1152.

Attempts at testing the reproducibility of coupling with cyclohexanone using $P^{Cy_2}N^{ArCF3_2}$ as a ligand and TMP as a base (**Table 14, entry 3**) were unsuccessful, typically only providing trace yields of the desired product, and quickly confirmed that the 30% yield we got from the HTE screen was a one-off observation. Such reproducibility issues can take a long time to understand and resolve and therefore could serve as an exciting project in the future for reductive addition onto diaryl or dialkyl ketones.

Similar reproducibility issues were also observed for some of the hits observed for coupling with *N*-methyl isatin, however, some ligands showed promising results when replicated in a vial (**Table 16**). It should be noted that for the HTE plate, a concentration of 0.1 M was chosen to avoid running into solubility issues when preparing stock solutions. For subsequent experiments, a reaction concentration of 0.2 M was used.

Table 16: Attempts to reproduce the HTE hits for coupling with *N*-methyl isatin

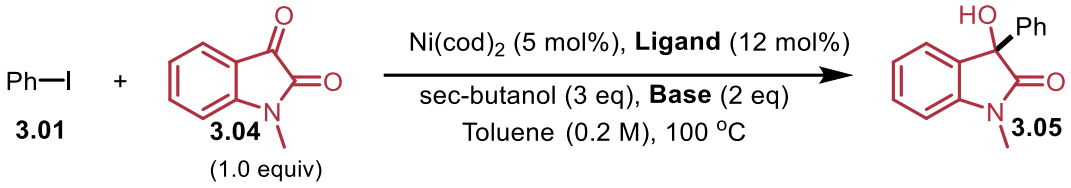

Entry	Ligand	Base	Yield 3.05[a]
1	$P^{Ph}{}_2N^{Bn}{}_2$	TMP	Trace
2	$P^{Cy}{}_2N^{ArOMe}{}_2$	TMP	<10%
3	$P^{tBu}{}_2N^{ArCF3}{}_2$	TMP	<10%
4	$P^{Ph}{}_2N^{ArCF3}{}_2$	TMP	30%
5	$P^{Cy}{}_2N^{ArCF3}{}_2$	TMP	43%

General conditions: aryl iodide (0.15 mmol), *N*-methyl isatin (0.15 mmol), Base (0.30 mmol), *sec*-butanol (0.45 mmol), $Ni(cod)_2$ (5 mol%), Ligand (12 mol%) in PhMe (0.20 M), 100 °C for 16 h, under an inert atmosphere (set-up inside the glovebox). [a]Yields are calculated by ^1H NMR with 1,3,5-trimethoxybenzene as the internal standard.

These reproducibility experiments revealed that most P_2N_2 ligands providing a low-to-moderate yield of the desired alcohol **3.05** in the HTE experiment gave only trace amounts of product on the benchtop (**entries 1-3**). The two ligands that emerged as promising choices were $P^{Ph}{}_2N^{ArCF3}{}_2$ and $P^{Cy}{}_2N^{ArCF3}{}_2$, providing the product in 30% and 43% yields, respectively (**entry 4, 5**). Therefore, $P^{Cy}{}_2N^{ArCF3}{}_2$ was used as the ligand of choice for all subsequent experiments.

We conducted a series of preliminary control experiments to make sure that the reactivity that we were observing did in fact require a catalyst. In the absence of base,

ligand or a nickel catalyst, no coupling was observed, further convincing us that this was indeed a catalytic reaction (**Table 17, entries 2-4**). Increasing the amount of base used (**entry 5**) or doubling the stoichiometry of the isatin or aryl iodide (**entry 6, 7**) seemed to have either no impact on the yield or decreased the yield only slightly. Due to the ease of availability, low cost, and air-stability of Ni(II) precursors, we conducted the reaction using $NiBr_2$•diglyme and found that it performs just as well as $Ni(cod)_2$ (**entry 8**).

Table 17: Control Experiments for reductive 1,2-addition of *N*-methyl isatin

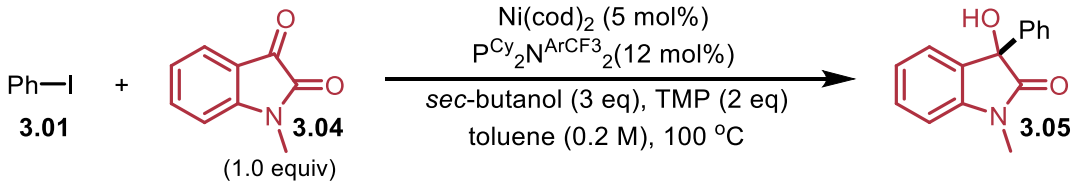

Entry	Deviation from conditions	Yield 3.05[a]
1	None	43%
2	No base	0%
3	No ligand	0%
4	No nickel catalyst	0%
5	3 equivalents of base	40%
6	2 equivalents of *N*-methyl isatin	33%
7	2 equivalents of aryl iodide	35%
8	$NiBr_2$•diglyme as catalyst	41%

General reaction conditions: aryl iodide (0.15 mmol), *N*-methyl isatin (0.15 mmol), TMP (0.30 mmol), *sec*-butanol (0.45 mmol), Ni catalyst (5 mol%), $P^{Cy}{}_2N^{ArCF3}{}_2$ (12 mol%) in PhMe (0.20 M), 100 °C for 16 h, under an inert atmosphere (set-up inside the glovebox). [a]Yields are calculated by ^1H NMR with 1,3,5-trimethoxybenzene as the internal standard.

We performed a small screen comparing toluene with other solvents commonly employed in Ni-catalysed cross-coupling reactions (**Table 18**). When toluene is used as a solvent, the desired alcohol **3.05** is obtained in a 43% yield (**entry 1**), while dioxane gives a 28% yield (**entry 2**). Other solvents such as DMA, MeCN and xylenes only gave trace yields of the product (**entries 3-5**).

Table 18: Solvent screen for reductive 1,2-addition on *N*-methyl isatin

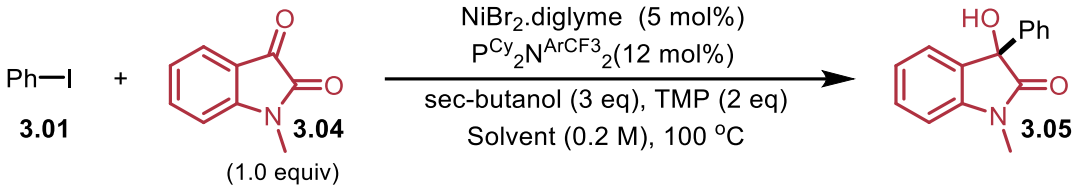

Entry	Solvent	Yield 3.05[a]
1	Toluene	43%
2	Dioxane	28%
3	DMA	0%
4	MeCN	Trace
5	Xylenes	Trace

General reaction conditions: aryl iodide (0.15 mmol), *N*-methyl isatin (0.15 mmol), TMP (0.30 mmol), *sec*-butanol (0.45 mmol), $NiBr_2$•diglyme (5 mol%), $P^{Cy_2}N^{ArCF_3{}_2}$ (12 mol%) in PhMe (0.20 M), 100 °C for 16 h, under an inert atmosphere (set-up inside the glovebox). [a]Yields are calculated by ^1H NMR with 1,3,5-trimethoxybenzene as the internal standard.

In Chapter 2, we established that for these types of transformations it was imperative to have the ligand in a large excess relative to the catalyst. For this reason, we tested different loadings of the $NiBr_2$•diglyme catalyst and the ligand (**Table 19**). We found 10 mol% of Ni and 24 mol% of $P^{Cy_2}N^{ArCF_3{}_2}$ to be optimal since it increased the yield from 43% to 67% for the desired product (**entry 2**). Further increasing the catalyst and ligand loadings to 15 mol% and 30 mol%, respectively, provided a 56% yield of **3.05** (**entry 3**). Such high catalyst and ligand loadings often gave us significant mixing issues and therefore impacted the reproducibility.

Table 19: Testing different catalyst and ligand concentrations

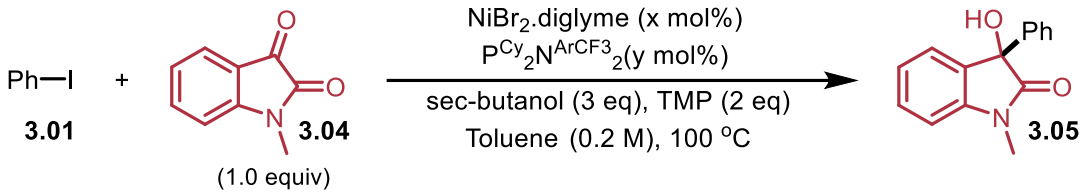

Entry	Catalyst (x mol%)	Ligand (y mol%)	Yield 3.05[a]
1	5 mol%	12 mol%	43%
2	10 mol%	24 mol%	67%
3	15 mol %	30 mol%	56%

General conditions: General reaction conditions: aryl iodide (0.15 mmol), *N*-methyl isatin (0.15 mmol), TMP (0.30 mmol), *sec*-butanol (0.60 mmol), $NiBr_2$•diglyme (x mol%), $P^{Cy}{}_2N^{ArCF3}{}_2$ (y mol%) in PhMe (0.20 M), 100 °C for 16 h, under an inert atmosphere (set-up inside the glovebox). [a]Yields are calculated by ^1H NMR with 1,3,5-trimethoxybenzene as the internal standard.

While searching for conditions that would further improve the yield for our desired product, we performed a few other tests that have been summarized in **Table 20**. From these results, we found that increasing the amount of the *sec*-butanol reducing agent to 4 equivalents gave a slight boost to the yield from 67% to 75% and we switched to this for future experiments (**entry 2**). Increasing the reaction concentration to 0.4 M gave a poorer yield compared to the standard 0.2 M concentration (**entry 3**). The reduction in yield at a higher reaction concentration could be attributed to poor solubility and lack of homogeneity of the reaction mixture. Running the reaction at a slightly lower

temperature of 85 °C or higher temperature of 120 °C plummets the yield significantly (**entry 4, 5**).

Table 20: Summary of optimization experiments for coupling between Iodobenzene and *N*-methyl isatin

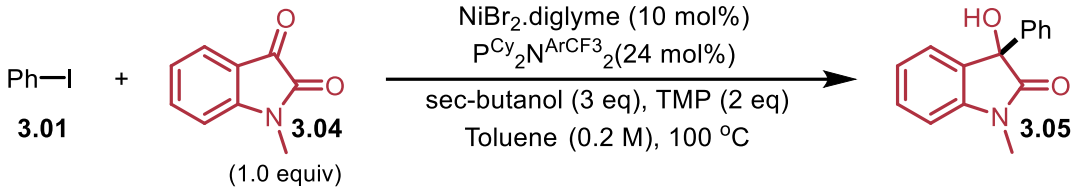

Entry	Deviation from conditions	Yield 3.05[a]
1	None	67%
2	4 equivalents of *sec*-butanol	75%
3	0.4 M concentration	45%
4	85 °C reaction temperature	38%
5	120 °C reaction temperature	31%

General reaction conditions: aryl iodide (0.15 mmol), *N*-methyl isatin (0.15 mmol), TMP (0.30 mmol), *sec*-butanol (0.60 mmol), $NiBr_2$•diglyme (10 mol%), $P^{Cy}{}_2N^{ArCF3}{}_2$ (24 mol%) in PhMe (0.20 M), 100 °C for 16 h, under an inert atmosphere (set-up inside the glovebox). [a]Yields are calculated by ^1H NMR with 1,3,5-trimethoxybenzene as the internal standard.

When we employed other aryl halides or pseudo halides such as napthyl triflate, bromobenzene and chlorobenzene as coupling partners, we only obtained trace yields of the desired product suggesting a possibly difficult oxidative addition with these substrates (**Table 21, entries 2-4**).

Table 21: Other aryl (pseudo)halides as coupling partners with *N*-methyl isatin

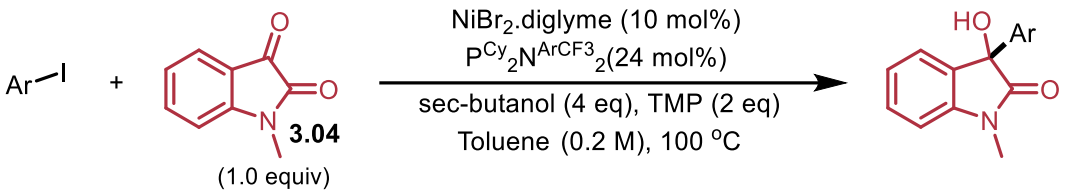

Entry	Deviation from conditions	% Yield
1	None	75%
2	Bromobenzene instead of iodobenzene	Trace
3	Chlorobenzene instead of iodobenzene	0%
4	Napthyl triflate instead of iodobenzene	0%

General reaction conditions: aryl halide (0.15 mmol), *N*-methyl isatin (0.15 mmol), TMP (0.30 mmol), *sec*-butanol (0.60 mmol), $NiBr_2$•diglyme (10 mol%), $P^{Cy}{}_2N^{ArCF3}{}_2$ (24 mol%) in PhMe (0.20 M), 100 °C for 16 h, under an inert atmosphere (set-up inside the glovebox). [a]Yields are calculated by ^1H NMR with 1,3,5-trimethoxybenzene as the internal standard.

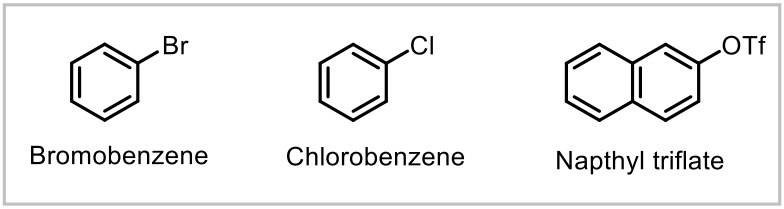

We directed our last few optimization efforts to the more interesting aryl iodide, 1-iodo-3-trifluormethyl-benzene, because we wanted to ensure that the results that we were observing were not specific to a simple aryl iodide such as iodobenzene and could be translated to a wide range of substrates (**Table 22**). Moreover, we wanted to rule out the possibility of other conditions existing and working more favourably. Under the established conditions, 1-iodo-3-trifluormethyl-benzene gave a decent yield of 74% for the desired product **3.07** (**entry 1**). A small screen of other available Ni(II) precursors

generally diminished the yield (**entries 2-5**). Using Zn as a reducing agent gave a trace yield of the desired alcohol (**entry 6**). Employing 1-phenyl ethanol, the reducing agent used for the reductive 1,2-addition of aldehydes, gave a slightly lower yield of 56% (**entry 7**). We quickly realized that no further modifications boosted the yield further.

Table 22: Selected optimization experiments with 1-iodo-3-trifluoromethyl-benzene and *N*-methyl isatin

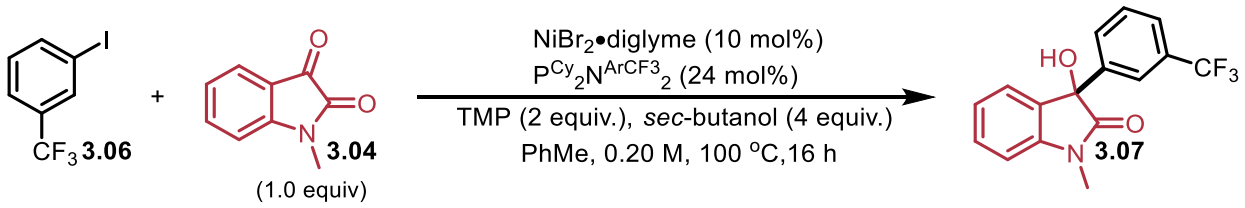

Entry	Deviation from conditions	Yield 3.07[a]
1	None	74%
2	$NiBr_2(EtPy)_2$ as catalyst	60%
3	$NiCl_2$.glyme as catalyst	51%
4	$Ni(OTf)_2$ as catalyst	23%
5	$NiCl_2(PPh_3)_2$ as catalyst	15%
6	Zn as a reducing agent	<10%
7	1-phenylethanol as a reducing agent	56%

General conditions: aryl iodide (0.15 mmol), *N*-methyl isatin (0.15 mmol), TMP (0.30 mmol), reducing agent (0.60 mmol), Ni catalyst (10 mol%), $P^{Cy}{}_2N^{ArCF3}{}_2$ (24 mol%) in PhMe (0.20 M), 100 °C for 16 h, under an inert atmosphere. [a]Yields are calculated by ^1H NMR with 1,3,5-trimethoxybenzene as the internal standard.

After we had thoroughly vetted our system, we were convinced that the conditions we had at hand (**Scheme 39**) were indeed fully optimized.

Scheme 39: Standard conditions for the reductive 1,2-arylation of N-methyl isatin

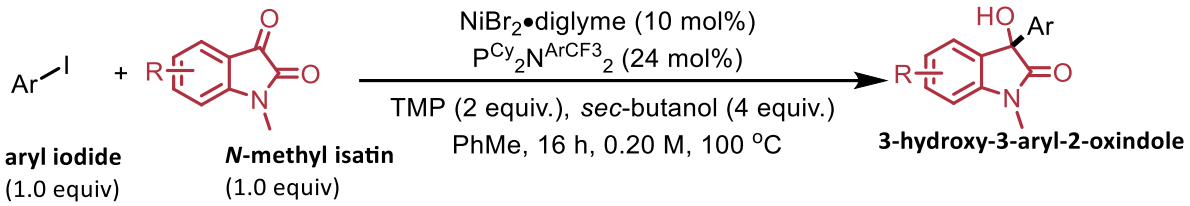

3.2: Scope of the reductive 1,2-addition of *N*-methyl isatins

We then went on to explore the scope of this transformation by first modifying the aryl iodide substrate and subjecting it to our standard conditions in the presence of *N*-methyl isatin. We were pleased to observe that several sensitive functionalities were well-tolerated and yields ranging from 50-90% were obtained (**Table 23**). Fluorine-containing aryl iodides were especially favourable under these conditions. 4-Fluoro-1-iodo-benzene (**3.09**) gave an excellent yield of 91% and was used as a model substrate for coupling with various isatins. It was also interesting to note the prevalence of the trifluoromethyl functionality in our scope which is highly desired from a medicinal chemistry point of view. Electron-donating groups (**3.10, 3.11**), electron-withdrawing aryl iodides (**3.12, 3.13**) and heterocyclic compounds (**3.14, 3.15**) were successfully incorporated in moderate to high yields. Other halogenated aryl iodides such as 4-chloro-1-iodo-benzene (**3.15**)

cooperated well and gave a decent yield of 73%. This could later be subjected to late-stage modification of the product to synthesise industrially useful heterocycles.

Table 23: Scope of aryl iodides for the reductive 1,2-arylation of *N*-methyl isatin

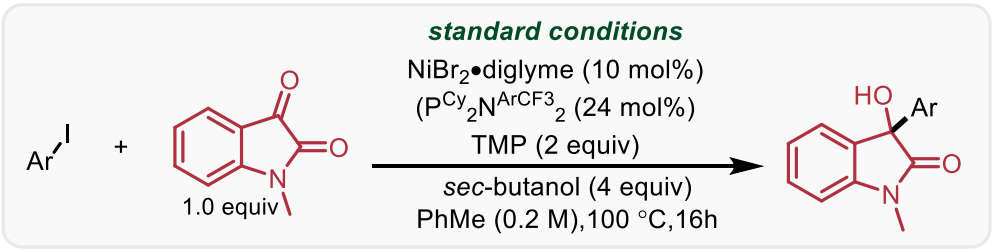

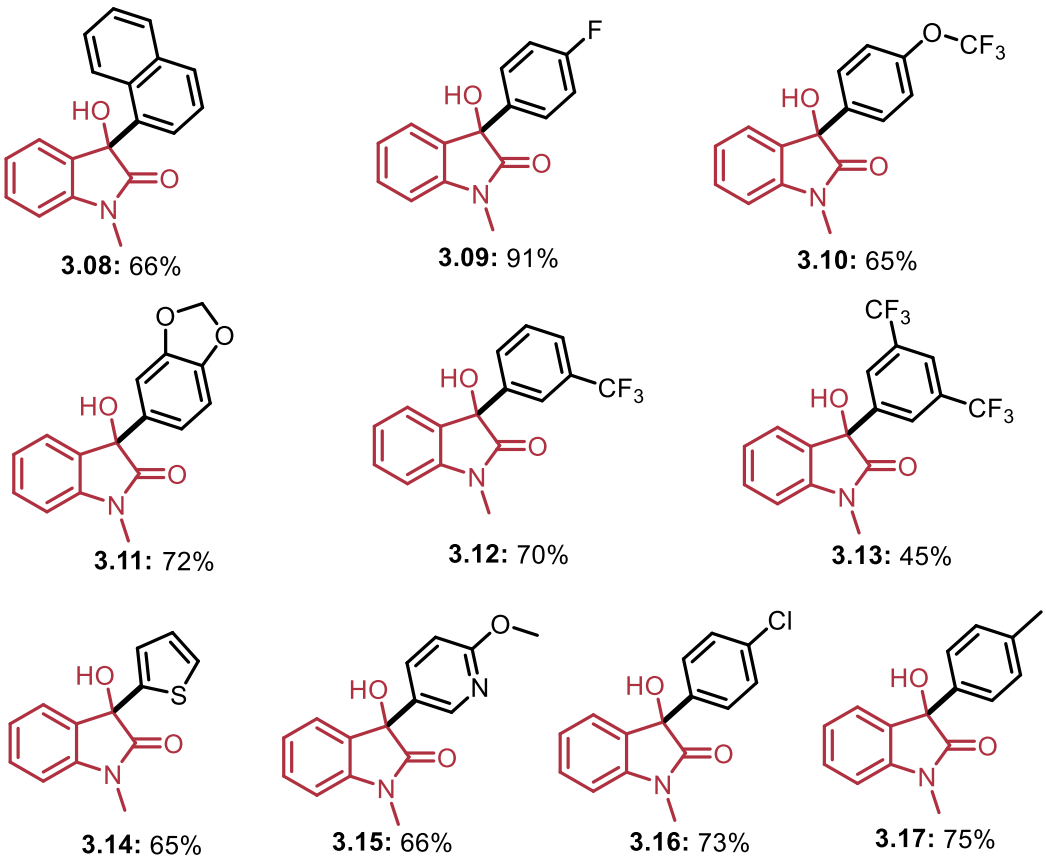

General reaction conditions: aryl iodide (0.15 mmol), *N*-methyl isatin (0.15 mmol), TMP (0.30 mmol), *sec*-butanol (0.60 mmol), $NiBr_2$•diglyme (10 mol%), $P^{Cy}{}_2N^{ArCF3}{}_2$ (24 mol%) in PhMe (0.20 M), 100 °C for 16 h, under an inert atmosphere (set-up inside the glovebox).

Following the satisfying results from the aryl iodide scope, we attempted to couple our highest yielding example (4-fluoro-1-iodo-benzene) with various commercially

available isatins that we methylated (**Table 24**). Although the scope for *N*-methyl isatins was more scarce compared to that of aryl iodides, we were pleased to observe modest yields with most of the ones we tested. Methoxy groups and fluorine containing isatins gave up to an 80% yield of the desired product (**3.18, 3.19, 3.20**). Electron-neutral isatins such as *N*-methyl-5,7-dimethylisatin provided the desired 3-hydroxy-2-oxindole product in 75% yield (**3.21**). Interestingly, isatins containing multiple fluorine atoms such as *N*-methyl-4,6-difluoroisatin gave a significantly lower yield of 52% for the desired product (**3.22**). As was the case with the aryl iodide substrates, trifluoromethyl and chloro functionalities were moderately tolerated and gave yields of around 55% (**3.23, 3.24)**.

Table 24: Scope of *N*-methyl isatins for the reductive 1,2-arylation with 4-fluoroiodobenzene

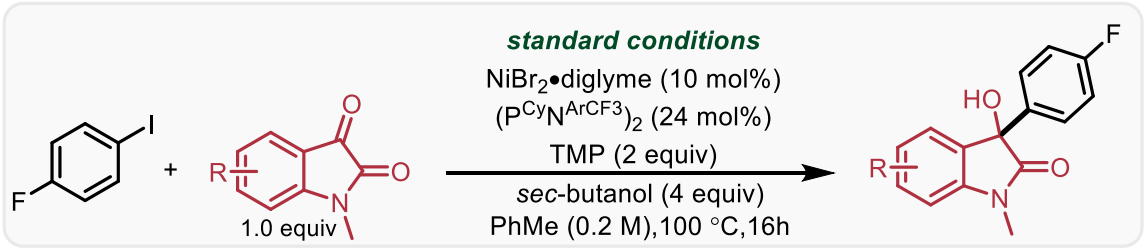

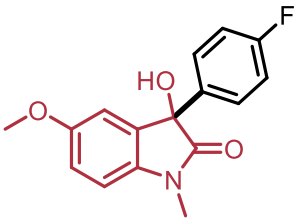

3.18: 82%

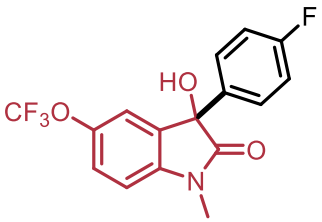

3.19: 40%

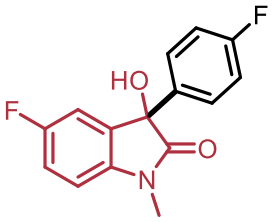

3.20: 80%

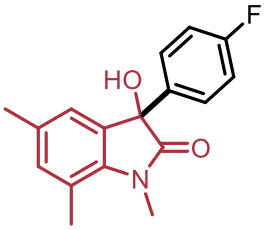

3.21: 75%

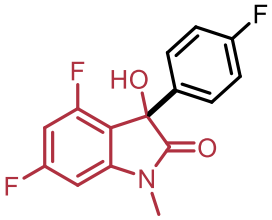

3.22:52%

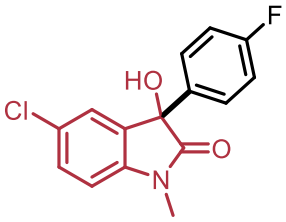

3.23: 50%

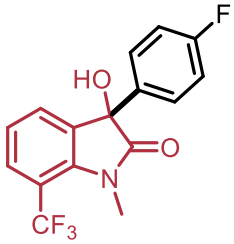

3.24: 55%

General reaction conditions: aryl iodide (0.15 mmol), *N*-methyl isatin (0.15 mmol), TMP (0.30 mmol), *sec*-butanol (0.60 mmol), $NiBr_2$•diglyme (10 mol%), $P^{Cy}{}_2N^{ArCF3}{}_2$ (24 mol%) in PhMe (0.20 M), 100 °C for 16 h, under an inert atmosphere (set-up inside the glovebox).

3.3: Preliminary mechanistic insights and discussion

Reaction with a $Ni^{(0)}(P_2N_2)_2$ complex

In order to get a deeper understanding of the mechanism of the coupling between aryl iodides and isatins to generate 3-aryl-3-hydroxy-2-oxindoles, we decided to conduct some preliminary mechanistic experiments. Although a closer investigation would be required to be convinced of the actual mechanism, this initial data was still a valuable starting point for us. We started off by attempting to synthesise a $Ni^{(0)}(P_2N_2)_2$ complex because we wanted to make sure that the active catalytic species involved ligation of the P_2N_2 ligand to the nickel center (**Scheme 40**.[73] It has been previously proposed in the literature that the bulky phosphine atoms of the P_2N_2 ligands are both bound to nickel, with the nitrogen fragment pendant, enabling the complex to adopt a tetrahedral geometry.[74] In our attempts to probe the previously underexplored catalytic reactivity of these complexes we synthesized the $Ni^0(P^{Cy}{}_2N^{ArCF3}{}_2)_2$ and the $Ni^0(P^{Ph}{}_2N^{ArCF3}{}_2)_2$ species.

[73] Das, A. K.; Engelhard, M. H.; Bullock, R. M.; Roberts, J. A. *Inorg. Chem.* **2014**, *53*, 6875.
[74] Wiedner, E. S.; Yang, J. Y.; Chen, S.; Raugei, S.; Dougherty, W. G.; Kassel, W. S.; Helm, M. L.; Bullock, R. M.; Rakowski DuBois, M.; DuBois, D. L. *Organometallics.* **2011**, *31*, 144.

Scheme 40: Synthesis of the $Ni^{(0)}(P^{Cy}{}_2N^{ArCF3}{}_2)_2$ and $Ni^{(0)}(P^{Ph}{}_2N^{ArCF3}{}_2)_2$ complexes

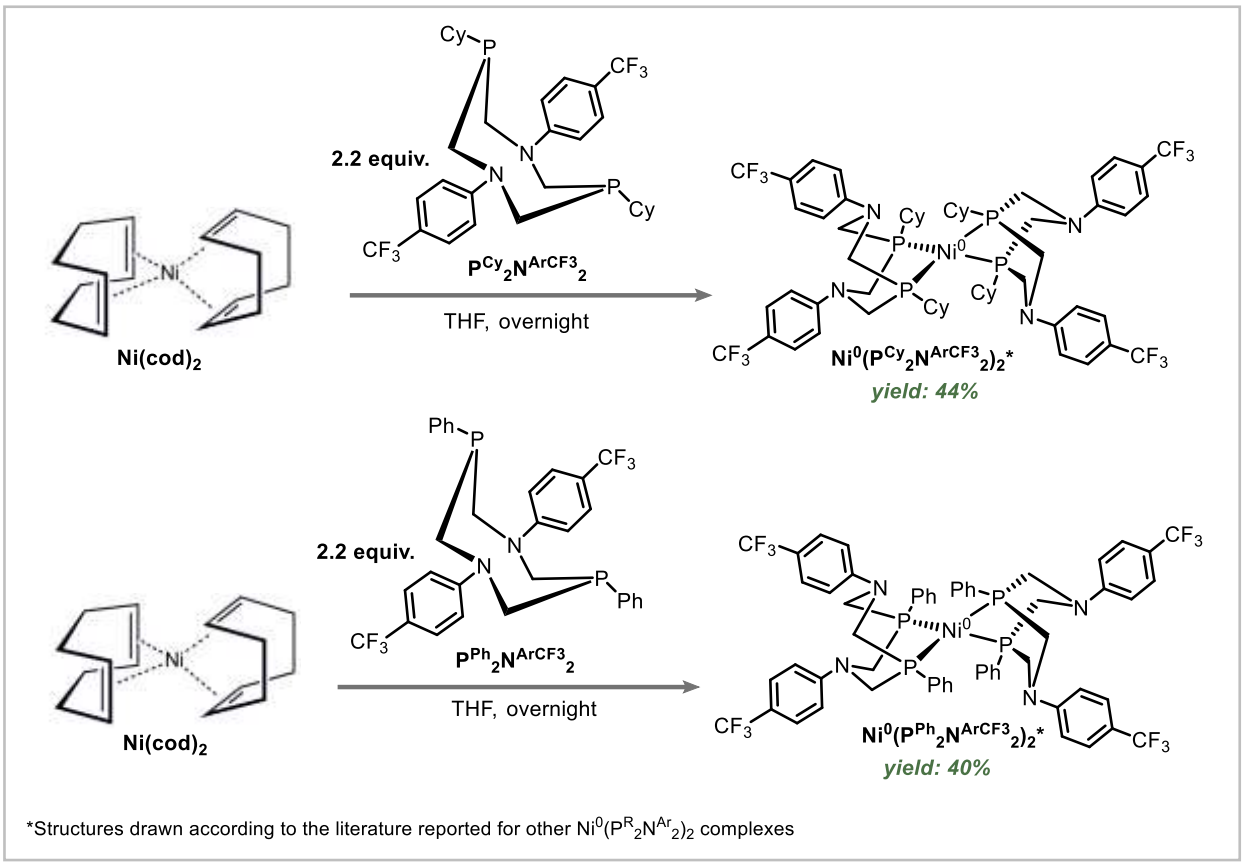

*Structures drawn according to the literature reported for other $Ni^0(P^R{}_2N^{Ar}{}_2)_2$ complexes

After we had successfully synthesised the above complexes, we first used $Ni^{(0)}(P^{Cy}{}_2N^{ArCF3}{}_2)_2$ in catalytic amounts in the 1,2-arylation of *N*-methyl isatin and observed product formation. For this, we used 1-iodonapthalene as the aryl iodide substrate simply because the product and by-products could be visualized and quantified using the GC-MS (**Table 25**).

Table 25: Attempting the 1,2-arylation of *N*-methyl isatin with $Ni^{(0)}(P^{Cy}{}_2N^{ACF3}{}_2)_2$

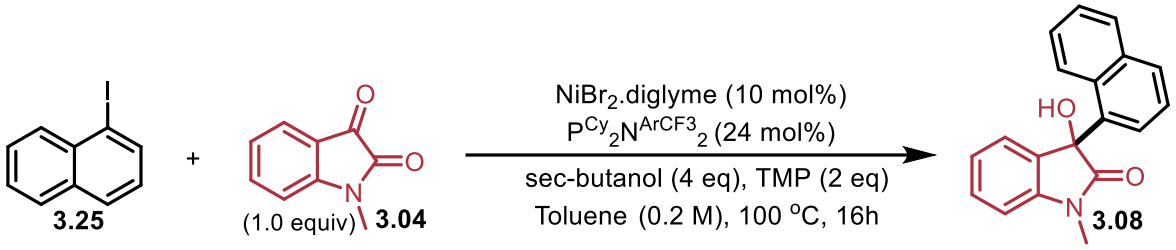

Entry	Deviation from standard conditions	Yield 3.08[a]
1	None	65%
2	$Ni^{(0)}(P^{Cy}{}_2N^{ArCF3}{}_2)_2$ as a catalyst	45%

General reaction conditions: aryl iodide (0.15 mmol), *N*-methyl isatin (0.15 mmol), TMP (0.30 mmol), *sec*-butanol (0.60 mmol), $NiBr_2$•diglyme (10 mol%), $P^{Cy}{}_2N^{ArCF3}{}_2$ (24 mol%) in PhMe (0.20 M), 100 °C for 16 h, under an inert atmosphere (set-up inside the glovebox). [a]Yields are calculated by ^1H NMR with 1,3,5-trimethoxybenzene as the internal standard.

We were exceptionally pleased to see that the $Ni^{(0)}(P^{Cy}{}_2N^{ArCF3}{}_2)_2$ behaves as a catalyst in this transformation and provides appreciable amounts of the desired product **3.08** (**entry 2**). The yield, however, was about 20% lower than the standard reaction (**entry 1**). To our knowledge, this is the first use of such a $Ni^{(0)}(P_2N_2)_2$ species being used in catalytic coupling, therefore, further investigation would be required to fully understand the role it plays in this transformation. A hypothetical mechanism for the reductive 1,2-arylation reaction starting from a $Ni^{(0)}(P_2N_2)_2$ complex, would resemble our proposed catalytic cycle previously discussed in Chapters 1 and 2. Presumably, one of the P_2N_2 ligands would fall off to generate a monoligated $Ni^{(0)}(P_2N_2)$ species that is coordinatively unsaturated to perform oxidative addition (**Scheme 41**).

Scheme 41: Proposed mechanism for the reductive 1,2-arylation of *N*-methyl isatin catalyzed by a $Ni^{(0)}(P_2N_2)_2$ complex

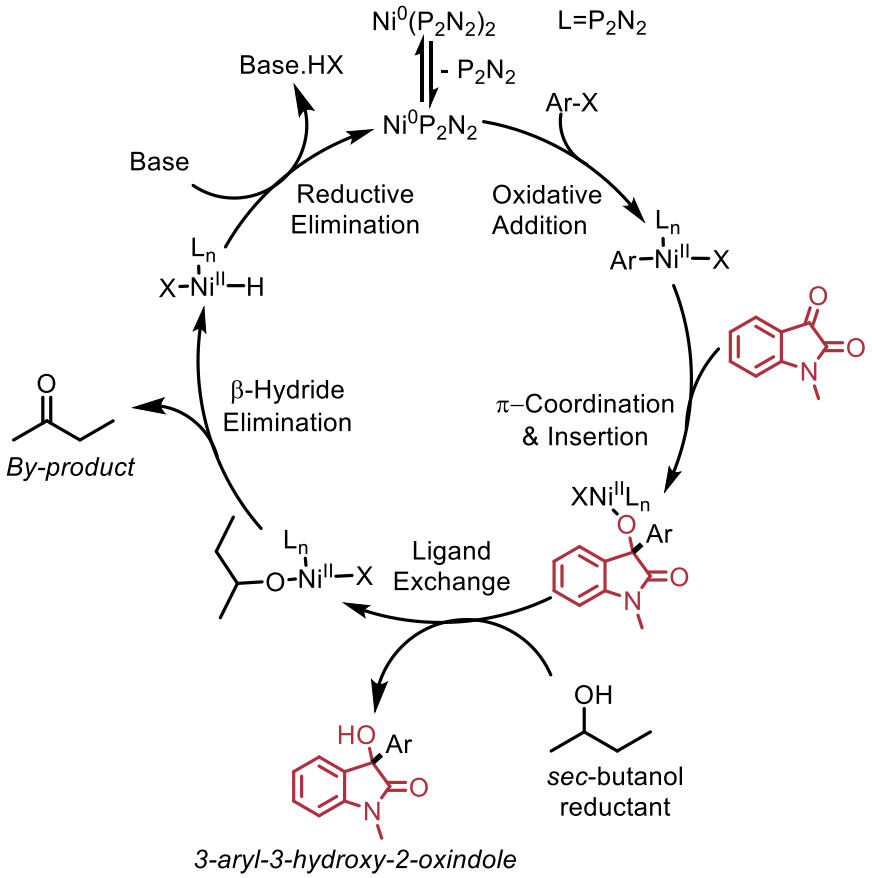

X-ray Crystal Structure of the $Ni^{(0)}(P_2N_2)_2$ complex

Our next aim was to get a better understanding of the structure of the complex we had synthesized and to prove that this species was in fact a nickel center with doubly ligated P_2N_2 ligands. For this, we needed to get an X-ray crystal structure of the complex. Unfortunately, any attempts to crystallize $Ni^{(0)}(P^{Cy}{}_2N^{ArCF3}{}_2)_2$ had failed and there was a lack of prior evidence in the literature that cyclohexyl phosphine containing metal-P_2N_2 complexes had been successfully crystallized.

We then decided to see if this transformation worked with a suboptimal P_2N_2 ligand, the complex of which can be crystallized. From our HTE experimentation we knew the reaction works in reduced yields with the $P^{Ph_2}N^{ArCF3_2}$ ligand. This compelled us to synthesise the $Ni^{(0)}(P^{Ph_2}N^{ArCF3_2})_2$ complex instead as shown in **Scheme 38**, and attempt its crystallization. **Table 26** demonstrates a comparison in yield between $P^{Cy_2}N^{ArCF3_2}$ and the $P^{Ph_2}N^{ArCF3_2}$ ligand as well as the $Ni^{(0)}(P^{Ph_2}N^{ArCF3_2})_2$ catalytic complex. Under our standard conditions, the yield for the desired alcohol **3.08** was 65% (**entry 1**) but when $P^{Ph_2}N^{ArCF3_2}$ is used as a ligand, the yield drops to 40% (**entry 2**). Using the $Ni^{(0)}(P^{Ph_2}N^{ArCF3_2})_2$ complex as a catalyst does give the desired product but further drops the yield to 25% (**entry 3**), which was comparatively less effective than the previously tested $Ni^{(0)}(P^{Cy_2}N^{ArCF3_2})_2$ complex (**entry 4**).

Table 26: Attempting the 1,2-arylation of *N*-methyl isatin with $Ni^{(0)}(P^{Ph}{}_2N^{ArCF3}{}_2)_2$

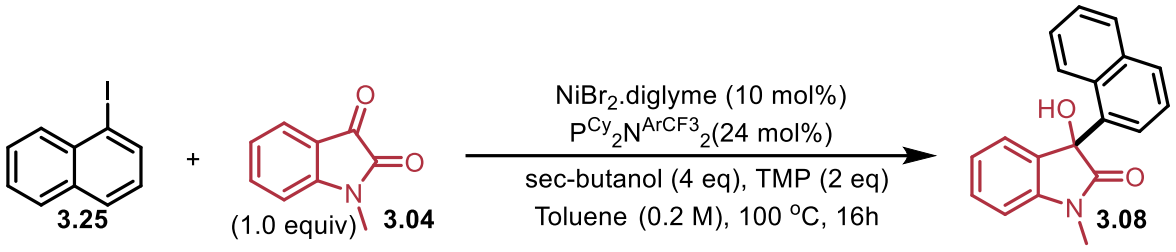

Entry	Deviation from standard conditions	Yield 3.08[a]
1	None	65%
2	$P^{Ph}{}_2N^{ArCF3}{}_2$ as a ligand	40%
3	$Ni^{(0)}(P^{Ph}{}_2N^{ArCF3}{}_2)_2$ as a catalyst	25%
4	$Ni^{(0)}(P^{Cy}{}_2N^{ArCF3}{}_2)_2$ as a catalyst	45%

General reaction conditions: aryl iodide (0.15 mmol), *N*-methyl isatin (0.15 mmol), TMP (0.30 mmol), *sec*-butanol (0.60 mmol), $NiBr_2$•diglyme (10 mol%), $P^{Cy}{}_2N^{ArCF3}{}_2$ (24 mol%) in PhMe (0.20 M), 100 °C for 16 h, under an inert atmosphere (set-up inside the glovebox). [a]Yields are calculated by ^1H NMR with 1,3,5-trimethoxybenzene as the internal standard.

Once we had established that the synthesised $Ni^{(0)}(P^{Ph}{}_2N^{ArCF3}{}_2)_2$ was catalytically active, albeit in lower yields, we attempted to crystallize it using literature procedures that have previously reported the crystallization of other phenyl phosphine containing metal-P_2N_2 complexes.

We were at last successful in obtaining crystals of the $Ni^{(0)}(P^{Ph}{}_2N^{ArCF3}{}_2)_2$ and were able to get a well-resolved X-ray crystal structure of the complex that we formed (**Figure 5**).

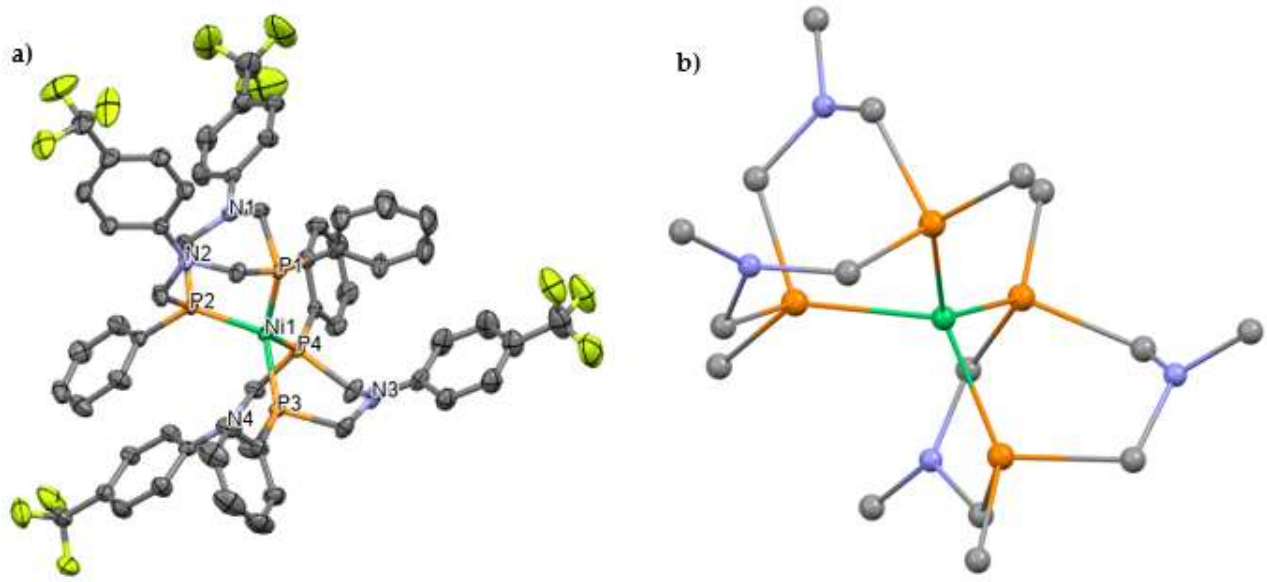

Figure 5: X-ray crystal diagrams of the $Ni^{(0)}(P^{Ph_2}N^{ArCF3_2})_2$ complex. a) X-ray crystal structure with phenyl rings shown and some atoms labeled. b) Simplified image with phenyl rings on the nitrogen and phosphorus atoms replaced by ipso carbons. Selected bond distances (A˚) and angles (°): Ni(1)–P(3), 2.133(6); Ni(1)–P(4), 2.142(8); P(1)–Ni(1)–P(2), 85.16(2); P(3)–Ni(1)–P(4), 85.05(3). Thermal ellipsoids are shown at the 40% probability level. For clarity, hydrogens and solvent molecules have been removed and carbon and fluorine atoms have not been labeled.

X-Ray diffraction studies were carried out on yellow crystals of $Ni^{(0)}(P^{Ph_2}N^{ArCF3_2})_2$ grown from a solution of acetonitrile and diethyl ether at -20 °C. The molecule has a distorted tetrahedral geometry with Ni–P bond lengths ranging from 2.13–2.14 Å and $P^{Ph_2}N^{ArCF3}$ bite angles of 85.2° and 85.1°.[74] From **Figure 5b**, it can be seen that three out of the four six-membered rings formed upon coordination of the diphosphine ligands to the nickel are in boat conformations, while one adopts a chair-like conformation. The average

non-bonding Ni· · ·N distance is 3.52 Å.[75] The phenyl rings on the two ligands seem to be rotated about 90° to one another and π-stacking as well as edge-on stacking of the phenyl substituents can be observed.

NMR experiment:

Once we had a better understanding of the structure of the active Ni catalytic complex, we wanted to see if we could observe changes in the ^{31}P (proton decoupled phosphorus-31) NMR spectrum at room temperature following the addition of nickel and an aryl iodide to the ligand in toluene-d_8 (**Figure 6**).

[75] Yang, J. Y.; Chen, S.; Dougherty, W. G.; Kassel, W. S.; Bullock, R. M.; DuBois, D. L.; Raugei, S.; Rousseau, R.; Dupuis, M.; DuBois, M. R. *Chem. Commun.* **2010**, *46*, 8618.

^{31}P[1H] NMR in toluene-*d*$_8$

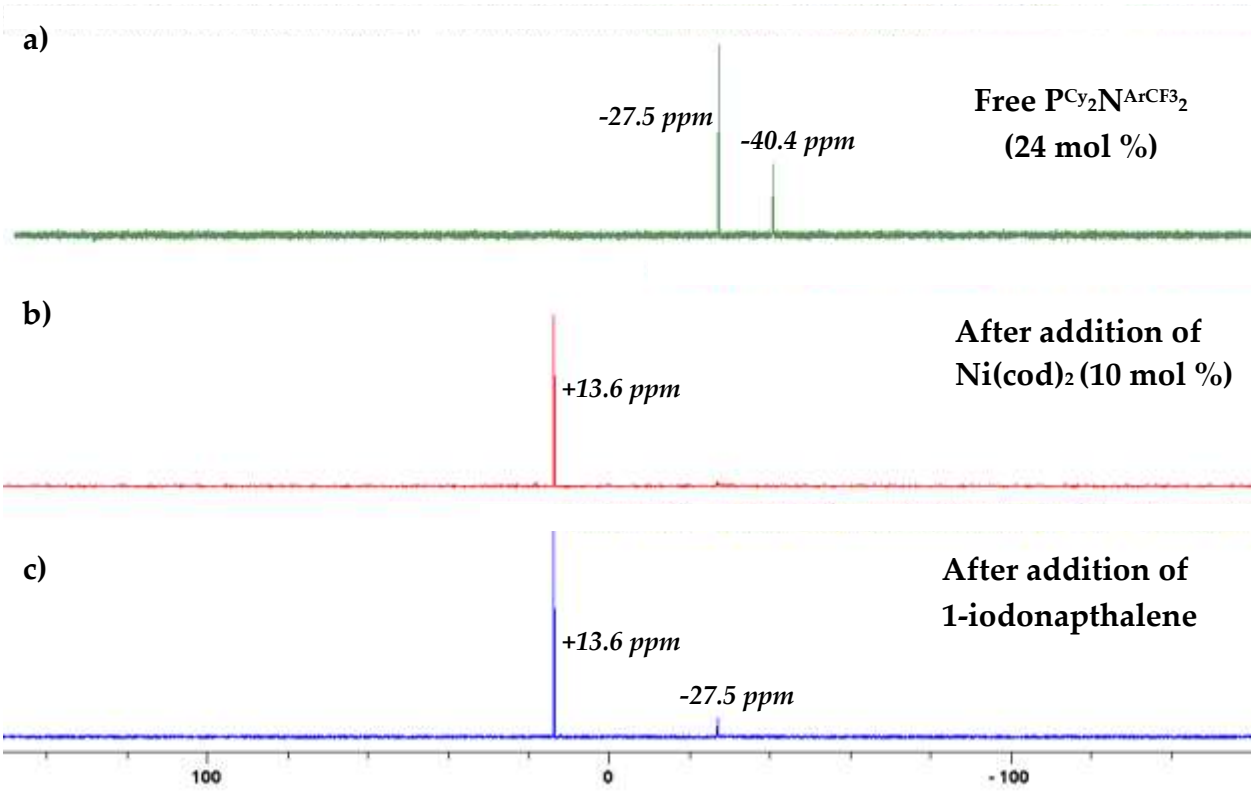

Figure 6: Overlay of the proton decoupled ^{31}P NMR spectra in toluene-*d*$_8$ for addition of 1-iodonapthalene. a) NMR spectrum for the free $P^{Cy_2}N^{ArCF_3{}_2}$ ligand. b) NMR spectrum after addition of Ni(0). c) NMR spectrum after addition of 1-iodonapthalene.

It was quite interesting to observe that following the addition of Ni(cod)$_2$ all of the free P_2N_2 ligates to the Ni(0). The peaks at **-27.5ppm** and **-40.4ppm** for the free P_2N_2 ligand represents the different conformations that this ligand can exist in. This was further evidence for the affinity of $P^{Cy_2}N^{ArCF_3{}_2}$ to bind to nickel because the peak at **+13.6ppm** matched the ^{31}P NMR spectrum for the $Ni^{(0)}(P^{Cy_2}N^{ArCF_3{}_2})_2$ isolated complex we synthesised (refer to **Appendix B**). We did not observe significant changes following the addition of 1-iodonapthalene, which is not very surprising since these experiments were conducted at room temperature and there is a possibility that the oxidative addition complex does not form at room temperature. We did, however, attempt high-temperature (100 ^{o}C)

NMR experiments hoping to see discernible changes in the phosphorus NMR that could be attributed to the oxidative-addition complex. Unfortunately, we only saw complete disappearance of peaks from the ^{31}P NMR spectra potentially due to peak broadening because of the formation of paramagnetic species.

We then went on to perform the same test as we did above on *N*-methyl isatin instead, where it was added to an NMR tube along with $Ni(cod)_2$ and $P^{Cy}{}_2N^{ArCF3}{}_2$ in toluene-d_8 and the change in the ^{31}P NMR spectra was tracked (**Figure 7**).

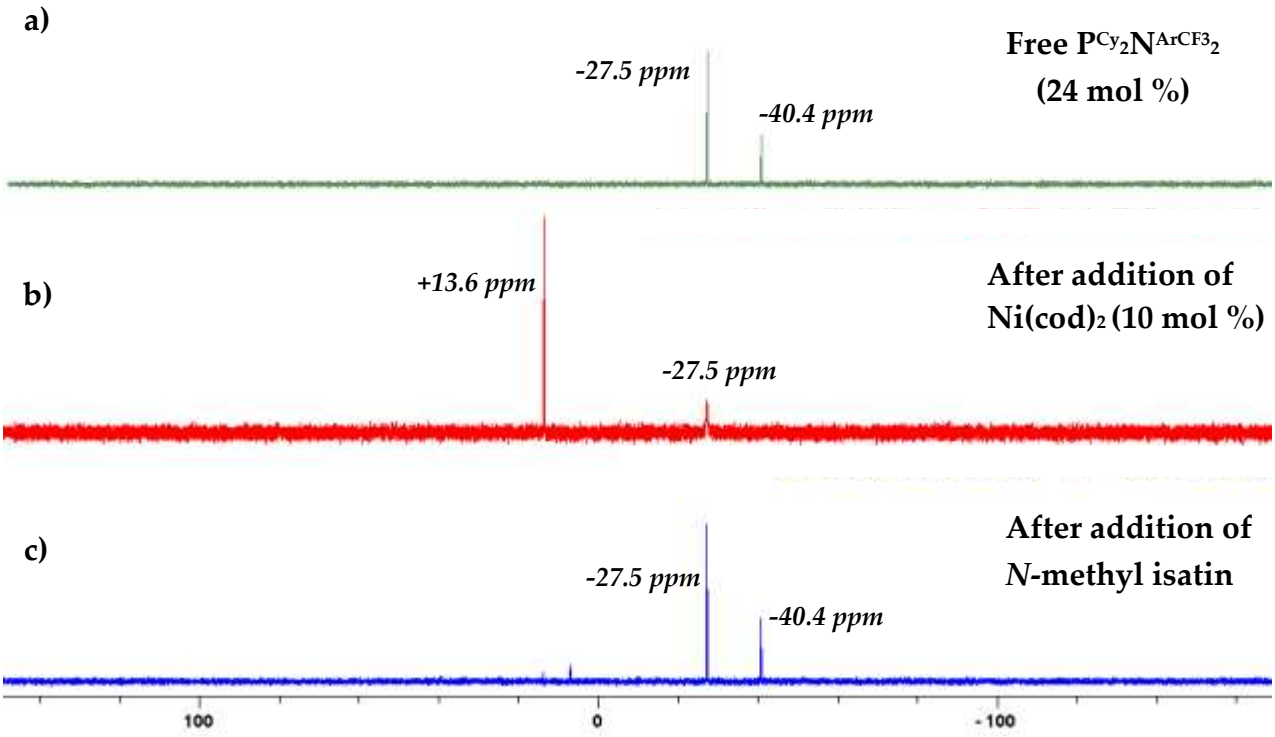

Figure 7: Overlay of the proton decoupled ^{31}P NMR spectra in toluene-d_8 for addition of *N*-methyl isatin. a) NMR spectrum for the free $P^{Cy_2}N^{ArCF_3{}_2}$ ligand. b) NMR spectrum after addition of Ni(0). c) NMR spectrum after addition of *N*-methyl isatin.

It was intriguing to observe the formation of a complex between *N*-methyl isatin and nickel. Following the addition of *N*-methyl isatin, it seems as though it completely displaces the ligand from the $Ni^{(0)}(P^{Cy_2}N^{ArCF_3{}_2})_2$ complex that forms in-situ because we predominantly see peaks corresponding to the unligated, free $P^{Cy_2}N^{ArCF_3{}_2}$. It should be noted, however, that in order to get quantitative values for the relative amounts of free and metal-bound ligand, a phosphorus internal standard should have been added. We were unable to find prior literature precedence for this type of complexation between α-ketoamides and nickel and so further experimentation would be required to fully understand the role of this complex formation in the mechanism of the experiment.

We had also originally aimed to synthesise and isolate an oxidative addition complex of the Ar-[$Ni^{II}(P_2N_2)$]-X species. We hypothesised that this complex, when employed stoichiometrically in our model reaction, might give rise to the desired 3-aryl-3-hydroxy-2-oxindole product, suggesting that oxidative addition of the aryl iodide potentially takes place before any other plausible step in the mechanism. However, our initial attempts to isolate and crystallize this complex failed and we were unable to obtain any meaningful data from those attempts.

3.4: Summary and Future work

3-Aryl-3-hydroxy-2-oxindoles, and their derivatives, are found in many natural products and pharmaceutical agents, and have a variety of biological activities.[76] Some commonly used metal-catalyzed methods of functionalizing the 3-position of isatins or oxindoles involve coupling with aryl boronic acids[77] or intramolecular ring-closure of α-keto amides containing a halide.[38] These methods have been discussed in **Chapter 1**. However, the direct intermolecular addition of aryl halides to isatins was previously elusive. In our work, we demonstrated a simple one-pot strategy for the reductive 1,2-adition of isatins and were able to create a decent scope with several interesting examples.

[76] Hewawasam, P.; Meanwell, N. A.; Gribkoff, V. K.; Dworetzky, S. I.; Biossard, C. G. *Bioorg. Med. Chem. Lett*. **1997**, 7, 1255.
[77] Toullec, P. Y.; Jagt, R. B. C.; de Vries, J. G.; Feringa, B. L.; Minnaard, A. *J. Org. Lett*. **2006**, *8*, 2715.

Although our method is quite robust, there are still some limitations which need to be addressed before we could envision this as being an industrially applicable strategy. For example, *N*-methylation of the isatin starting material adds an additional step to the overall synthetic procedure. In the future, we should aim to optimize further using unprotected isatins as starting materials (**Scheme 42**). Alternatively, we could also look at using boc-protected or acetylated substrates, that allow the synthesis of more complex isatins.

Scheme 42: Reductive 1,2-addition of unprotected isatins

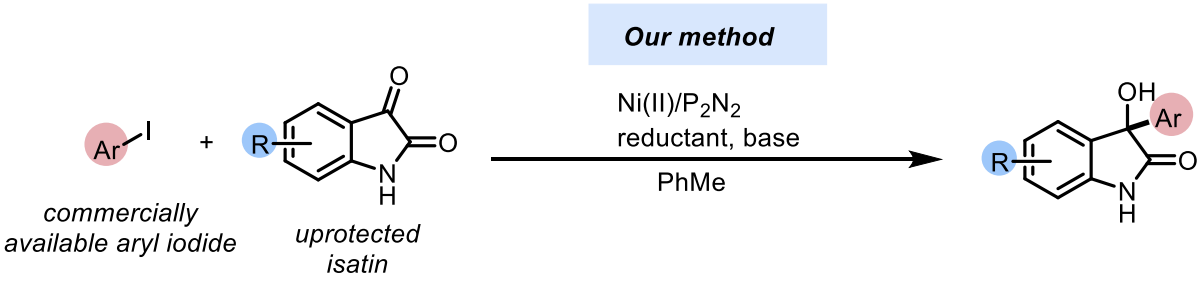

In our scope, we fell short of apsplying our methodology to the synthesis of drug precursor compounds or currently marketed pharmaceutical intermediates. Our goal going forward should be to explore the synthetic applicability of this transformation to access and derivatize bioactive compounds. **Scheme 43** shows the general synthesis of a patented BRD4 inhibitor which is studied for application in cancer treatment.[78] The patented synthesis of this drug involves the use of aryl magnesium bromide to

[78] GMBH BII, Engelhardt, H.; Gianni, D.; Mantoulidis, A.; Smethurst, C, eds. *Indoline analogs as BRD4 inhibitors.* **2014**; (WO2014/154760).

functionalize the carbonyl at the 3-position. Using our method, we could completely circumvent the need to use any stoichiometric organometallic reagents or harsh reaction conditions.

Scheme 43: Coupling of isatin with aryl halides to generate a pharmaceutically relevant compound

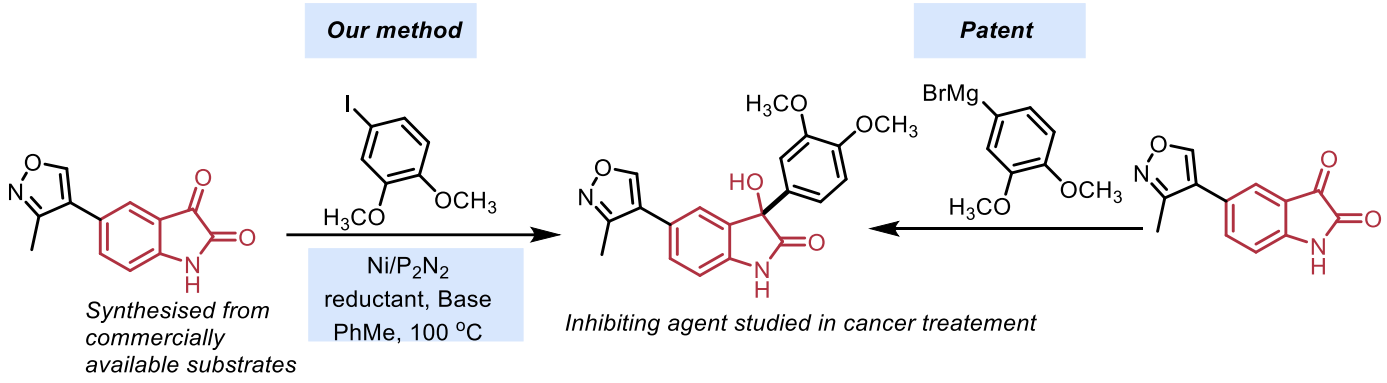

Since time constraints in this project left us with several unanswered mechanistic questions, our priority going forward is to understand the mechanism through extensive mechanistic investigations. Getting access to an isolated oxidative addition complex which we can characterize by NMR spectroscopy, mass spectrometry, and X-ray crystallography, and one that leads to product formation, would help us immensely in confirming our proposed catalytic cycle. According to our hypothesis, an equivalent of the P_2N_2 ligand must fall off for the metal to be coordinatively unsaturated and for the oxidative addition to take place. Quantitatively tracking the relative amounts of free and bound ligand could be a potential way to identify the presence of the oxidative-addition complex.

In conclusion, we discovered new reactivity with highly ubiquitous isatins, which are essentially cyclic α-ketoamides, and we were able to selectively functionalize the carbonyl at the 3-position while the neighbouring amide remained unaffected. This was an exciting HTE discovery for us and there is a lot still left to explore in this area. We also got a deeper understanding of the 3-dimensional structure of a $Ni^{(0)}(P_2N_2)_2$ complex by obtaining its X-ray crystal information and were able to demonstrate that it is catalytically active in our reaction.

3.5: Experimental

3.5.1: General experimental details

Unless otherwise indicated, reactions were conducted under an atmosphere of nitrogen in 8 mL screw-capped vials that were oven dried (120 °C) or flame dried and shipped into a glovebox. Column chromatography was either performed manually using Silicycle F60 40−63 μm silica gel or by using a Combiflash Rf+ automated chromatography system with commercially available Biotage normal-phase Silica Flash columns (35−70 μm). Analytical thin layer chromatography (TLC) was conducted with aluminum backed EMD Millipore Silica Gel 60 F_{254} pre-coated plates. Visualization of developed plates was performed under UV light (254 nm). For certain purifications, cerium ammonium molybdate (CAM) or potassium permanganate ($KMnO_4$) stains were used to better visualize the compounds on the TLC plates.

3.5.2: Instrumentation

^{1}H NMR and ^{13}C NMR were recorded on a Bruker AVANCEII 300 MHz spectrometer, a Bruker AVANCEII 400 MHz spectrometer, or a Bruker AVANCEIII 500 MHz spectrometer. ^{1}H NMR spectra were internally referenced to the residual solvent signal (e.g., $CDCl_3$ = 7.27 ppm). ^{13}C NMR spectra were internally referenced to the residual solvent signal (e.g., $CDCl_3$ = 77.00 ppm). Data for ^{1}H NMR are reported as follows: chemical shift (δ ppm), multiplicity (s = singlet, d = doublet, t = triplet, q = quartet, m = multiplet), coupling constant (Hz), integration. NMR yields for optimization studies were obtained by ^{1}H NMR analysis of the crude reaction mixture using 1,3,5-trimethoxybenzene as an internal standard. IR spectra were obtained using a Cary 630 FTIR (Agilent Technologies) and are reported in terms of frequency of absorption (cm^{-1}). Melting point ranges were determined on a Canlab Gallen Kamp Melting Point Apparatus. Accurate mass data (EI) was obtained from an Agilent 5977A GC/MSD using

MassWorks 4.0 from CERNO Bioscience.[1] HRMS data was obtained from a Micromass Q-TOF 2 quadrupole – time-of-flight mass spectrometer with ESI source.

3.5.3: Materials

Organic solvents were purified by rigorous degassing with nitrogen before passing through a PureSolv solvent purification system. Low water content was confirmed by Karl Fischer titration (<25 ppm for all solvents). Unless otherwise noted, reagents were used as received. $NiBr_2$•diglyme was purchased from Sigma Aldrich. Phenylphosphine was obtained as a 10% wt. solution in hexanes from Sigma Aldrich. Cyclohexylphosphine, isobutylphosphine and tertbutylphosphine were generously donated from Cytec-Solvay as neat liquids. Monophosphines were stored and used in the glovebox to avoid any reaction with oxygen. Commercial ligands were purchased from Sigma Aldrich, Combi-Blocks, and Strem Chemicals. 2,2,6,6-Tetramethylpiperidine (TMP) (99%) was obtained from Combi-Blocks. *S*ec-butanol was purchased from Acros Organics (97%) with no discernable difference between suppliers. Unless otherwise noted, all other commercially available starting materials were obtained from Sigma-Aldrich, TCI America, Fisher Scientific, Acros Organics, Alfa Aesar, Combi-Blocks, or Oakwood Chemicals and used as received.

3.5.4: General Procedure for the methylation of isatins:

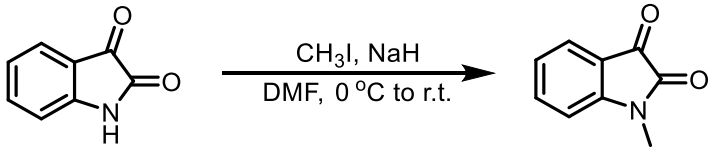

Isatins were all commercially obtained were subjected to methylation according to literature protocols.[79] Dissolve 3 mmol of the isatin (indolin-2,3-dione) starting material in 15 mL DMF. Cool the solution to 0 °C and then add NaH (3.5 mmol) in 3 equal portions.

[79] Ni, Q.; Wang, X.; Zeng, D.; Wu, Q.; Song, X. *Org. Lett.* **2021**, *23*, 2273–2278.

Stir for 5 minutes then add iodomethane (3.5 mmol). Stir the reaction at 0°C for 3 hours. Monitor by TLC. Pour the reaction mixture over saturated aqueous NH_4Cl. Extract with EtOAc. Wash the combined organic portions with water and brine. Dry, filter and concentrate.

3.5.5: Procedure for the synthesis of $Ni^0(P_2N_2)_2$

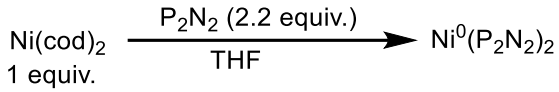

$Ni^0(P^{Cy}_2N^{ArCF3}_2)_2$ and **$Ni^0(P^{Ph}_2N^{ArCF3}_2)_2$** were synthesized using a modified literature procedure.[73] $Ni(cod)_2$ (50.6 mg, 0.181 mmol) in THF (2 mL) was added to a stirred slurry of the P_2N_2 ligand (0.362 mmol) in THF (5 mL). The solution was stirred overnight under an inert atmosphere in the glovebox and filtered through a plug of celite. The solvent was removed under vacuum on Schlenk line in a sealed Schlenk flask which was backfilled with argon post-evaporation. The dried powder was then crystallized.

$Ni^0(P^{Cy}_2N^{ArCF3}_2)_2$ crashed out after addition of MeCN to the dried residue and was isolated as a pale-yellow powder (100 mg, 44% yield). This fine powder was filtered, dried and used in the reaction. All attempts to crystallize this complex had failed. Note: **^{1}H NMR** (C_6D_6, 300 MHz) for this complex was paramagnetic and well-resolved peaks were not obtained. **^{19}F NMR** (C_6D_6, 282 MHz) δ -60.7, -60.9. **^{31}P{^{1}H}** (C_6D_6, 121 MHz) δ 19.4, 13.8.

$Ni^0(P^{Ph}_2N^{ArCF3}_2)_2$ was crystallized by addition of MeCN/Et_2O to the dried residue until it dissolved. The solution was kept in a -20 °C freezer under an inert atmosphere, up to a week. Shiny, bright-yellow crystals crashed out of the solution and were filtered and dried. They were submitted for X-ray crystal analysis and used directly in the reaction (85 mg, 38% yield). **^{1}H NMR** (C_6D_6, 300 MHz) δ 7.61-7.51 (m, 8H), 7.27 (d, J = 8.7 Hz, 8H), 7.04-6.99 (m, 4H), 6.95-6.87 (m, 8H), 6.53 (d, J = 8.7 Hz, 8H), 3.74-3.58 (m, 16H). **^{19}F NMR** (C_6D_6, 282 MHz) δ -60.9. **^{31}P{^{1}H}** (C_6D_6, 121 MHz) δ 5.8.

3.5.6: General Procedure for the reductive coupling of aryl iodides with *N*-methyl isatins

Inside the glovebox, to a dry 8 mL screw-capped reaction vial equipped with a magnetic stir bar, Ni source (0.10 equiv, 0.015 mmol) and ligand (0.24 equiv, 0.036 mmol) were added and dissolved in the reaction solvent (0.75 mL). Base (2 equiv, 0.3 mmol), aryl halide (1 equiv, 0.15 mmol), and *N*-methyl isatin (1 equiv, 0.15 mmol) were added to the stirring solution followed by the reducing agent (4 equiv, 0.6 mmol). The vial was capped, removed from the glovebox, and placed in a stirring (350 rpm) pre-heated mineral oil bath at 100 ^{o}C. After stirring for 16 hours, the reaction vial was removed from the oil bath and cooled down to room temperature. For optimization experiments, 1,3,5-Trimethoxybenzene (0.05 mmol) was added as an internal standard and the mixture was diluted with ethyl acetate. The reaction was filtered through a plug of silica gel with thin layers of sodium sulfate and celite at the bottom of the frit. For very polar products, a mixture of ethyl acetate and acetone was used to flush the compound off the silica gel. The filtrate was diluted to an appropriate concentration and analyzed by GC-MS. Solvent was removed *in vacuo* and the crude sample was analyzed with NMR spectroscopy. For scope examples, the sample was dry loaded onto silica by diluting with DCM, drying *in vacuo*, and then purifying by column chromatography.

3.5.7 Procedure for the ^{31}P NMR studies

These NMR studies were conducted at room temperature. High temperature NMR (100 ^{o}C) was attempted but led to paramagnetic NMR spectra. Inside the glovebox, to a dry screw-cap NMR tube $P^{Cy}{}_2N^{ArCF3}{}_2$ (0.24 equiv, 0.024 mmol) was added and dissolved in toluene-d^8 (0.2 M). The tube was sealed and shipped out of the glovebox followed by rigorous agitation on the vortex. The solution goes from a white suspension to a mostly homogenous solution. The NMR sample was analyzed on the Bruker AVANCEII 300 MHz spectrometer on the proton-decoupled ^{31}P method. The NMR tube was shipped back into the glovebox and Ni(cod)$_2$ (0.10 equiv, 0.01 mmol) was added. The tube was

sealed and shipped out of the glovebox and analyzed NMR spectrometry. The same preliminary steps were repeated and the starting material (aryl iodide or *N*-methyl isatin (1.0 equiv, 0.10 mmol)) was added (Figures 6 and 7). The NMR studies were conducted at room temperature. Note: Although not shown as part of Figures 6 and 7, addition of base (2.0 equiv, 0.2 mmol) led to no change in the appearance and relative intensity of the peaks observed. When the reducing agent (3 equiv, 0.30 mmol) was added, several uncharacterizable and unidentifiable peaks were observed suggesting the formation of different of conformers of the ligand. A more extensive analysis would be required to identify each of the peaks observed.

3.5.8: Characterization for the reductive coupling of aryl iodides and *N*-methyl isatin

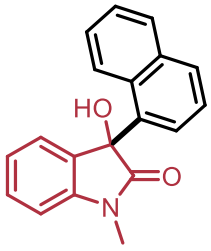

3-hydroxy-1-methyl-3-(naphthalen-1-yl) oxindole (3.08) was prepared according to the general procedure. The product was purified by column chromatography using a gradient of 5→40% EtOAc in hexanes to afford **3.08** as a colourless oil (28.6 mg, 66% yield). **^{1}H NMR** ($CDCl_3$, 400 MHz) δ 7.91 (d, J = 7.0 Hz, 1H), 7.86-7.83 (m, 3H), 7.51-7.47 (m, 1H), 7.45-7.41 (m, 1H), 7.39-7.35 (m, 2H), 7.25 (d, J = 7.1 Hz, 1H), 7.02-6.98 (m, 2H), 3.41 (s, 3H), 3.26 (brs, 1H). **^{13}C NMR** ($CDCl_3$, 100 MHz) δ 177.4, 143.4, 135.6, 134.4, 131.4, 130.2, 129.7, 129.1, 126.4, 125.6, 125.0, 124.9, 124.7,124.3, 123.6, 109.0, 77.2, 26.7. Characterization of **3.08** matched previously reported spectra.[38]

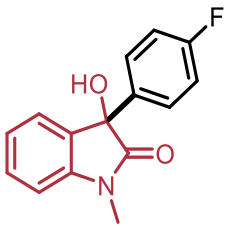

3-(4-fluorophenyl)-3-hydroxy-1-methylindolin-2-one (3.09) was prepared according to the general procedure. The product was purified by column chromatography with a gradient of 0%→30% EtOAc in hexanes to afford **3.09** as a white solid (35.1 mg, 91% yield). **^{1}H NMR** ($CDCl_3$, 400 MHz) δ 7.39-7.33 (m, 3H), 7.28-7.26 (m, 1H), 7.11 (t, J = 7.5 Hz, 1H), 7.03-6.97 (m, 2H), 6.92 (d, J = 7.8 Hz, 1H), 3.83 (br s, 1H), 3.24 (s, 3H).**^{13}C NMR** ($CDCl_3$, 100 MHz) δ 177.4, 162.7 (d, J = 249 Hz), 143.4, 135.9 (d, J = 3.3 Hz), 131.4, 130.0, 127.4 (d, J = 8.5 Hz), 124.9, 123.7, 115.4 (d, J = 20.2 Hz), 108.0, 77.5, 26.6. **^{19}F NMR** ($CDCl_3$, 377 MHz) δ -113.9. Characterization of **3.09** matched previously reported spectra.[80]

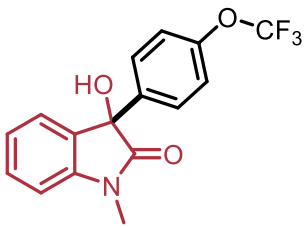

3-(4-(trifluoromethoxy)phenyl)-3-hydroxy-1-methylindolin-2-one (3.10) was prepared according to the general procedure. The product was purified by column chromatography using a gradient of 5%→45% EtOAc in hexanes to afford **3.10** as a pale-yellow solid (21.8 mg, 65% yield). **^{1}H NMR** ($CDCl_3$, 400 MHz) δ 7.43-7.31 (m, 3H), 7.28 (d, J = 6.5 Hz, 1H), 7.17-7.10 (m, 3H), 6.93 (d, J = 8.0 Hz, 1H), 3.67 (br s, 1H), 3.25 (s, 3H). **^{13}C NMR** ($CDCl_3$, 100 MHz) δ 177.2, 149.1, 143.4, 138.7, 131.2, 130.2, 127.2, 124.5 (d, J = 120 Hz), 121.7, 120.9, 119.1, 108.9, 77.5, 26.6. **^{19}F NMR** ($CDCl_3$, 377 MHz) δ -57.8. **Accurate mass (EI):** $H_{12}C_{16}F_3NO_3$ Theoretical: 323.0769. Found: 323.0647. Spectral Accuracy: 95.6%.

[80] Tang, R.-Y.; Zheng, W.-X.; Liao, Y.-Y.; Xu, L. *Synthesis.* **2018**, *50*, 4645–4650.

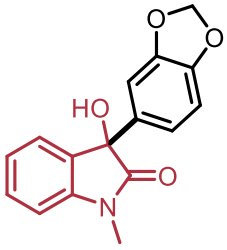

3-(benzo[*d*][1,3]dioxol-5-yl)-3-hydroxy-1-methylindolin-2-one (3.11) was prepared according to the general procedure. The product was purified by column chromatography using a gradient of 0%→20% EtOAc in hexanes to afford **3.11** as a white solid (30.7 mg, 72% yield). **^{1}H NMR** ($CDCl_3$, 400 MHz) δ 7.36 (td, J = 7.8 Hz, 1.2 Hz, 1H), 7.29 (dd, J = 7.4 Hz, 0.7 Hz, 1H), 7.10 (td, J = 7.5 Hz, 0.9 Hz, 1H), 6.92-6.89 (m, 2H), 6.83 (dd, J = 8.0 Hz, 1.8 Hz, 1H), 6.74-6.72 (m, 1H), 5.94 (dd, 3.2 Hz, 1.4 Hz, 2H), 3.24 (s, 3H). **^{13}C NMR** ($CDCl_3$, 100 MHz) δ 177.4, 147.9, 147.7, 143.4, 133.9, 131.5, 129.9, 124.8, 123.6, 118.9, 108.7, 108.2, 106.4, 101.2, 76.7, 26.5. Characterization of **3.12** matched previously reported spectra.[38]

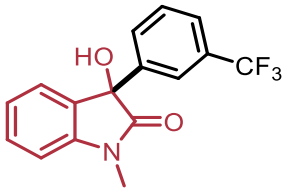

3-hydroxy-1-methyl-3-(3-(trifluoromethyl)phenyl)indolin-2-one (3.12) was prepared according to the general procedure. The product was purified by column chromatography using a gradient of 0% → 25% EtOAc in hexanes to afford **3.12** as a colourless oil (32.2 mg, 70% yield). **^{1}H NMR** ($CDCl_3$, 400 MHz) δ 7.71 (d, J = 0.6 Hz, 1H), 7.58-7.56 (m, 1H), 7.53-7.51 (m, 1H), 7.46-7.44 (m, 1H), 7.40 (td, J = 7.8 Hz, 1.8 Hz, 1H), 7.28-7.25 (m, 1H), 7.12 (td, J = 7.6 Hz, 0.9 Hz, 1H), 6.96 (d, J = 7.8 Hz, 1H), 3.45 (br s, 1H), 3.28 (s, 3H). **^{13}C NMR** ($CDCl_3$, 100 MHz) δ 176.9, 143.5, 141.2, 130.9, 130.8, 130.4, 129.1, 128.9, 125.4, 125.2 (d, J = 3.7 Hz), 124.9, 123.9, 122.3, (d, J = 3.8 Hz), 109.0, 77.6, 26.8. **^{19}F NMR** ($CDCl_3$, 377 MHz) δ -62.6. **Accurate mass (EI):** $H_{12}C_{16}F_3NO_2$ Theoretical: 307.0820. Found: 307.0815. Spectral Accuracy: 98.8%.

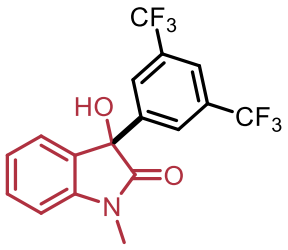

3-(3,5-bis(trifluoromethyl)phenyl)-3-hydroxy-1-methylindolin-2-one (3.13) was prepared according to the general procedure. The product was purified by column chromatography using a gradient of 0%→30% EtOAc in hexanes to afford **3.13** as a white solid (25.5 mg, 45% yield). **^{1}H NMR** ($CDCl_3$, 400 MHz) δ 7.82 (s, 3H), 7.44 (td, J = 7.7 Hz, 1.3 Hz, 1H), 7.25-7.22 (m, 1H), 7.17-7.13 (m, 1H), 6.99 (d, J = 7.8 Hz, 1H), 3.85 (br s, 1H), 3.29 (s, 3H). **^{13}C NMR** ($CDCl_3$, 100 MHz) δ 176.2, 143.1, (d, J = 66.2 Hz), 131.9 (d, J = 35.2 Hz), 130.9, 130.3, 126.1, 124.9, 124.5, 124.2, 122.4 (d, J = 3.5 Hz), 121.8, 109.3, 77.2, 26.8. **^{19}F NMR** ($CDCl_3$, 377 MHz) δ -62.8. Characterization of **3.13** matched previously reported spectra.[81]

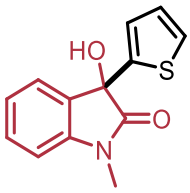

3-hydroxy-1-methyl-3-(thiophen-2-yl)indolin-2-one (3.14) was prepared according to the general procedure. The product was purified by column chromatography using a gradient of 0%→50% EtOAc in hexanes to afford **3.14** as a white solid (24.0 mg, 65% yield). **^{1}H NMR** ($CDCl_3$, 400 MHz) δ 7.54 (d, J = 7.9 Hz, 1H), 7.39 (td, J = 7.8 Hz, 1.2 Hz, 1H), 7.33 (dd, J = 5.2 Hz, 1.2 Hz, 1H), 7.16 (td, J = 7.8 Hz, 0.8 Hz, 1H), 7.00-6.98 (m, 1H), 6.89 (d, J = 7.8 Hz, 1H), 6.94-6.92 (m, 1H), 3.24 (s, 3H). **^{13}C NMR** ($CDCl_3$, 100 MHz) δ 176.1, 143.4, 143.2, 130.4, 130.3, 126.8, 126.7, 125.9, 125.0, 123.5, 108.8, 75.4, 26.6. Characterization of **3.14** matched previously reported spectra.[37]

[81] Hu, J. X.; Wu, H.; Li, C. Y.; Sheng, W. J.; Jia, Y. X.; Gao, J. R. *Chem. Eur. J.* **2011**, *17*, 5234–5237.

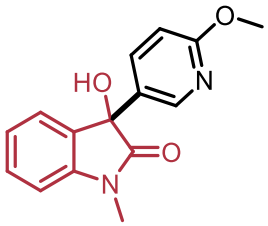

3-Hydroxy-1-methyl-3-(pyridine-5-yl-2-methoxy)-2-oxindole (3.15) was prepared according to the general procedure. The product was purified by column chromatography using a gradient of 0%→30% EtOAc in hexanes to afford **3.15** as a white solid (26.7 mg, 66% yield). **^{1}H NMR** ($CDCl_3$, 400 MHz) δ 8.07 (d, J = 2.5 Hz, 1H), 7.71 (dd, J = 8.7 Hz, 2.6 Hz, 1H), 7.40-7.33 (m, 2H), 7.13 (t, J = 7.5 Hz, 1H), 6.91 (d, J = 7.8 Hz, 1H), 6.72 (d, J = 8.7 Hz, 1H), 3.89 (s, 3H), 3.22 (s, 3H). **^{13}C NMR** ($CDCl_3$, 100 MHz) δ 177.0, 164.2, 144.4, 143.3, 136.7, 130.6, 130.2, 128.6, 125.0, 123.7, 110.9, 108.9, 76.3, 53.6, 26.6. 824, 790, 745, 695. **Accurate mass (EI)** $H_{14}C_{15}N_2O_3$ Theoretical: 270.1004. Found: 270.0999. Spectral Accuracy: 98.2%

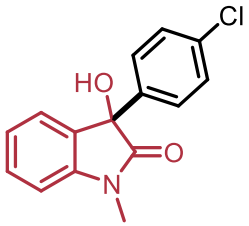

3-(4-chlorophenyl)-3-hydroxy-1-methylindolin-2-one (3.16) was prepared according to the general procedure. The product was purified by column chromatography using a gradient of 0%→30% EtOAc in hexanes to afford **3.16** as a colourless oil (30.0 mg, 73% yield). **^{1}H NMR** ($CDCl_3$, 400 MHz) δ 7.37 (td, J = 7.8 Hz, 1.3 Hz, 1H), 7.32 – 7.25 (m, 5H), 7.10 (td, J = 7.5 Hz, 0.9 Hz, 1H), 6.92 (d, J = 7.8 Hz, 1H), 3.81 (s, 1H), 3.24 (s, 3H). **^{13}C NMR** ($CDCl_3$, 100 MHz) δ 177.2, 143.4, 138.7, 134.3, 131.3, 130.1, 128.7, 126.9, 124.9, 123.7, 108.9, 77.6, 26.6. Characterization of **3.16** matched previously reported spectra.[38]

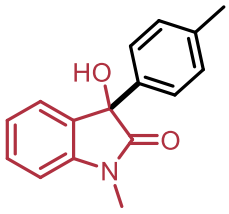

3-Hydroxy-1-methyl-3-p-tolyloxindole (3.17) was prepared according to the general procedure. The product was purified by column chromatography with using a gradient of 0%→30% EtOAc in hexanes to afford **3.17** as a white solid (28.6 mg, 75% yield). **^{1}H NMR** ($CDCl_3$, 400 MHz) δ 7.35 (td, J = 7.7 Hz, 1.3 Hz, 1H), 7.30-7.27 (m, 3H), 7.14-7.07 (m, 3H), 6.90 (d, J = 7.8 Hz, 1H), 3.67 (s, 1H), 3.24 (s, 3H), 2.33 (s, 3H). **^{13}C NMR** ($CDCl_3$, 100 MHz) δ 177.7, 143.5, 138.1, 137.2, 131.7, 129.8, 129.3, 125.3, 124.9, 123.5, 108.7, 77.9, 26.5, 21.1. Characterization of **3.17** matched previously reported spectra.[80]

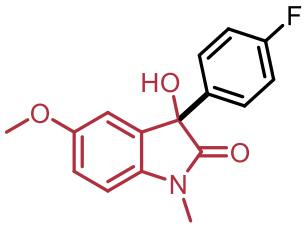

5-methoxy-1-methyl-3-(4-fluorophenyl)-3-hydroxy-2-oxindole (3.18) was prepared according to the general procedure. The product was purified by column chromatography using a gradient of 0%→55% EtOAc in hexanes to afford **3.18** as a yellow oil (35.0 mg, 82% yield). **^{1}H NMR** ($CDCl_3$, 400 MHz) δ 7.36-7.33 (m, 2H), 7.02-6.97 (m, 2H), 6.89-6.81 (m, 2H), 3.93 (br s, 1H), 3.56 (s, 3H), 3.20 (s, 3H). **^{13}C NMR** ($CDCl_3$, 100 MHz) δ 177.2, 162.7 (d, J = 250 Hz), 156.7, 136.7, 135.9 (d, J = 3.0 Hz), 127.4 (d, J = 8.3 Hz), 115.6 (d, J = 21.9 Hz), 114.7, 111.7, 109.3, 77.9, 55.8, 26.6. **^{19}F NMR** ($CDCl_3$, 377 MHz) δ -113.9. **Accurate mass (EI)** $H_{14}C_{16}FNO_3$ Theoretical: 287.0958. Found: 287.1091. Spectral Accuracy: 97.1%

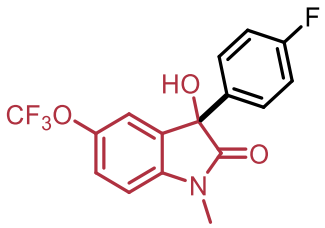

5-trifluoromethoxy-1-methyl-3-(4-fluorophenyl)-3-hydroxy-2-oxindole (3.19) was prepared according to the general procedure. The product was purified by column chromatography using a gradient of 0%→55% EtOAc in hexanes to afford **3.19** as a yellow-orange oil (20.5 mg, 40% yield). **^{1}H NMR** ($CDCl_3$, 400 MHz) δ 7.38-7.34 (m, 2H), 7.26-7.24 (m, 1H), 7.18-7.17 (m, 1H), 7.07-7.02 (m, 2H), 6.91 (d, J = 8.3 Hz, 1H), 3.27 (s, 3H). **^{13}C NMR** ($CDCl_3$, 100 MHz) δ 142.0, 132.7, 127.3, 127.2, 123.1, 118.9, 115.9, 115.6, 109.4, 77.5, 77.2, 26.8 (2 peaks were not resolved). **^{19}F NMR** ($CDCl_3$, 377 MHz) δ -113.0, -58.9. **Accurate mass (EI)** $H_{11}C_{16}F_4NO_2$ Theoretical: 341.0675. Found: 341.0670. Spectral Accuracy: 97.8%

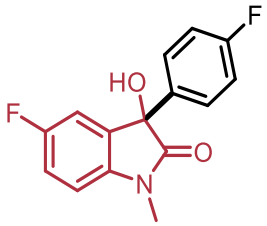

5-fluoro-1-methyl-3-(4-fluorophenyl)-3-hydroxy-2-oxindole (3.20) was prepared according to the general procedure. The product was purified by column chromatography using a gradient of 0%→35% EtOAc in hexanes to afford **3.20** as an orange solid (33.0 mg, 80% yield). **^{1}H NMR** ($CDCl_3$, 400 MHz) δ 7.35-7.31 (m, 2H), 7.09-6.98 (m, 4H), 6.86-6.83 (m, 1H), 4.06 (br s, 1H), 3.22 (s, 3H). **^{13}C NMR** ($CDCl_3$, 100 MHz) δ 177.3, 162.7 (d, J = 248.0 Hz), 159.7 (d, J = 245.0 Hz), 139.2, 135.4 (d, J = 3.0 Hz), 133.0 (d, J = 8.1 Hz), 127.3 (d, J = 8.3 Hz), 116.3 (d, J = 23.8 Hz), 115.6 (d, J = 21.8 Hz), 113.1 (d, J = 27.1 Hz), 109.5 (d, J = 7.7 Hz), 77.7, 26.7. **^{19}F NMR** ($CDCl_3$, 377 MHz) δ -113.4, -118.7. **Accurate mass (EI)** $H_{11}C_{15}F_2NO_2$ Theoretical: 275.0758. Found: 275.0752. Spectral Accuracy: 98.7%

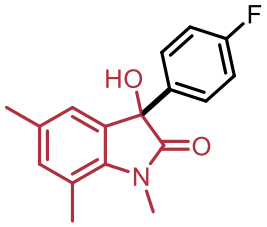

5,7-dimethyl-3-(4-fluorophenyl)-3-hydroxy-1-methyl-2-oxindole

(3.21) was prepared according to the general procedure. The product was purified by column chromatography using a gradient of 0%→25% EtOAc in hexanes to afford **3.21** as a pale-yellow solid (32.1 mg, 75% yield). **^{1}H NMR** ($CDCl_3$, 400 MHz) δ 7.36-7.31 (m, 2H), 7.02-6.96 (m, 2H), 6.89 (d, J = 3.3 Hz, 2H), 3.70 (br s, 1H), 3.48 (s, 3H), 2.56 (s, 3H), 2.24 (s, 3H). **^{13}C NMR** ($CDCl_3$, 100 MHz) δ 178.2, 162.4, 138.5, 136.4 (d, J = 3.8 Hz), 134.1, 133.3, 132.3, 127.3 (d, J = 8.9 Hz), 123.5, 120.2, 115.3 (d, J = 21.3 Hz), 77.3, 29.9, 20.7, 18.9. **^{19}F NMR** ($CDCl_3$, 377 MHz) δ -114.2. **Accurate mass (EI)** $H_{16}C_{17}FNO_2$ Theoretical: 285.3184. Found: 285.1384. Spectral Accuracy: 95.9%

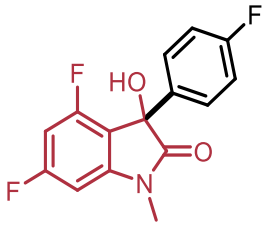

4,6-difluoro-3-(4-fluorophenyl)-3-hydroxy-1-methyl-2-oxindole

(3.22) was prepared according to the general procedure. The product was purified by column chromatography using a gradient of 0%→35% EtOAc in hexanes to afford **3.22** as a yellow-orange solid (22.9 mg, 52% yield). **^{1}H NMR** ($CDCl_3$, 400 MHz) δ 7.41-7.38 (m, 2H), 7.05-7.01 (m, 2H), 6.55-6.49 (m, 2H), 3.69 (br s, 1H), 3.22 (s, 3H). **^{13}C NMR** ($CDCl_3$, 100 MHz) δ 176.6, 165.9 (d, J = 12.9 Hz), 164.2, 163.4 (d, J = 13.0 Hz), 161.7, 160.4, (d, J = 13.9 Hz), 157.9 (d, J = 14.0 Hz), 146.2 (t, J = 10.8 Hz), 127.4 (d, J = 10.9 Hz), 115.5 (d, J = 22.0 Hz), 99.0 (t, J = 28.9 Hz), 94.4 (d, J = 3.8 Hz), 94.1 (d, J = 3.9 Hz), 27.1. **^{19}F NMR** ($CDCl_3$, 377 MHz) δ -104.8, -112.9. **Accurate mass (EI)** $H_{10}C_{15}F_3NO_2$ Theoretical: 293.0664. Found: 293.0692. Spectral Accuracy: 97.5%

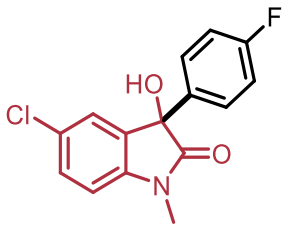

5-chloro-3-(4-fluorophenyl)-3-hydroxy-1-methyl-2-oxindole (3.23) was prepared according to the general procedure. The product was purified by column chromatography using a gradient of 0%→30% EtOAc in hexanes to afford **3.23** as a colourless oil (21.8 mg, 50% yield). **^{1}H NMR** ($CDCl_3$, 400 MHz) δ 7.36-7.33 (m, 3H), 7.25 (d, J = 2.1 Hz, 1H), 7.05-6.98 (m, 2H), 6.84 (d, J = 8.3 Hz, 1H), 3.73 (s, 1H), 3.24 (s, 3H). **^{13}C NMR** ($CDCl_3$, 100 MHz) δ 177.0, 162.8 (d, J = 248.0 Hz), 141.9, 135.3 (d, J = 3.1 Hz), 132.9, 129.5, 129.0, 127.3 (d, J = 8.7 Hz), 125.5, 115.7 (d, J = 22.0 Hz), 109.8, 77.5, 26.7. **^{19}F NMR** ($CDCl_3$, 377 MHz) δ -113.2. Characterization of **3.23** matched previously reported spectra.[82]

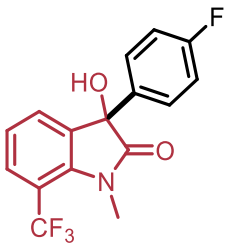

7-trifluoromethyl-3-(4-fluorophenyl)-3-hydroxy-1-methyl-2-oxindole (3.24) was prepared according to the general procedure. The product was purified by column chromatography using a gradient of 0%→15% EtOAc in hexanes to afford **3.24** as a pale-yellow oil (26.8 mg, 55% yield). **^{1}H NMR** ($CDCl_3$, 400 MHz) δ 7.66 (dd, J = 8.1 Hz, 1.0 Hz, 1H), 7.45 (dd, J = 7.4 Hz, 0.9 Hz, 1H), 7.36-7.31 (m, 2H), 7.18 (t, J = 7.8 Hz, 1H), 7.06-7.01 (m, 2H), 3.47 (s, 3H), 3.37 (br s, 1H). **^{13}C NMR** ($CDCl_3$, 100 MHz) δ 178.1, 164.1, 141.1, 135.3, 135.2, 133.9, 128.5, 127.9 (d, J = 5.8 Hz), 127.8, 127.2 (d, J = 8.5 Hz), 123.1, 115.8 (d, J = 21.6 Hz), 75.7, 29.3. **^{19}F NMR** ($CDCl_3$, 377 MHz) δ -53.3, -113.0.

[82] Yamamoto, Y.; Yohda, M.; Shirai, T.; Ito, H.; Miyaura, N. *Chem. Asian. J.* **2012**, *7*, 2446–2449.

Accurate mass (EI) $H_{11}C_{16}F_4NO_2$ Theoretical: 325.0726. Found: 325.0720. Spectral Accuracy: 98.6 %

Appendix A: NMR Spectra for Chapter 2

1,5-bis(*p*-benzotrifluoride)-3,7-bis(cyclohexyl)-1,5,3,7-diazadiphosphacyclooctane ($P^{Cy}N^{ArCF3}$)$_2$, ^{1}H, $CDCl_3$, 500 MHz, mixture of rotomers

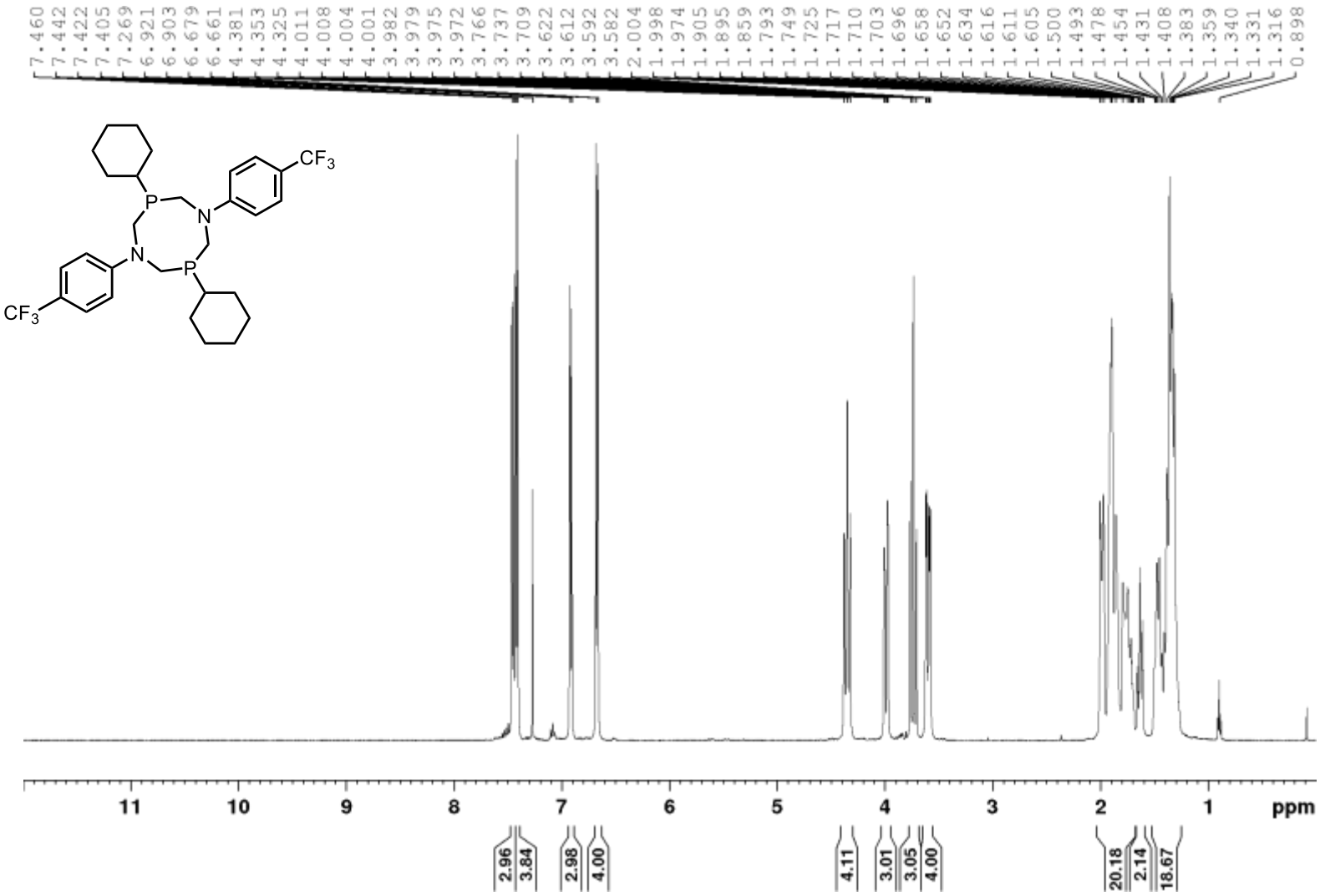

1,5-bis(*p*-benzotrifluoride)-3,7-bis(cyclohexyl)-1,5,3,7-diazadiphosphacyclooctane ($P^{Cy}N^{ArCF3}$)$_2$, ^{13}C, $CDCl_3$, 126 MHz, mixture of rotomers

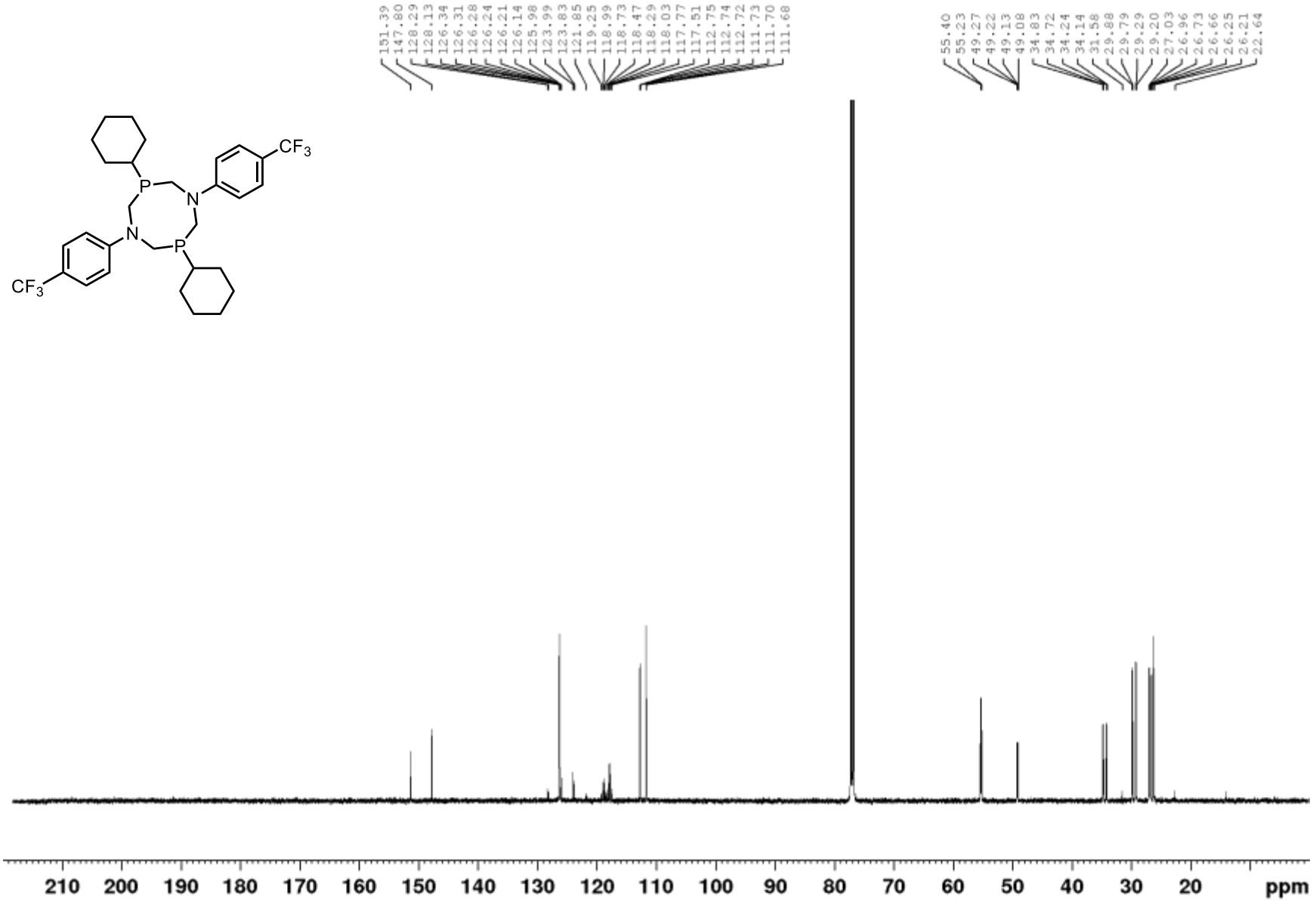

1,5-bis(*p*-benzotrifluoride)-3,7-bis(cyclohexyl)-1,5,3,7-diazadiphosphacyclooctane ($P^{Cy}N^{ArCF3}$)$_2$, ^{19}F, $CDCl_3$, 470 MHz, mixture of rotomers

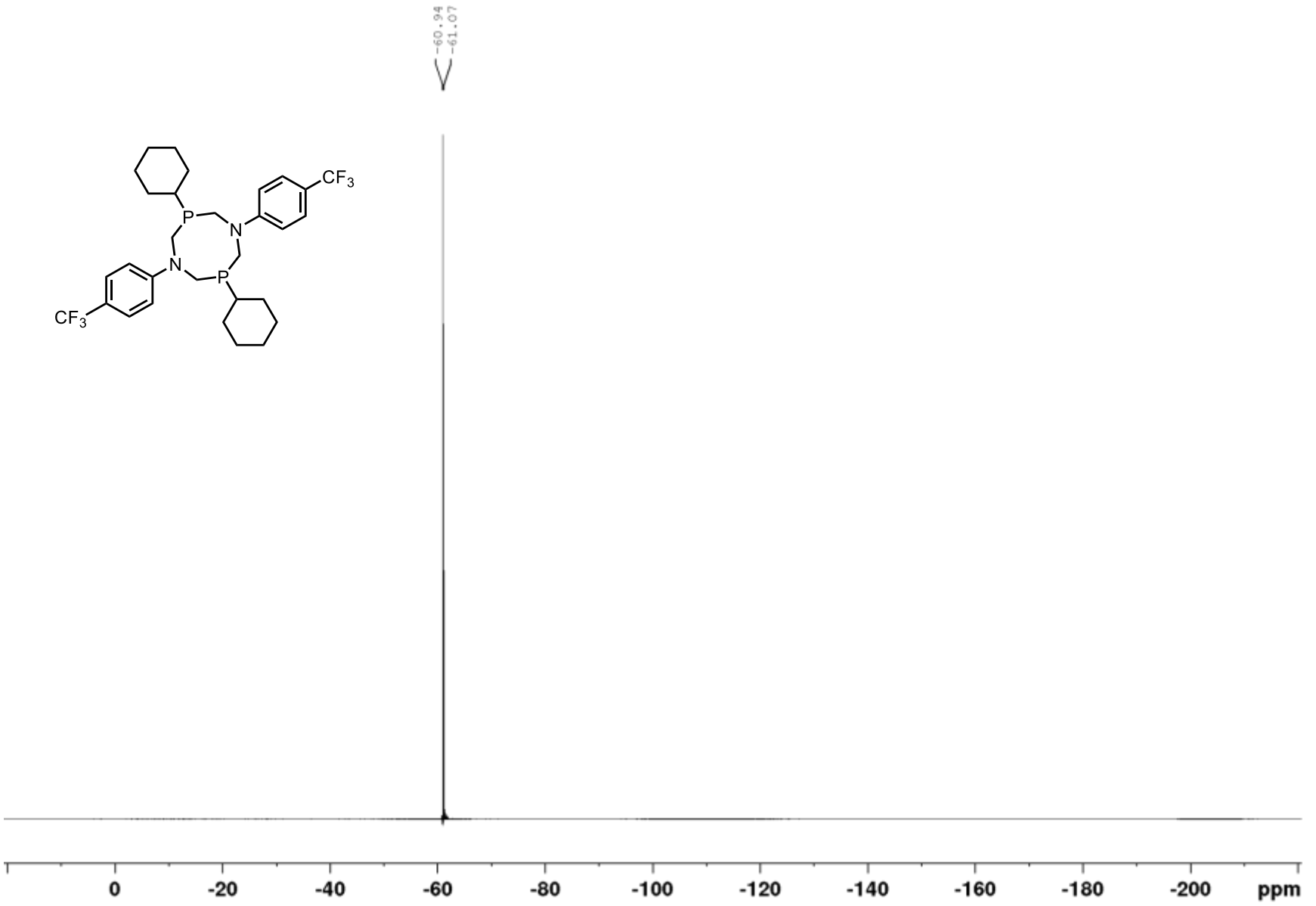

1,5-bis(*p*-benzotrifluoride)-3,7-bis(cyclohexyl)-1,5,3,7-diazadiphosphacyclooctane ($P^{Cy}N^{ArCF3}$)$_2$, ^{31}P, $CDCl_3$, 202 MHz, mixture of rotomers

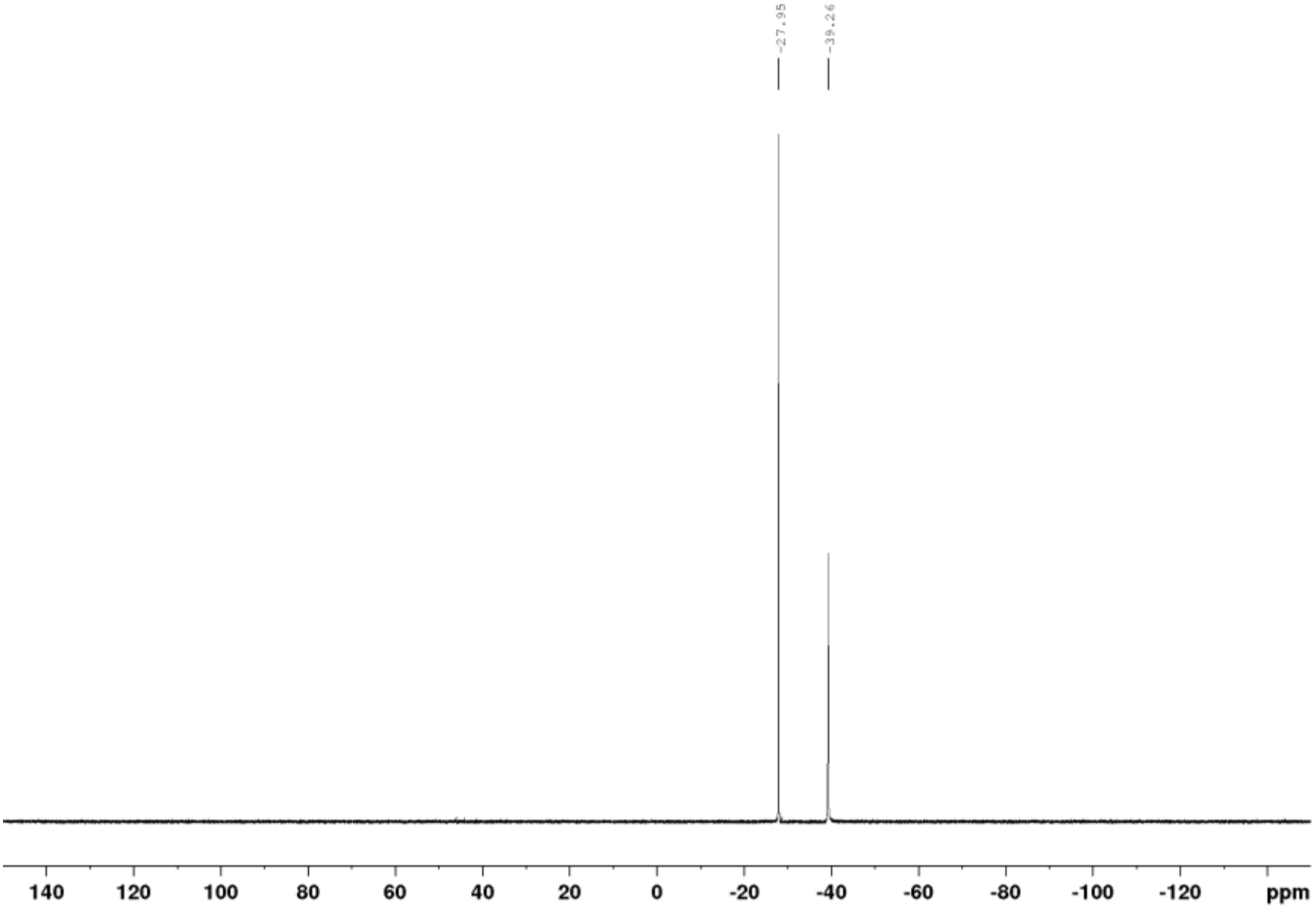

1,5-bis(*p*-benzotrifluoride)-3,7-bis(phenyl)-1,5,3,7-diazadiphosphacyclooctane ($P^{Ph}N^{ArCF3}$)$_2$, ^{1}H, C_6D_6, 300 MHz

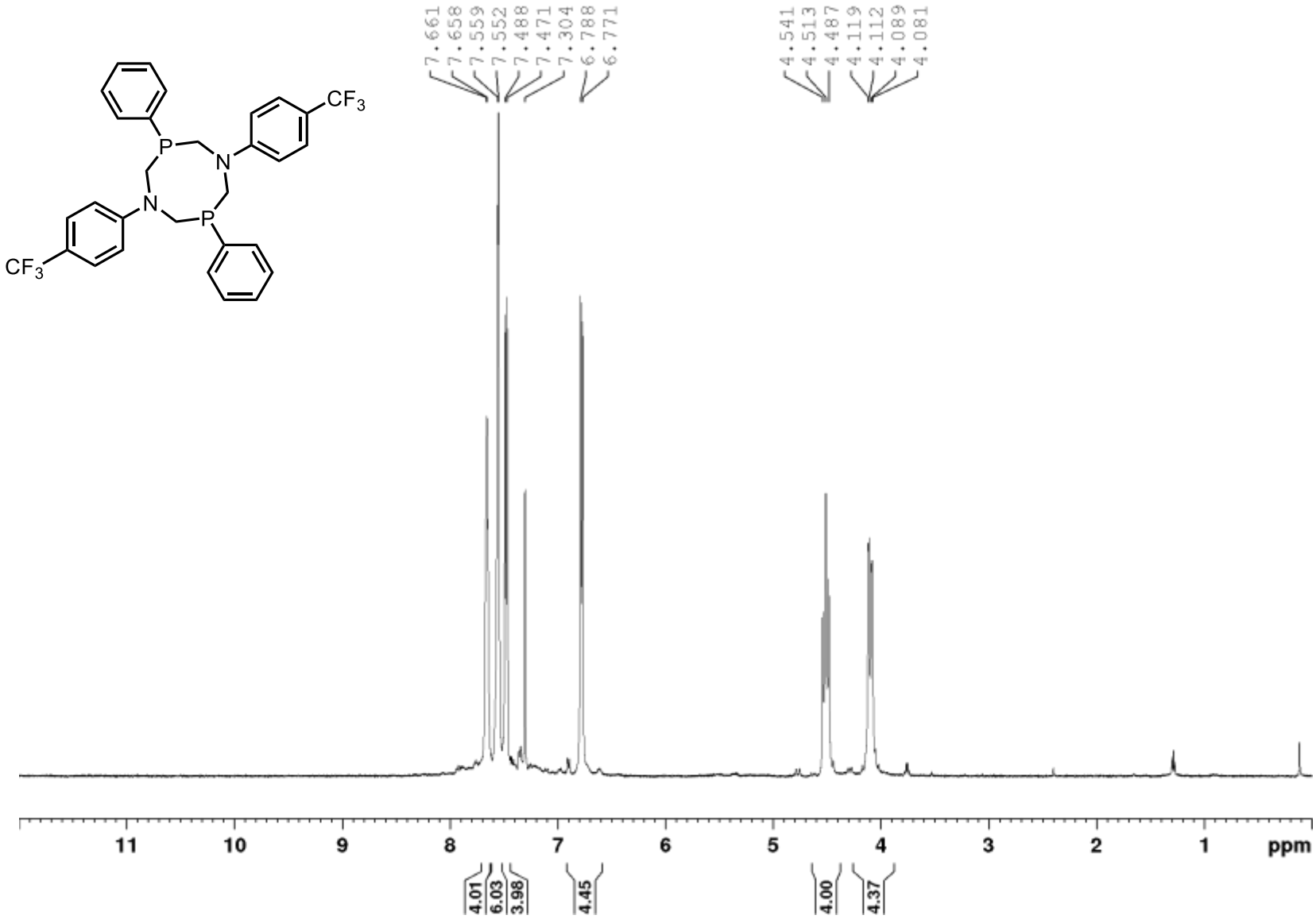

1,5-bis(*p*-benzotrifluoride)-3,7-bis(phenyl)-1,5,3,7-diazadiphosphacyclooctane ($P^{Ph}N^{ArCF3}$)$_2$, ^{19}F, C_6D_6, 282 MHz

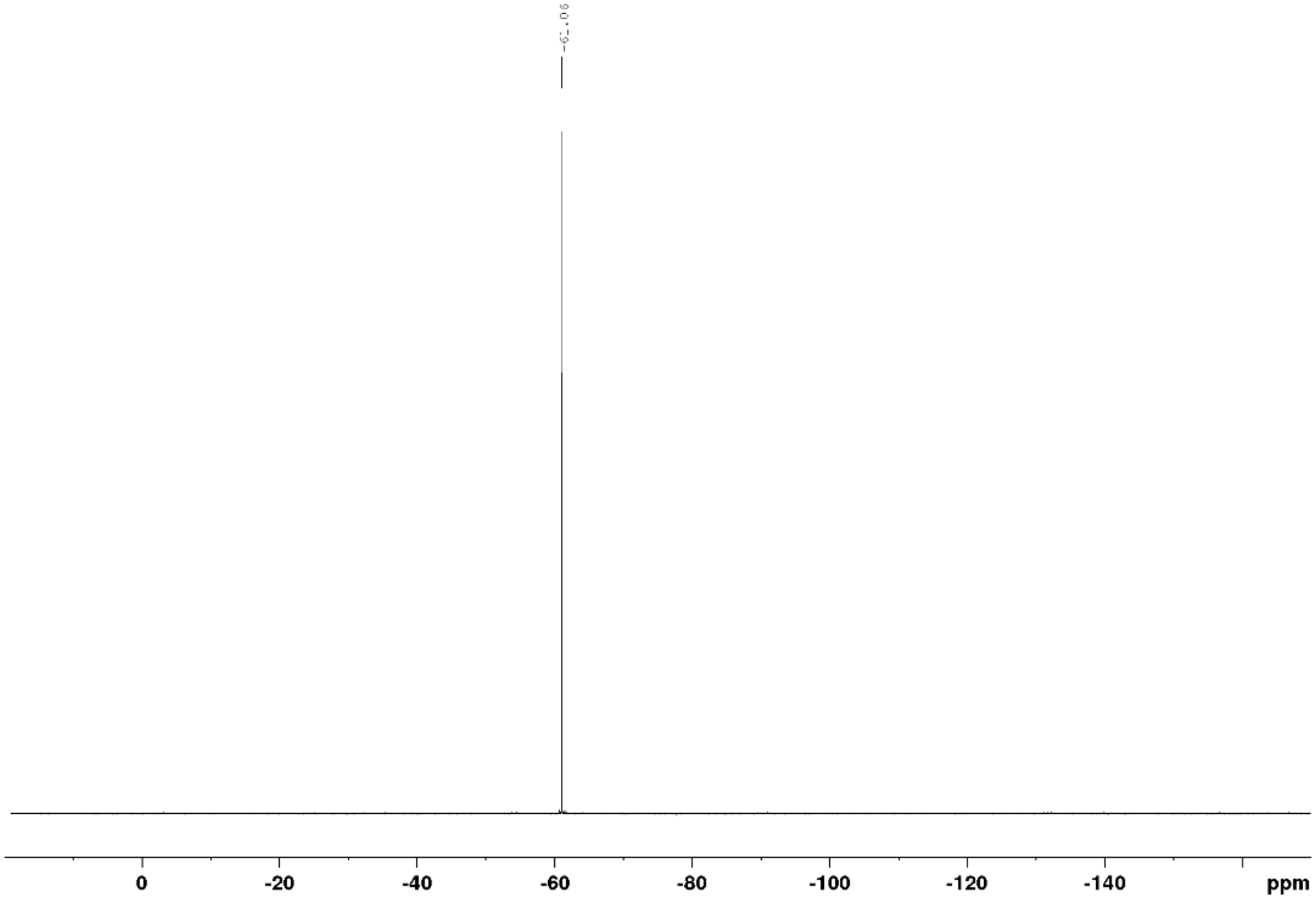

1,5-bis(*p*-benzotrifluoride)-3,7-bis(phenyl)-1,5,3,7-diazadiphosphacyclooctane ($P^{Ph}N^{ArCF3}$)$_2$, ^{31}P, C_6D_6, 121.5 MHz

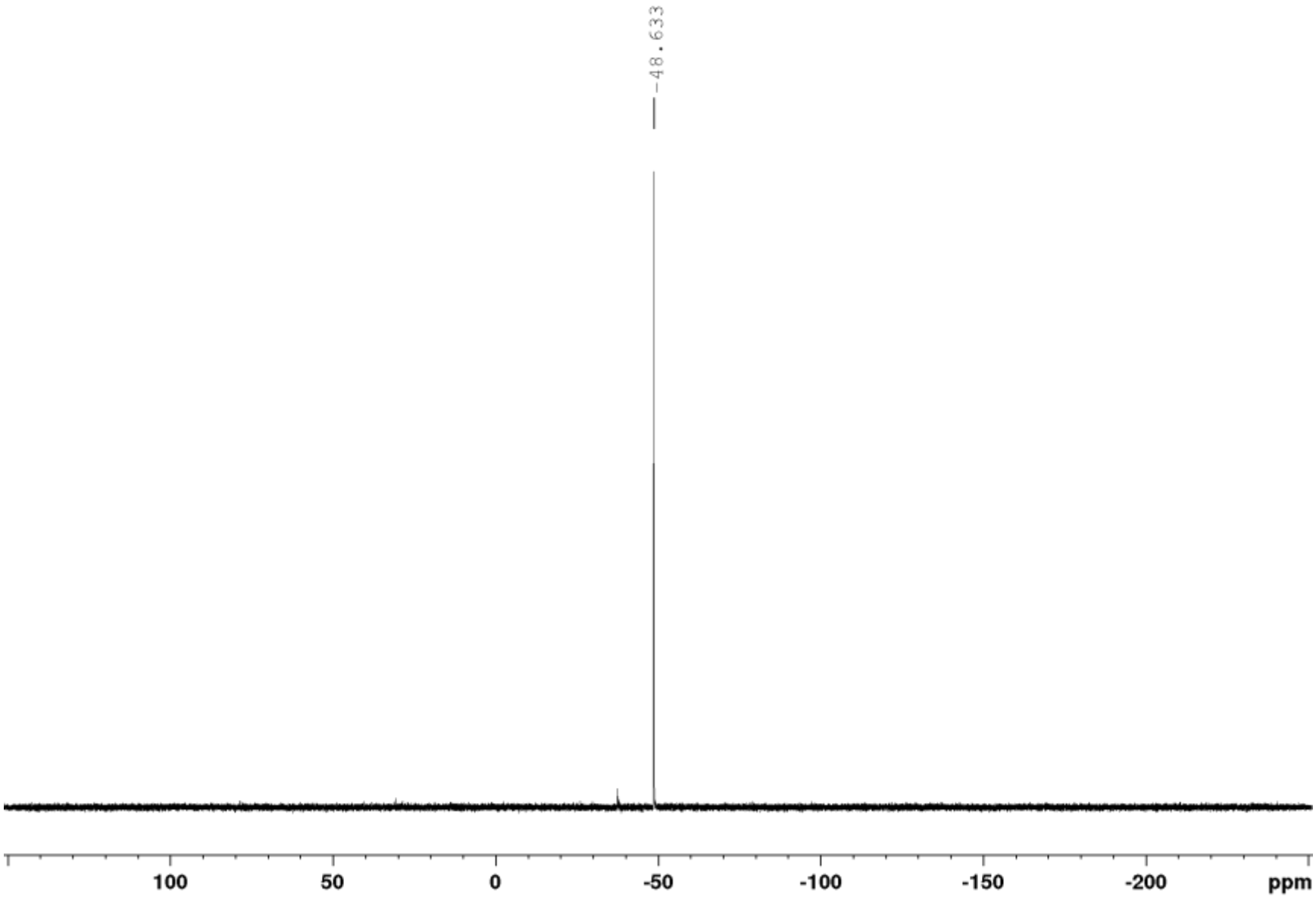

N-[4-[Hydroxy(1,3-Benzodioxol-5-yl) methyl]phenyl]acetamide (2.17), ^{1}H, CD_3OD, 400 MHz

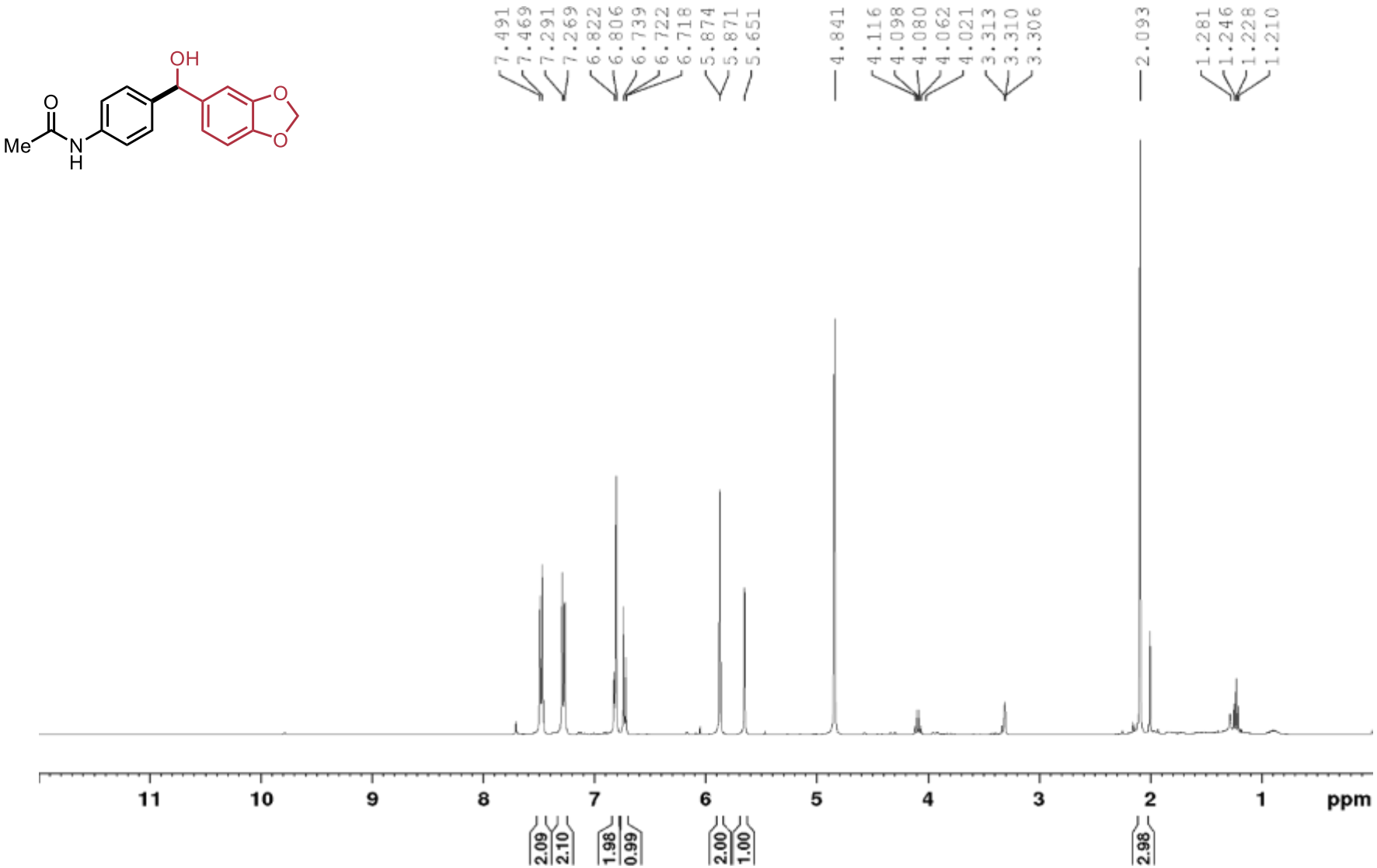

N-[4-[Hydroxy(1,3-Benzodioxol-5-yl) methyl]phenyl]acetamide (2.17), ^{13}C, CD_3OD, 100 MHz

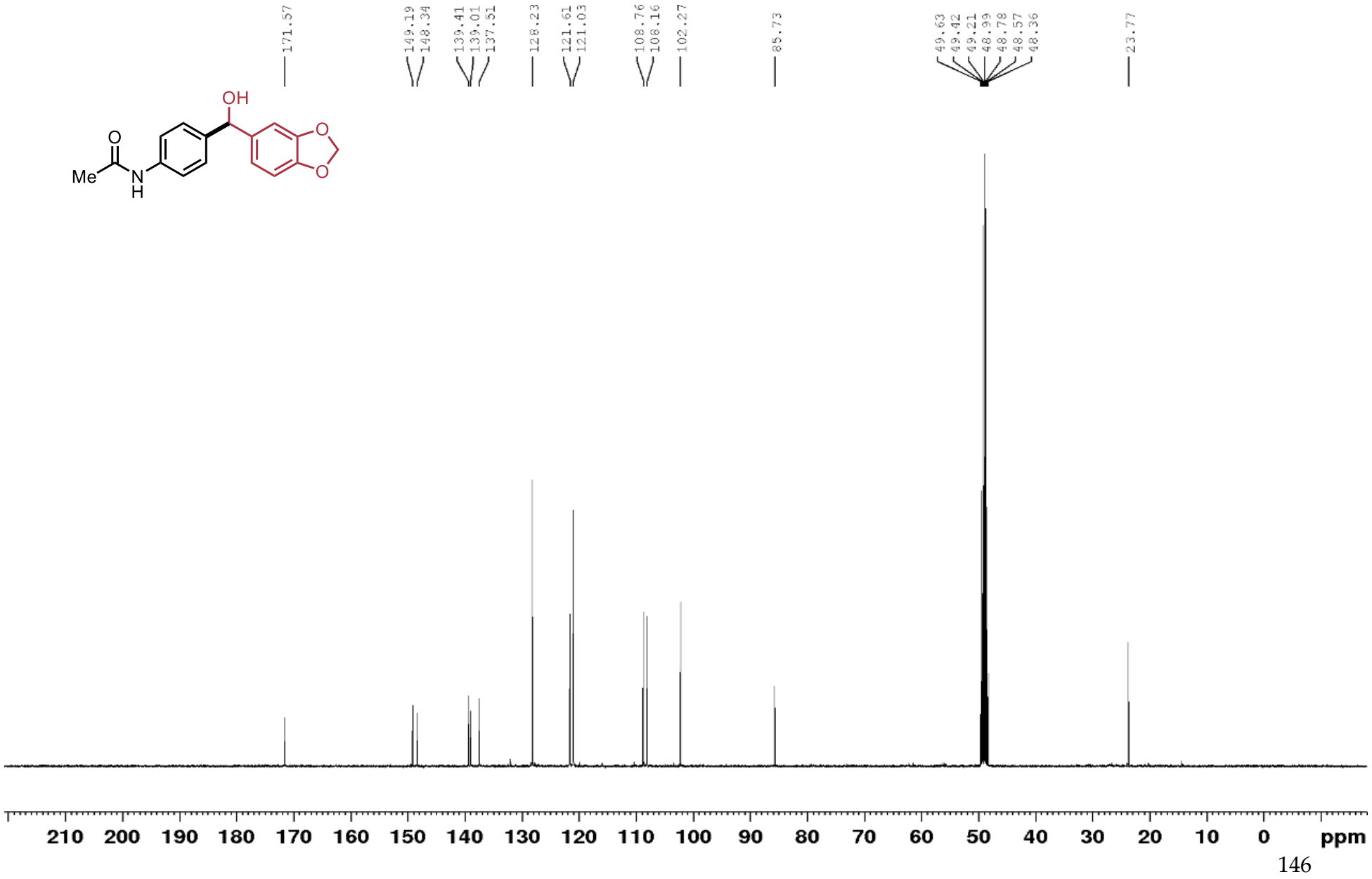

(4-(2-pyrimidinyloxy)phenyl)(6-quinolinyl)methanol (2.18), ^{1}H, $(CD_3)_2SO$, 400 MHz

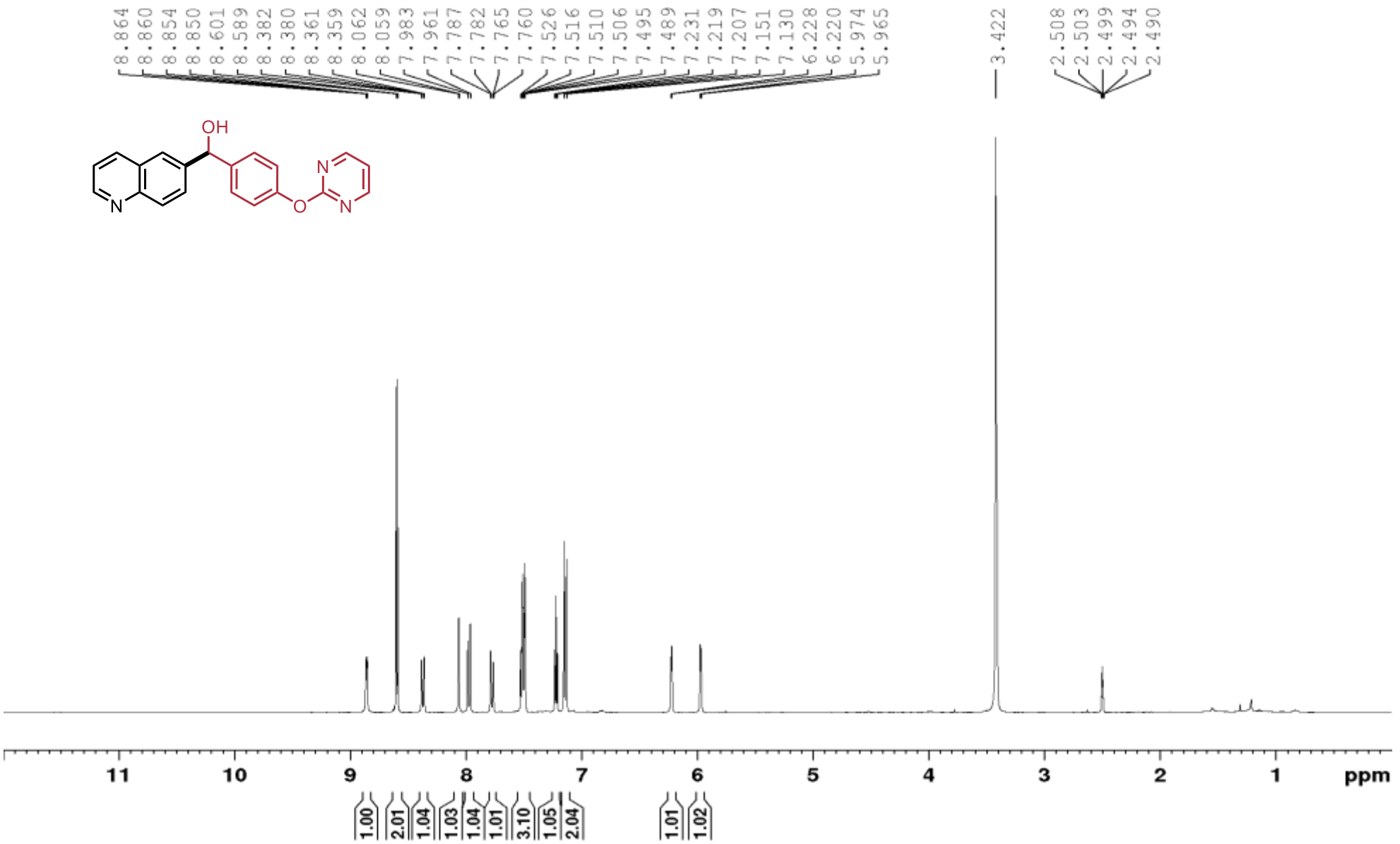

(4-(2-pyrimidinyloxy)phenyl)(6-quinolinyl)methanol (2.18), ^{13}C, $(CD_3)_2SO$, 100 MHz

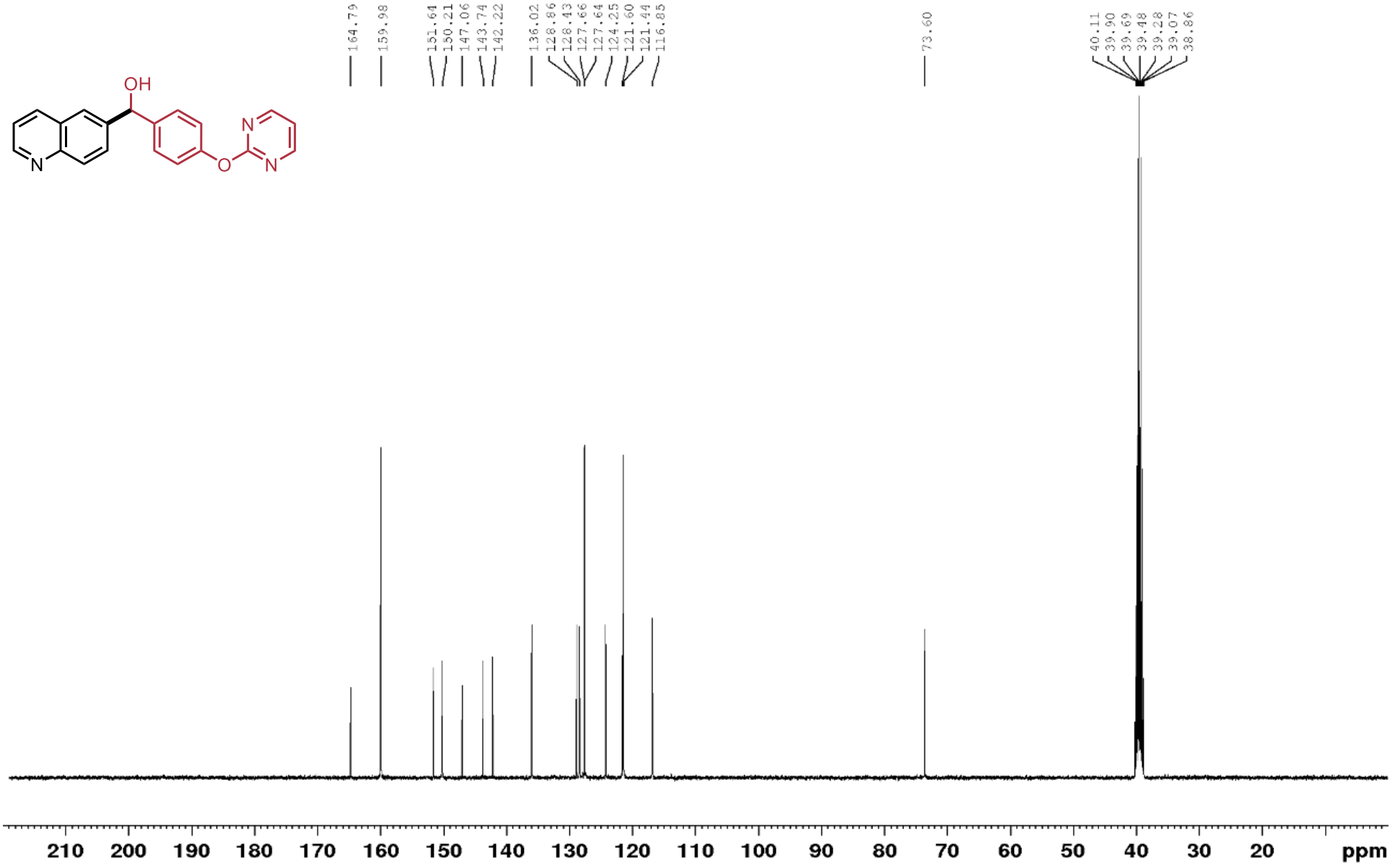

(4-bromophenyl)-quinolin-6-ylmethanol (2.19), ^{1}H, $(CD_3)_2SO$, 400 MHz

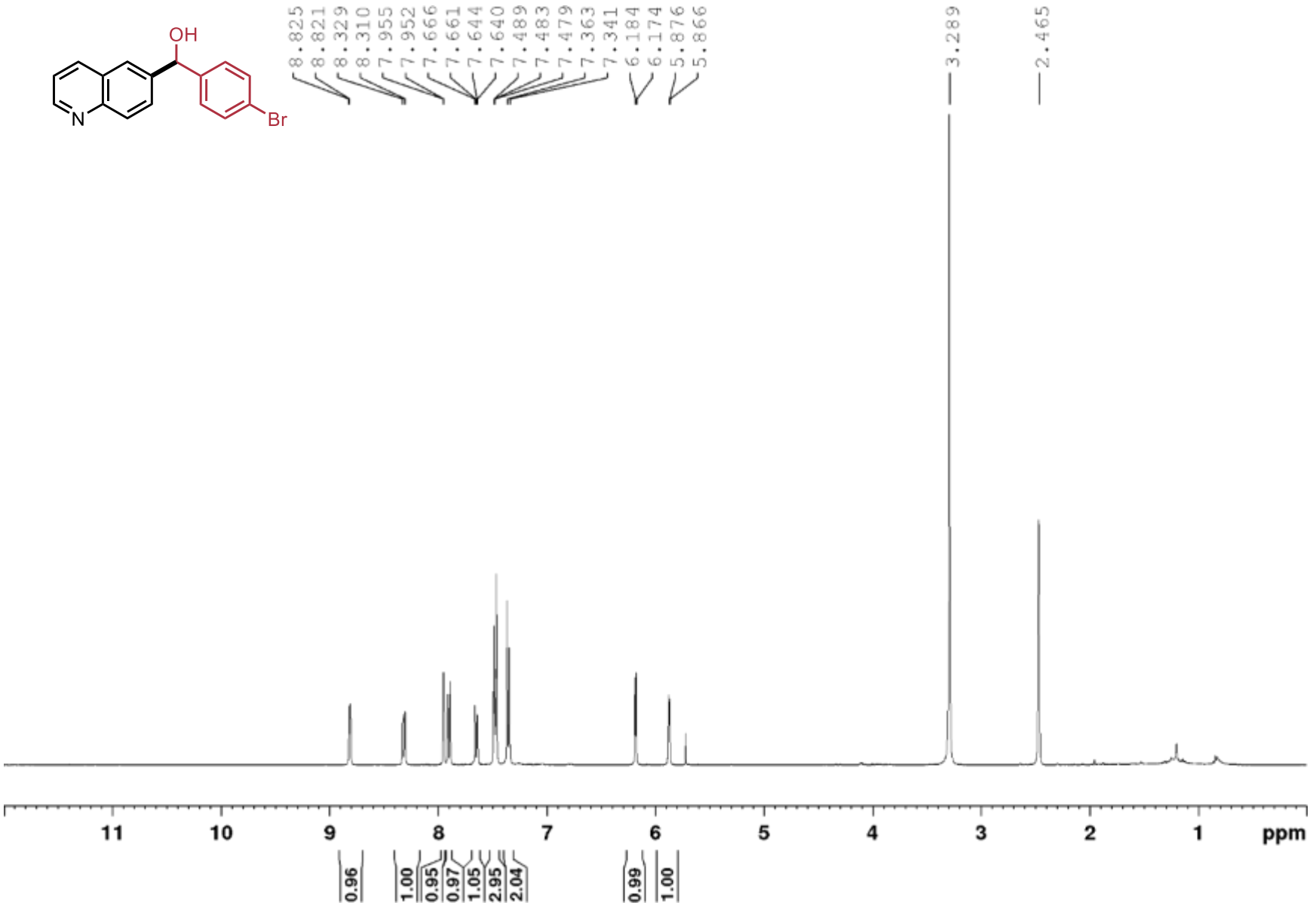

(4-bromophenyl)-quinolin-6-ylmethanol (2.19), ^{13}C, $(CD_3)_2SO$, 100 MHz

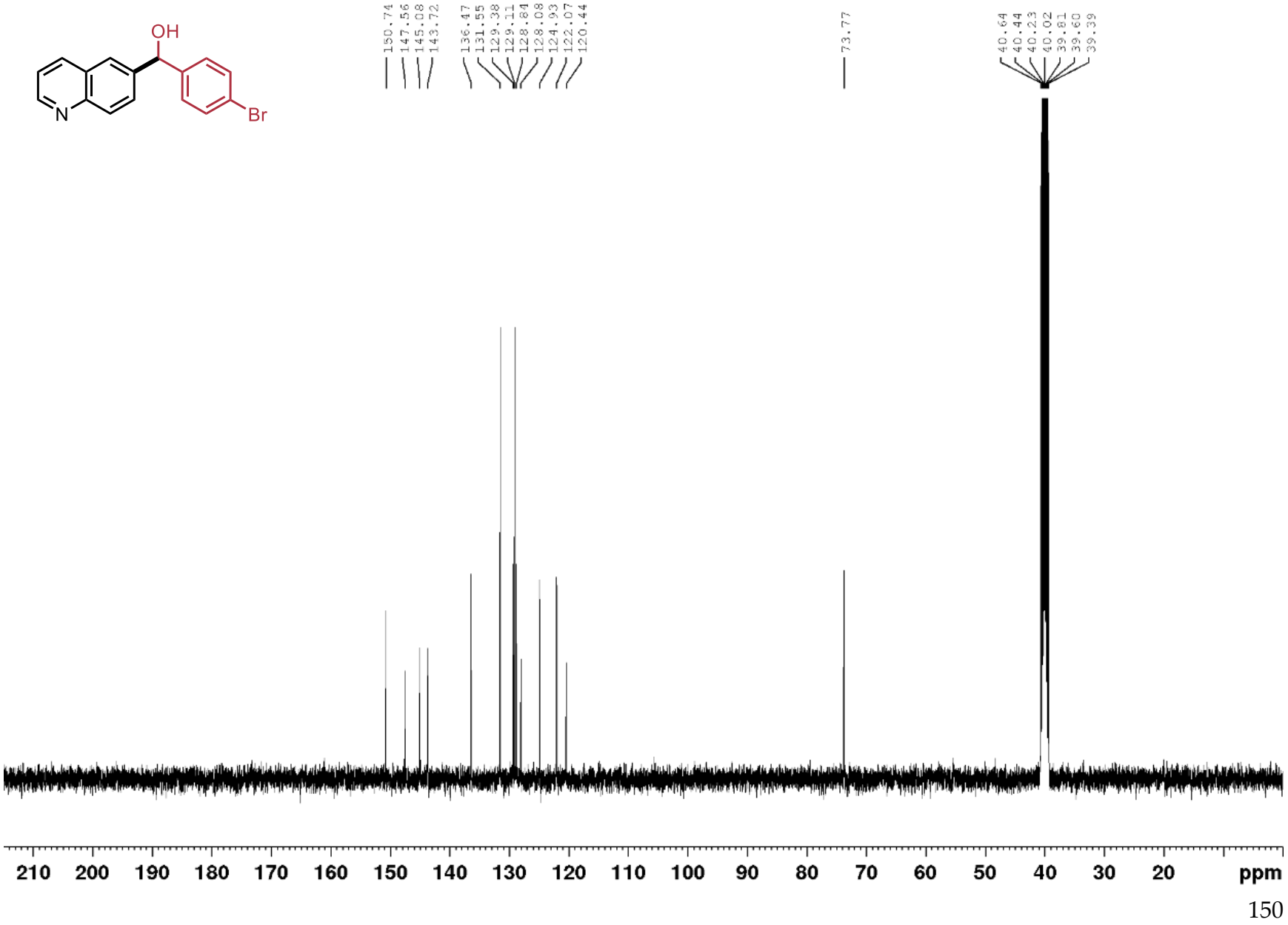

N-[3-Chloro-4-(3-fluorobenzyloxy)phenyl]-6-[Hydroxy(1,3-Benzodioxol-5-yl)methyl]quinazolin-4-amine (2.20), ^{1}H, $(CD_3)_2SO$, **400** MHz

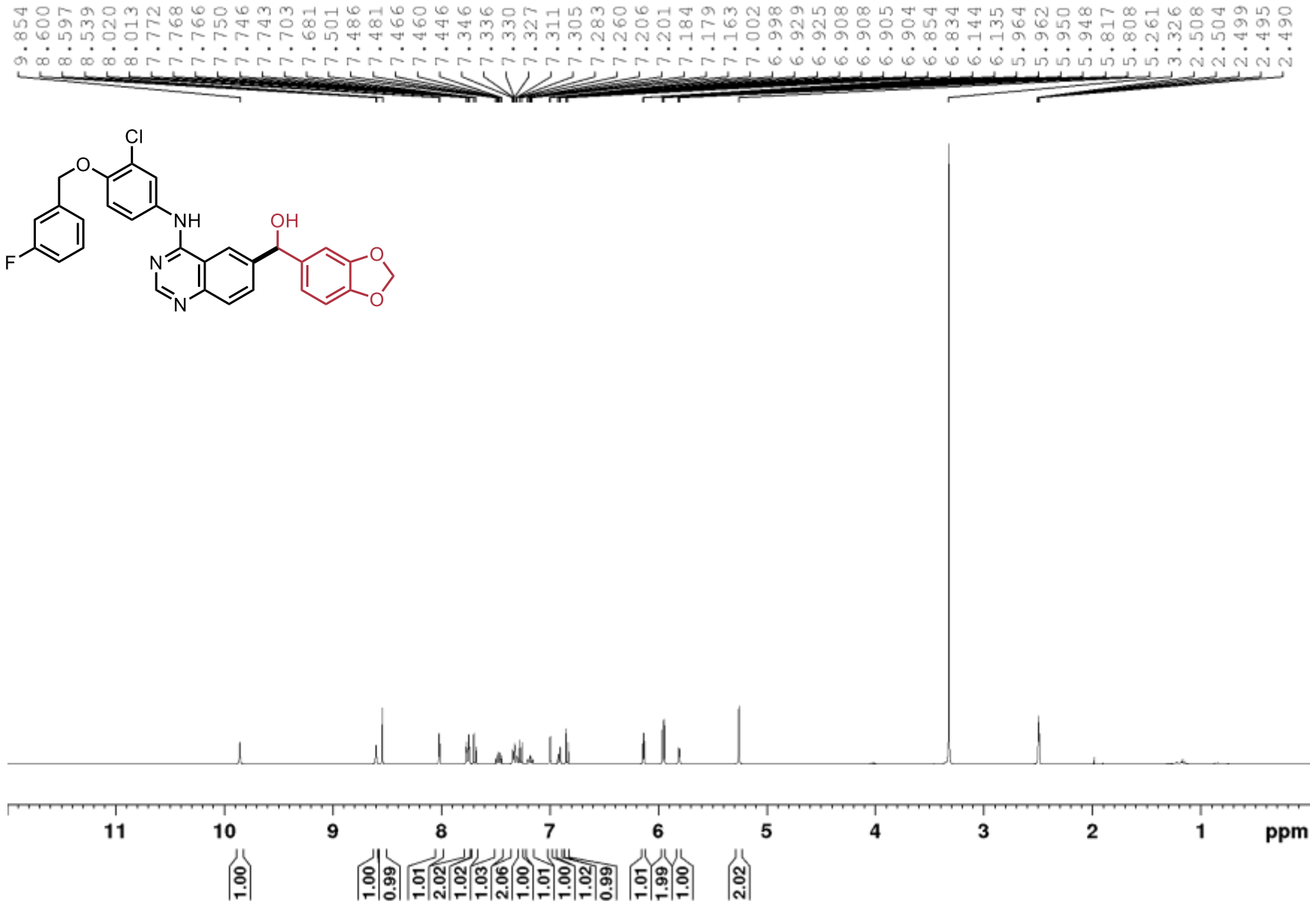

N-[3-Chloro-4-(3-fluorobenzyloxy)phenyl]-6-[Hydroxy(1,3-Benzodioxol-5-yl)methyl]quinazolin-4-amine (2.20), ^{13}C, $(CD_3)_2SO$, 100 MHz (zoomed in)

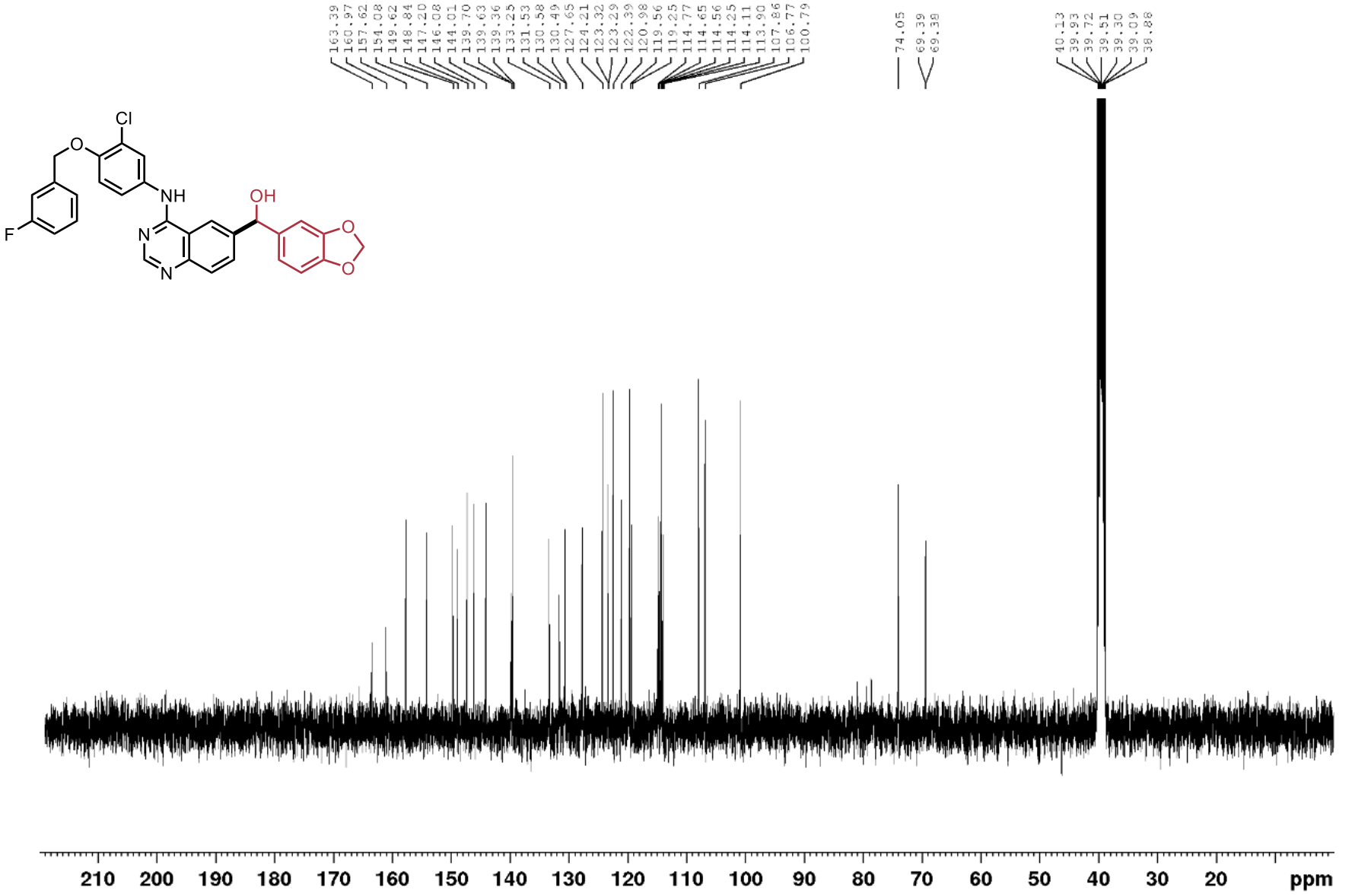

N-[3-Chloro-4-(3-fluorobenzyloxy)phenyl]-6-[Hydroxy(1,3-Benzodioxol-5 yl)methyl]quinazolin-4-amine (2.20), ^{19}F, ($(CD_3)_2SO$, 100 MHz

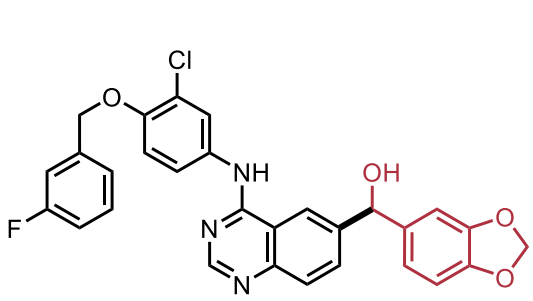

α-(4-chlorophenyl)-2-benzofuranmethanol (2.21), ^{1}H, $CDCl_3$, 400 MHz

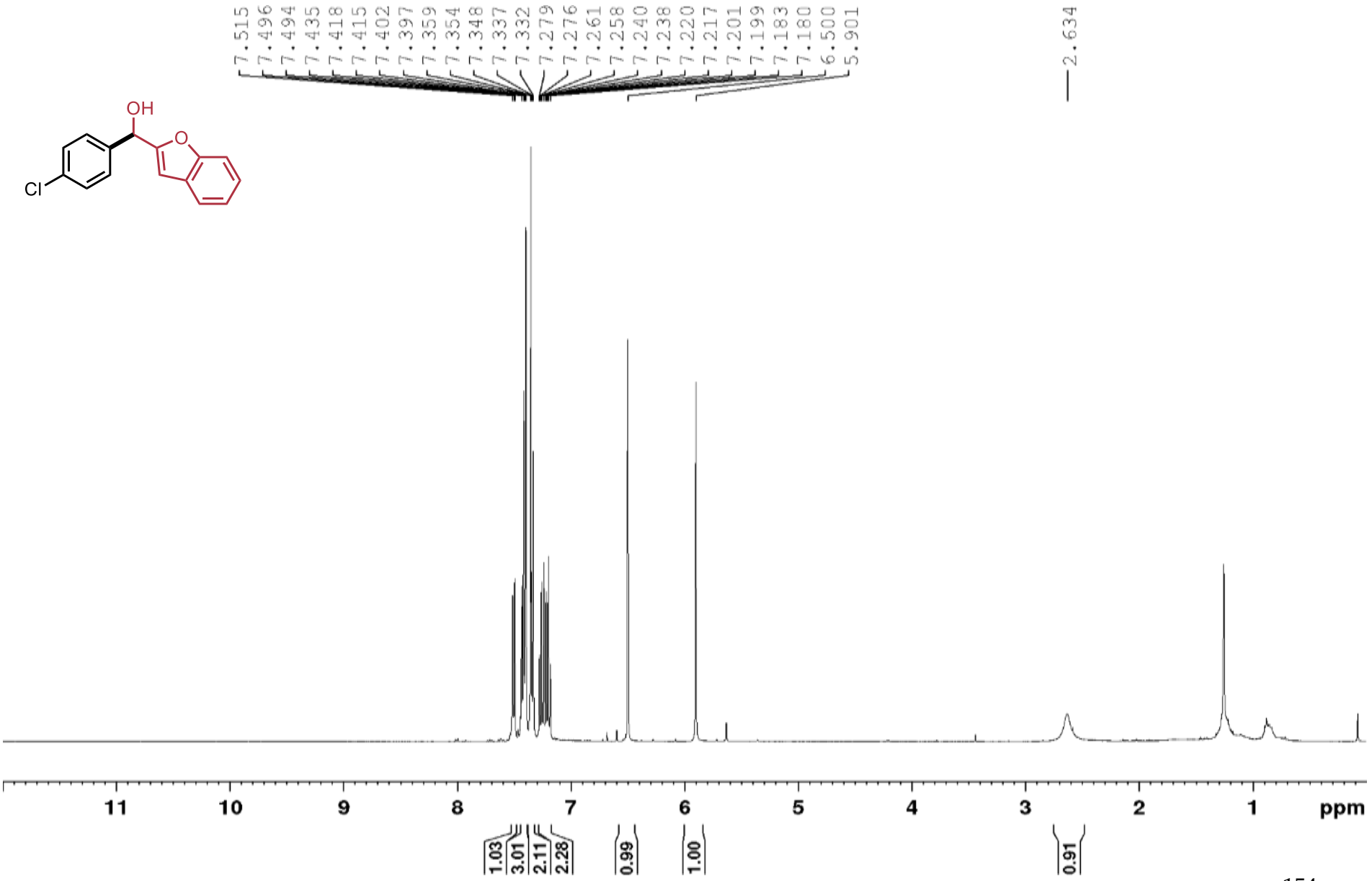

α-(4-Chlorophenyl)-2-benzofuranmethanol (2.21), ^{13}C, $CDCl_3$, 100 MHz

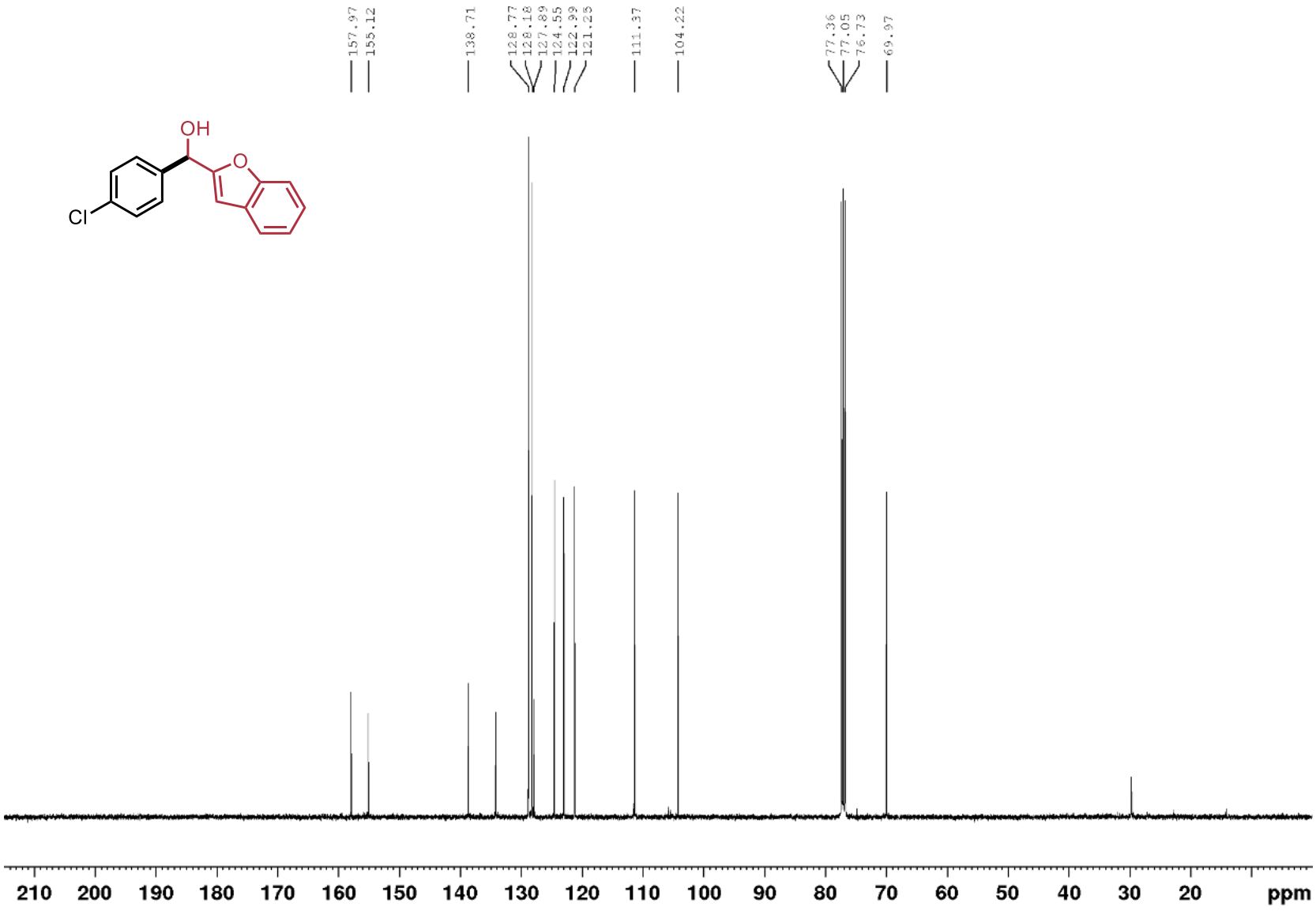

(1,3-benzodioxol-5-yl)-1,3-benzodioxole-5-methanol (2.22), ^{1}H, $CDCl_3$, 400 MHz

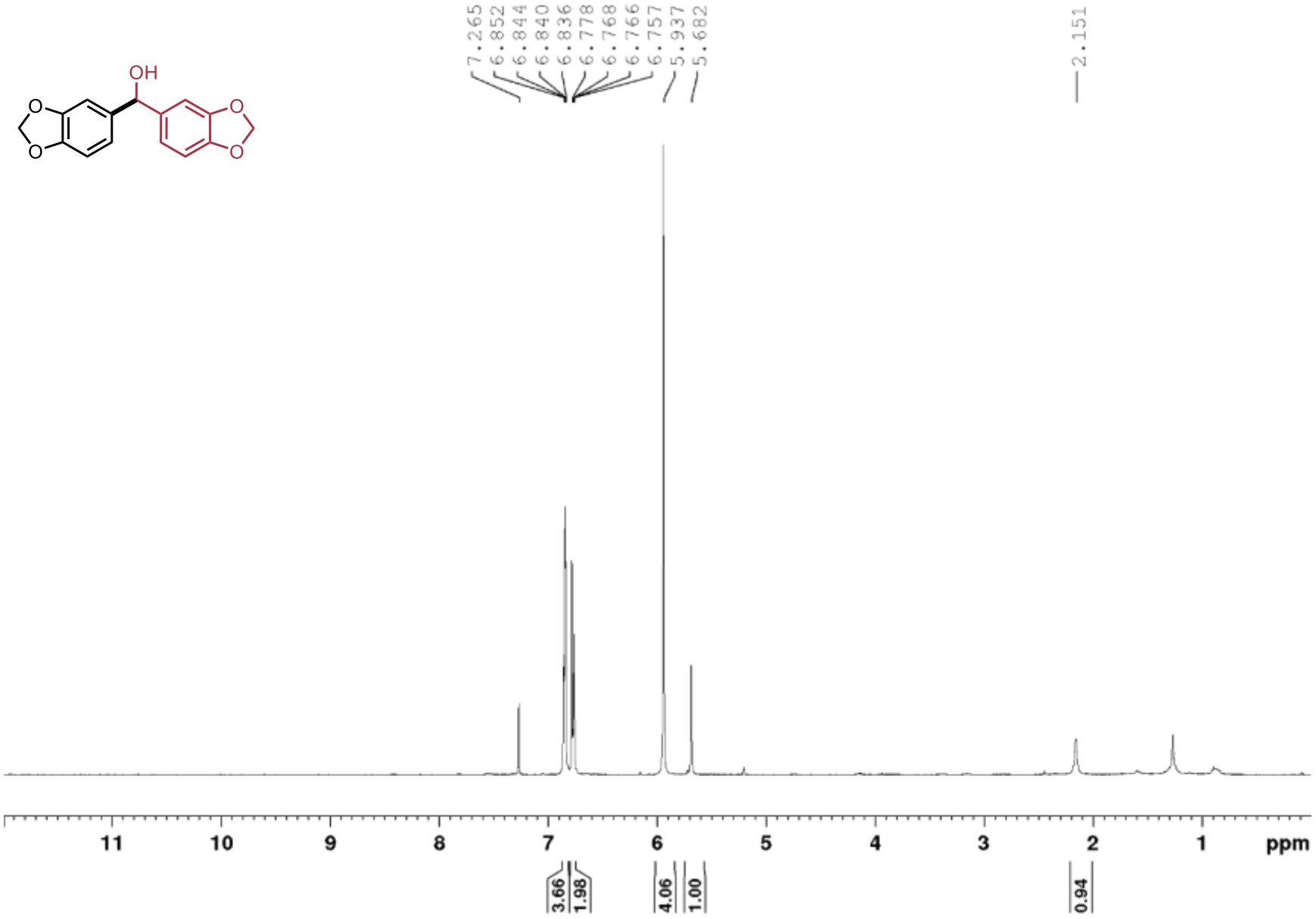

(1,3-benzodioxol-5-yl)-1,3-benzodioxole-5-methanol (2.22), ^{13}C, $CDCl_3$, 100 MHz

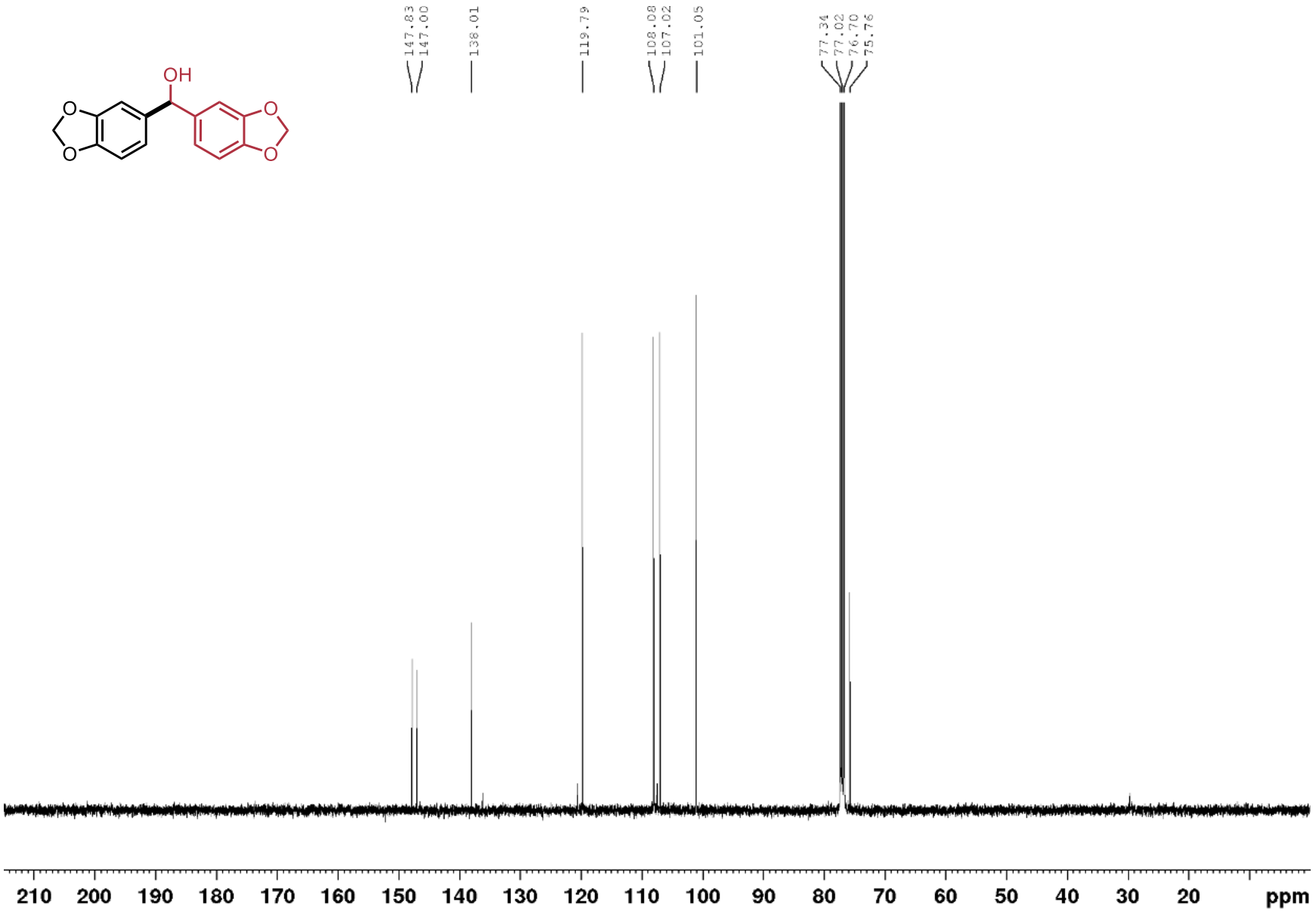

1-(naphthalen-1-yl)hexan-1-ol (2.23), ^{1}H, $CDCl_3$, 400 MHz

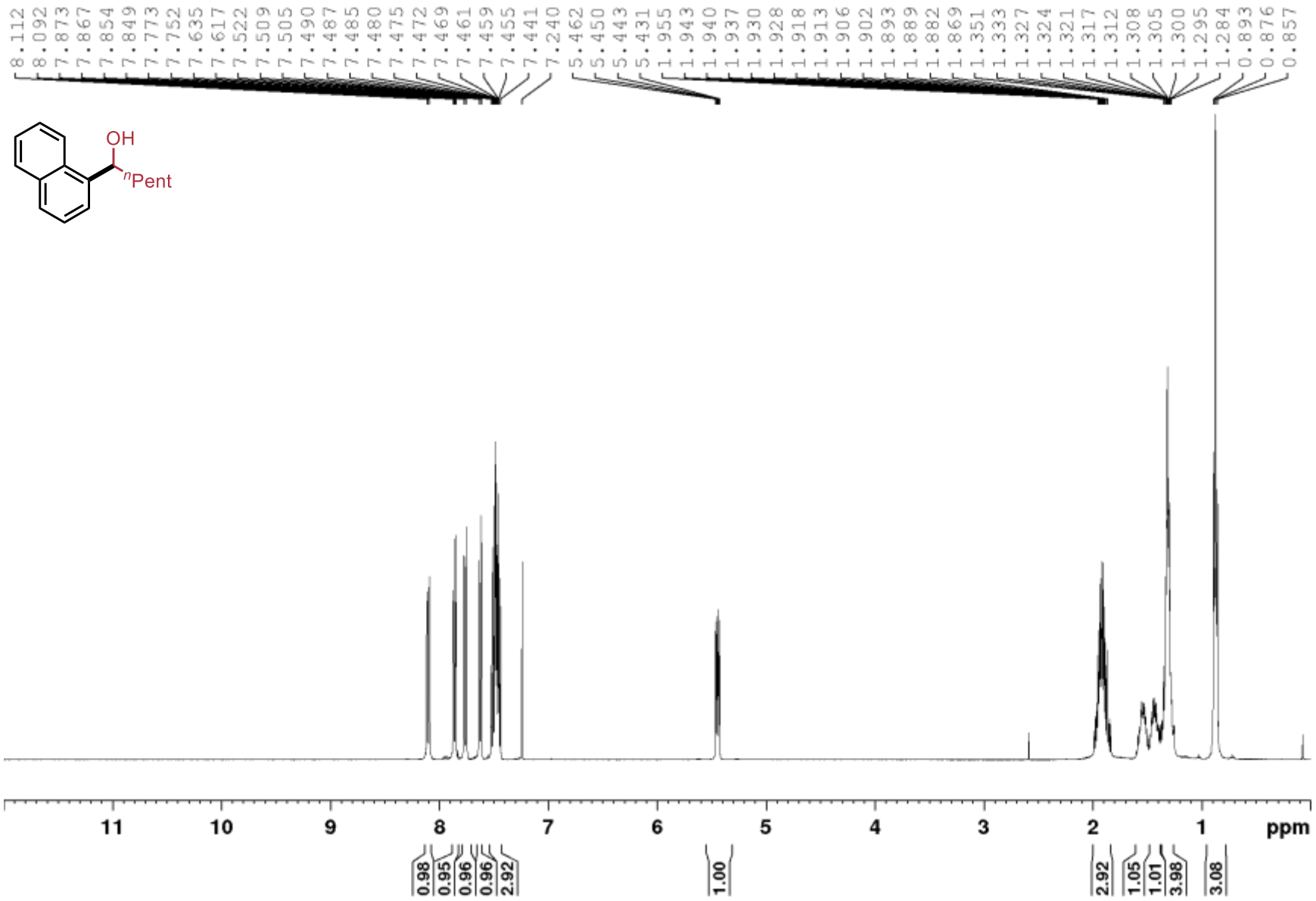

1-(naphthalen-1-yl)hexan-1-ol (2.23), ^{13}C, $CDCl_3$, 100 MHz

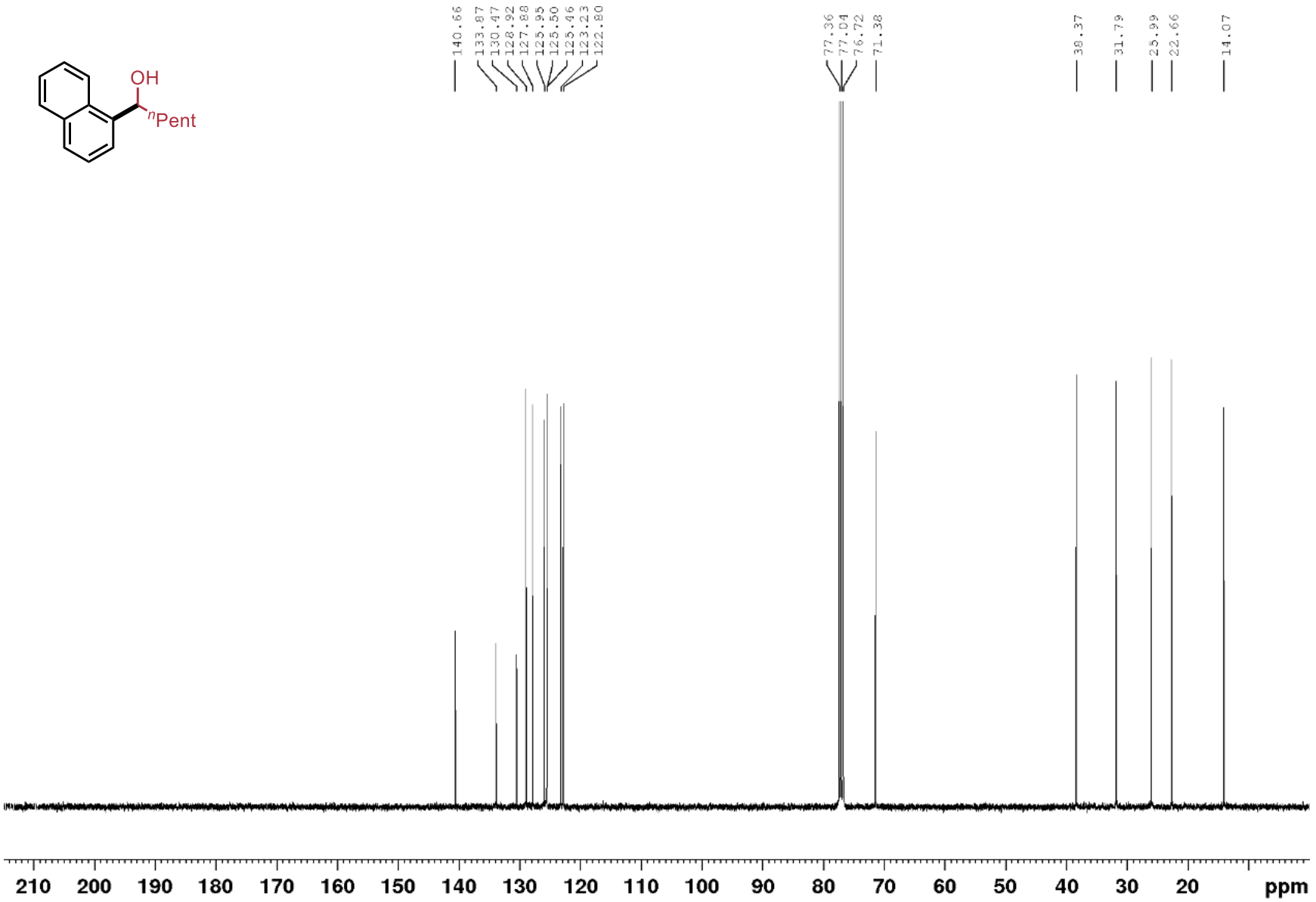

Cyclopropyl(naphthalen-1-yl)methanol (2.24), ^{1}H, $CDCl_3$, 400 MHz

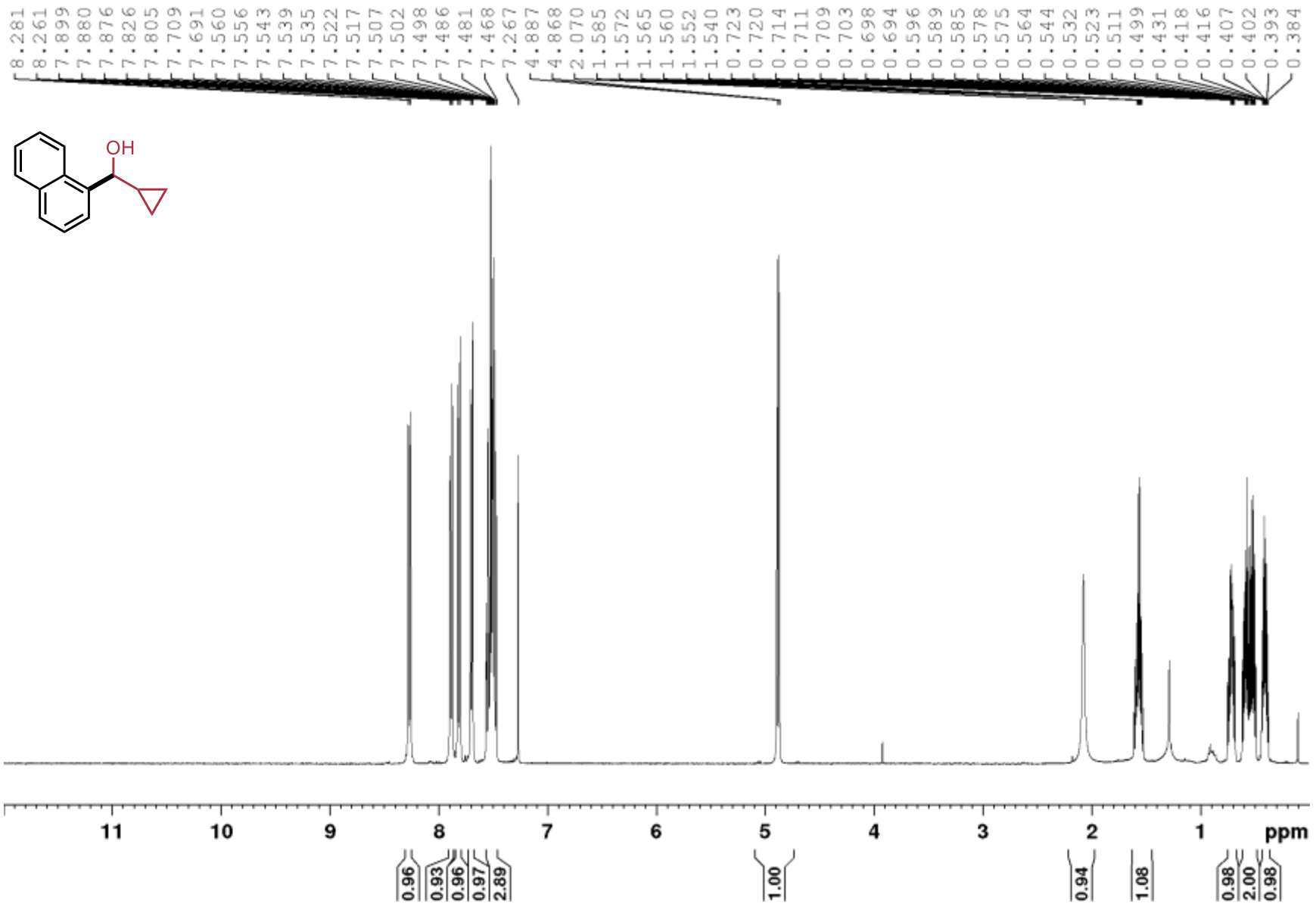

Cyclopropyl(naphthalen-1-yl)methanol (2.24), ^{13}C, $CDCl_3$, 100 MHz

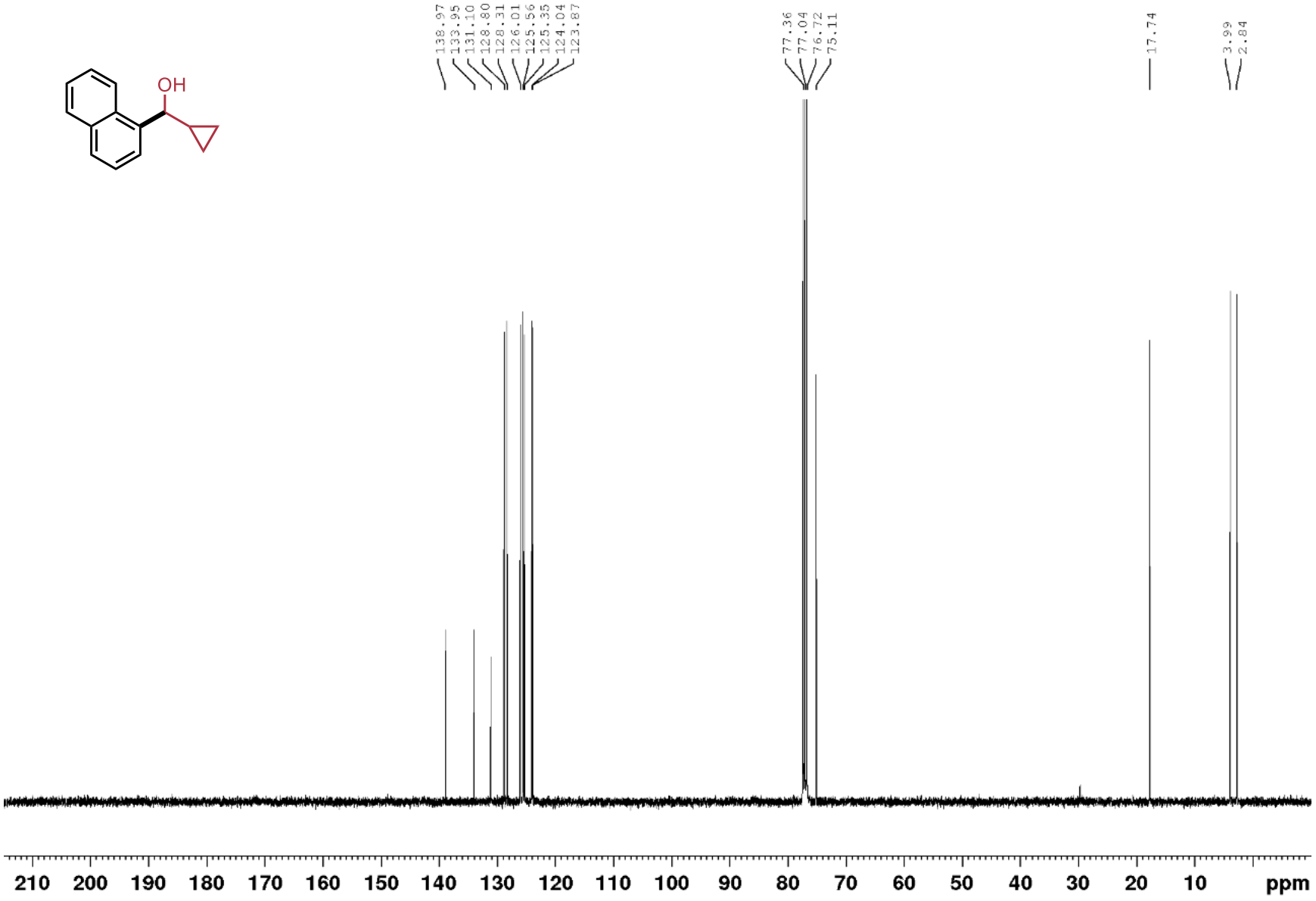

1-(α-naphthyl)-2-phenylethanol (2.25), ^{1}H, $CDCl_3$, 500 MHz

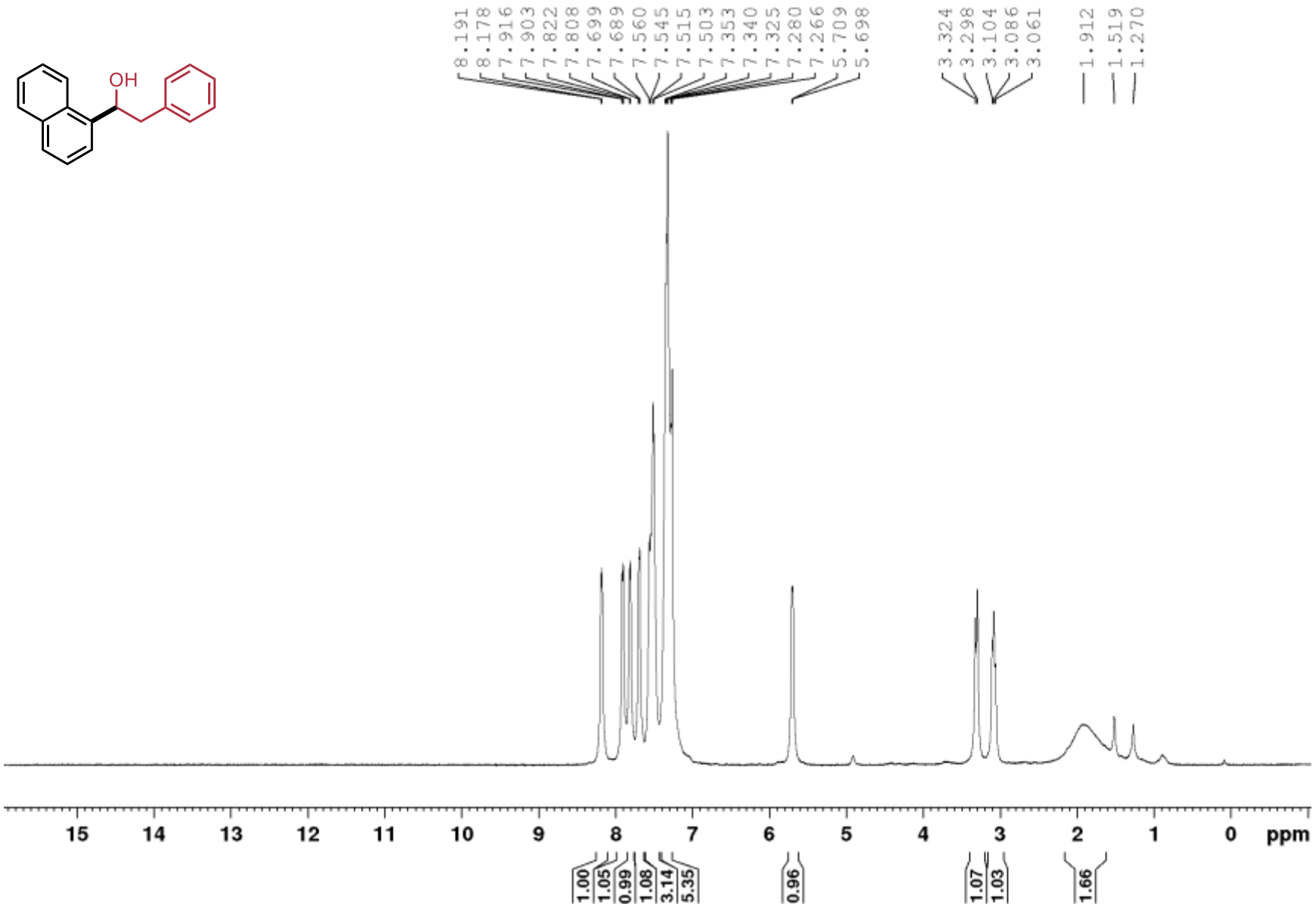

1-(α-naphthyl)-2-phenylethanol (2.25), ^{13}C, $CDCl_3$, 100 MHz

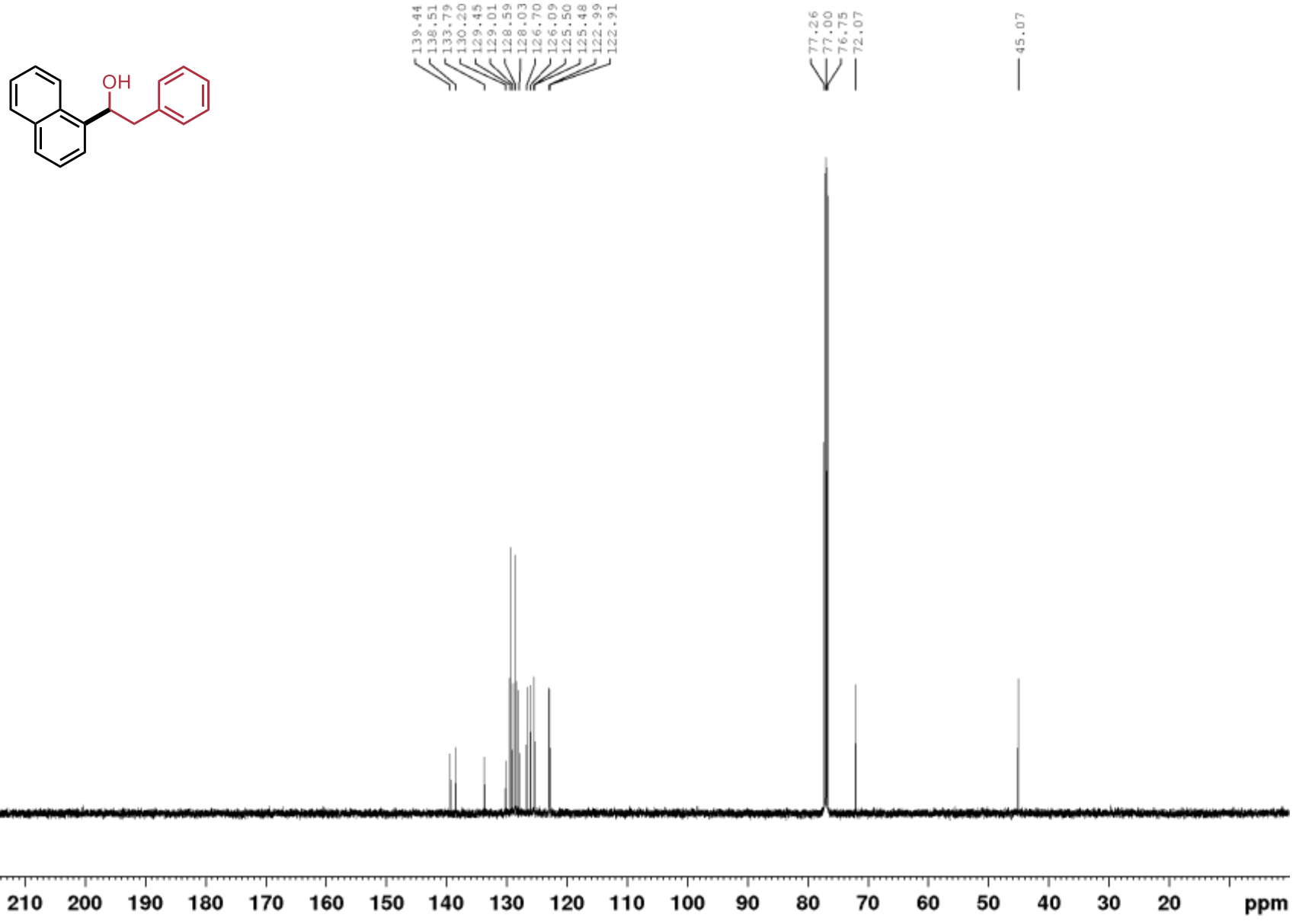

2H-1,3-benzodioxol-5-yl(4-(1H-Pyrazol-1-yl)phenyl)methanol (2.26), ^{1}H $CDCl_3$, 400 MHz

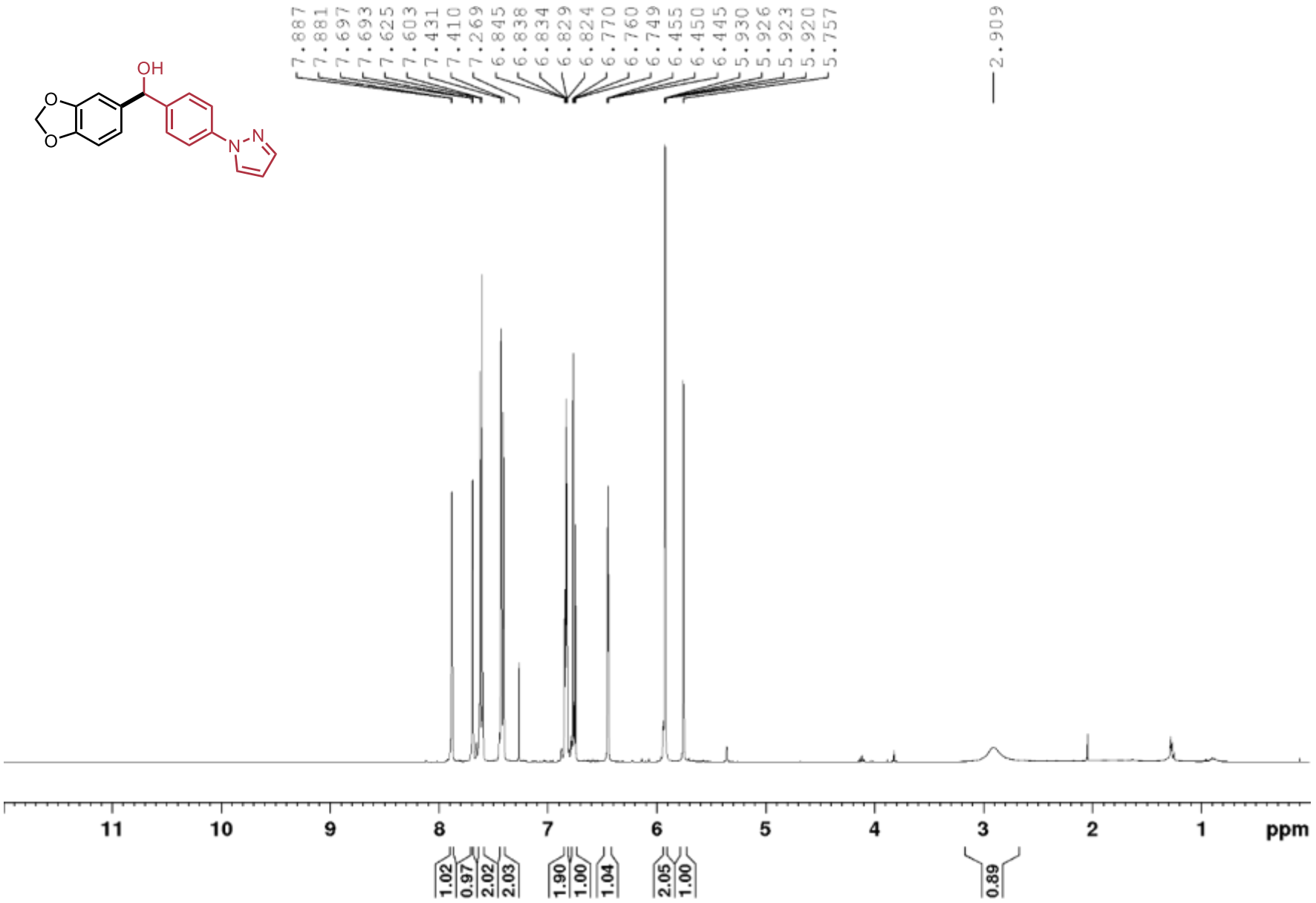

2H-1,3-benzodioxol-5-yl(4-(1H-Pyrazol-1-yl)phenyl)methanol (2.26), ^{13}C, $CDCl_3$, 100 MHz

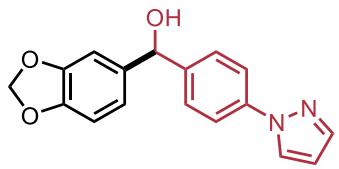

4-[4-(hydroxymethyl(α-(4-chloro-2-fluorophenyl))phenyl]-3-Morpholinone (2.27), $CDCl_3$, ^1H, 400 MHz

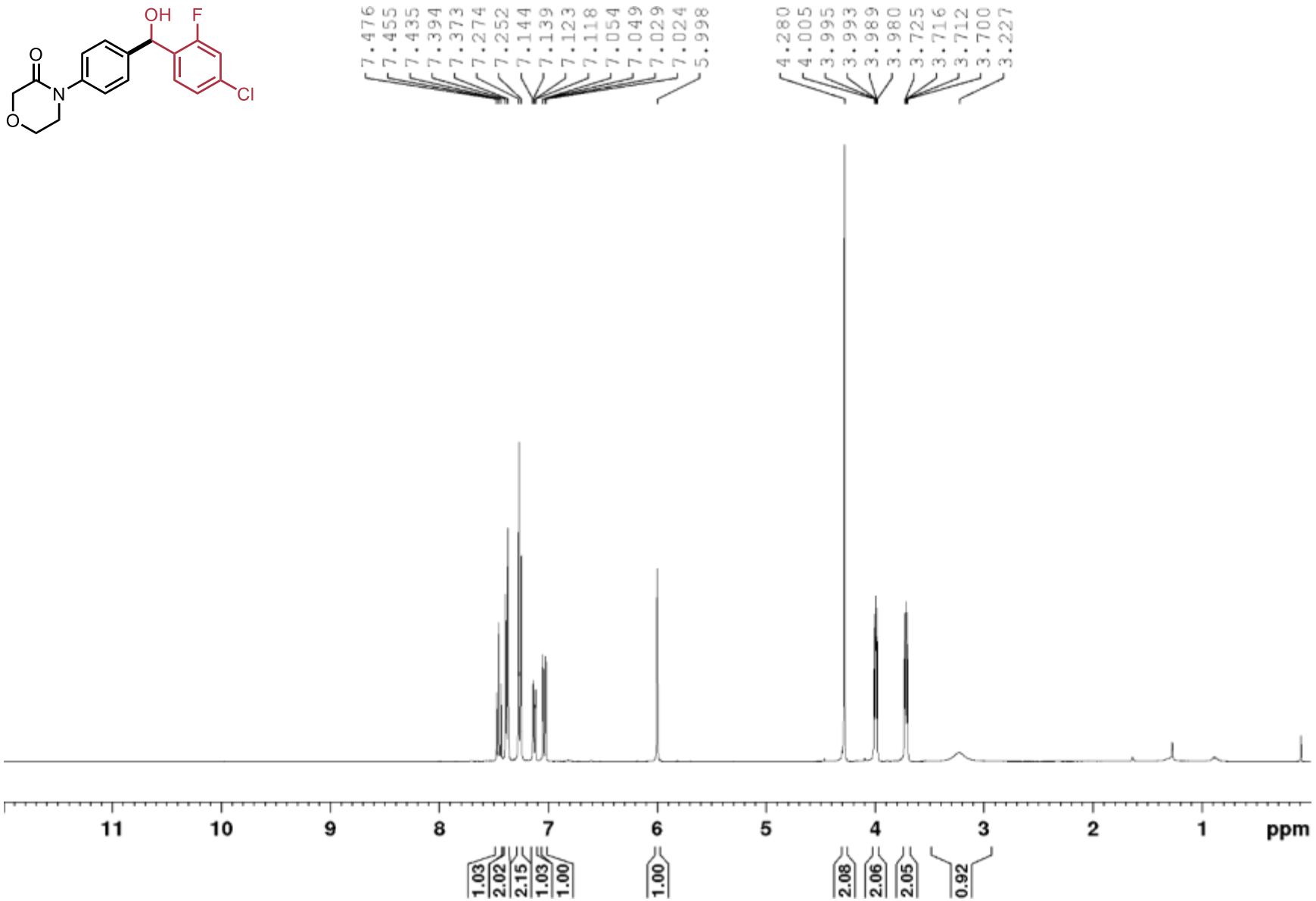

4-[4-(hydroxymethyl(α-(4-chloro-2-fluorophenyl))phenyl]-3-Morpholinone (2.27), $CDCl_3$, ^{13}C, 100 MHz

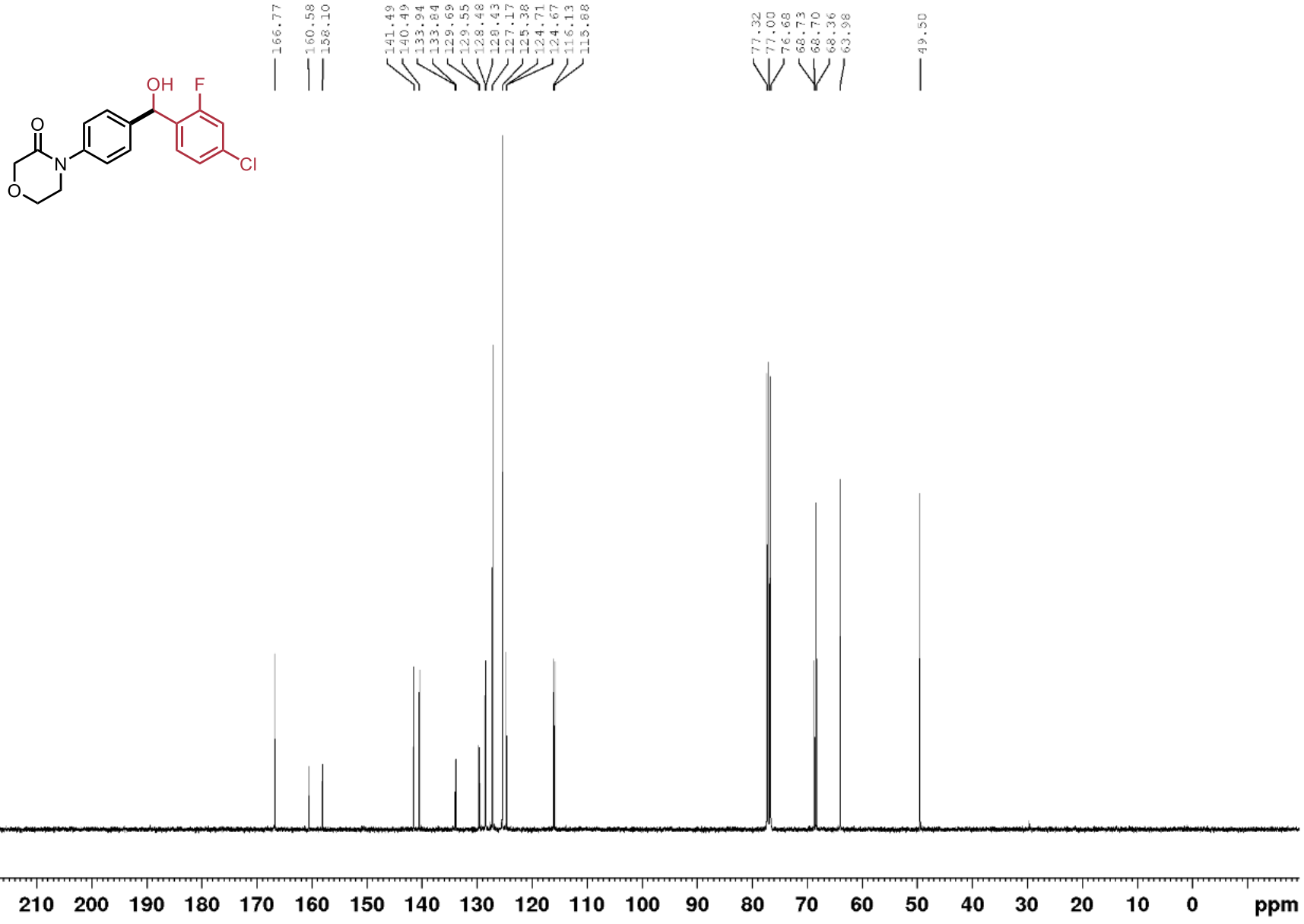

4-[4-(hydroxymethyl(α-(4-chloro-2-fluorophenyl))phenyl]-3-Morpholinone (2.27), $CDCl_3$, ^{19}F, 377 MHz

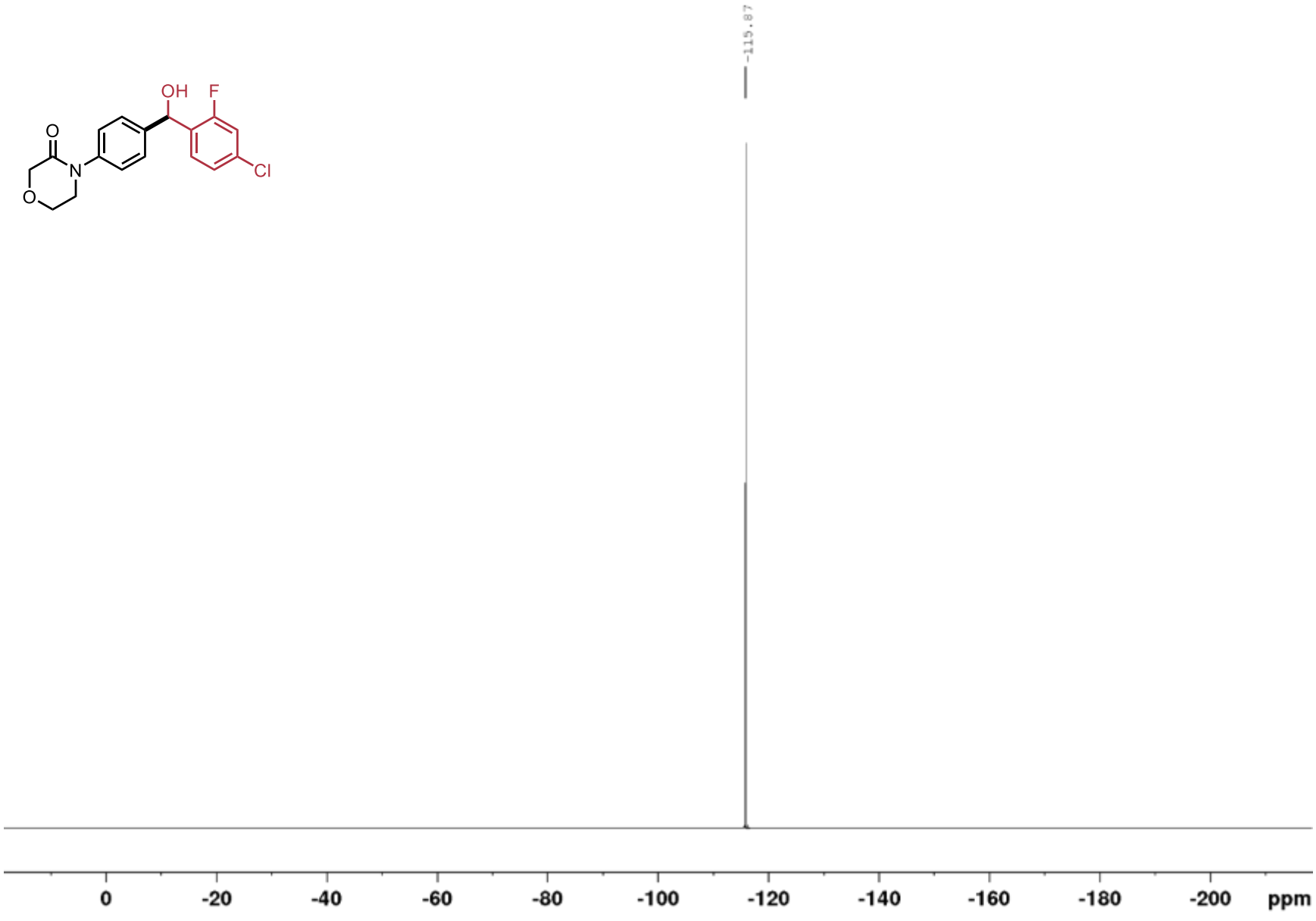

α-(4-chloro-2-fluorophenyl)-6-methoxy-3-Pyridinemethanol (2.28), $CDCl_3$, ^1H, 400 MHz

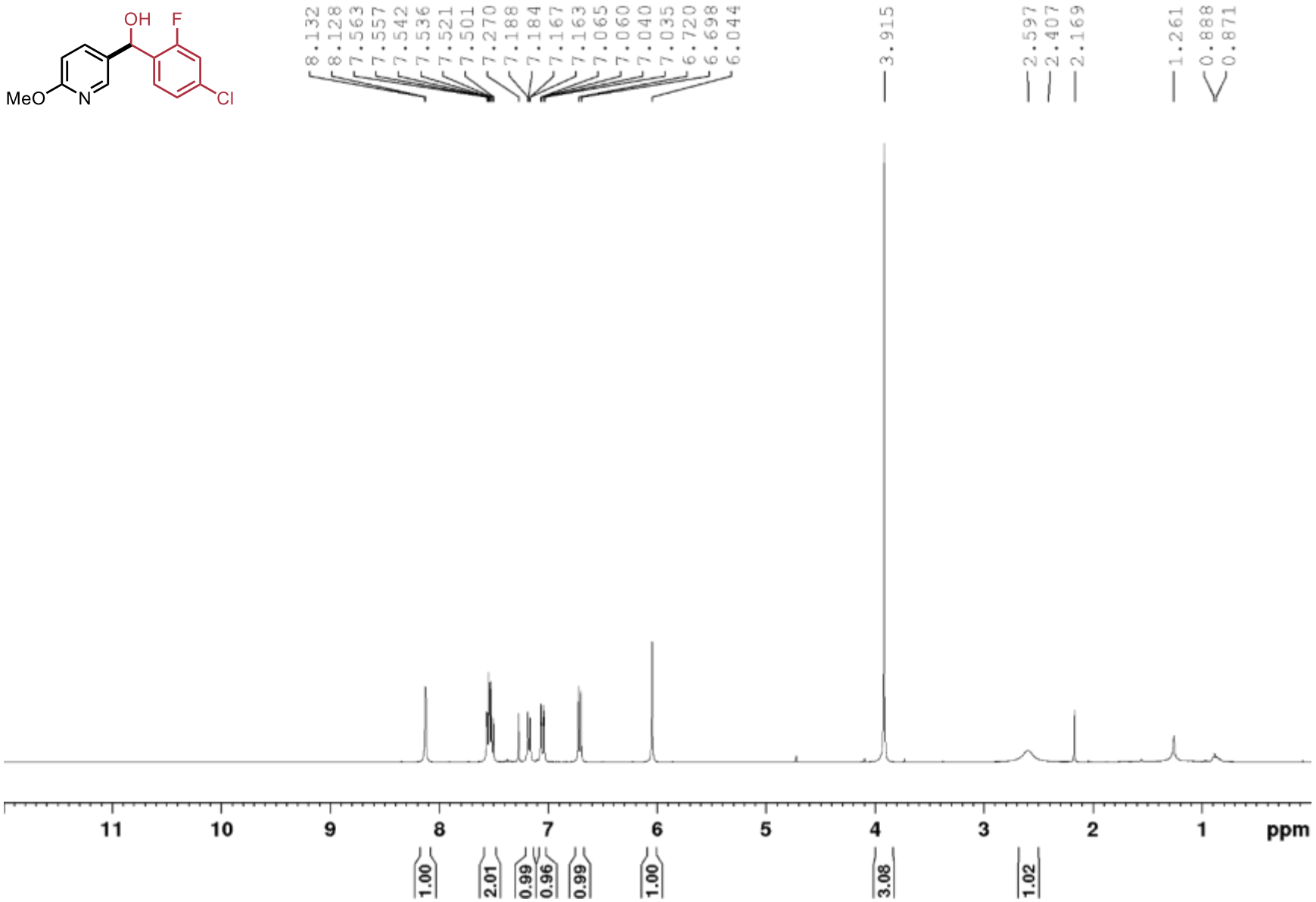

α-(4-chloro-2-fluorophenyl)-6-methoxy-3-Pyridinemethanol (2.28), $CDCl_3$, ^{13}C, 100 MHz

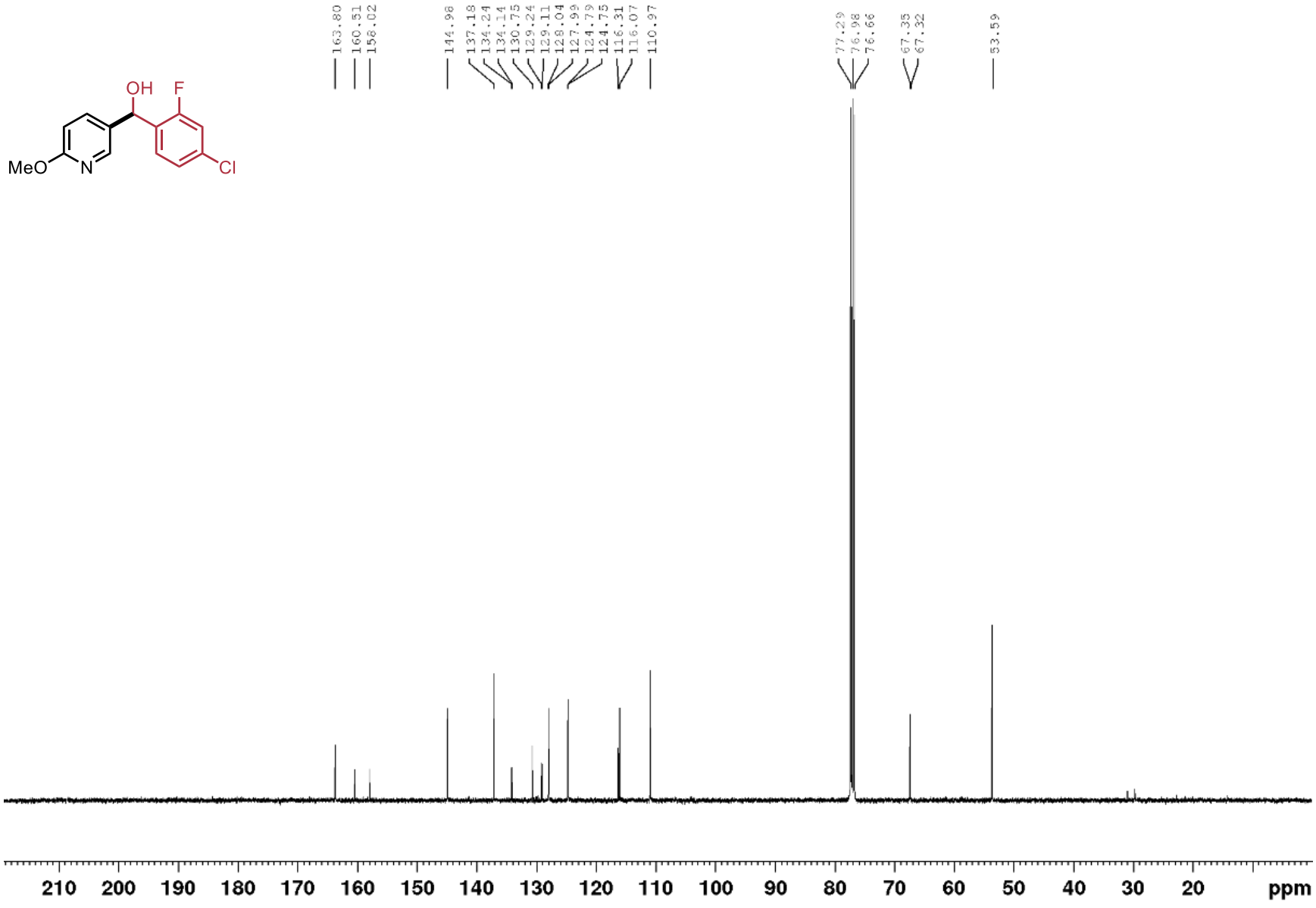

α-(4-chloro-2-fluorophenyl)-6-methoxy-3-Pyridinemethanol (2.28), $CDCl_3$, ^{19}F, 377 MHz

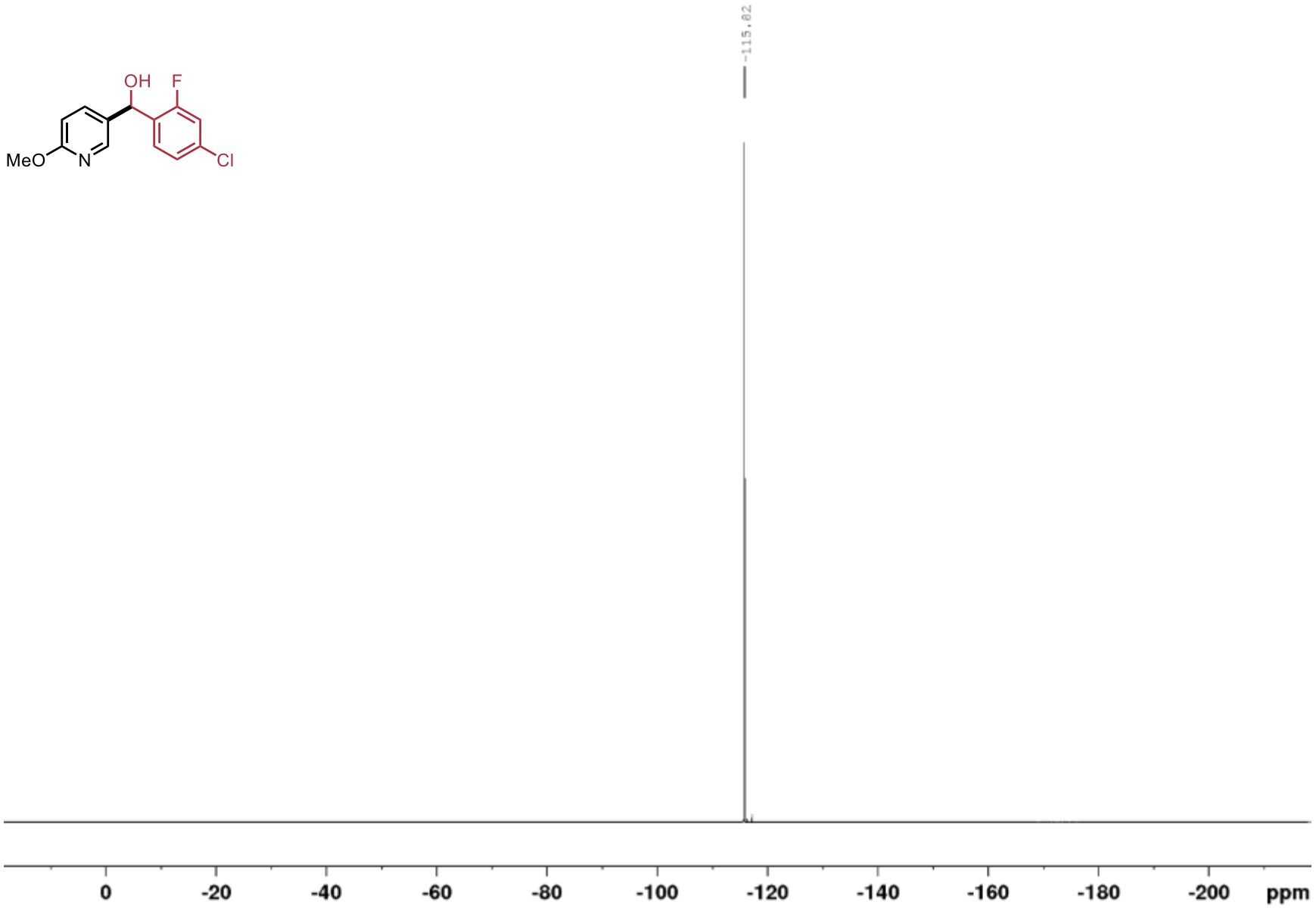

1-(naphthalen-5-yl)octan-1-ol (2.29), ^{1}H, $CDCl_3$, 400 MHz

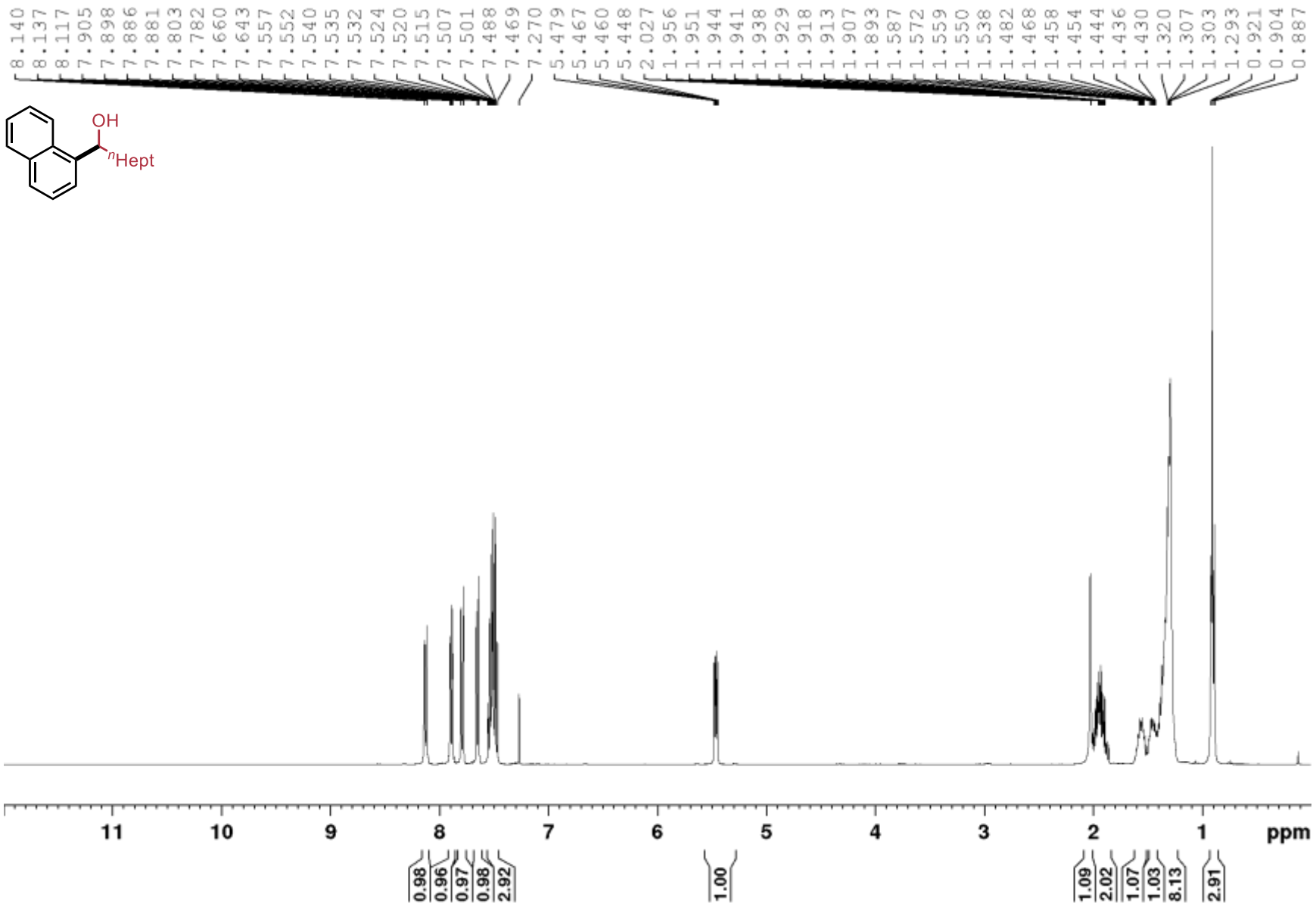

1-(naphthalen-5-yl)octan-1-ol (2.29), ^{13}C, $CDCl_3$, 100 MHz

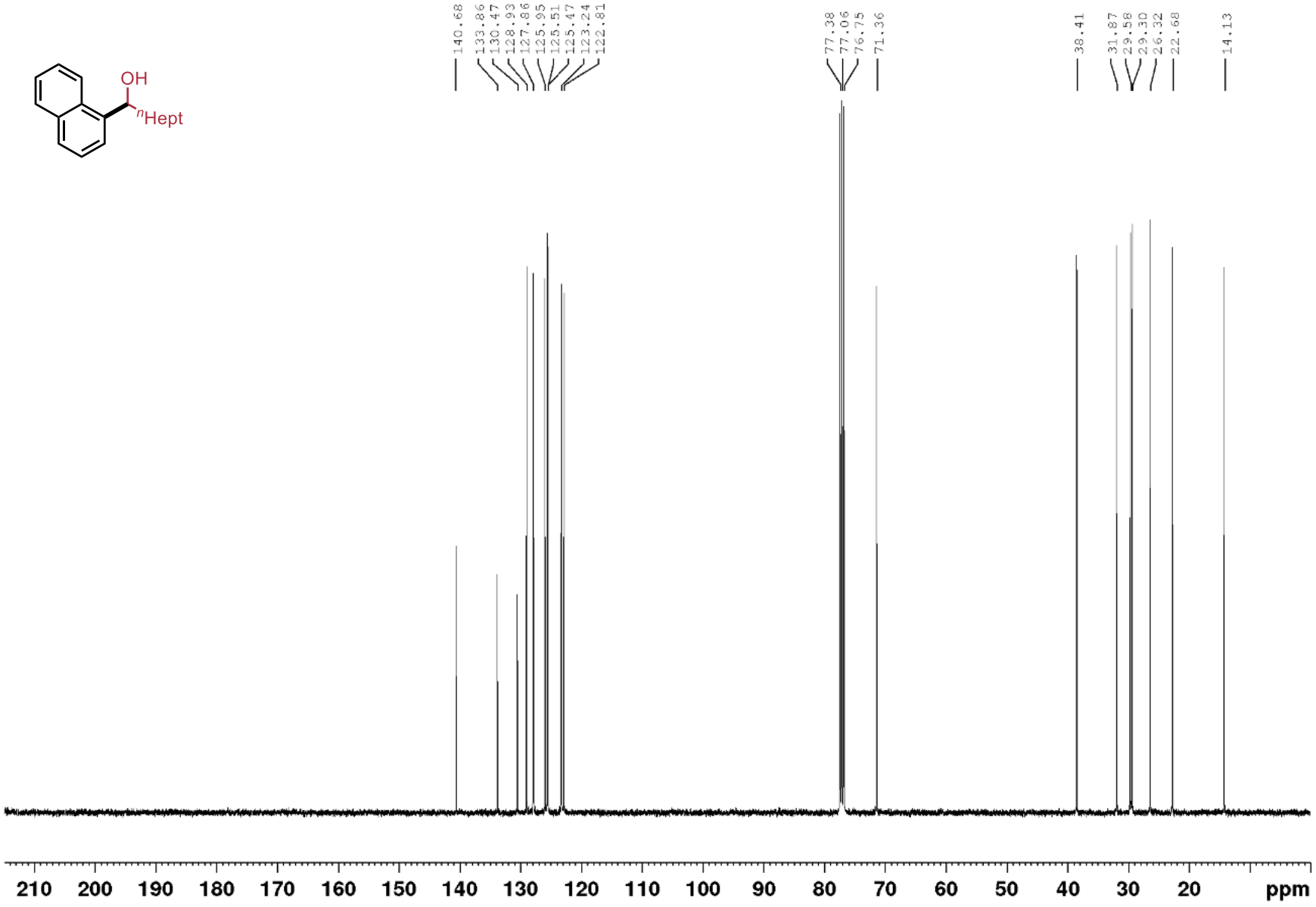

1-benzo[1,3]dioxol-5-yl-octan-1-ol (2.30), ^{1}H, $CDCl_3$, 400 MHz

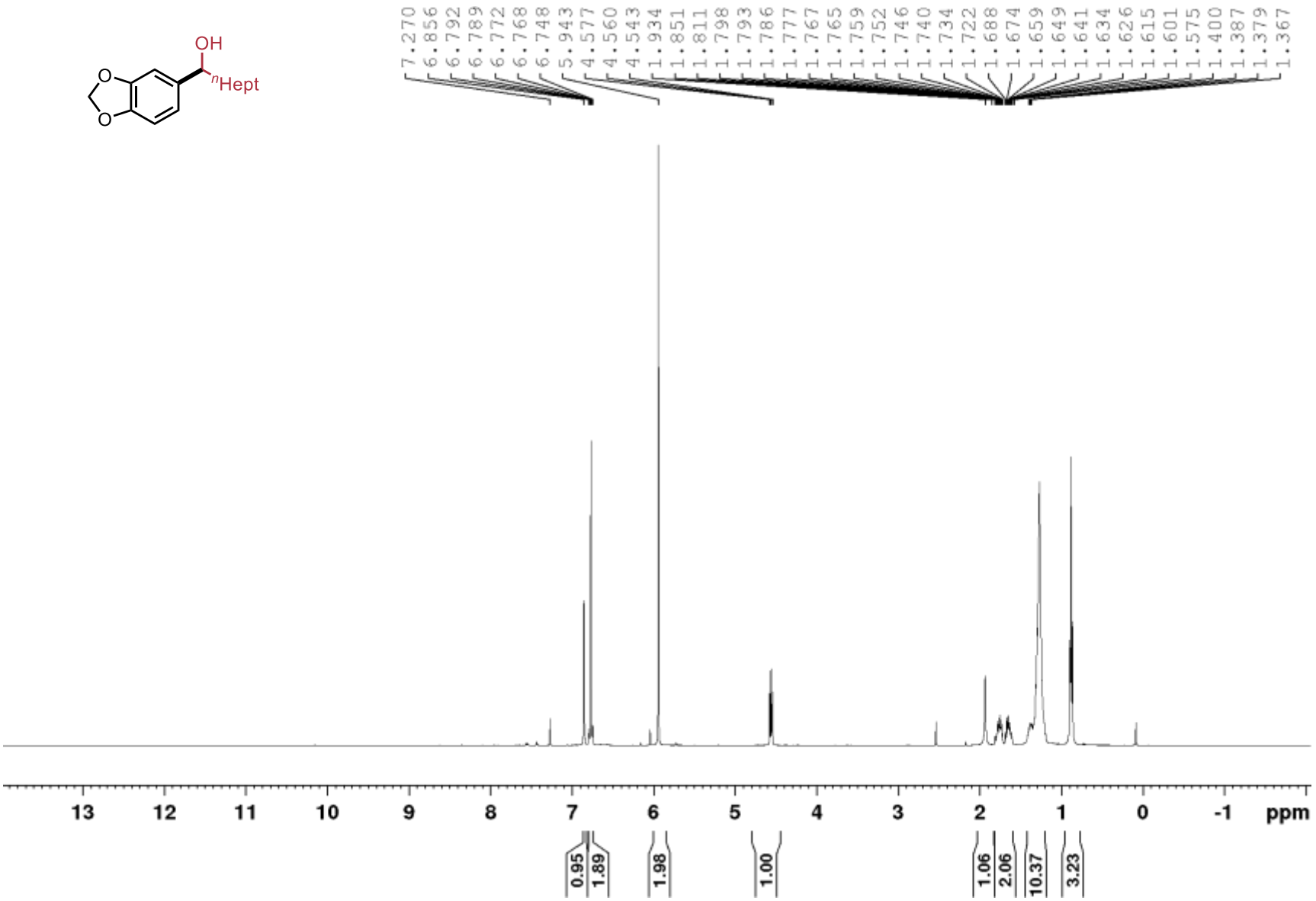

1-benzo[1,3]dioxol-5-yl-octan-1-ol (2.30), ^{13}C, $CDCl_3$, 100 MHz

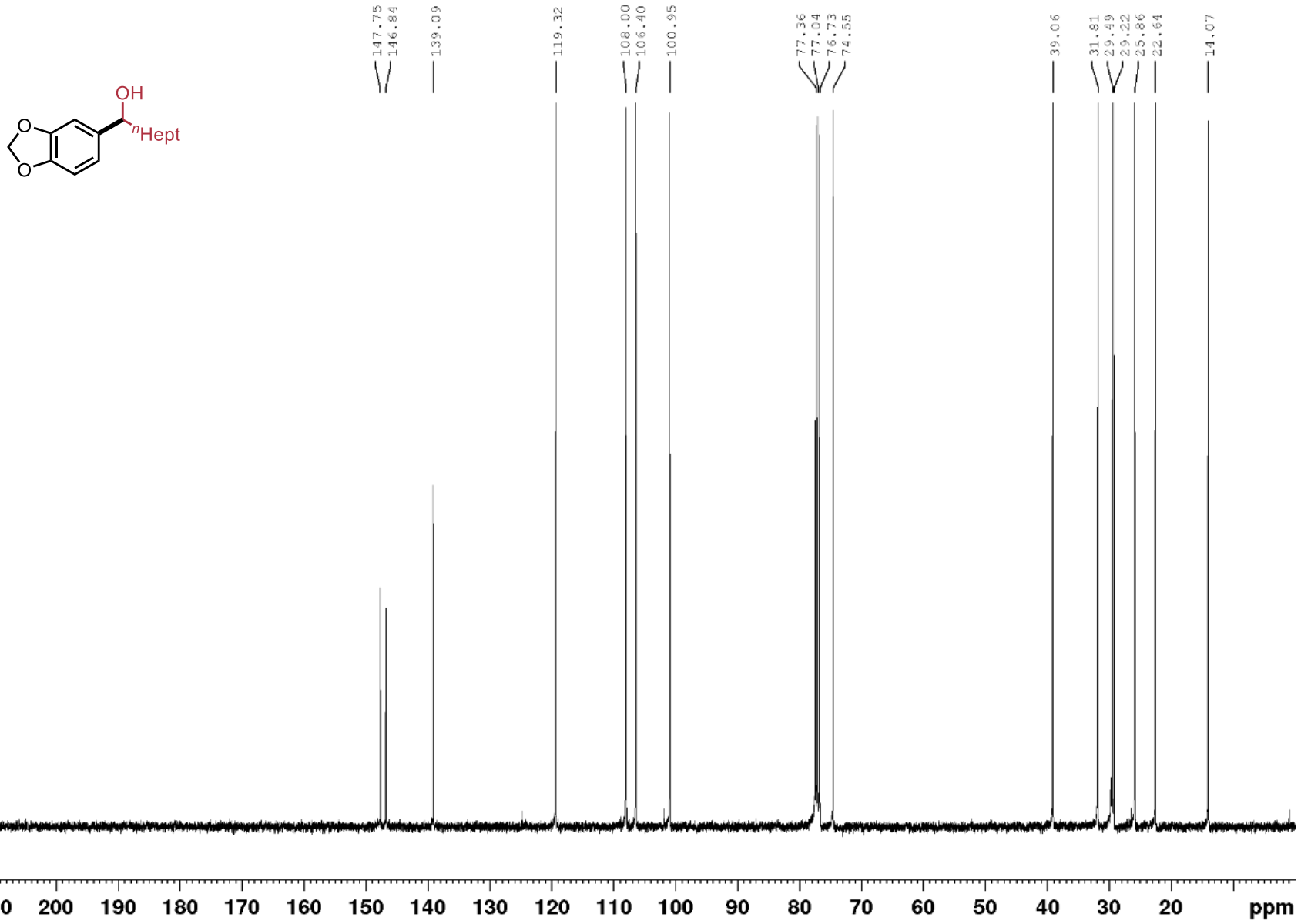

1-(naphthalen-1-yl)ethan-1-ol (2.31), ^{1}H, $CDCl_3$, 400 MHz

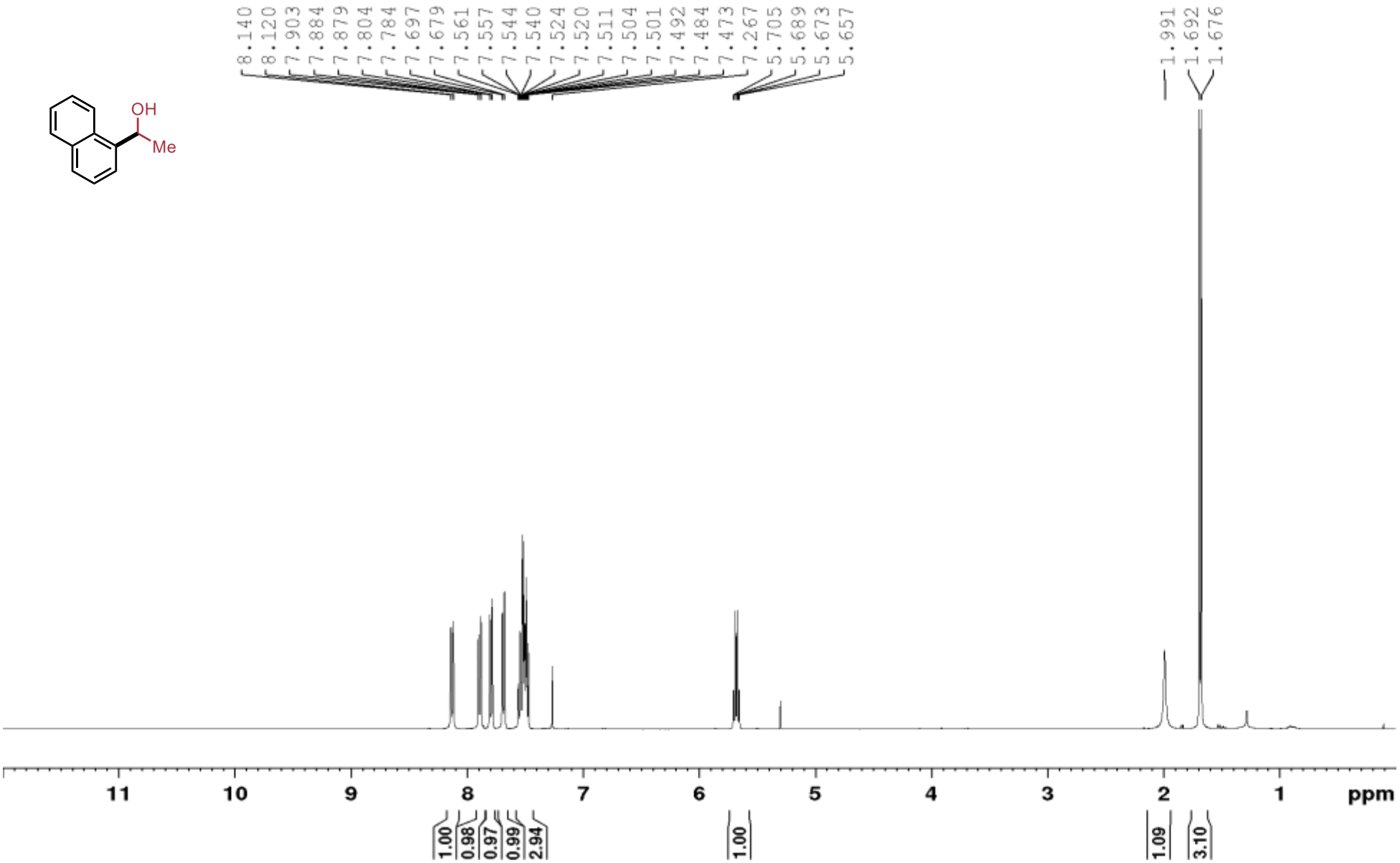

1-(naphthalen-1-yl)ethan-1-ol (2.31), ^{13}C, $CDCl_3$, 100 MHz

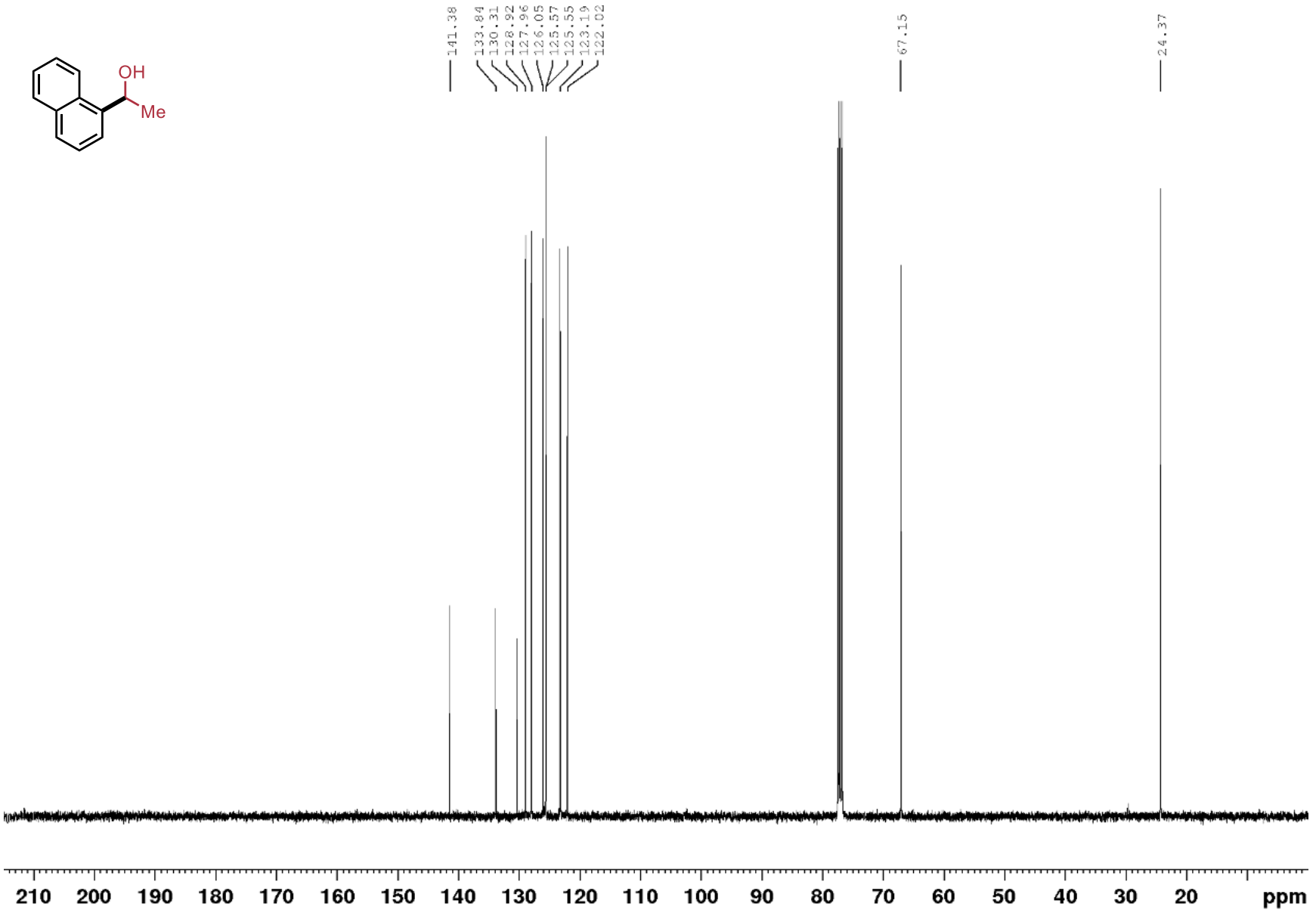

Cyclohexyl(naphthalen-1-yl)methanol (2.32), ^{1}H, $CDCl_3$, 400 MHz

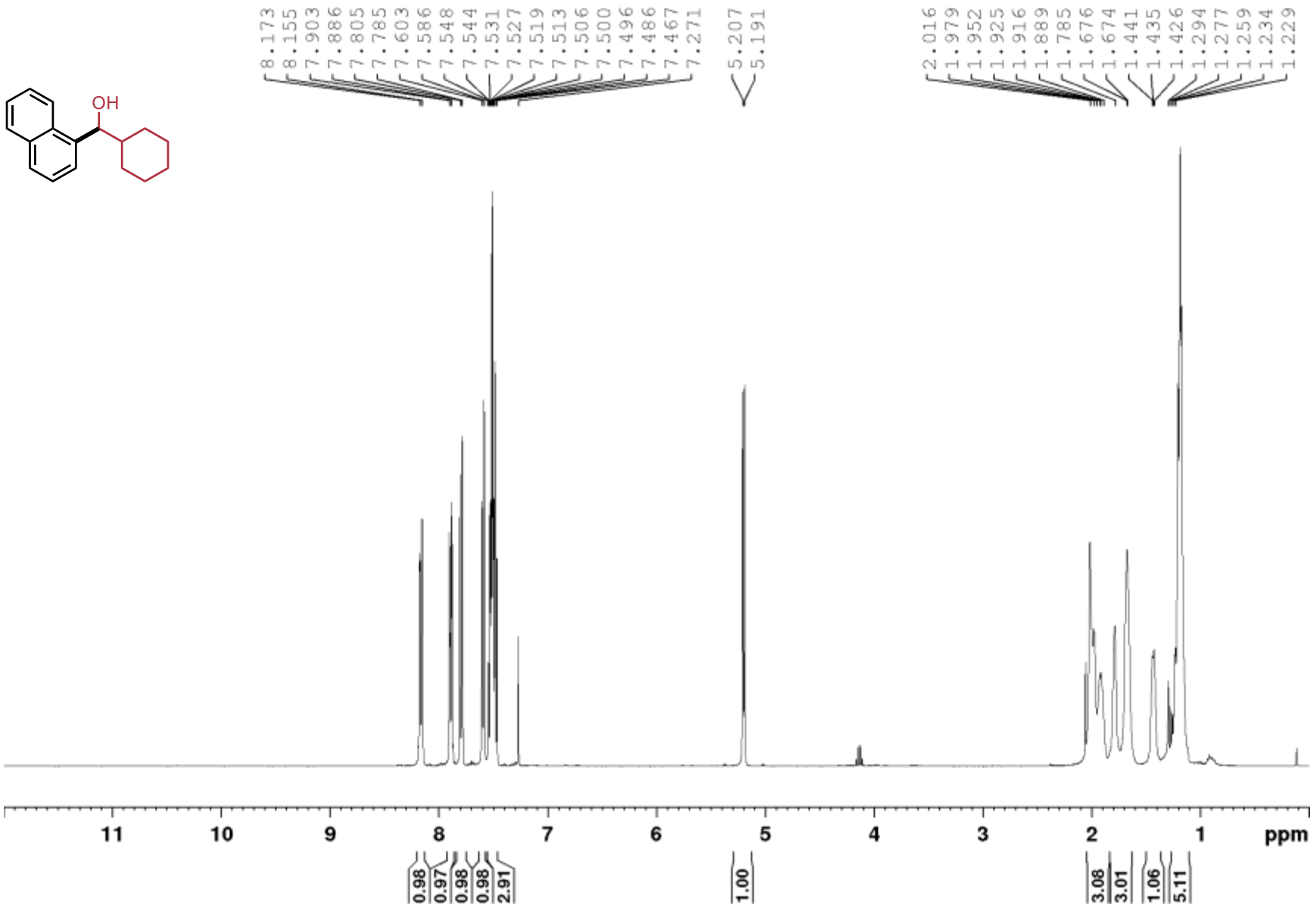

Cyclohexyl(naphthalen-1-yl)methanol (2.32), ^{13}C, $CDCl_3$, 100 MHz

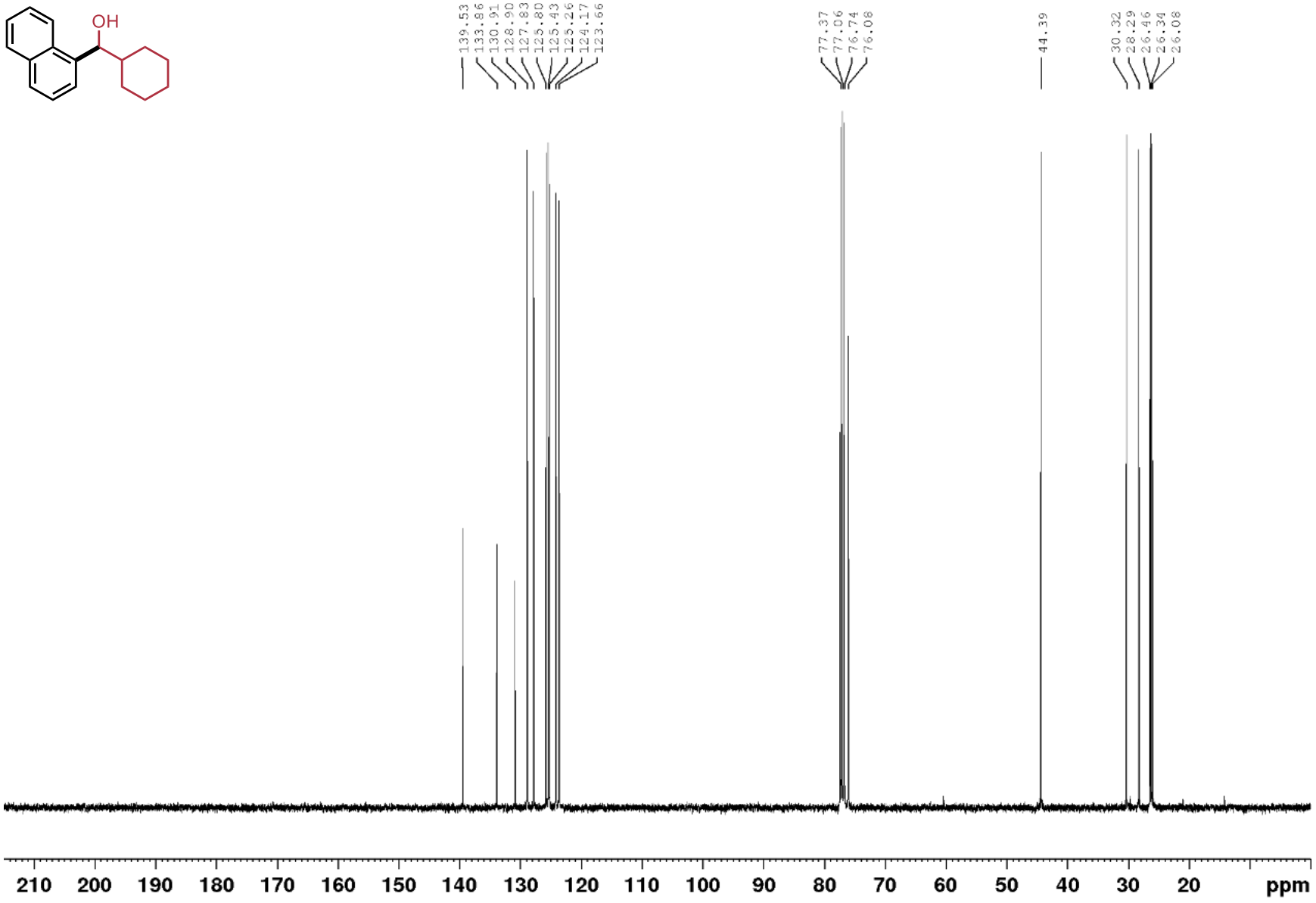

Cyclohex-3-en-1-yl(naphthalen-1-yl)methanol (1.33), ^{1}H, $CDCl_3$, 400 MHz

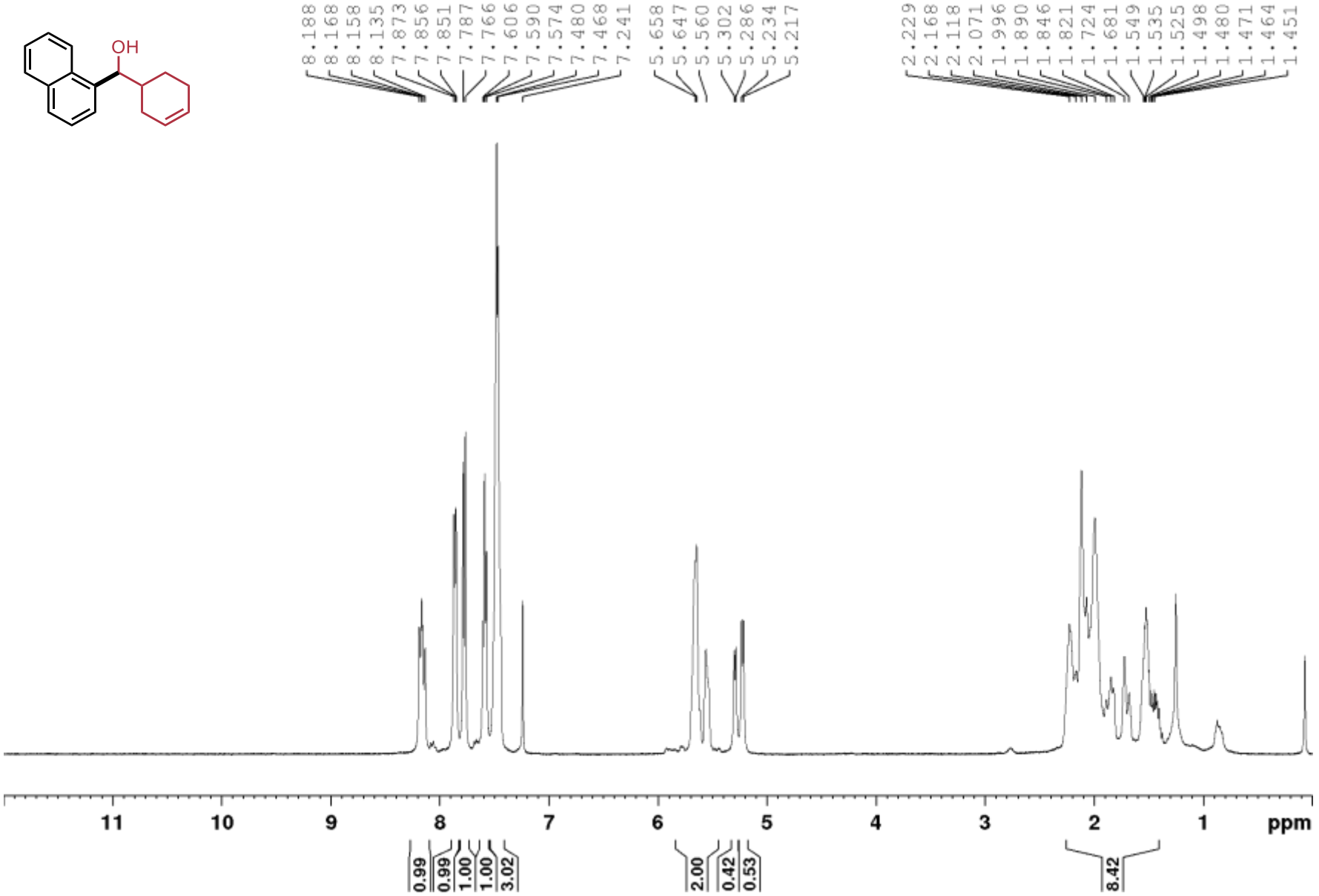

Cyclohex-3-en-1-yl(naphthalen-1-yl)methanol (2.33), ^{13}C,

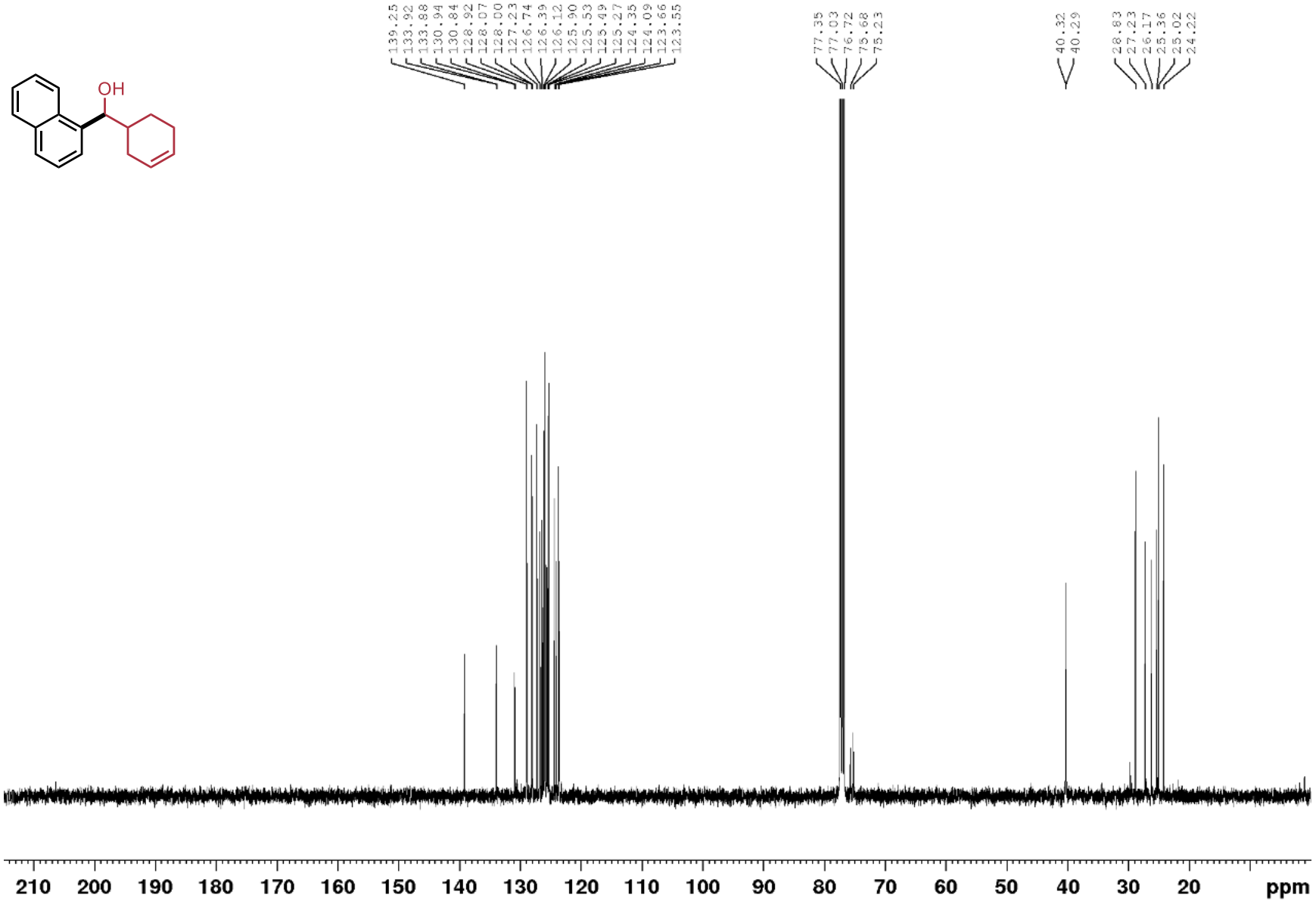

2-(4'-methoxyphenyl)-1-naphthalen-1-yl ethanol (2.34), ^{1}H, $CDCl_3$, 400 MHz

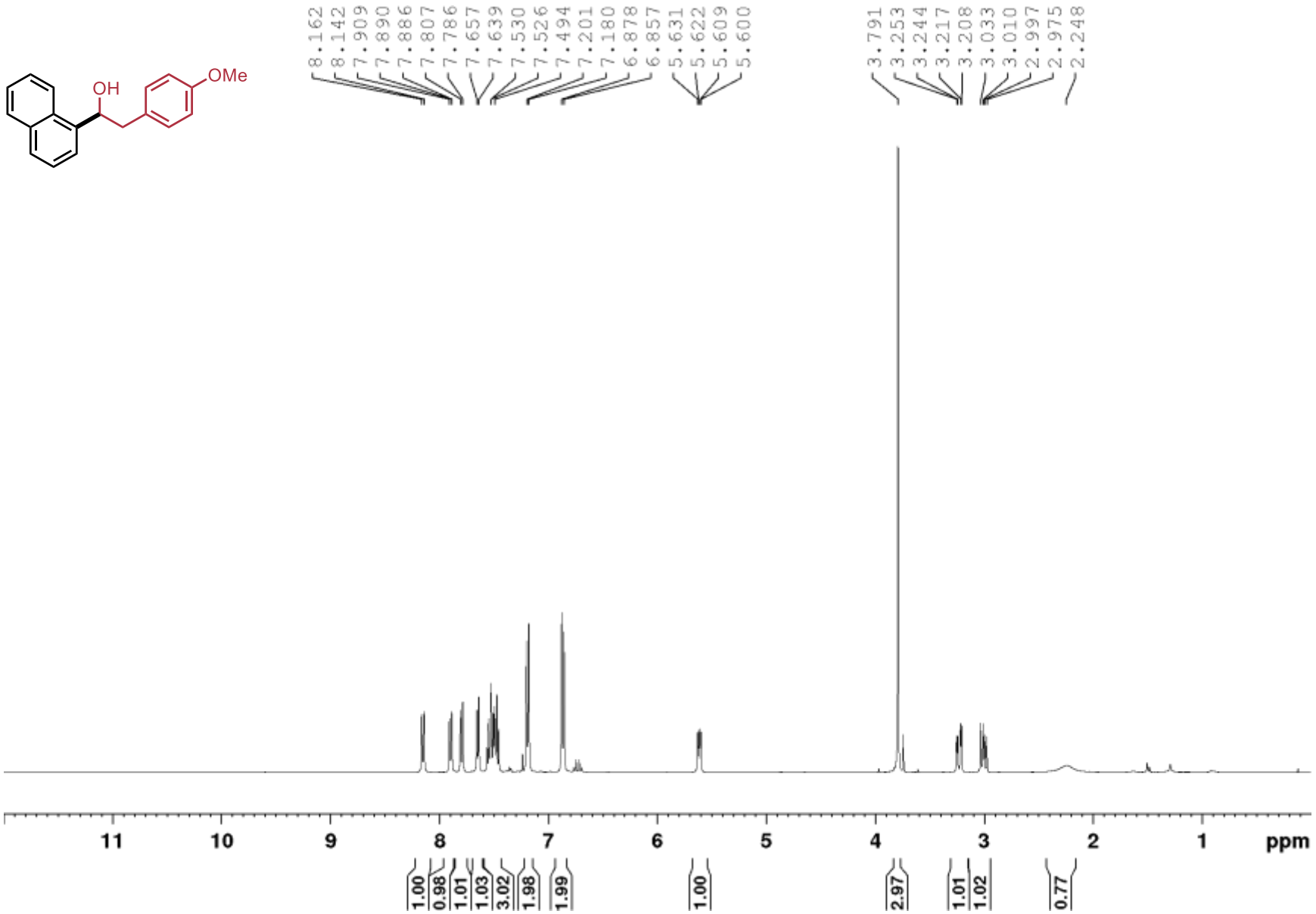

2-(4'-methoxyphenyl)-1-naphthalen-1-yl ethanol (2.34), ^{13}C, $CDCl_3$, 100 MHz

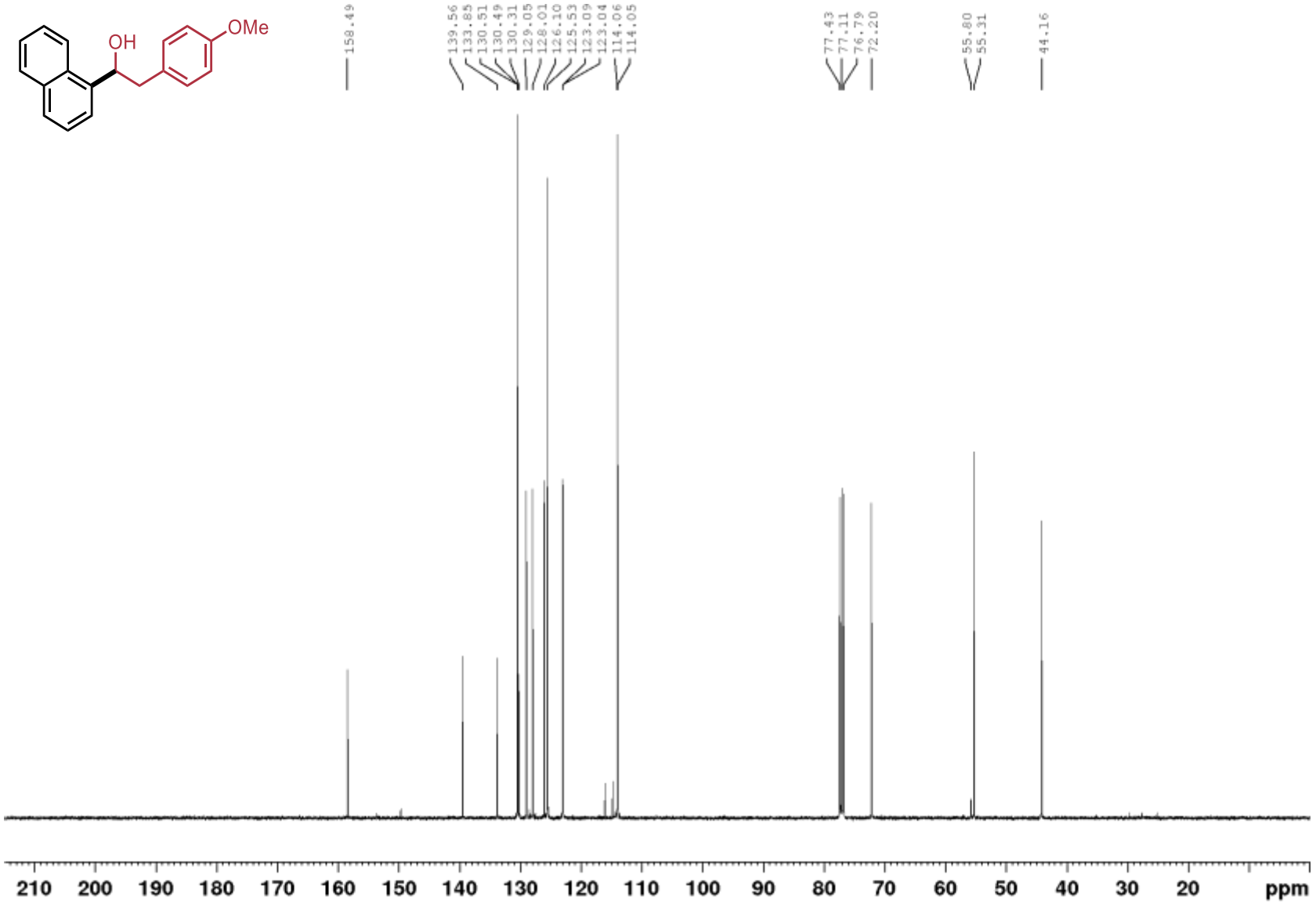

3-(hydroxy-1-naphthalenylmethyl)-1,1-dimethylethyl ester-1-Azetidinecarboxylic acid (2.35), ^{1}H, $CDCl_3$, 400 MHz

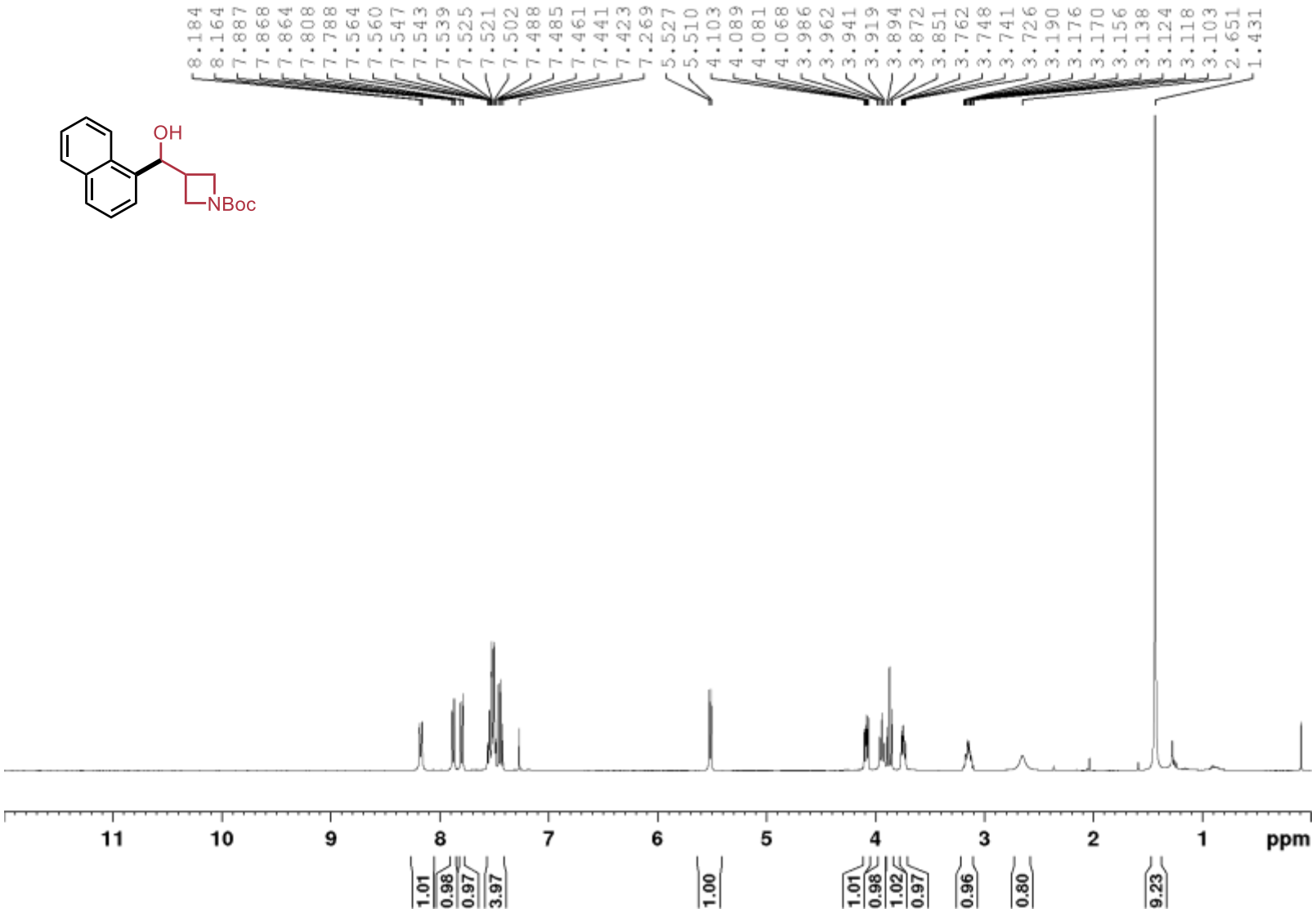

3-(hydroxy-1-naphthalenylmethyl)-1,1-dimethylethyl ester-1-Azetidinecarboxylic acid (2.35), ^{13}C, $CDCl_3$, 100 MHz

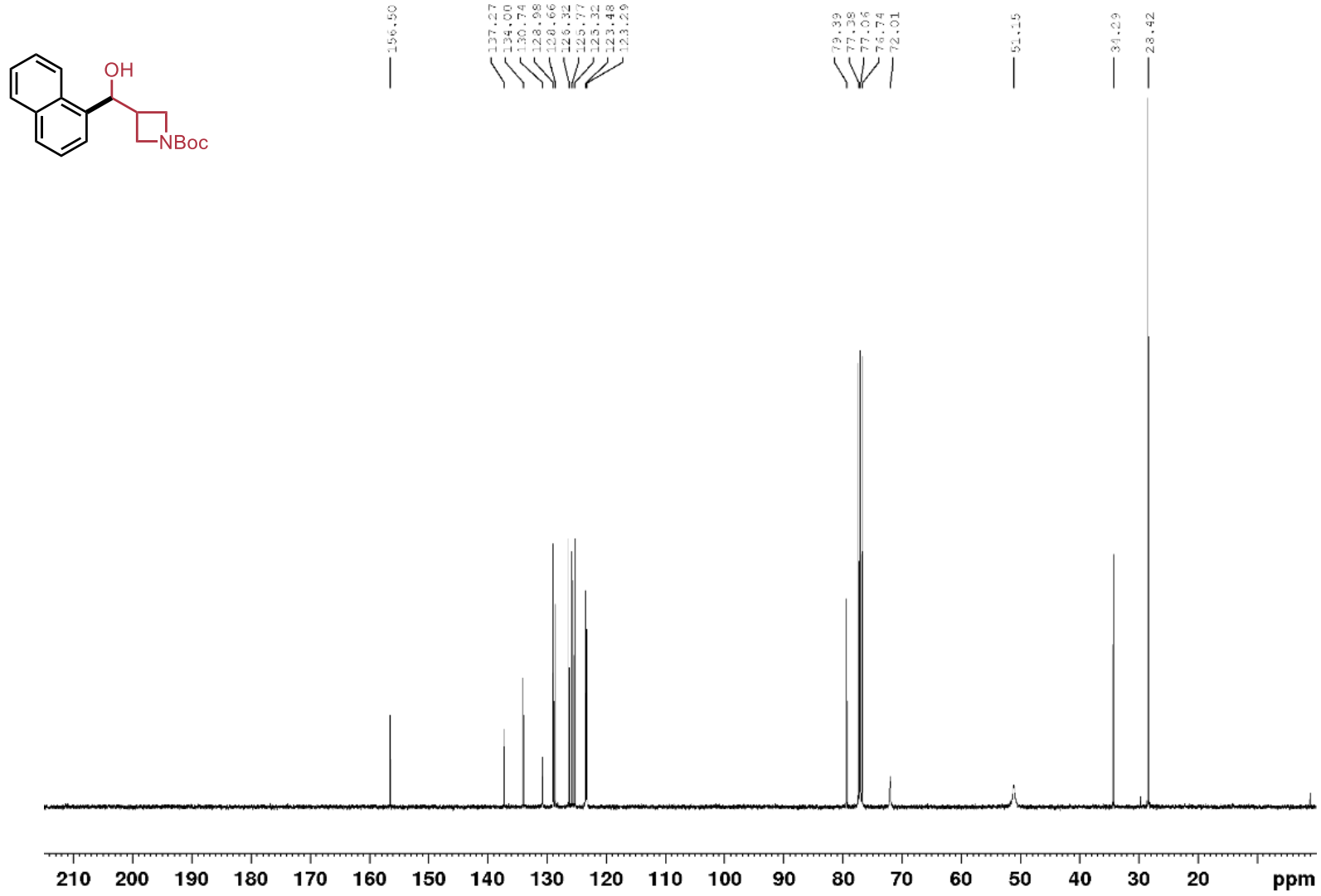

Cyclobutyl(naphthalen-1-yl)methanol (2.36), ^{1}H, $CDCl_3$, 400 MHz

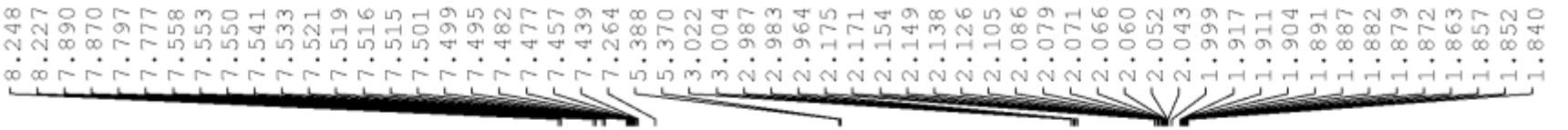

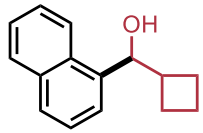

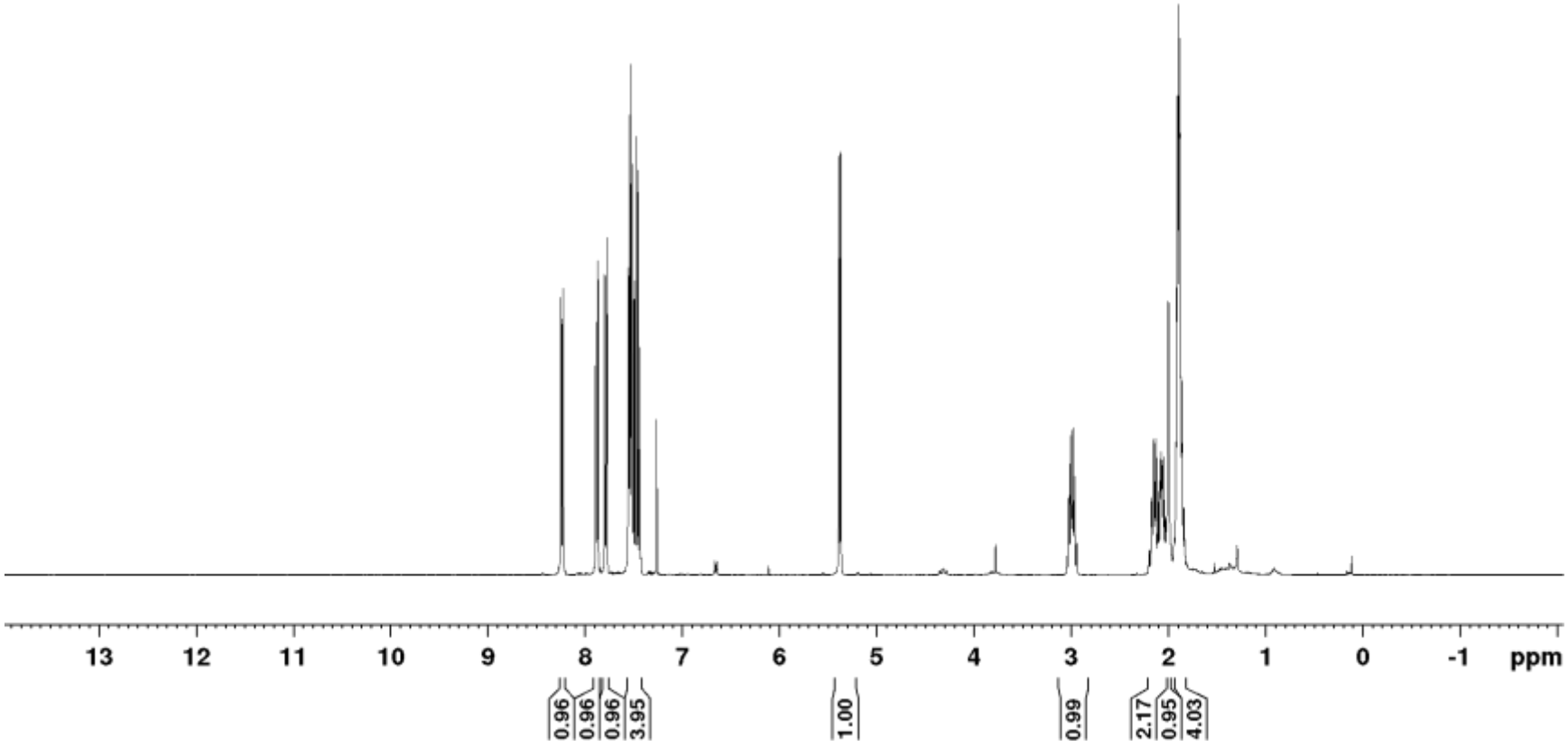

Cyclobutyl(naphthalen-1-yl)methanol (2.36), ^{13}C, $CDCl_3$, 100 MHz

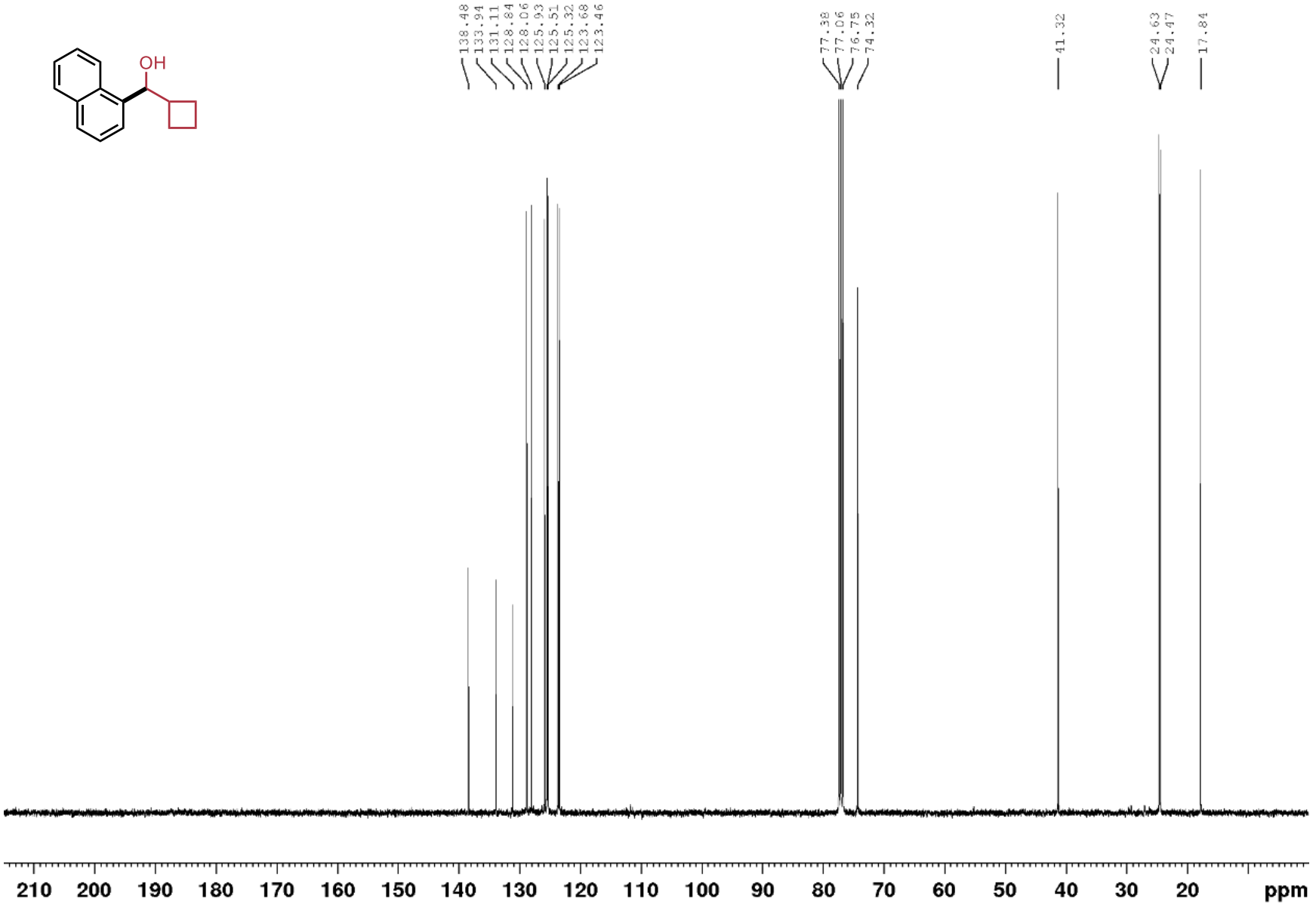

1-[4-[cyclobutyl(hydroxy)methyl]phenyl]ethanone (2.37), ^{1}H, $CDCl_3$, 400 MHz

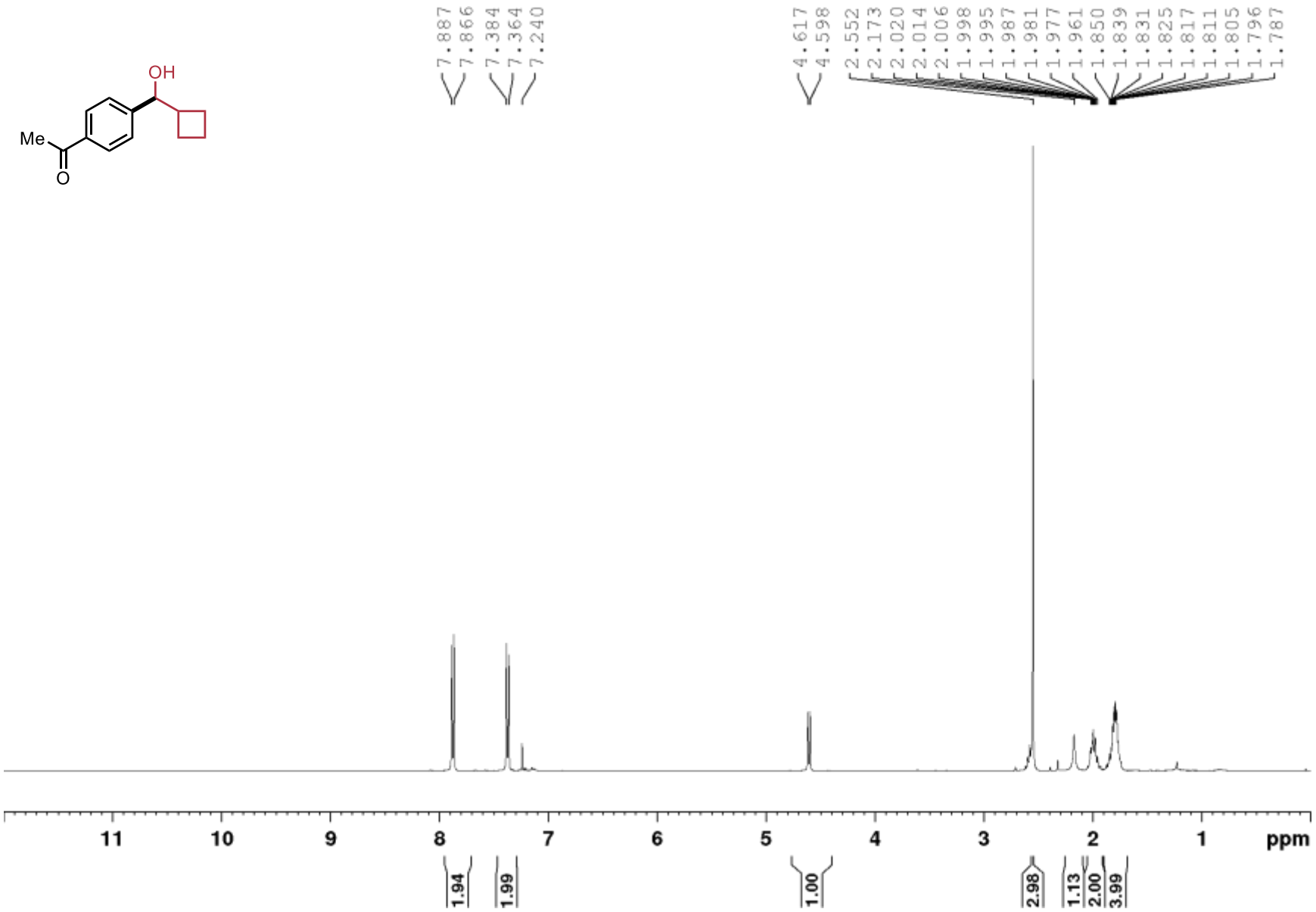

1-[4-[cyclobutyl(hydroxy)methyl]phenyl]ethanone (2.37), ^{13}C, $CDCl_3$, 100 MHz

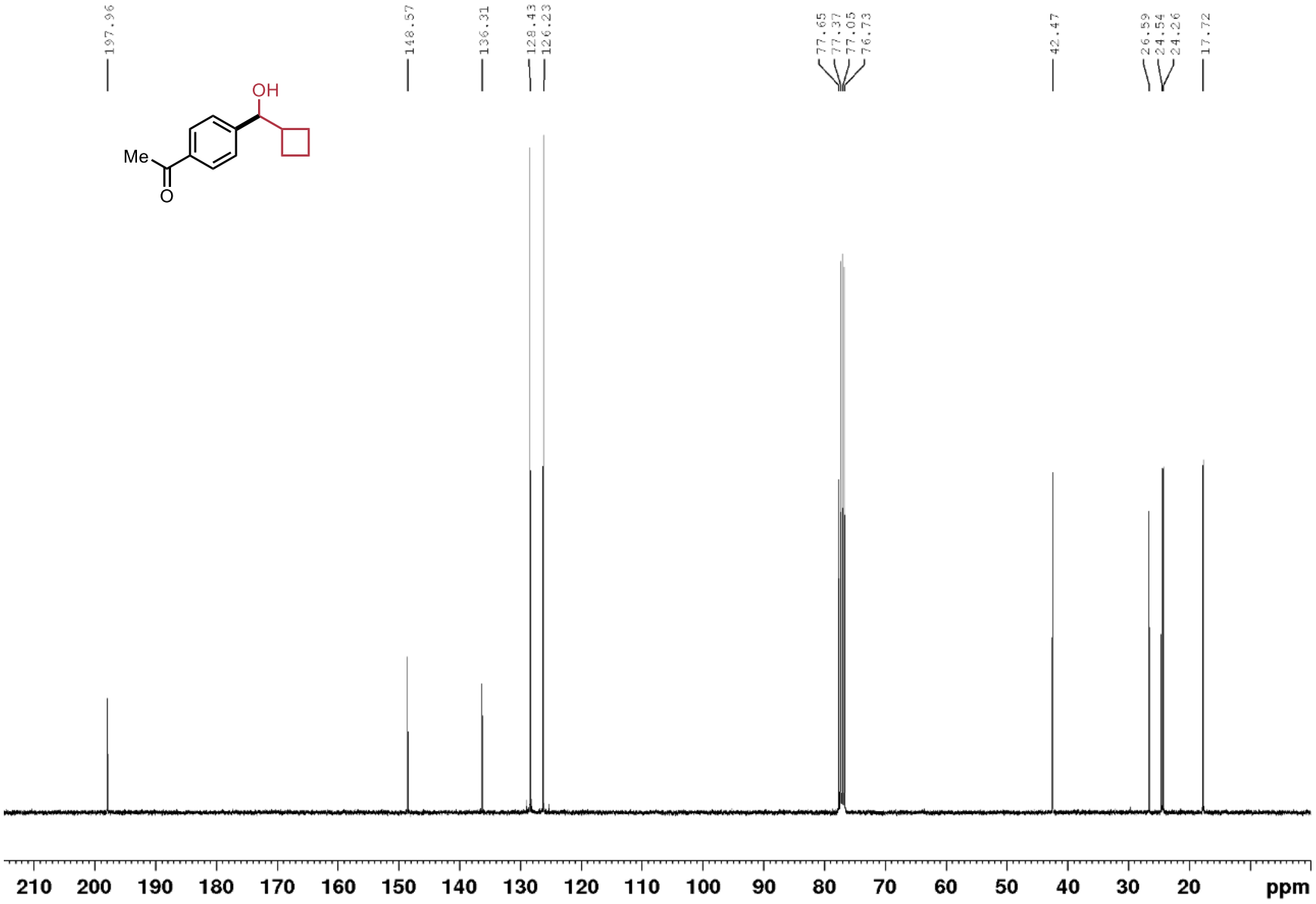

Cyclobutyl-(3,5-dichlorophenyl)methanol (2.38), ^{1}H, $CDCl_3$, 400 MHz

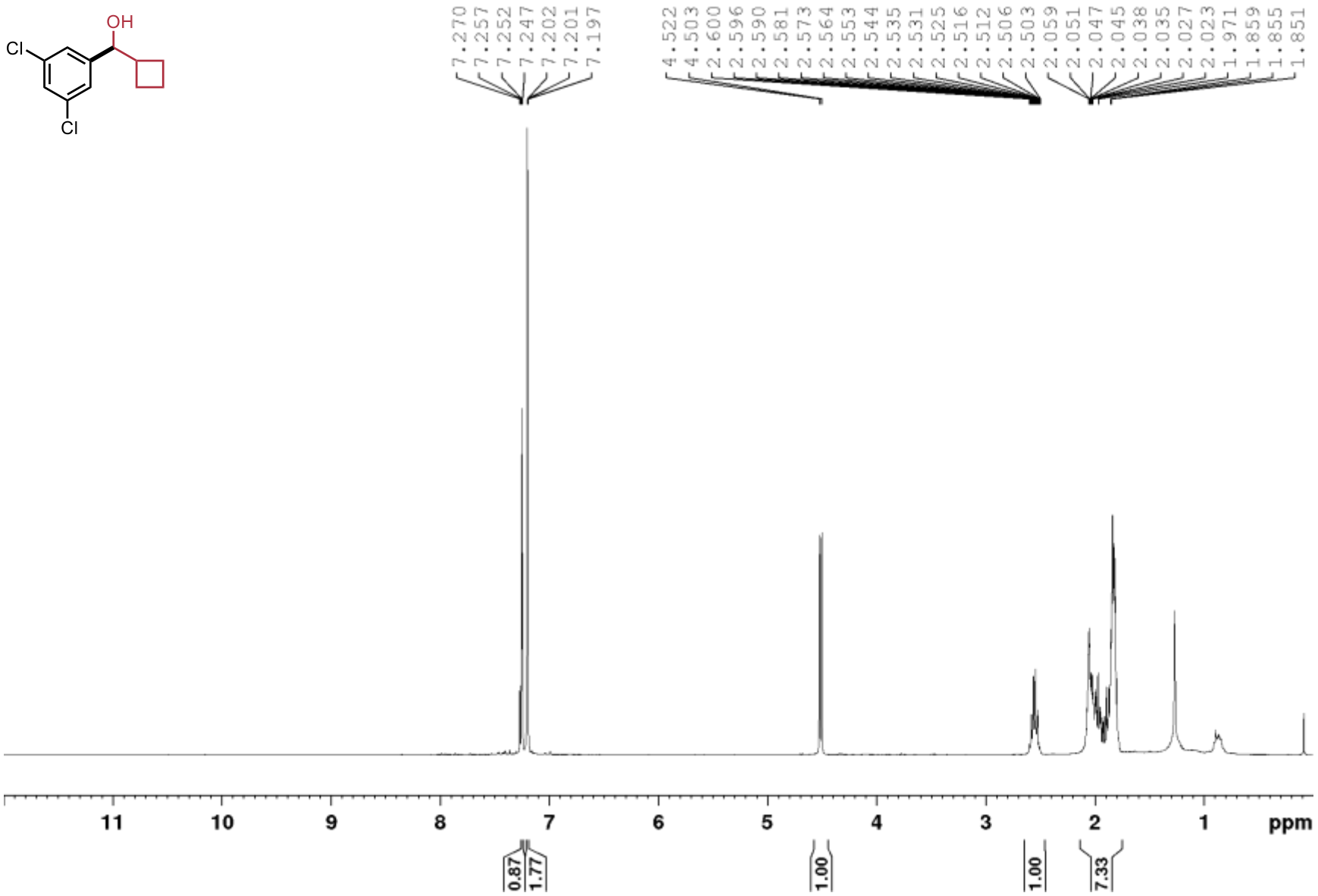

Cyclobutyl-(3,5-dichlorophenyl)methanol (2.38), ^{13}C, $CDCl_3$, 100 MHz

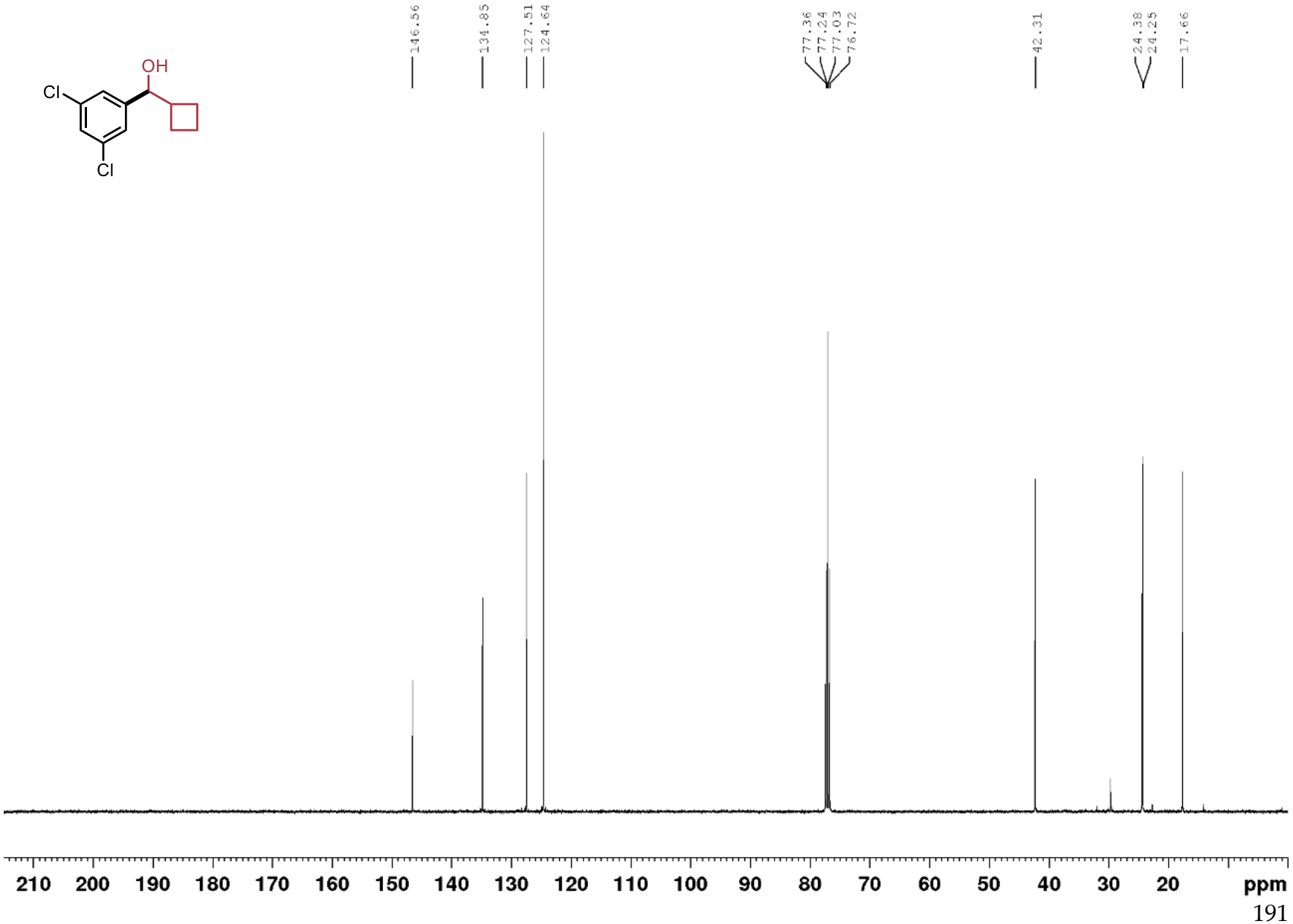

Cyclobutyl-[4-(trifluoromethoxy)phenyl]methanol (2.39), ^{1}H, $CDCl_3$, 400 MHz

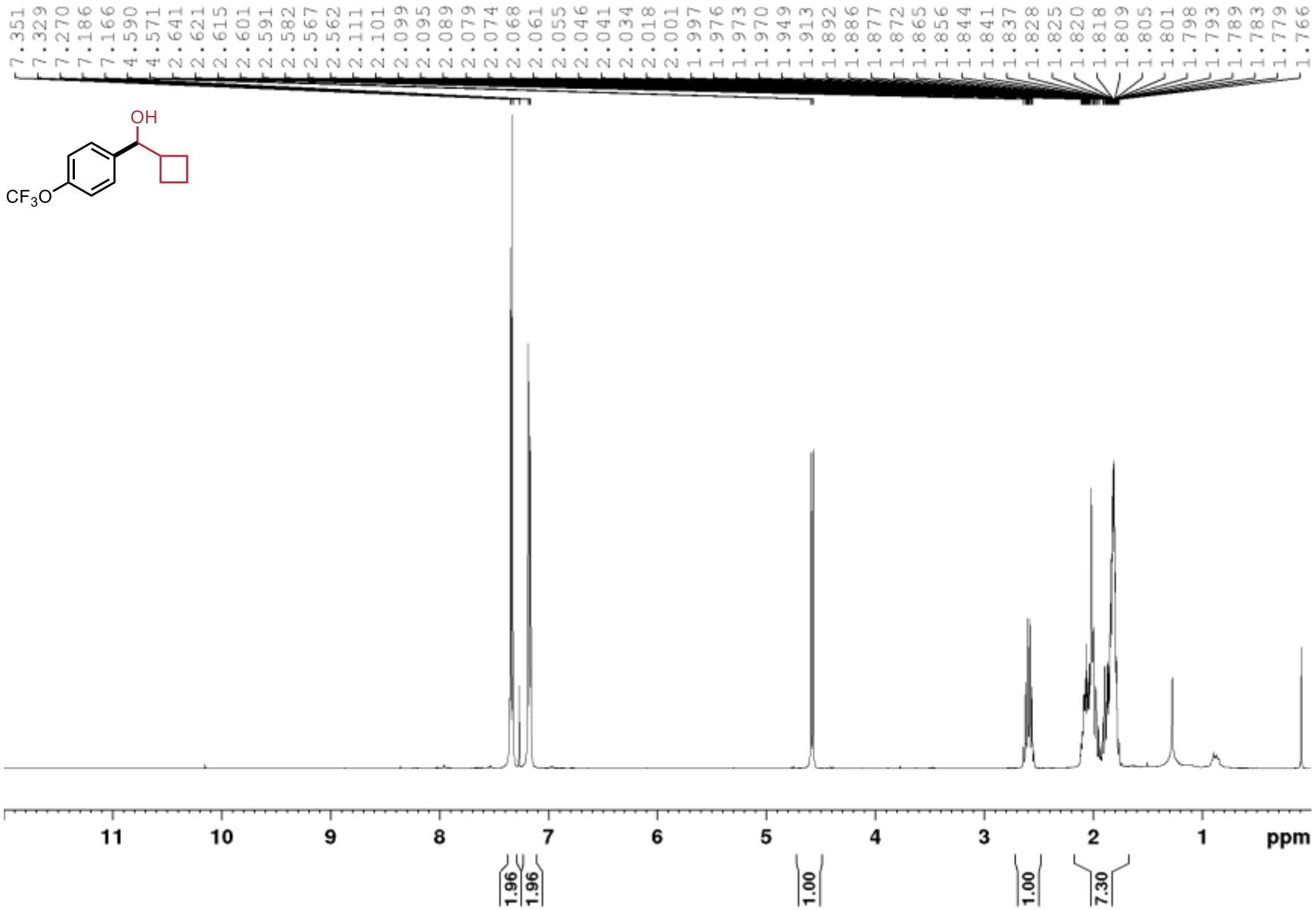

Cyclobutyl-[4-(trifluoromethoxy)phenyl]methanol (2.39), ^{13}C, $CDCl_3$, 100 MHz

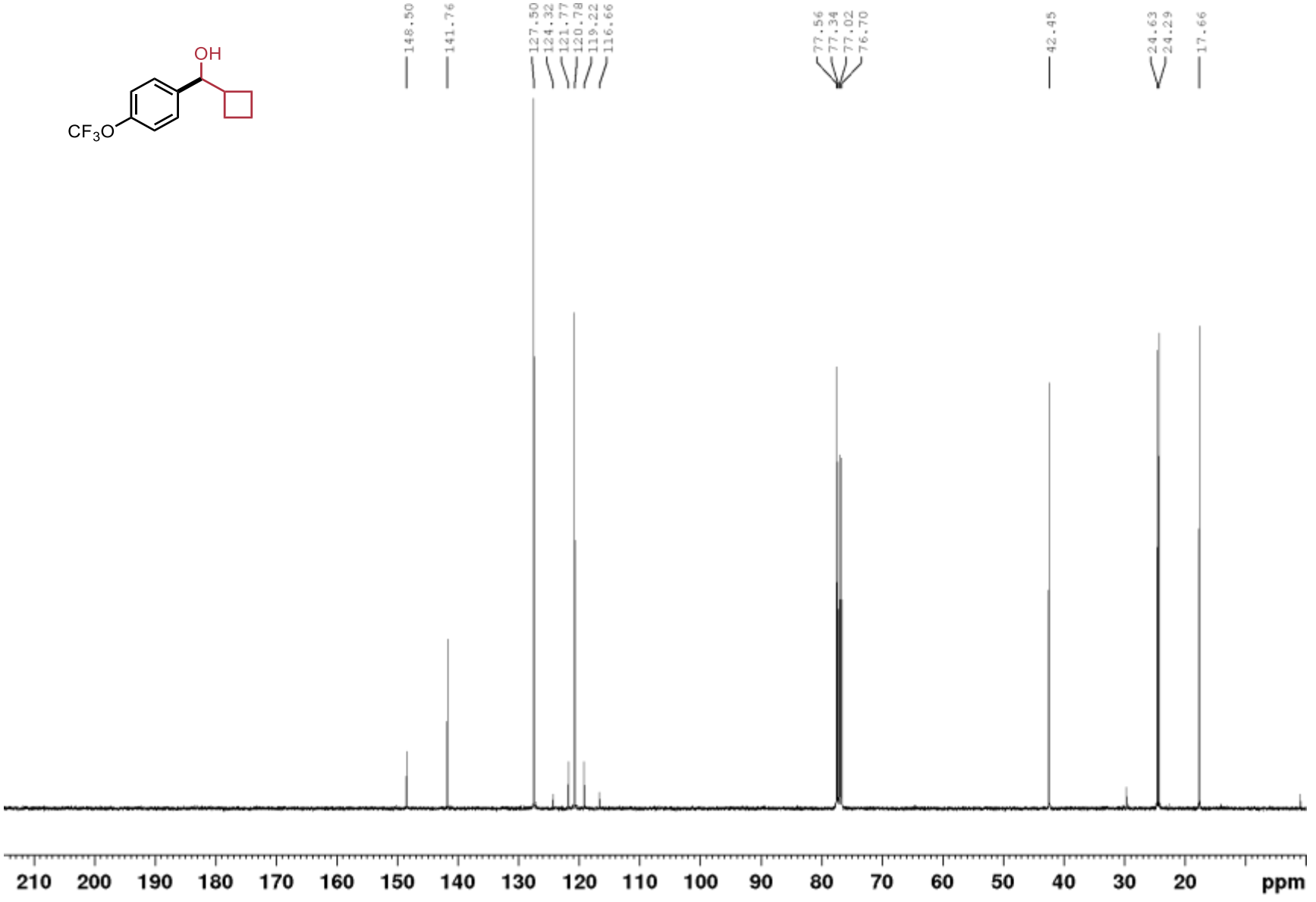

Cyclobutyl-[4-(trifluoromethoxy)phenyl]methanol (2.39), ^{19}F, $CDCl_3$, 377 MHz

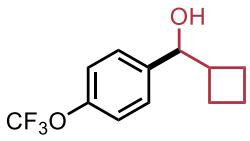

4-(cyclobutylhydroxymethyl)-benzoic acid methyl ester (2.40), ^{1}H, $CDCl_3$, 400 MHz

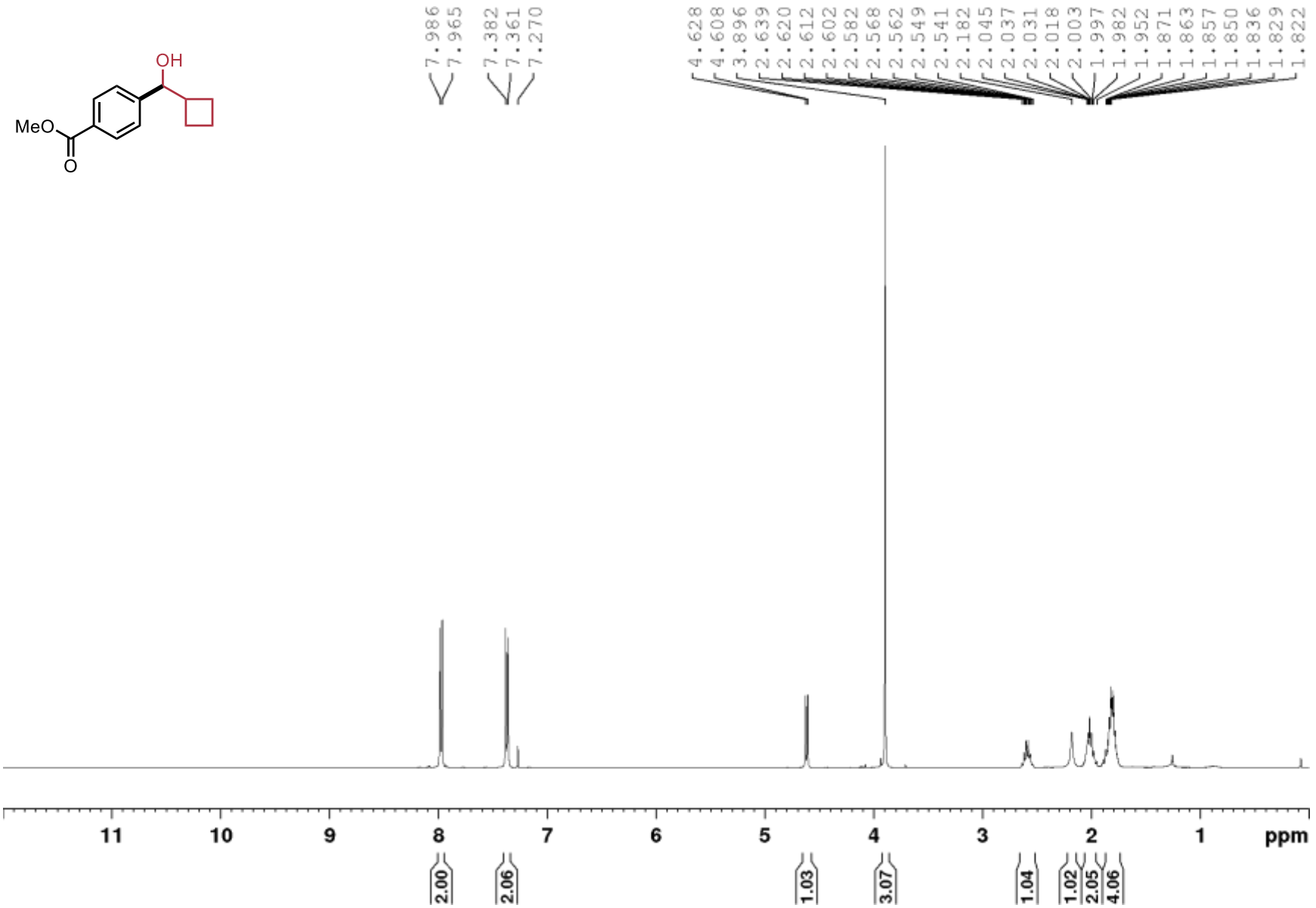

4-(cyclobutylhydroxymethyl)-benzoic acid methyl ester (2.40), ^{13}C, $CDCl_3$, 100 MHz

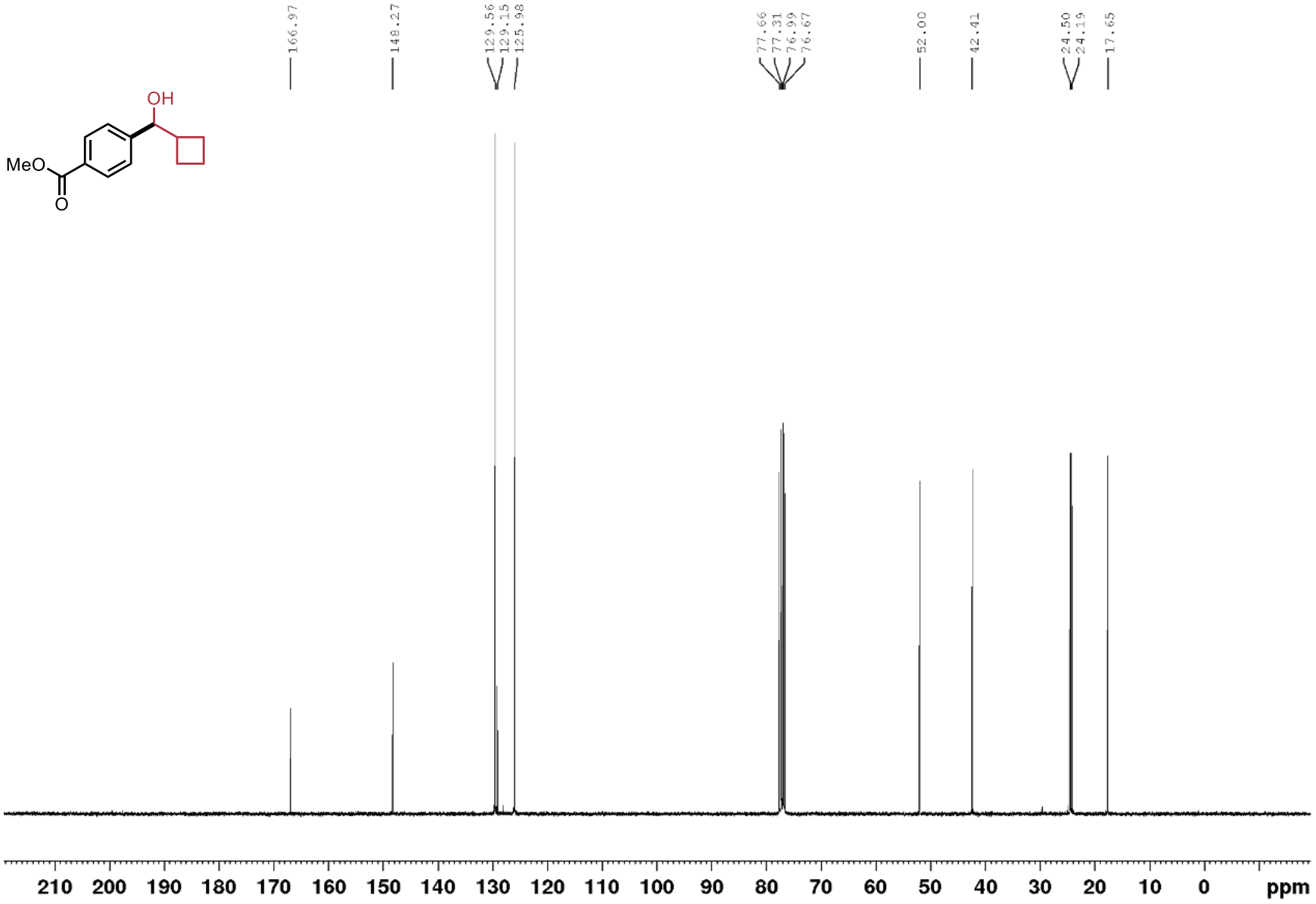

2-(1H-indol-3-yl)-1-(naphthalen-1-yl)ethanol (2.41), ^{1}H, $CDCl_3$, 400 MHz

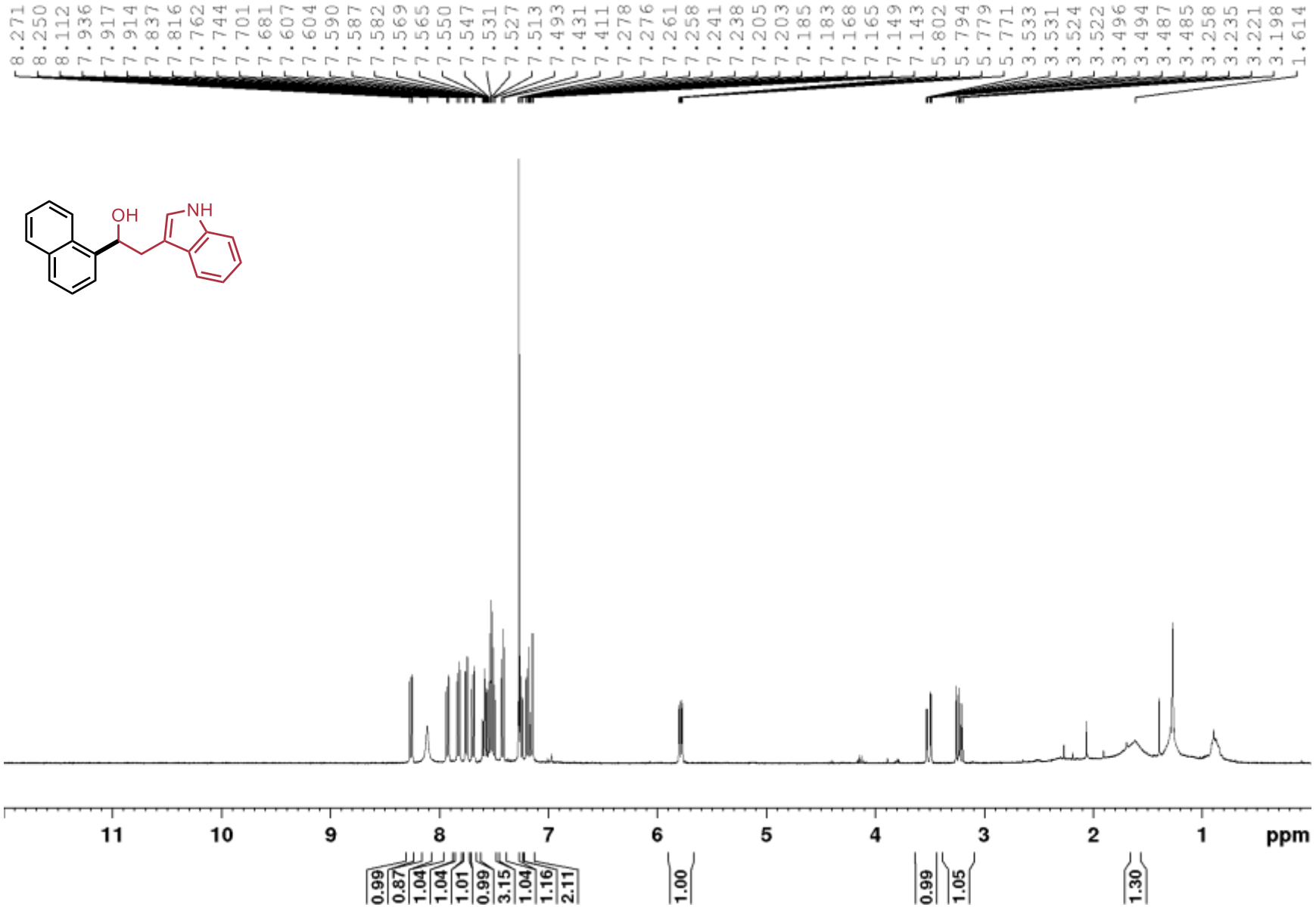

2-(1H-indol-3-yl)-1-(naphthalen-1-yl)ethanol (2.41), ^{13}C, $CDCl_3$, 100 MHz

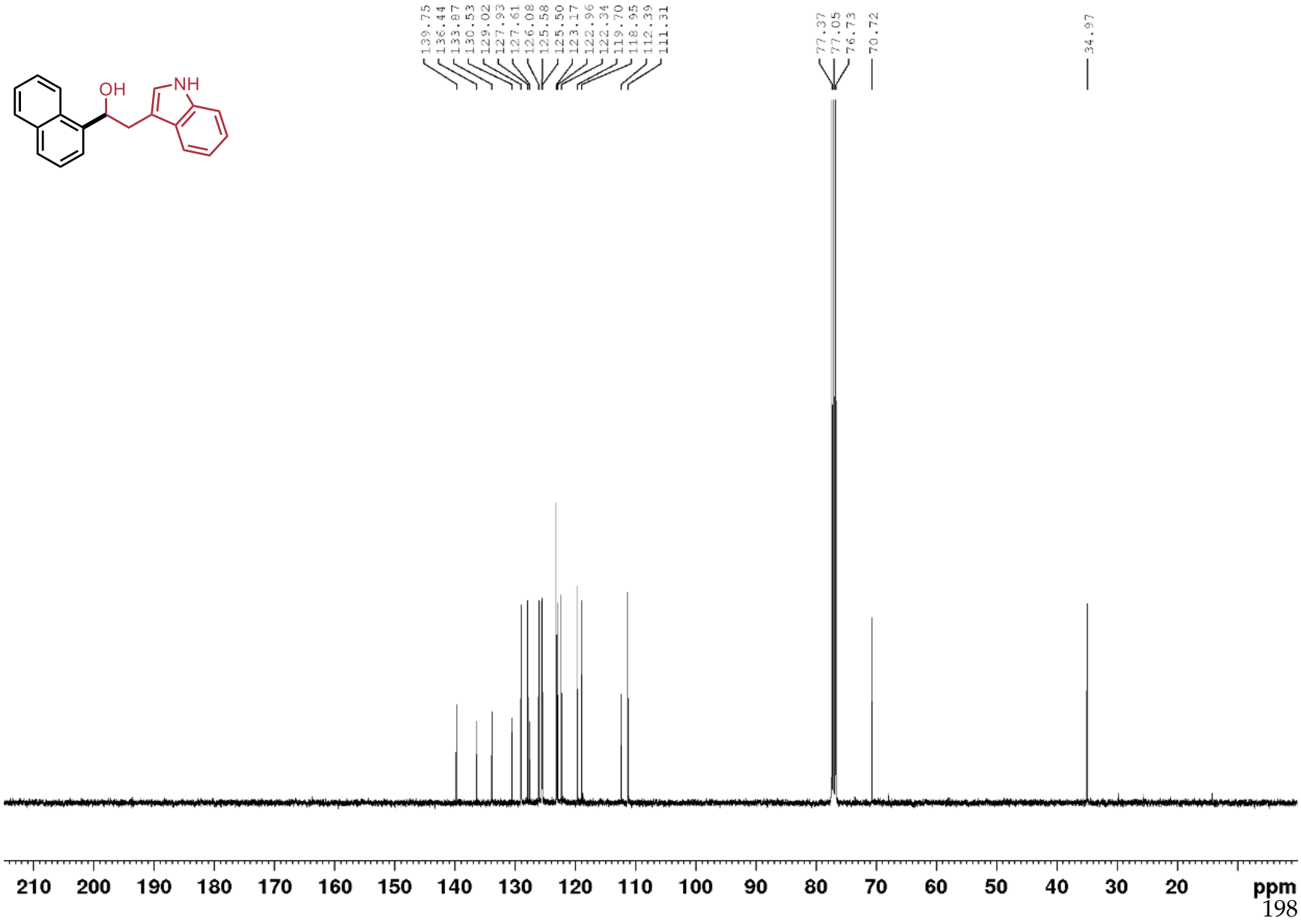

3-(hydroxy-[1-(11-(1-(Ethoxycarbonyl)piperidin-4-ylidene)-6,11-dihydro-5H-benzo[5,6]cyclohepta[1,2-b]pyridin-8-yl])-1,1-dimethylethyl ester-1-Azetidinecarboxylic acid (2.42), ^{1}H, $CDCl_3$, 400 MHz

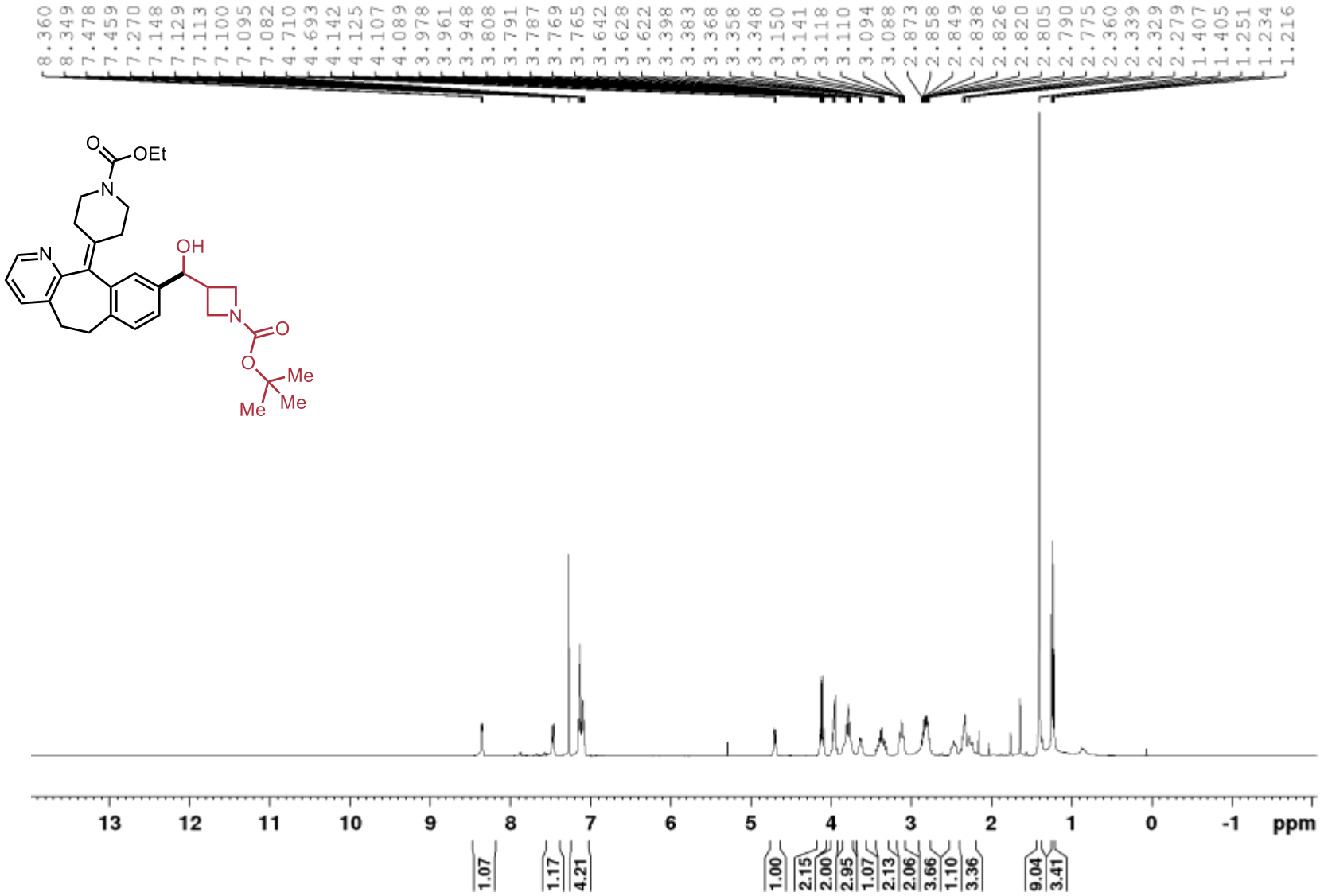

3-(hydroxy-[1-(11-(1-(Ethoxycarbonyl)piperidin-4-ylidene)-6,11-dihydro-5H-benzo[5,6]cyclohepta[1,2-b]pyridin-8-yl]) -1,1-dimethylethyl ester-1-Azetidinecarboxylic acid (2.42), ^{13}C, $CDCl_3$, 100 MHz

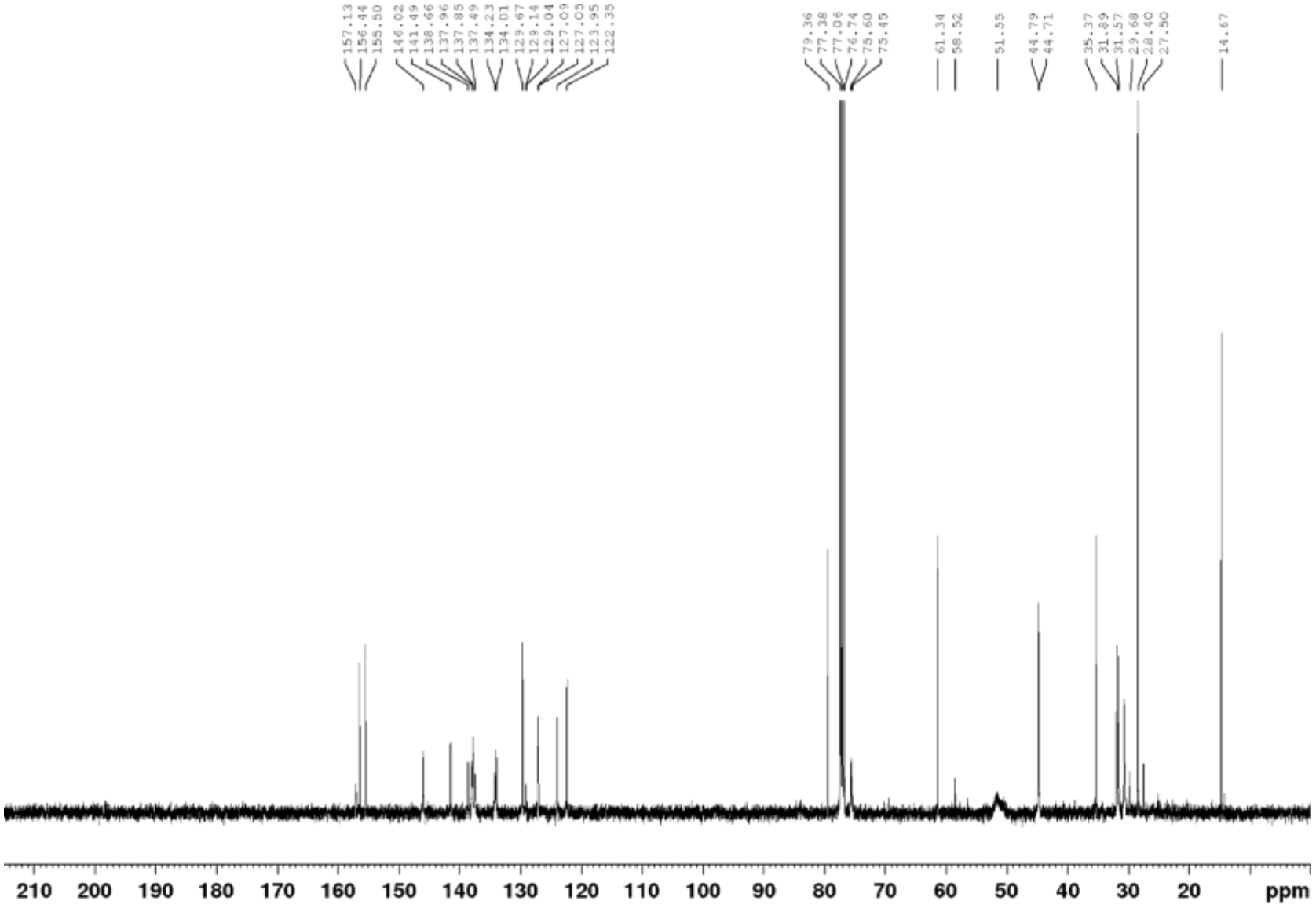

Appendix B: NMR Spectra for Chapter 3

Nickel(0)-1,5-bis(*p*-benzotrifluoride)-3,7-bis(cyclohexyl)-1,5,3,7-diazadiphosphacyclooctane $Ni^{0}(P^{Cy}_{2}N^{ArCF3}_{2})_{2}$, ^{19}F, C_6D_6, 282 MHz

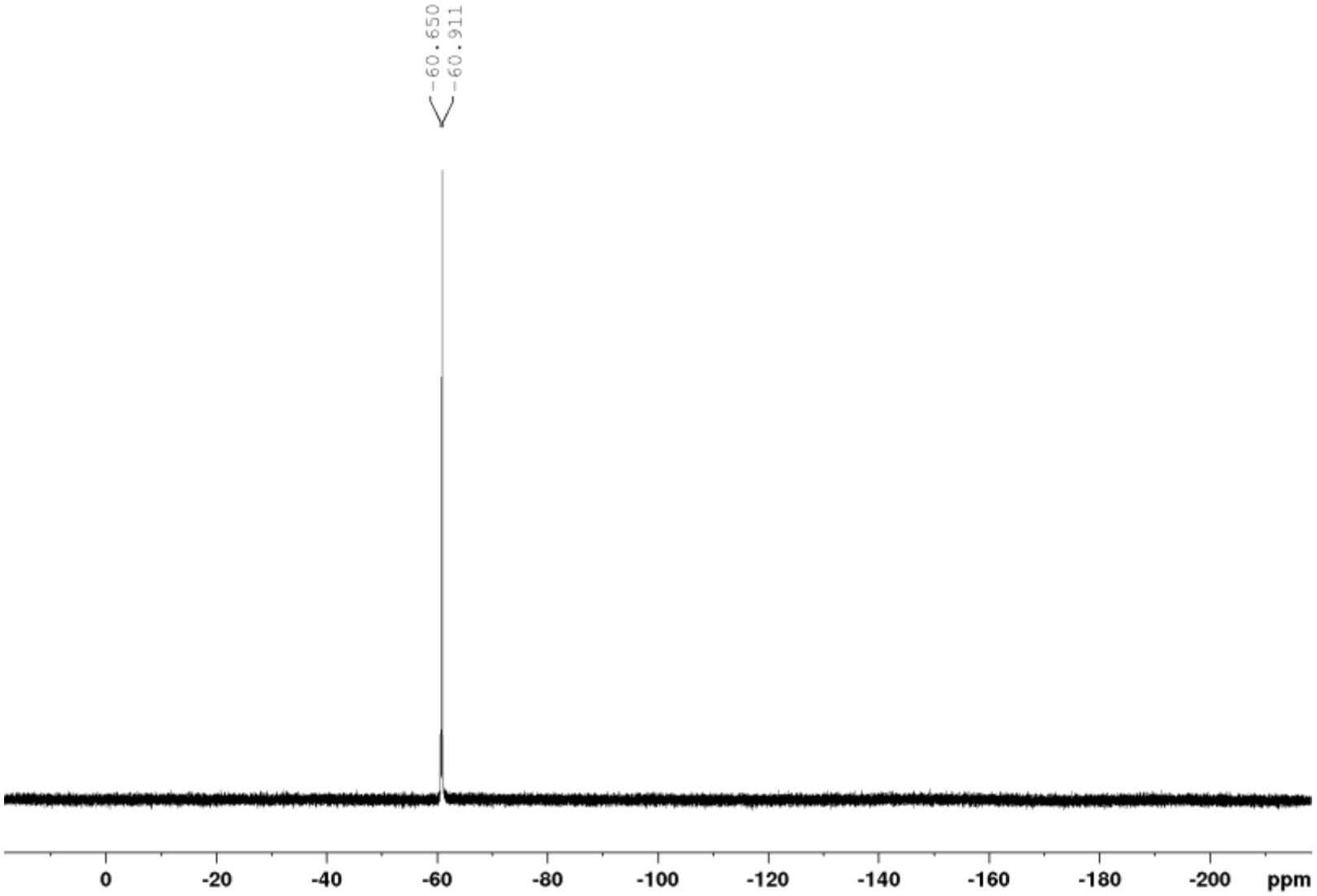

Nickel(0)-1,5-bis(*p*-benzotrifluoride)-3,7-bis(cyclohexyl)-1,5,3,7-diazadiphosphacyclooctane $Ni^0(P^{Cy}_2N^{ArCF3}_2)_2$, ^{31}P, C_6D_6, 121.5 MHz

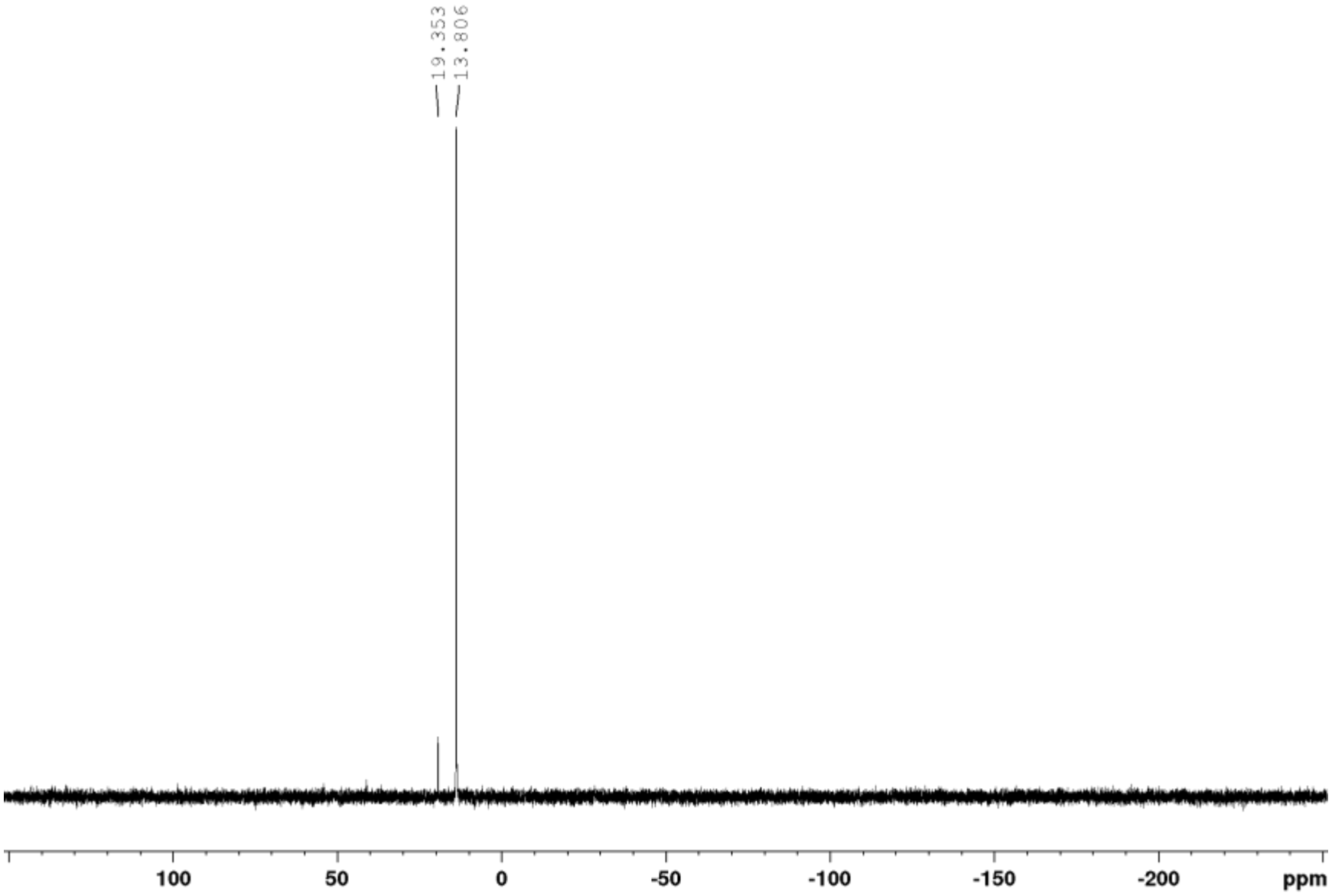

Nickel(0)-1,5-bis(*p*-benzotrifluoride)-3,7-bis(phenyl)-1,5,3,7-diazadiphosphacyclooctane $Ni^0(P^{Ph}_2N^{ArCF3}_2)_2$, ^1H, C_6D_6, 300 MHz

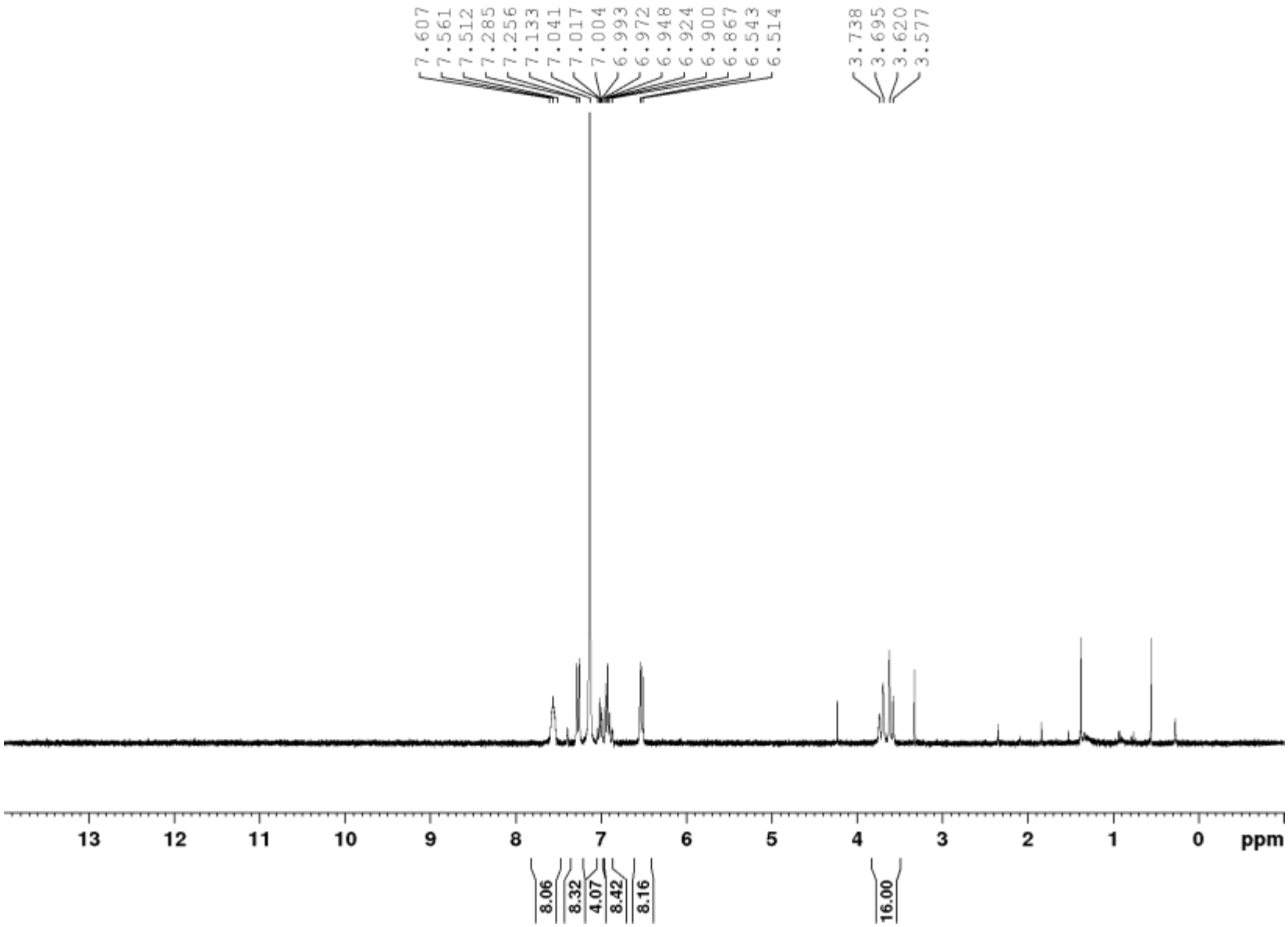

Nickel(0)-1,5-bis(*p*-benzotrifluoride)-3,7-bis(phenyl)-1,5,3,7-diazadiphosphacyclooctane $Ni^0(P^{Ph}{}_2N^{ArCF3}{}_2)_2$, ^{19}F, C_6D_6, 282 MHz

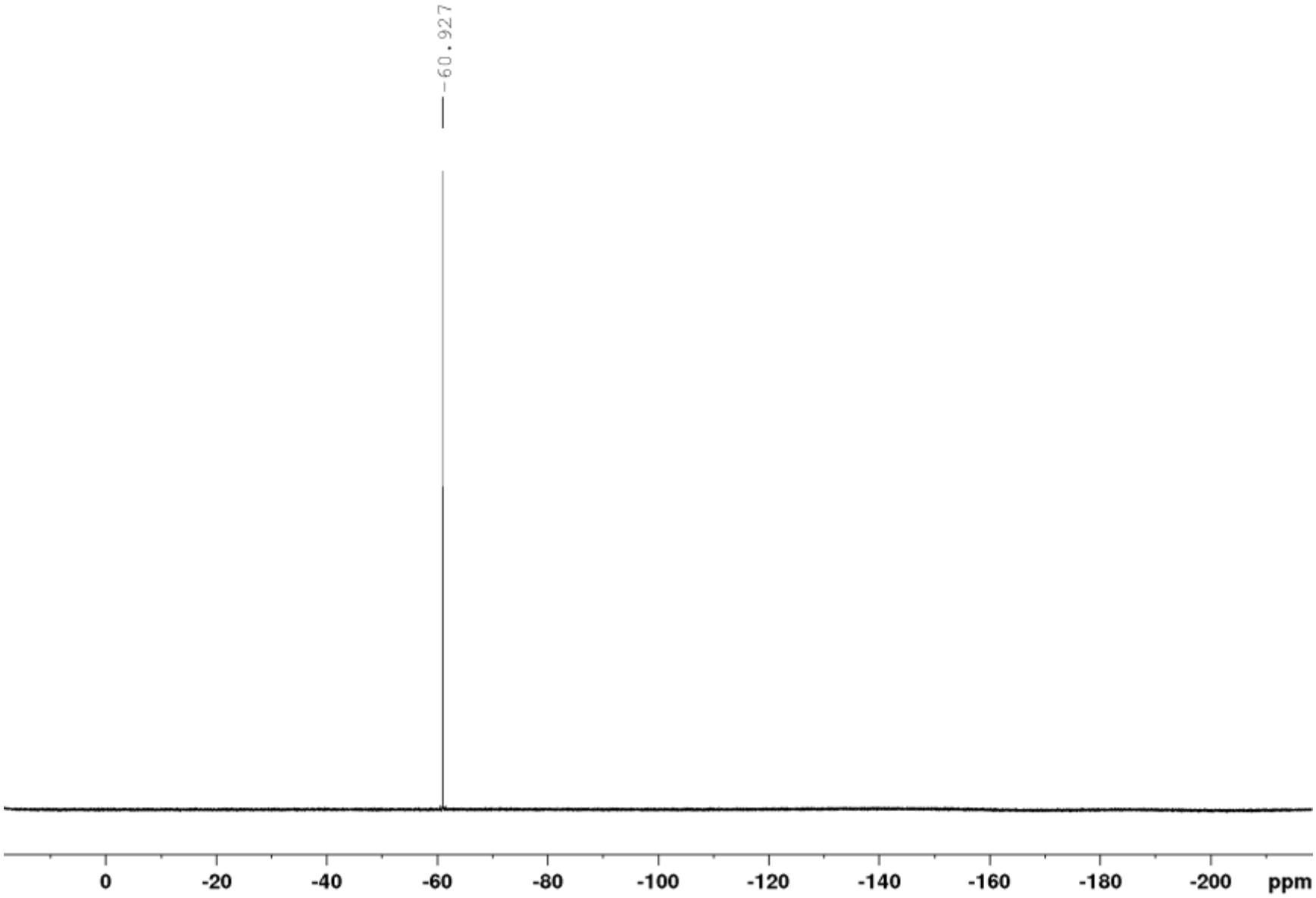

Nickel(0)-1,5-bis(*p*-benzotrifluoride)-3,7-bis(phenyl)-1,5,3,7-diazadiphosphacyclooctane $Ni^0(P^{Ph}{}_2N^{ArCF3}{}_2)_2$, ^{31}P, C_6D_6, 121.5 MHz

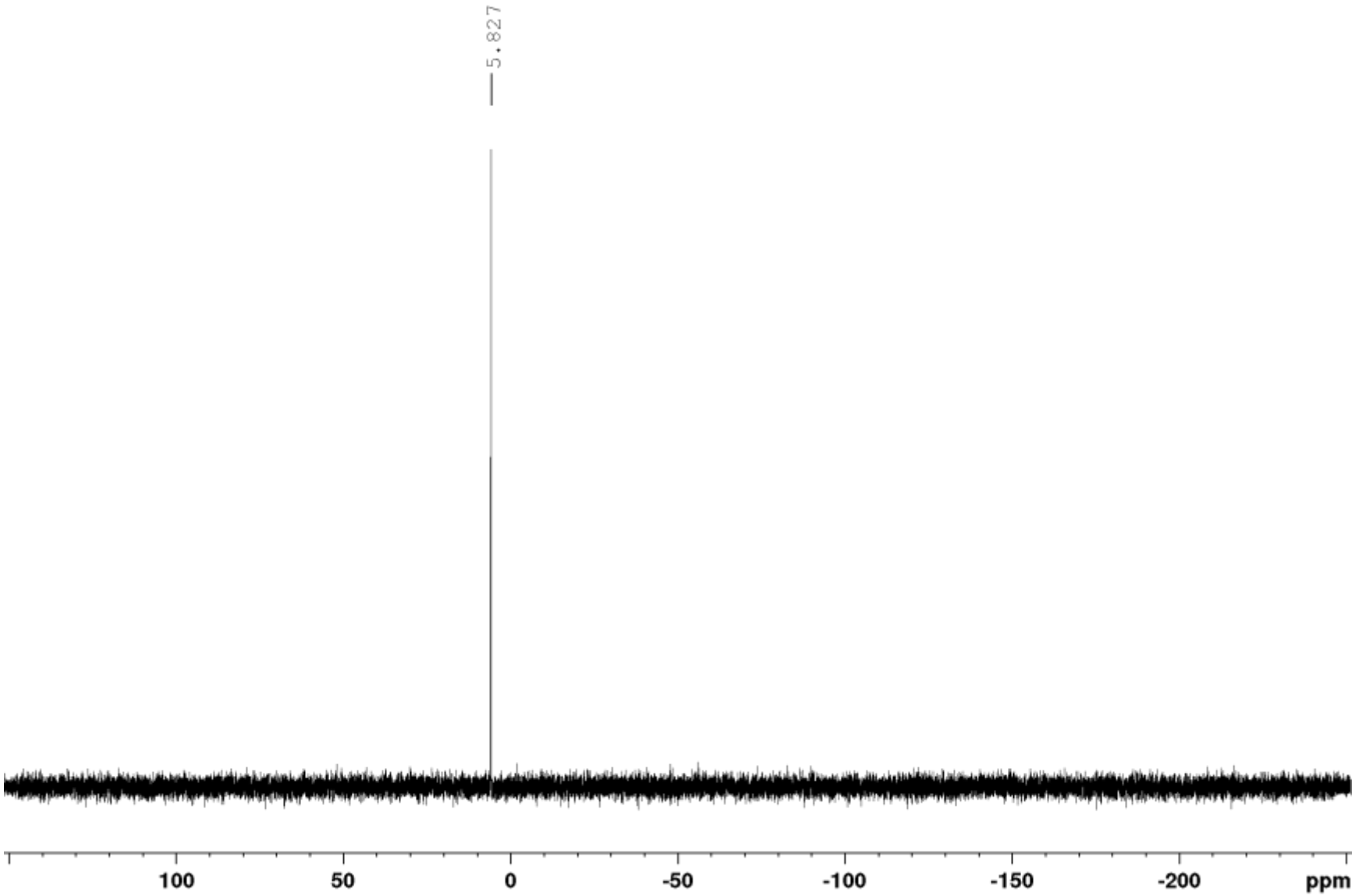

3-hydroxy-1-methyl-3-(naphthalen-1-yl)oxindole (3.08), ^{1}H, $CDCl_3$, 400 MHz

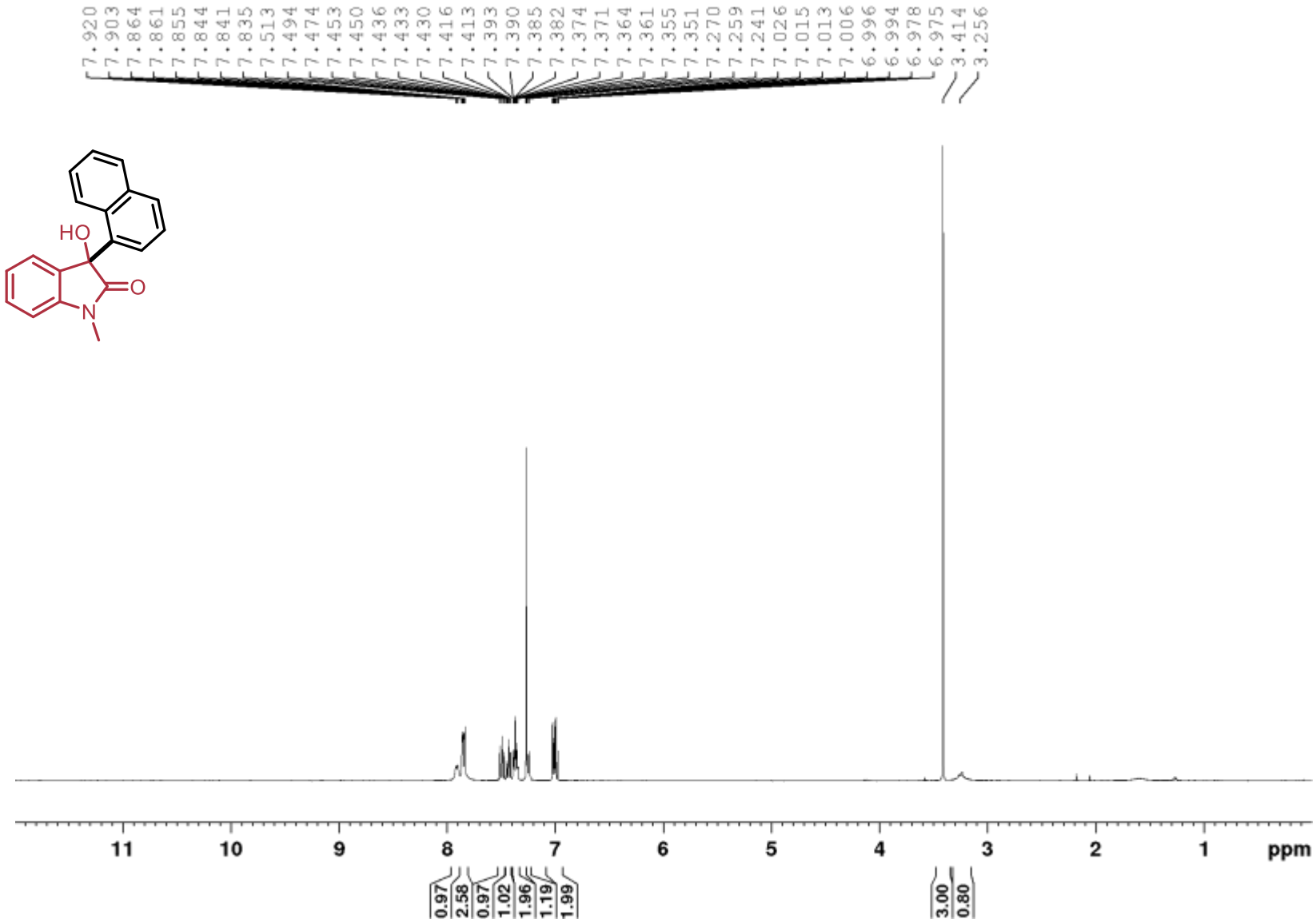

3-hydroxy-1-methyl-3-(naphthalen-1-yl)oxindole (3.08), ^{13}C, $CDCl_3$, 100 MHz

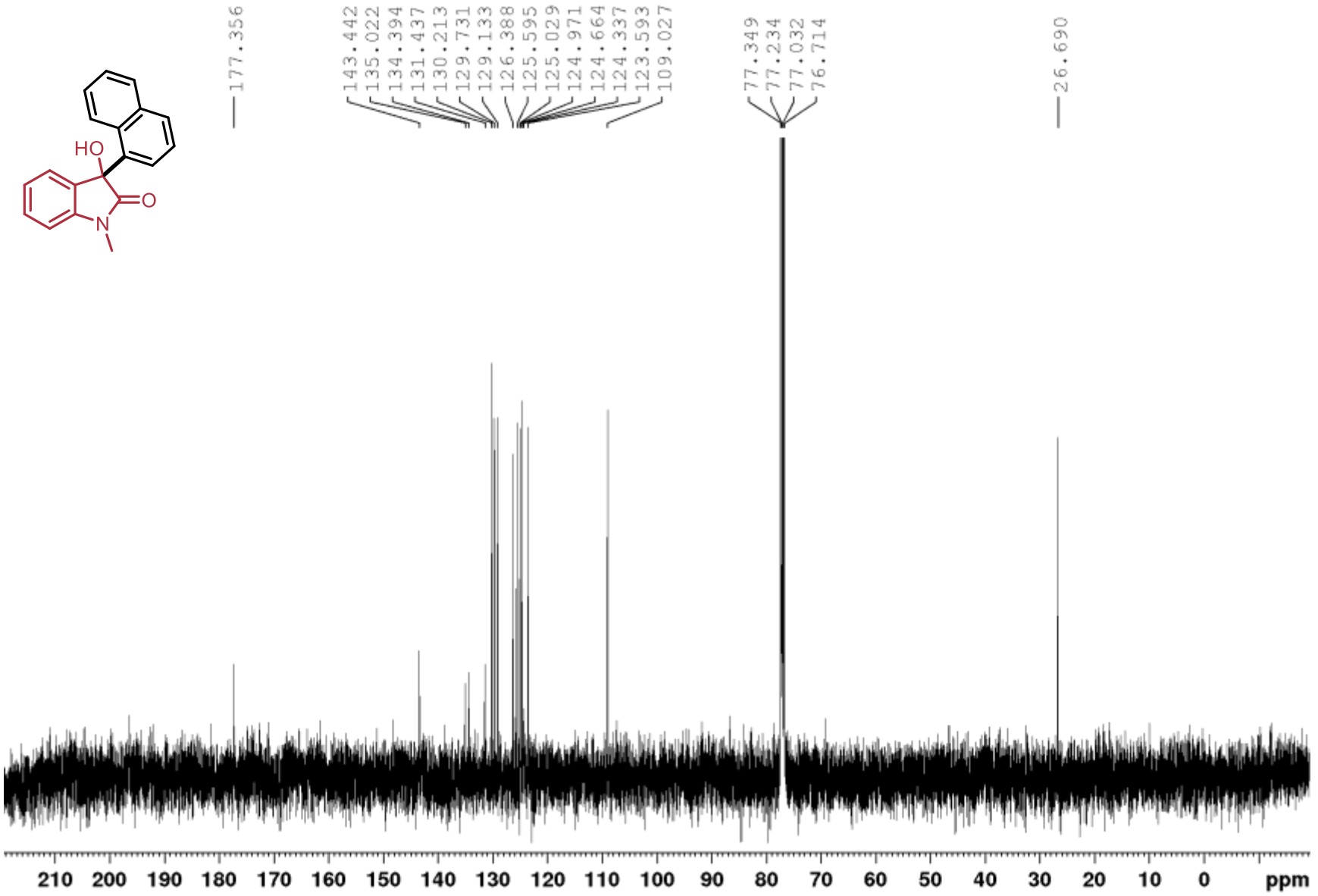

3-(4-fluorophenyl)-3-hydroxy-1-methylindolin-2-one (3.09), ^{1}H, $CDCl_3$, 400 MHz

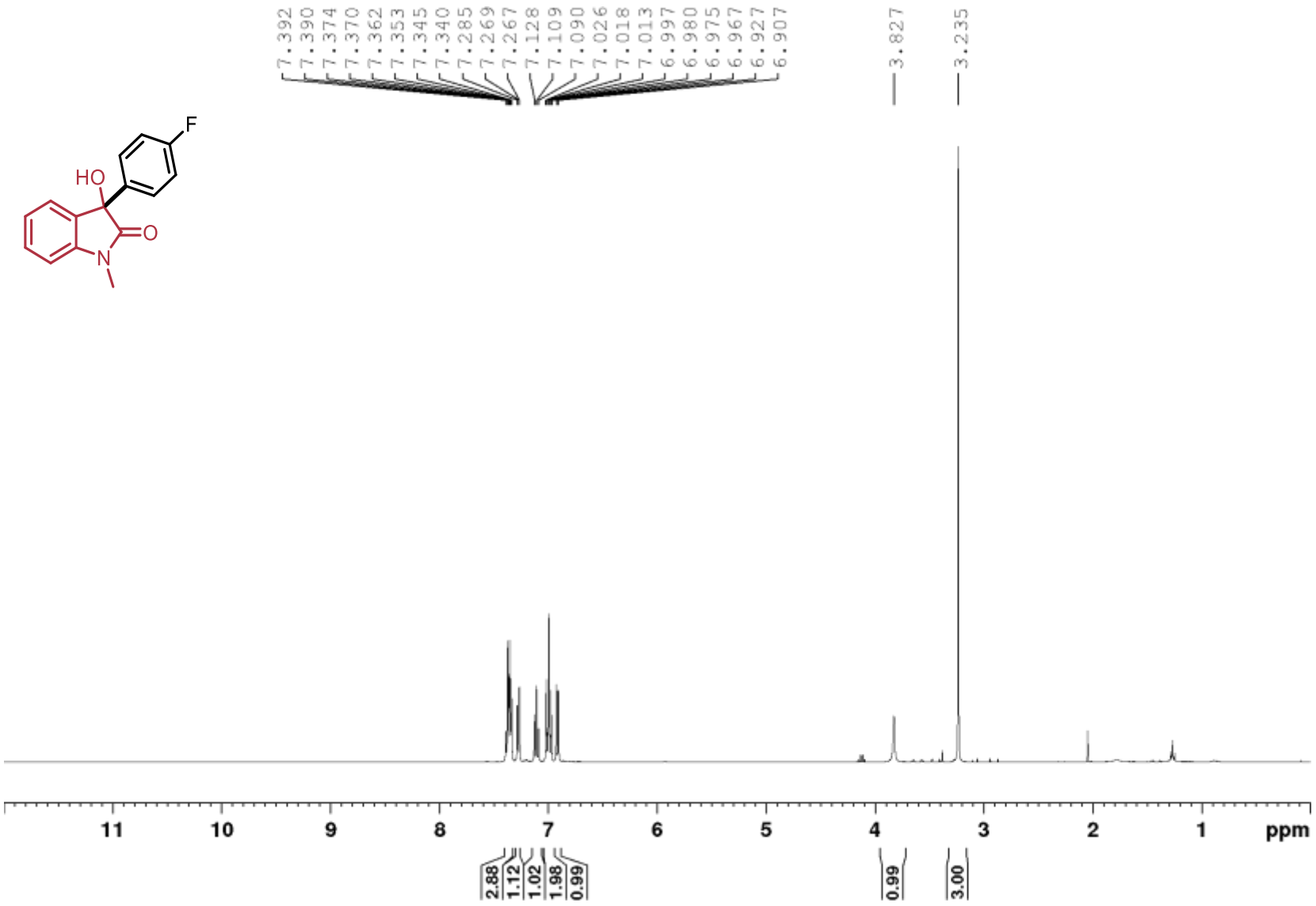

3-(4-fluorophenyl)-3-hydroxy-1-methylindolin-2-one (3.09), ^{13}C, $CDCl_3$, 100 MHz

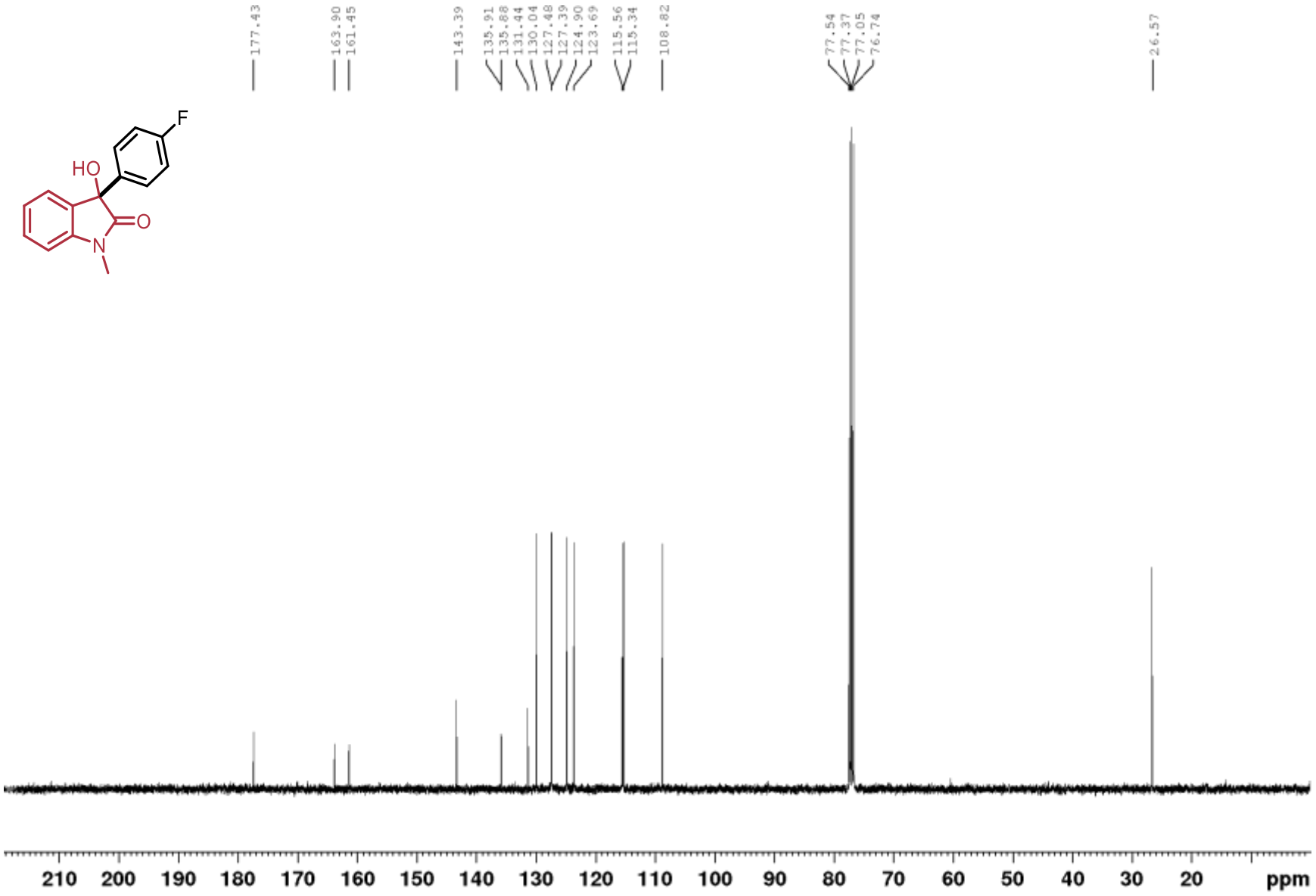

3-(4-fluorophenyl)-3-hydroxy-1-methylindolin-2-one (3.09), ^{19}F, $CDCl_3$, 377 M

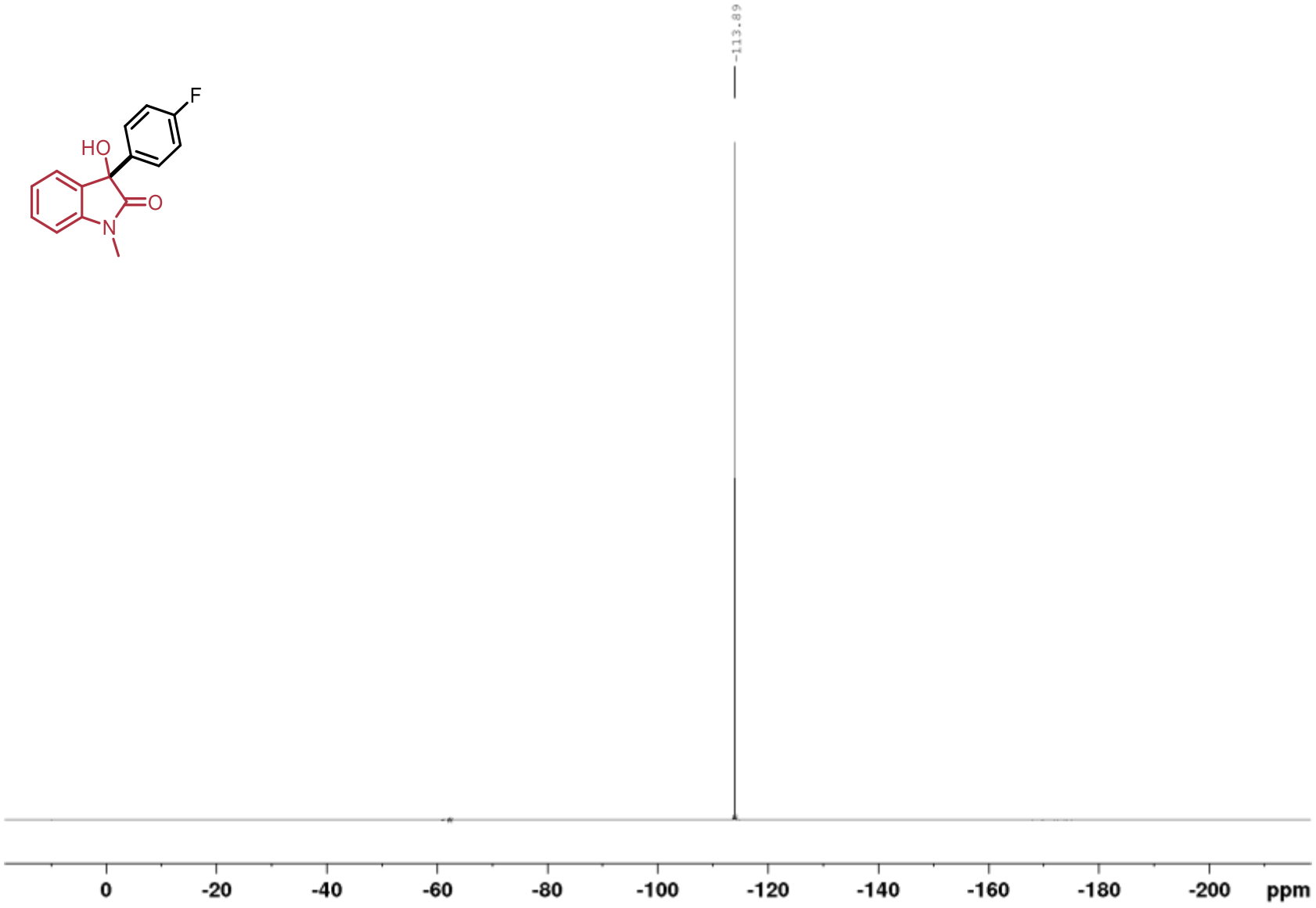

3-(4-(trifluoromethoxy)phenyl)-3-hydroxy-1-methylindolin-2-one (3.10), ^{1}H, $CDCl_3$, 400 MHz

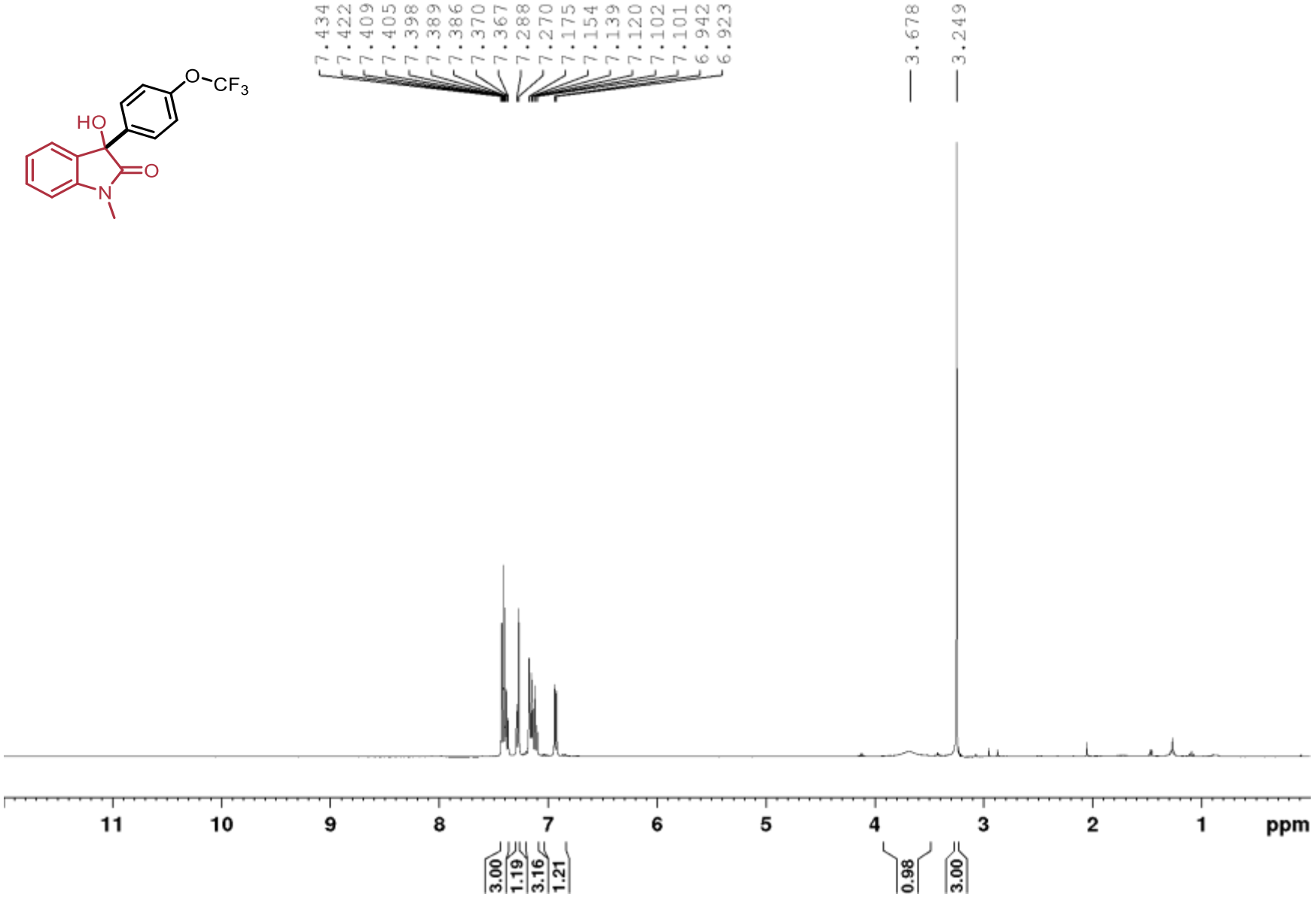

3-(4-(trifluoromethoxy)phenyl)-3-hydroxy-1-methylindolin-2-one (3.10), ^{13}C, $CDCl_3$, 100 MHz

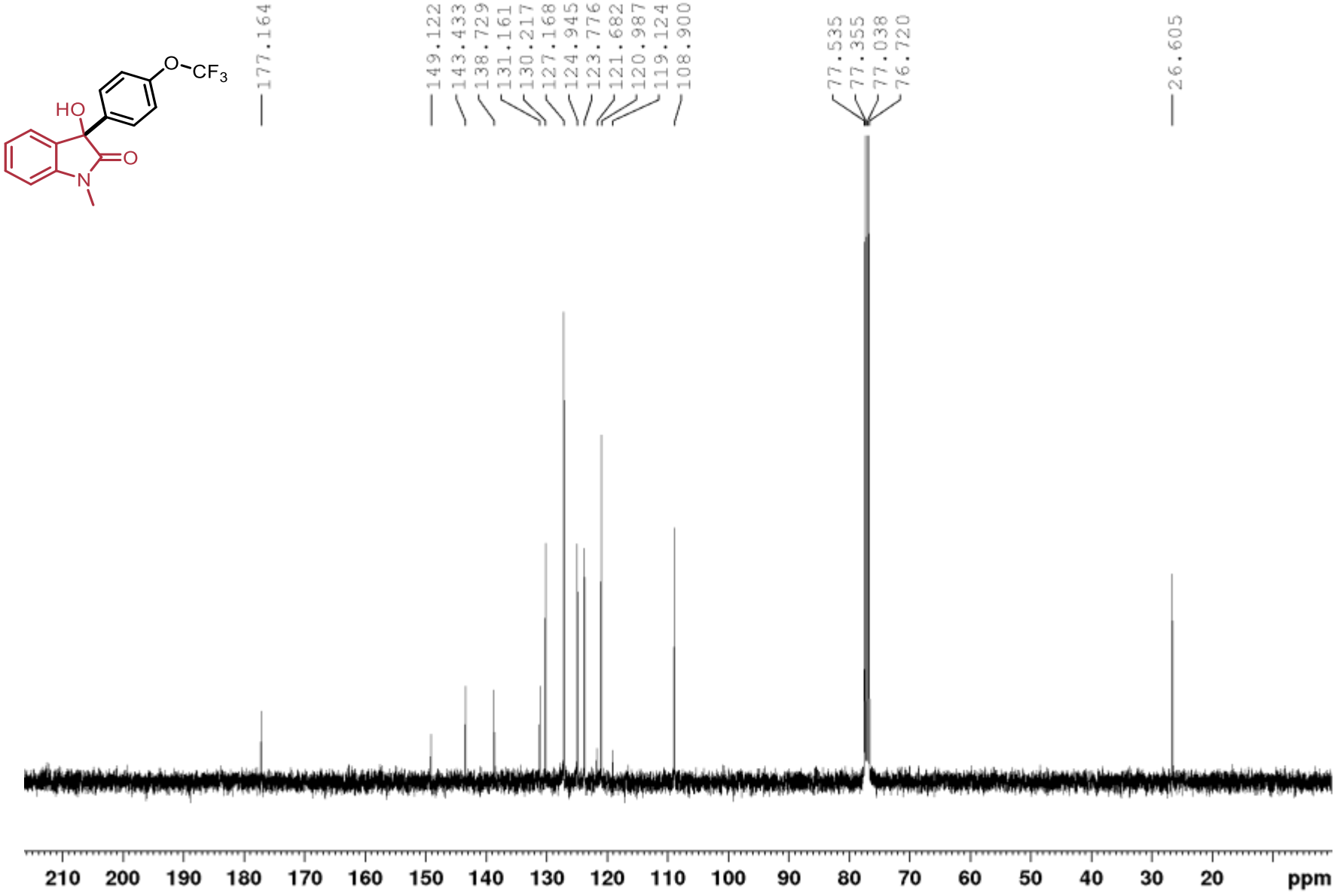

3-(4-(trifluoromethoxy)phenyl)-3-hydroxy-1-methylindolin-2-one (3.10), ^{19}F, $CDCl_3$, 377 MHz

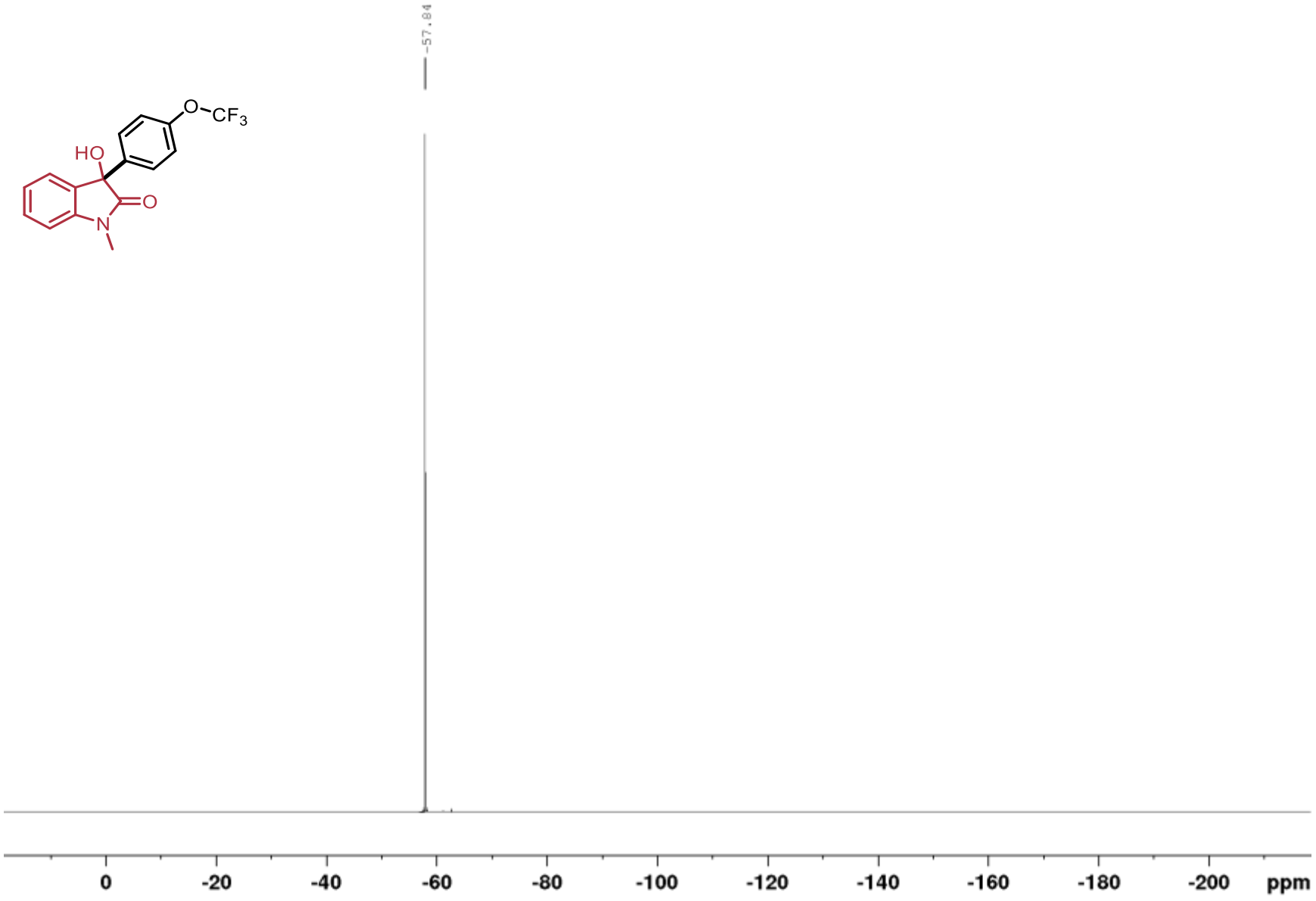

3-(benzo[*d*][1,3]dioxol-5-yl)-3-hydroxy-1-methylindolin-2-one (3.11), ^{1}H, $CDCl_3$, 400 MHz

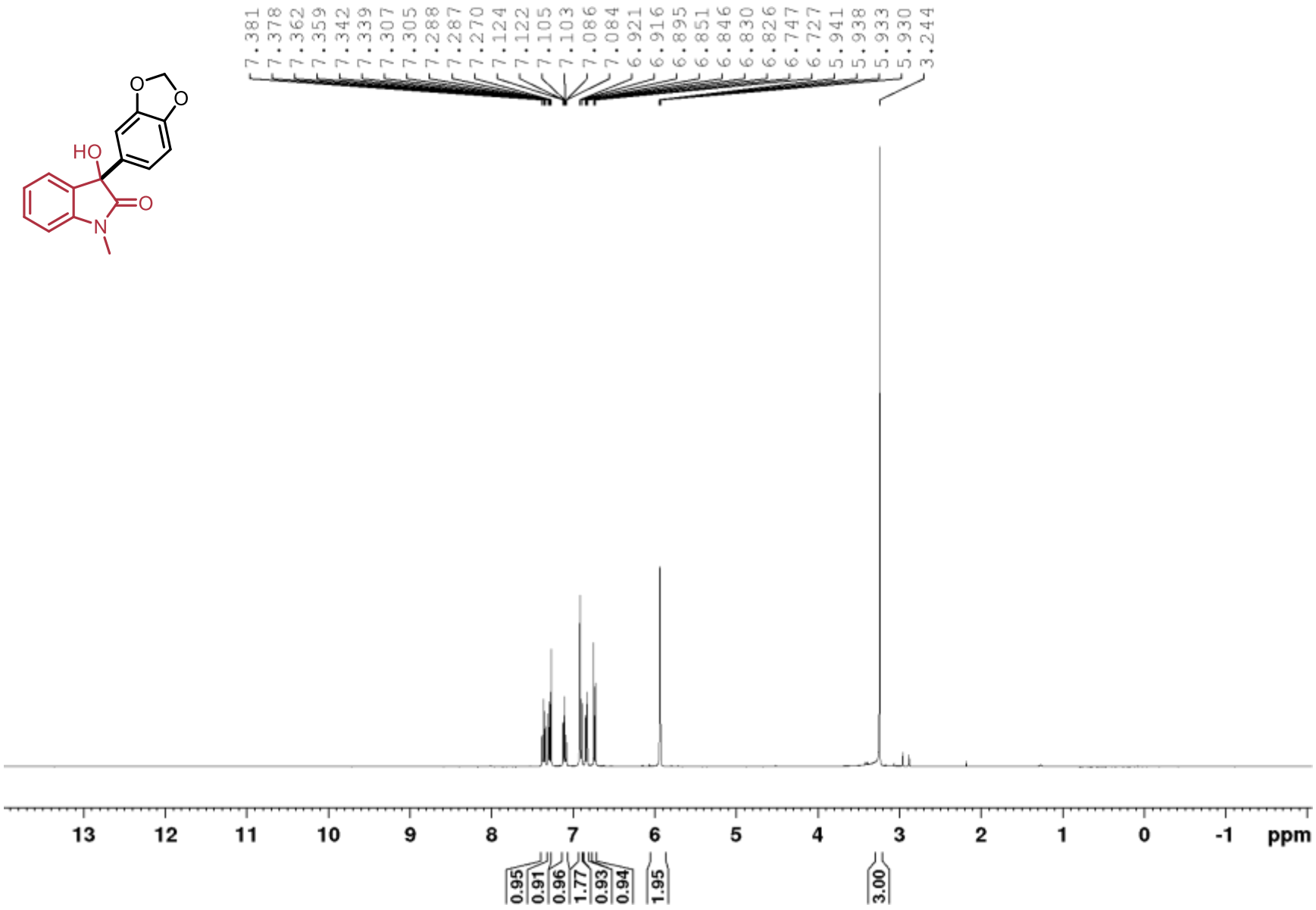

3-(benzo[*d*][1,3]dioxol-5-yl)-3-hydroxy-1-methylindolin-2-one (3.11), ^{13}C, $CDCl_3$, 100 MHz

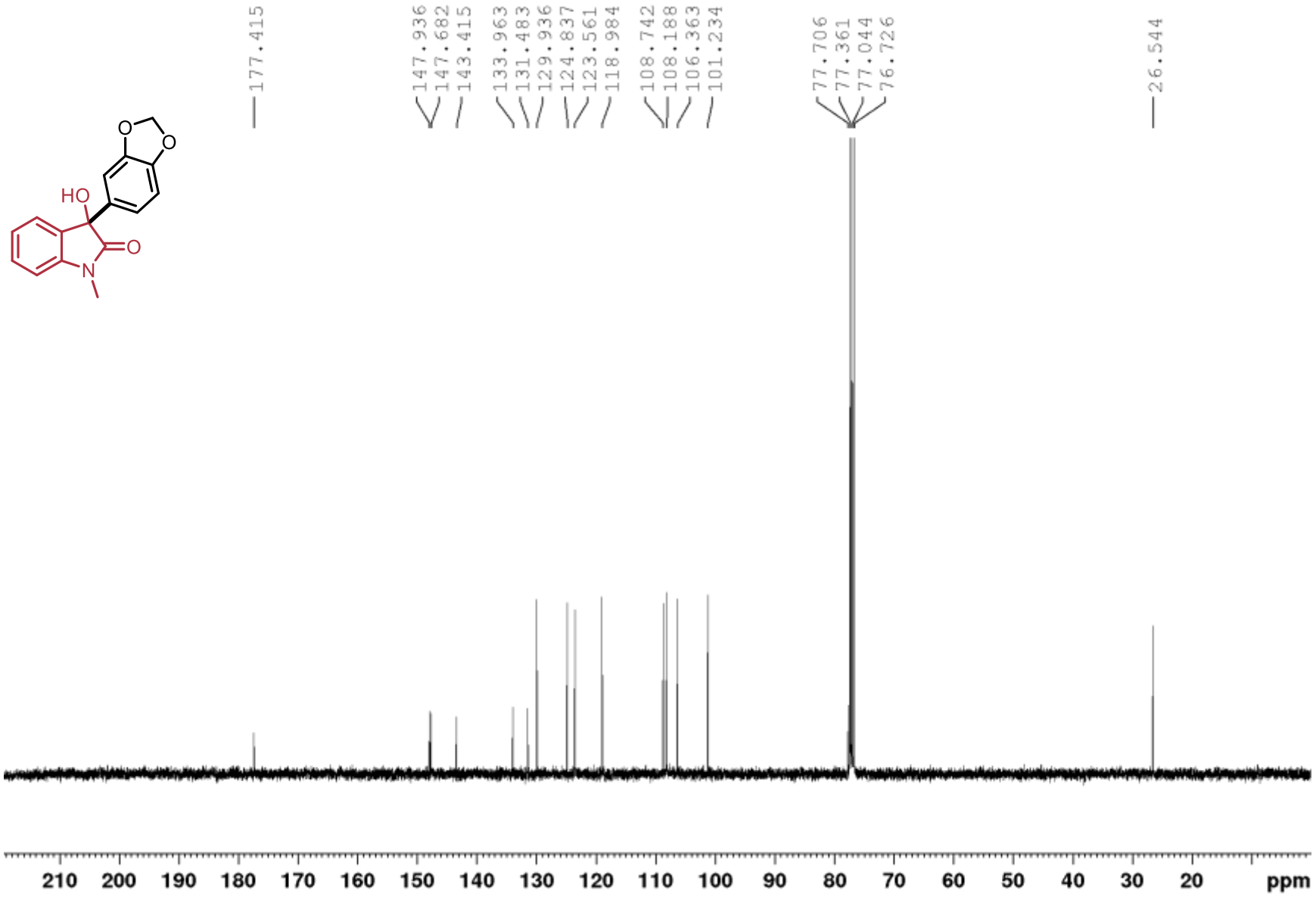

3-hydroxy-1-methyl-3-(3-(trifluoromethyl)phenyl)indolin-2-one (3.12), ^{1}H, $CDCl_3$, 400 MHz

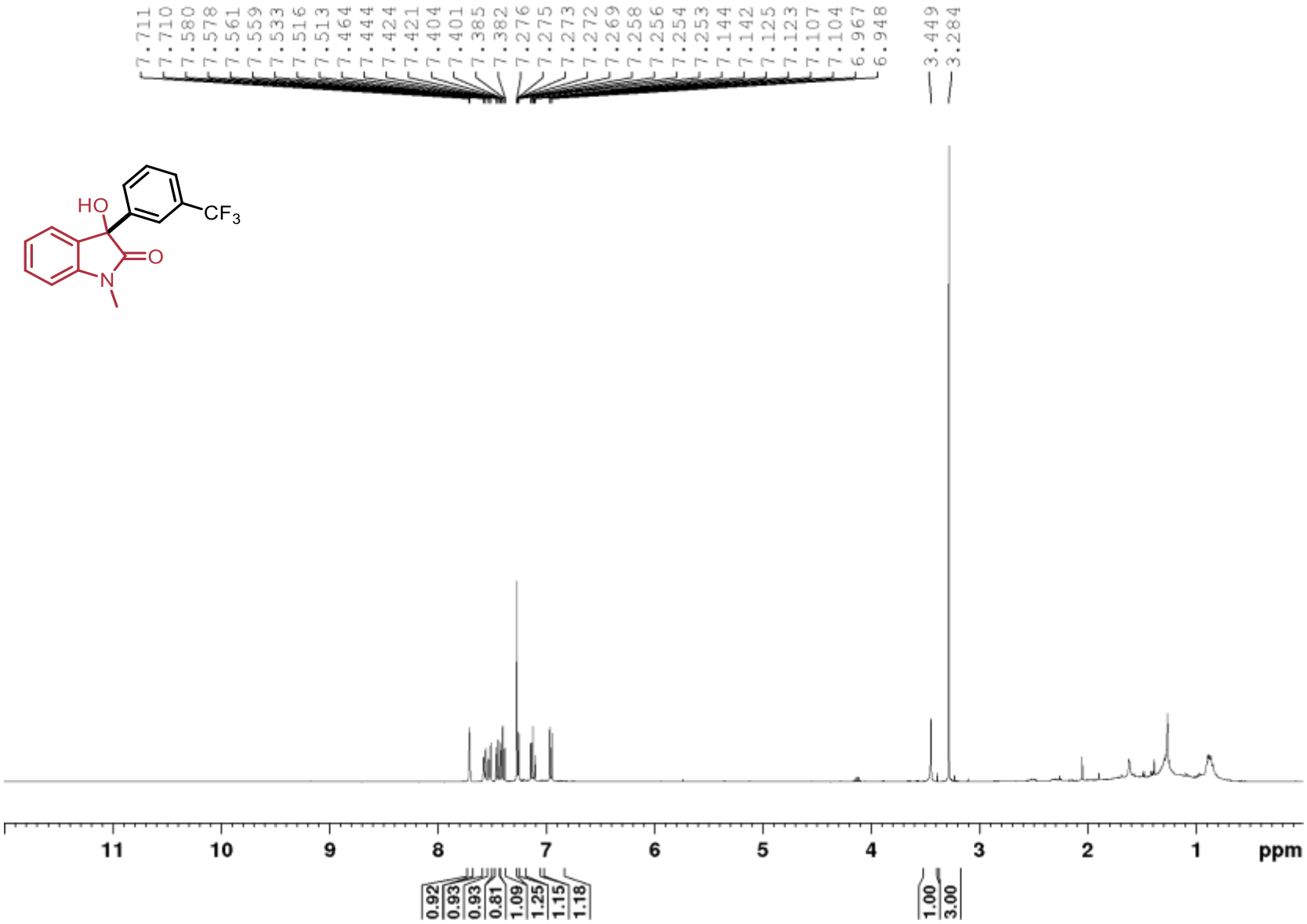

3-hydroxy-1-methyl-3-(3-(trifluoromethyl)phenyl)indolin-2-one (3.12), ^{13}C, $CDCl_3$, 100 MHz

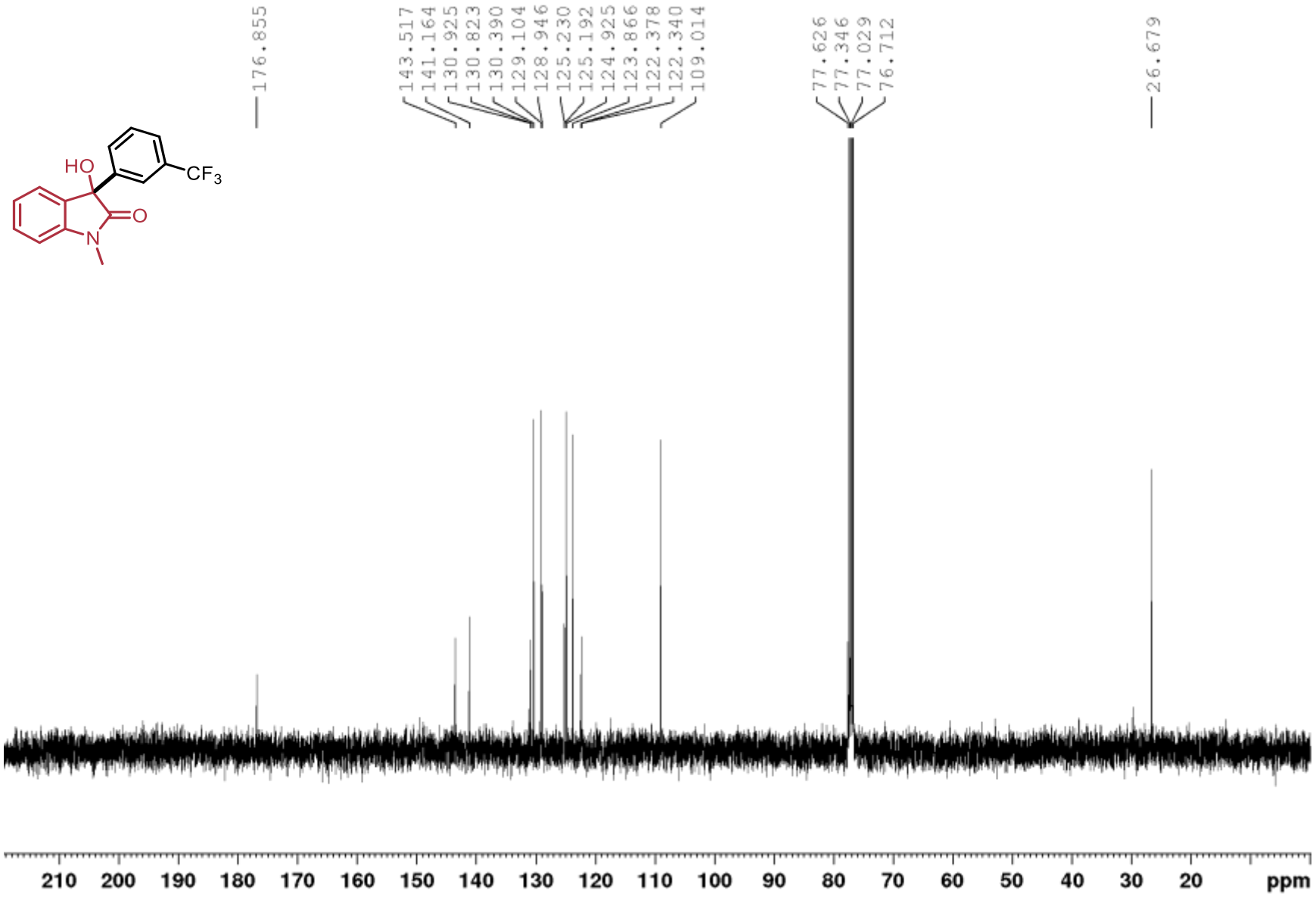

3-hydroxy-1-methyl-3-(3-(trifluoromethyl)phenyl)indolin-2-one (3.12), ^{19}F, $CDCl_3$, 377 MHz

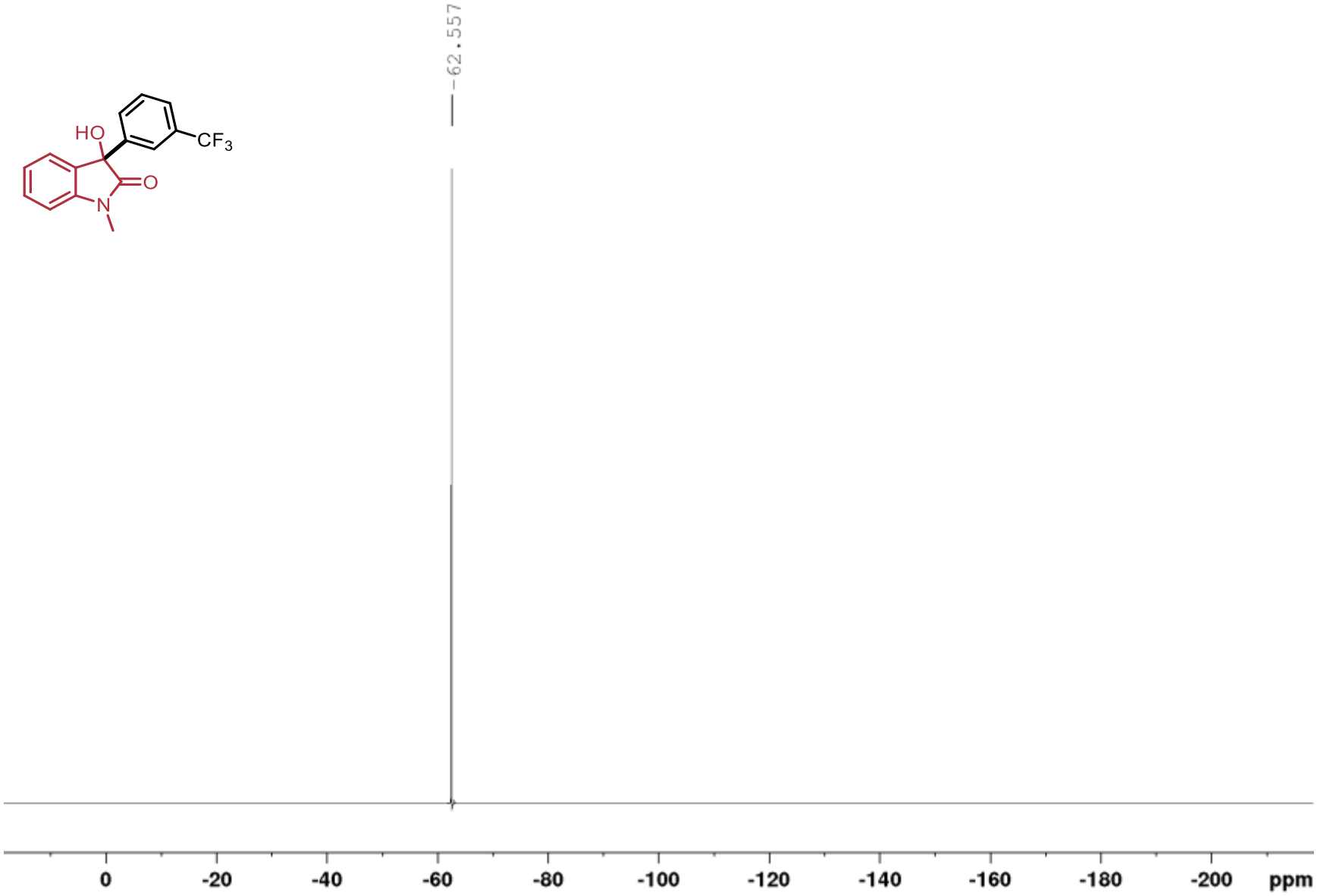

3-(3,5-bis(trifluoromethyl)phenyl)-3-hydroxy-1-methylindolin-2-one (3.13), ^{1}H, $CDCl_3$, 400 MHz

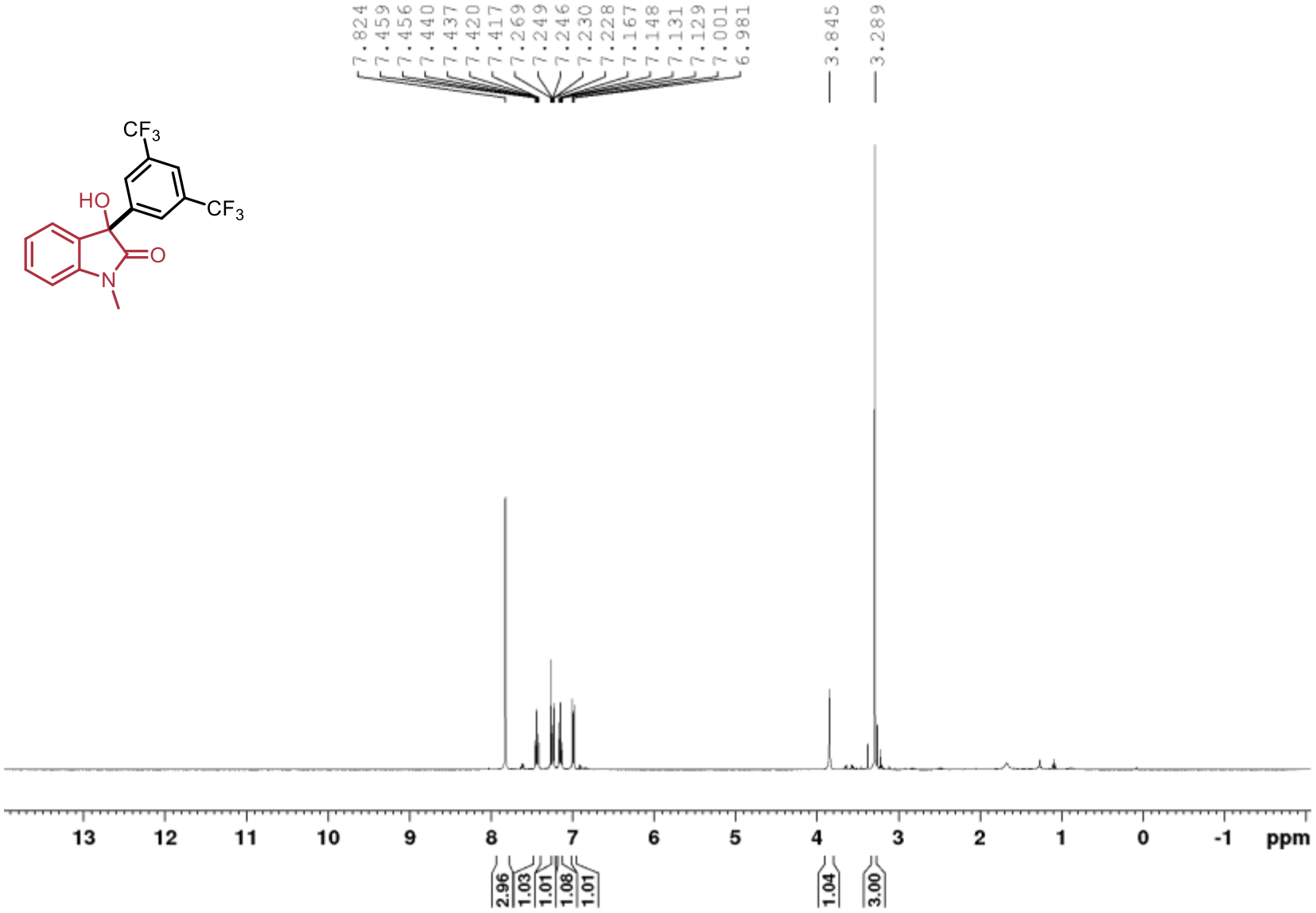

3-(3,5-bis(trifluoromethyl)phenyl)-3-hydroxy-1-methylindolin-2-one (3.13), ^{13}C, $CDCl_3$, 100 MHz

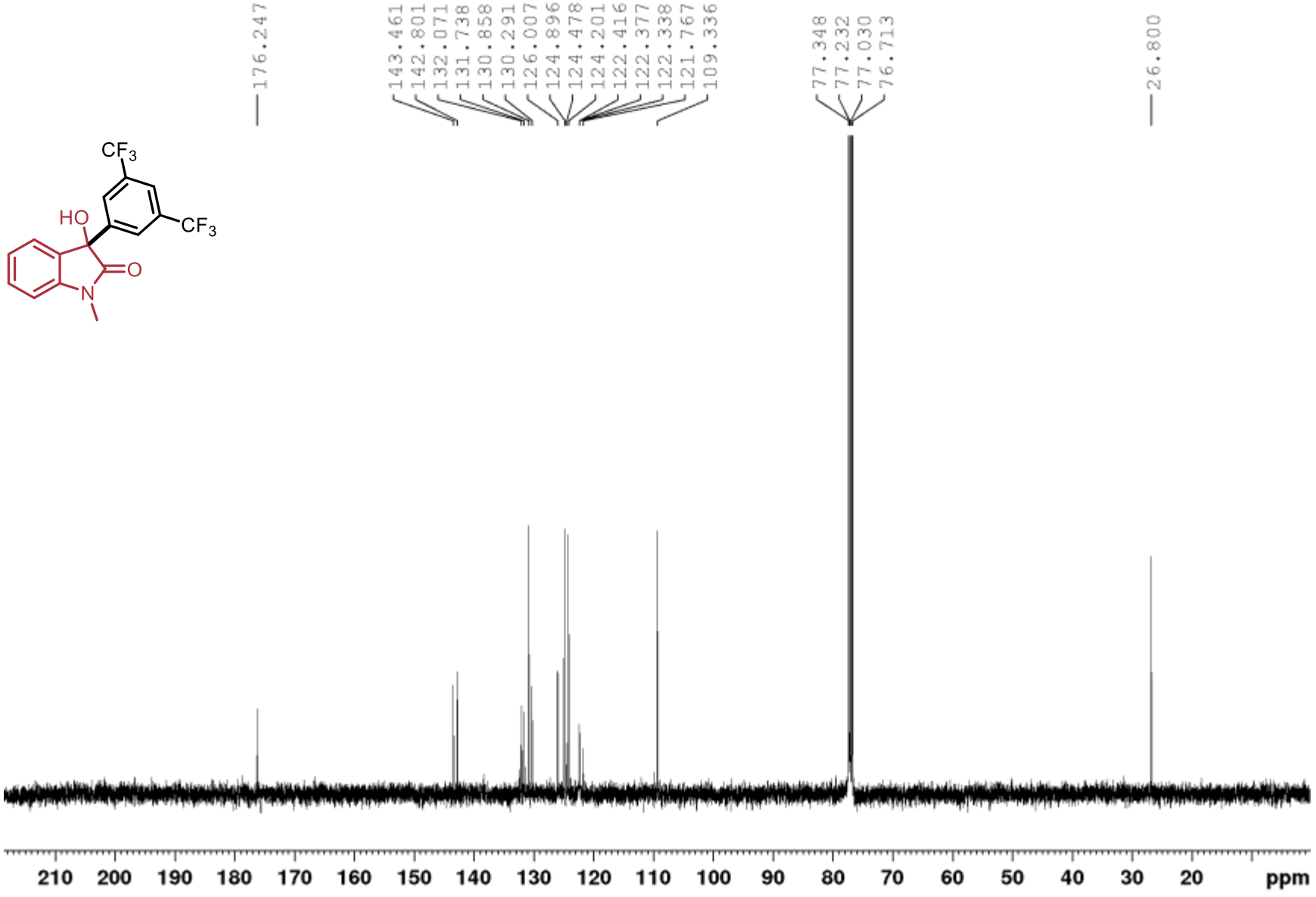

3-(3,5-bis(trifluoromethyl)phenyl)-3-hydroxy-1-methylindolin-2-one (3.13), ^{19}F, $CDCl_3$, 377 MHz

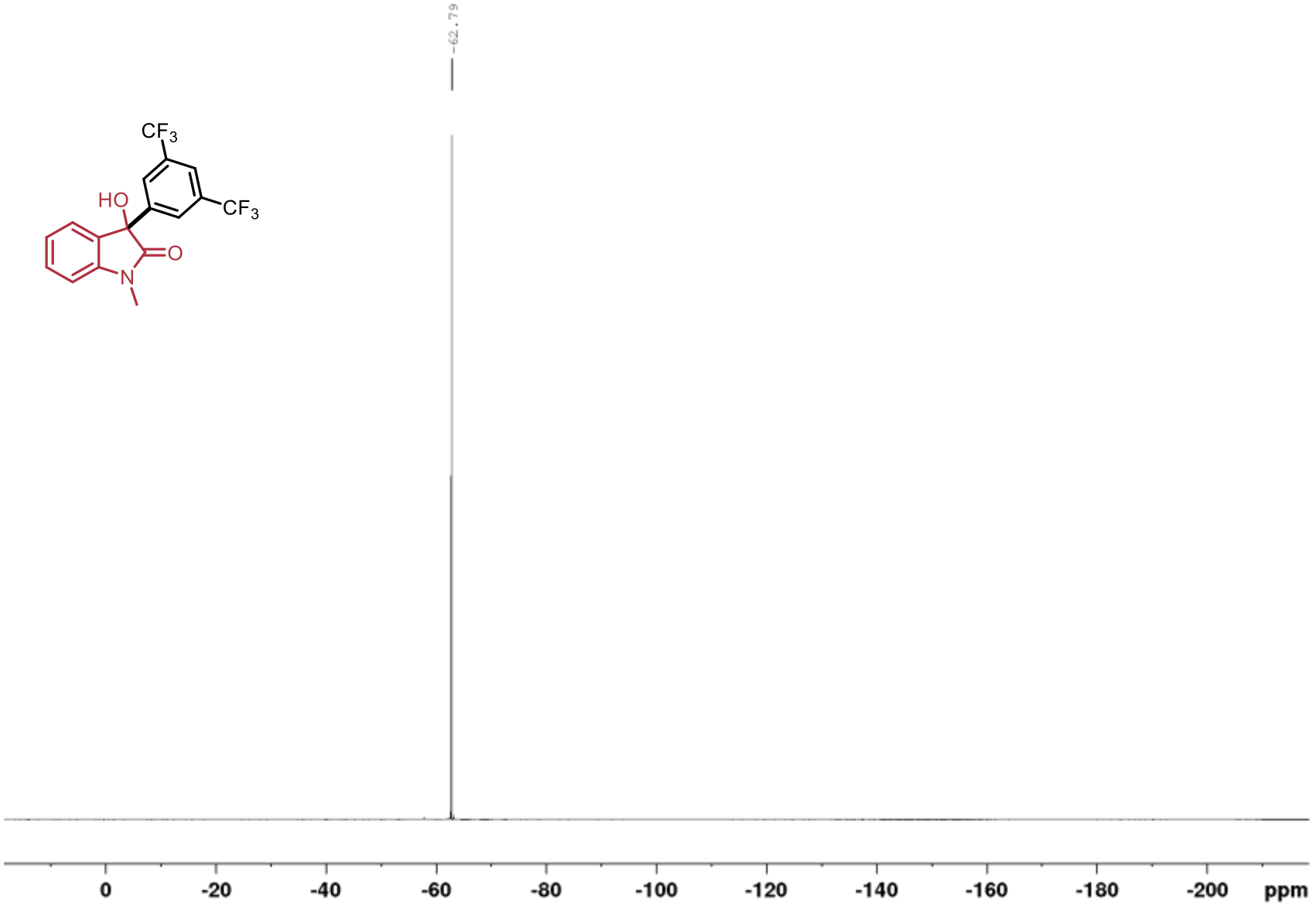

3-hydroxy-1-methyl-3-(thiophen-2-yl)indolin-2-one (3.14), ^{1}H, $CDCl_3$, 400 MHz

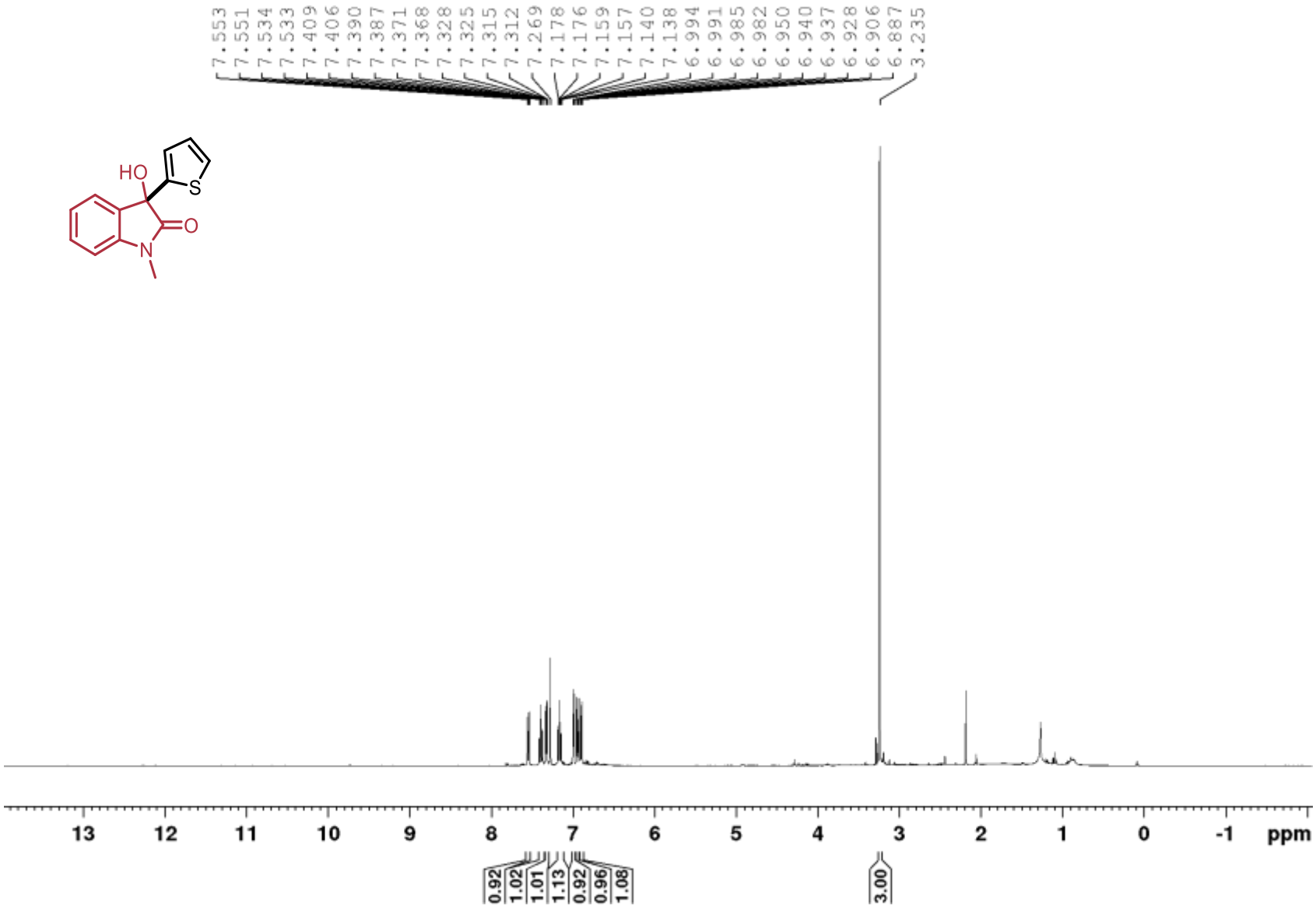

3-hydroxy-1-methyl-3-(thiophen-2-yl)indolin-2-one (3.14), ^{13}C, $CDCl_3$, 100 MHz

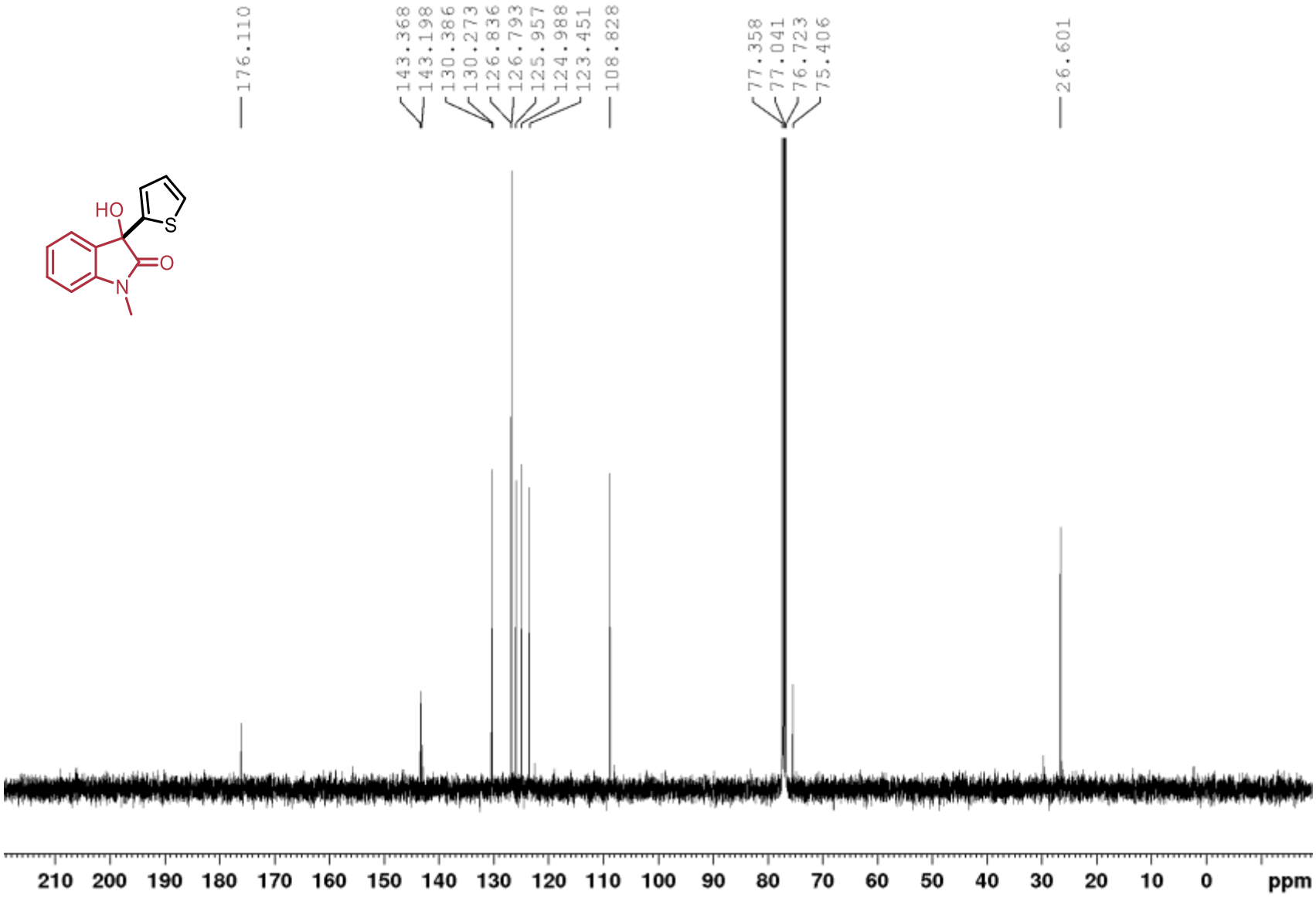

3-Hydroxy-1-methyl-3-(pyridine-5-yl-2-methoxy)-2-oxindole (3.15), ^{1}H, $CDCl_3$, 400 MHz

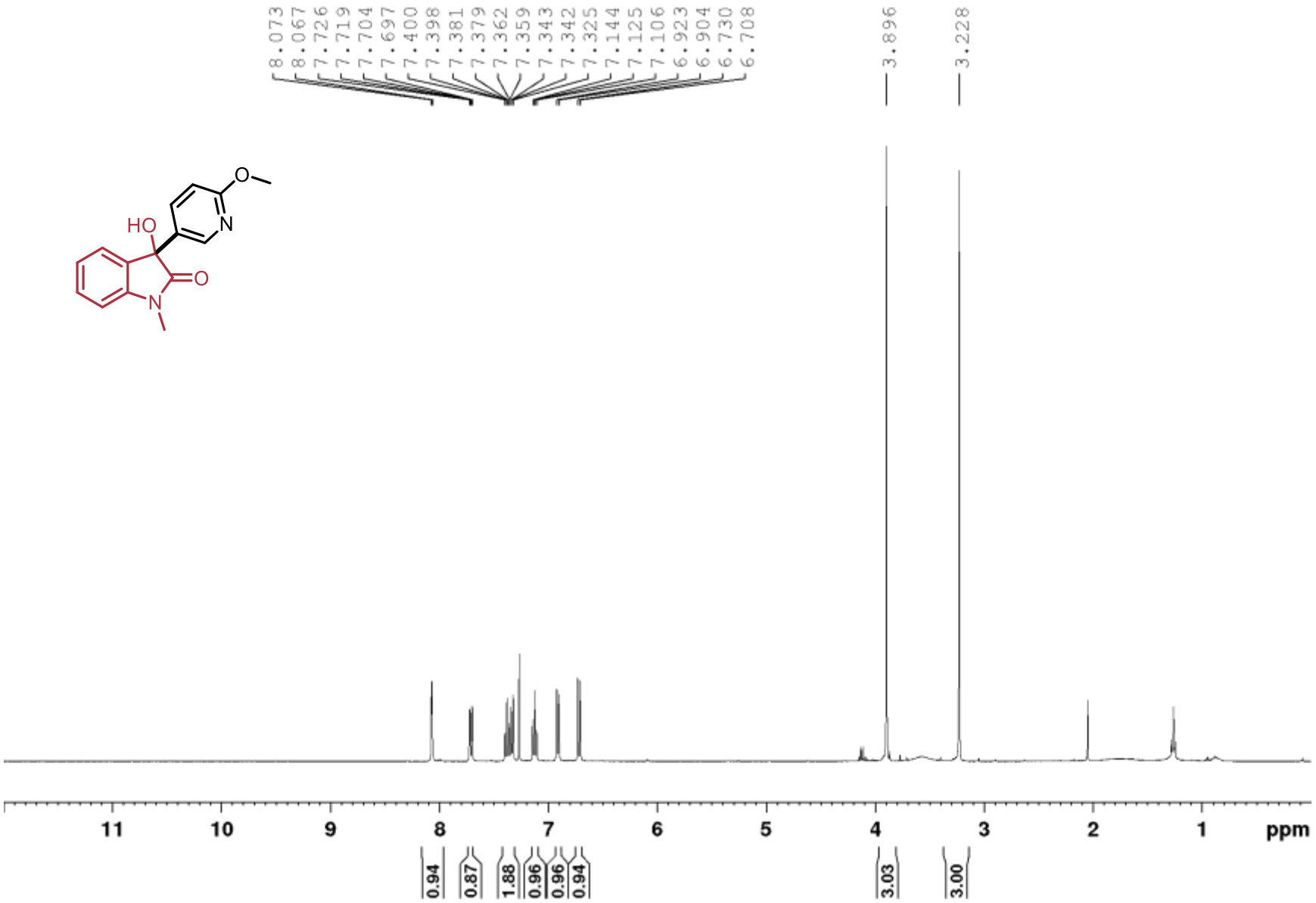

3-Hydroxy-1-methyl-3-(pyridine-5-yl-2-methoxy)-2-oxindole (3.15), ^{13}C, $CDCl_3$, 100 MHz

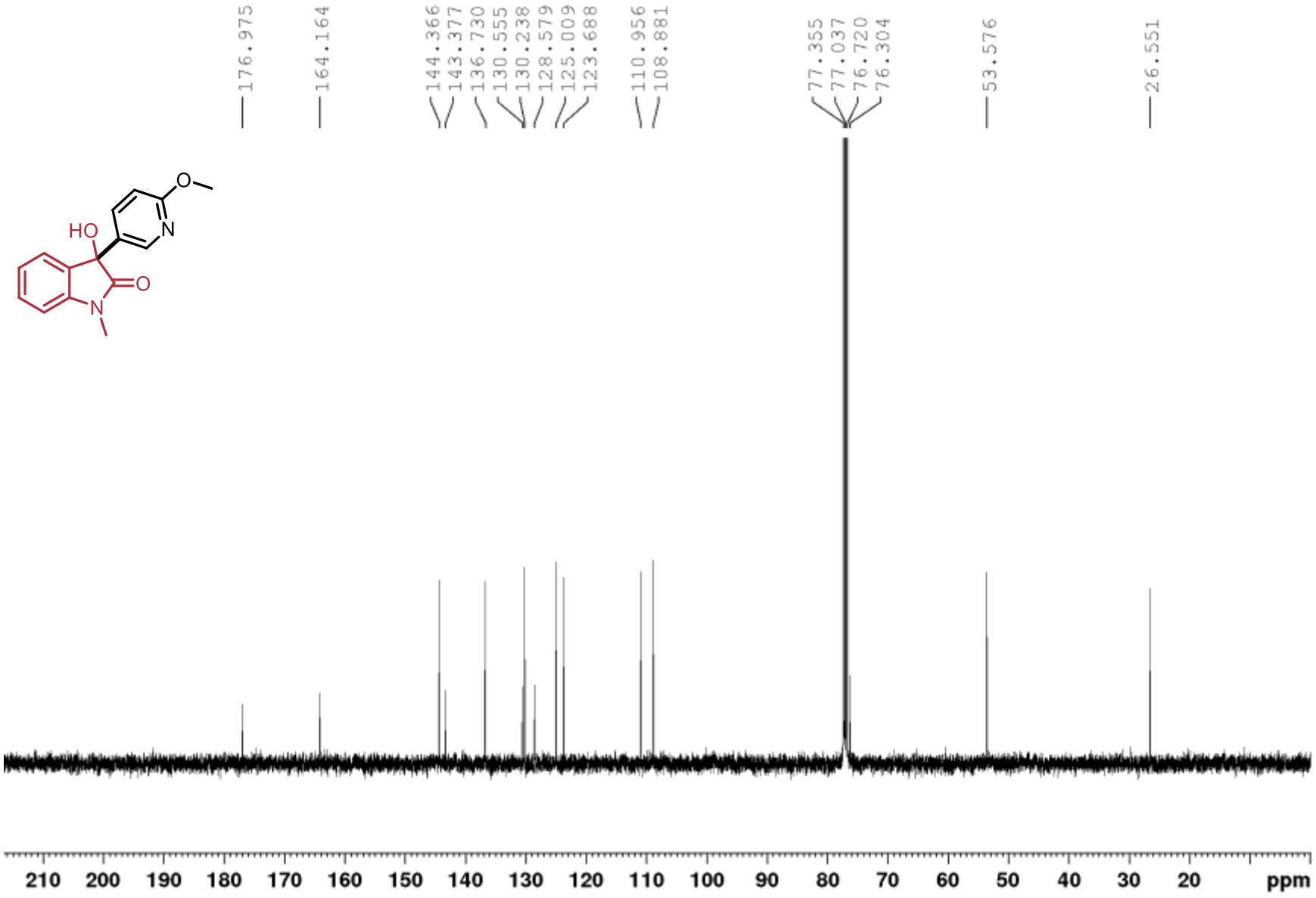

3-(4-chlorophenyl)-3-hydroxy-1-methylindolin-2-one (3.16), ^{1}H, $CDCl_3$, 400 MHz

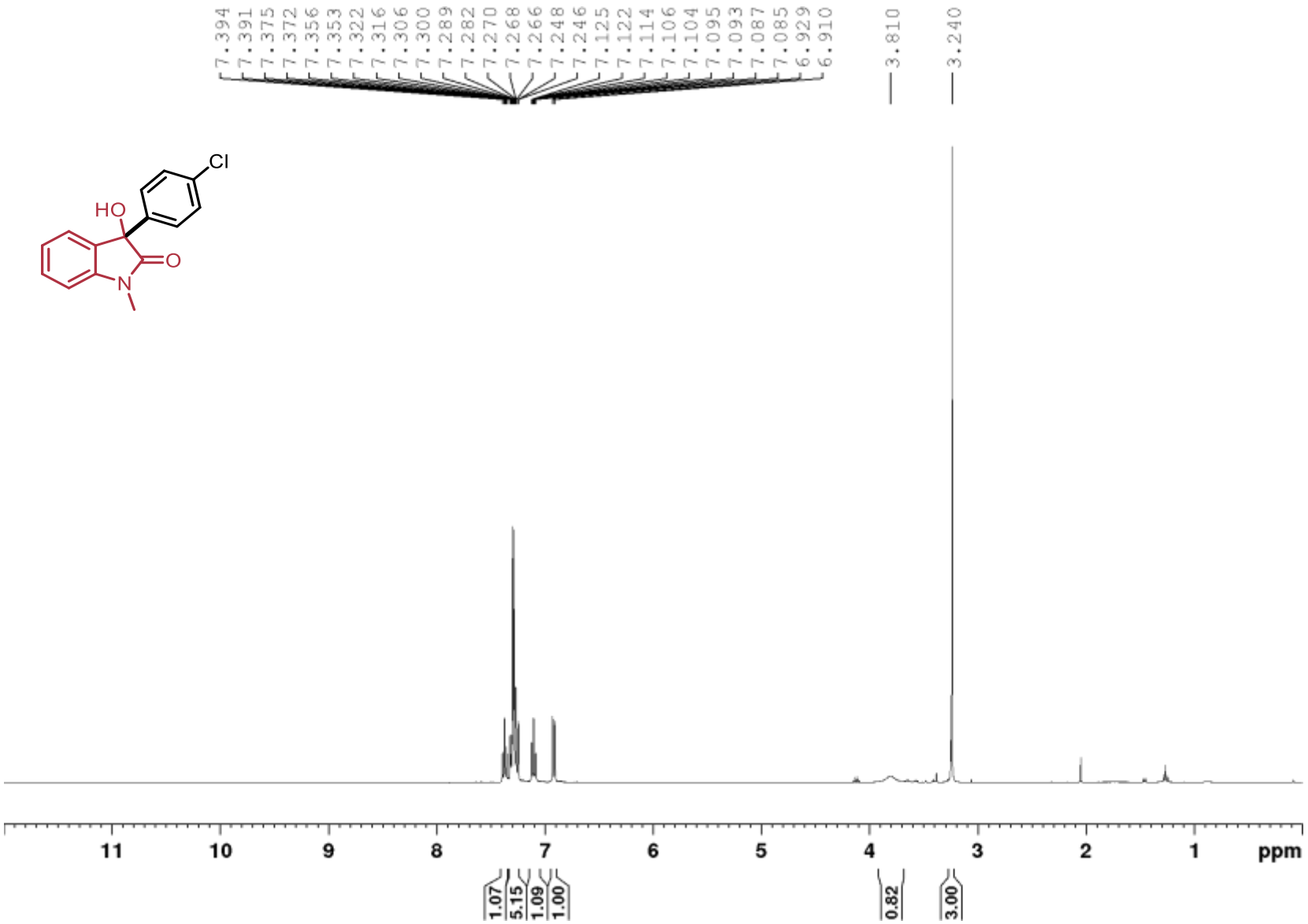

3-(4-chlorophenyl)-3-hydroxy-1-methylindolin-2-one (3.16), ^{13}C, $CDCl_3$, 100 MHz

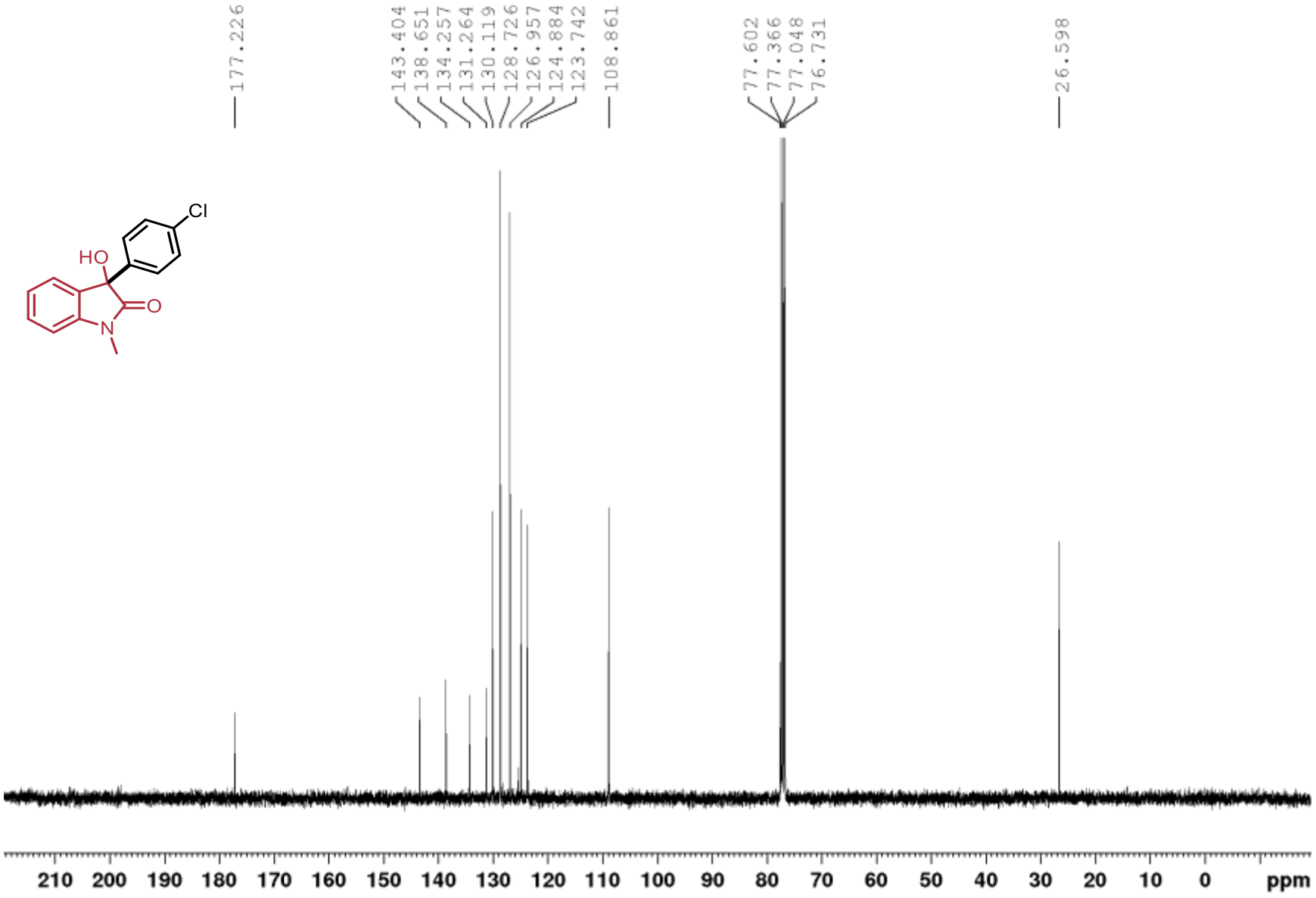

3-Hydroxy-1-methyl-3-p-tolyloxindole (3.17), ^{1}H, $CDCl_3$, 400 MHz

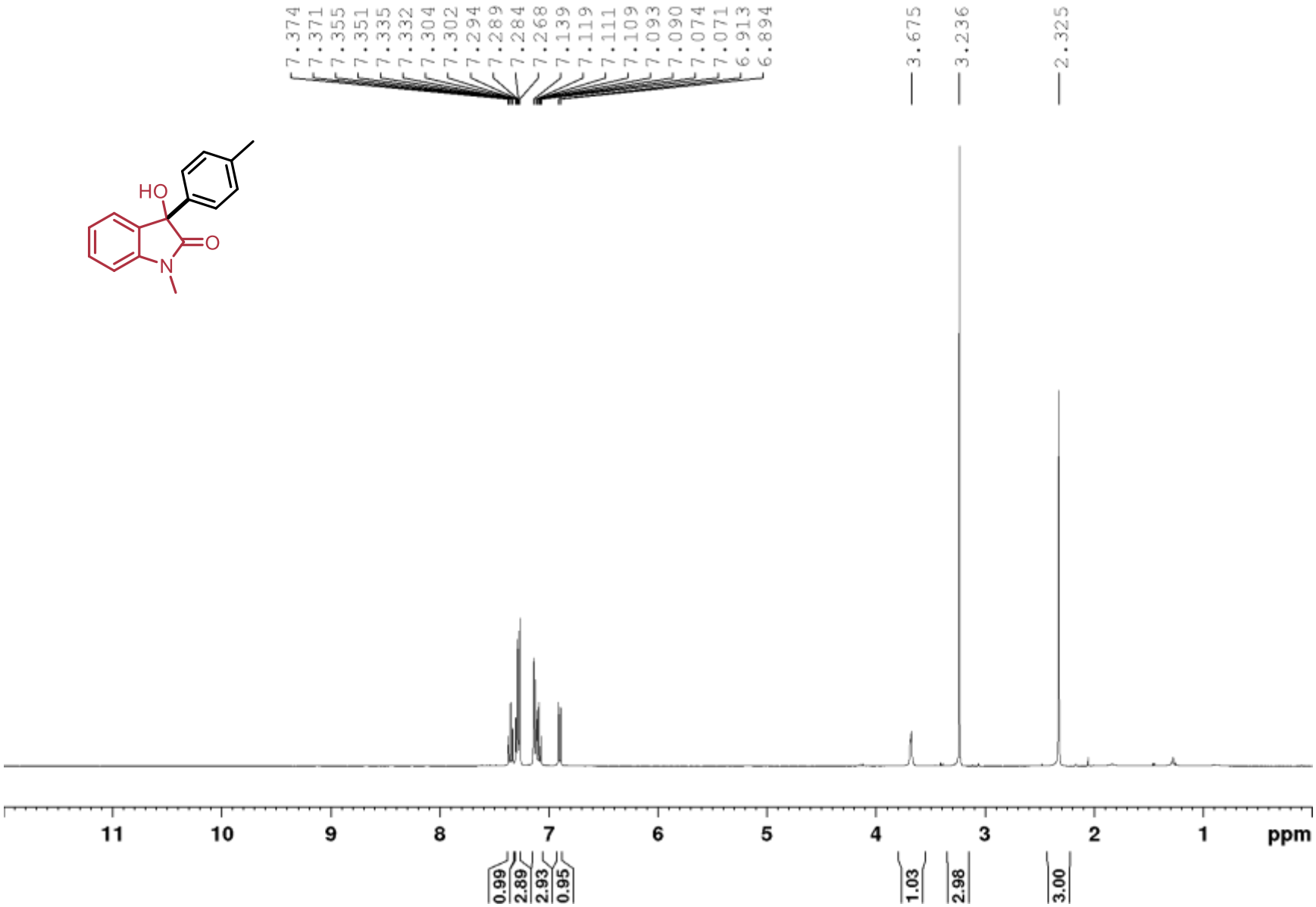

3-Hydroxy-1-methyl-3-p-tolyloxindole (3.17), ^{13}C, $CDCl_3$, 100 MHz

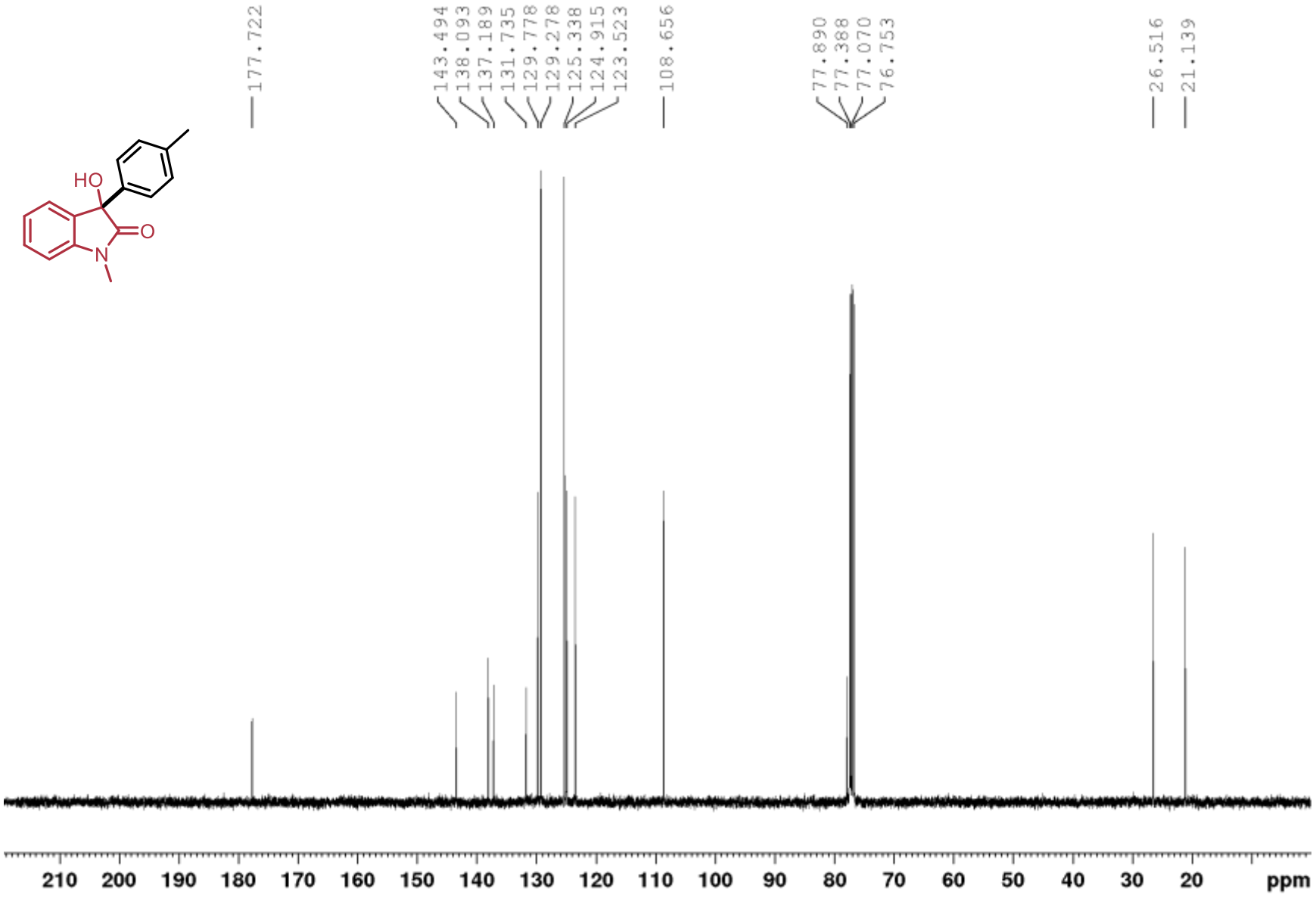

5-methoxy-1-methyl-3-(4-fluorophenyl)-3-hydroxy-2-oxindole (3.18), ^{1}H, $CDCl_3$, 400 MHz

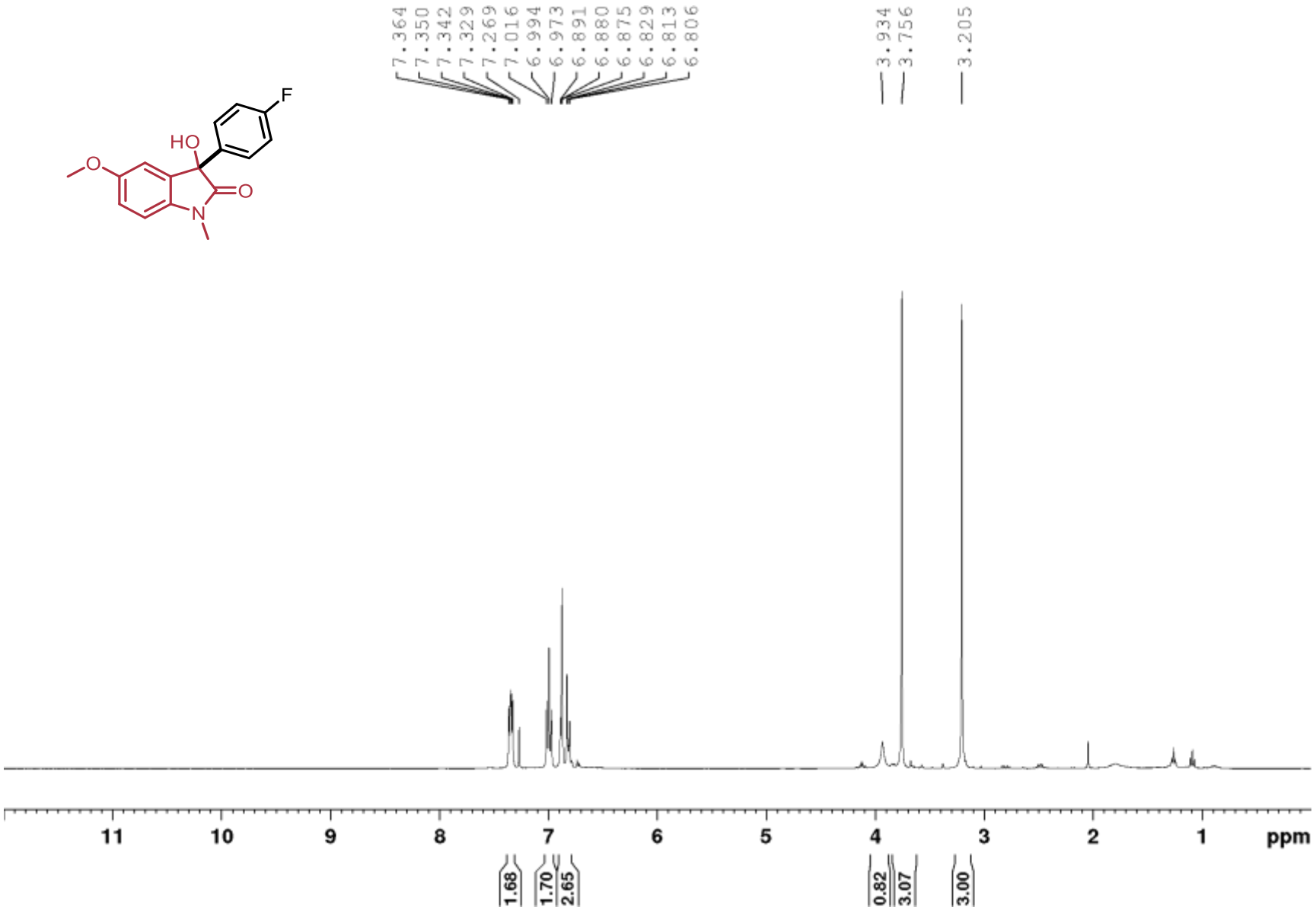

5-methoxy-1-methyl-3-(4-fluorophenyl)-3-hydroxy-2-oxindole (3.18), ^{13}C, $CDCl_3$, 100 MHz

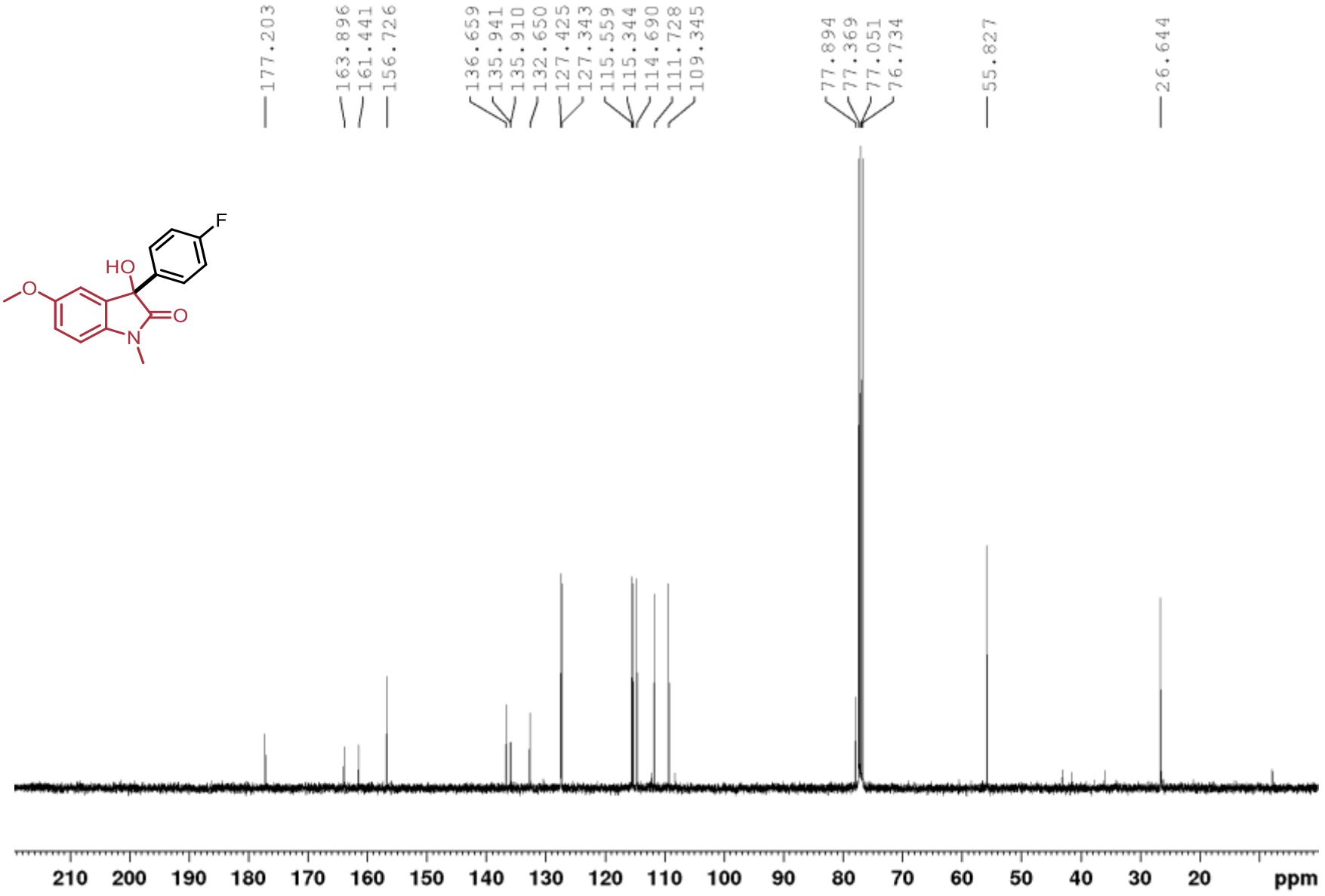

5-methoxy-1-methyl-3-(4-fluorophenyl)-3-hydroxy-2-oxindole (3.18), ^{19}F, $CDCl_3$, 377 MHz

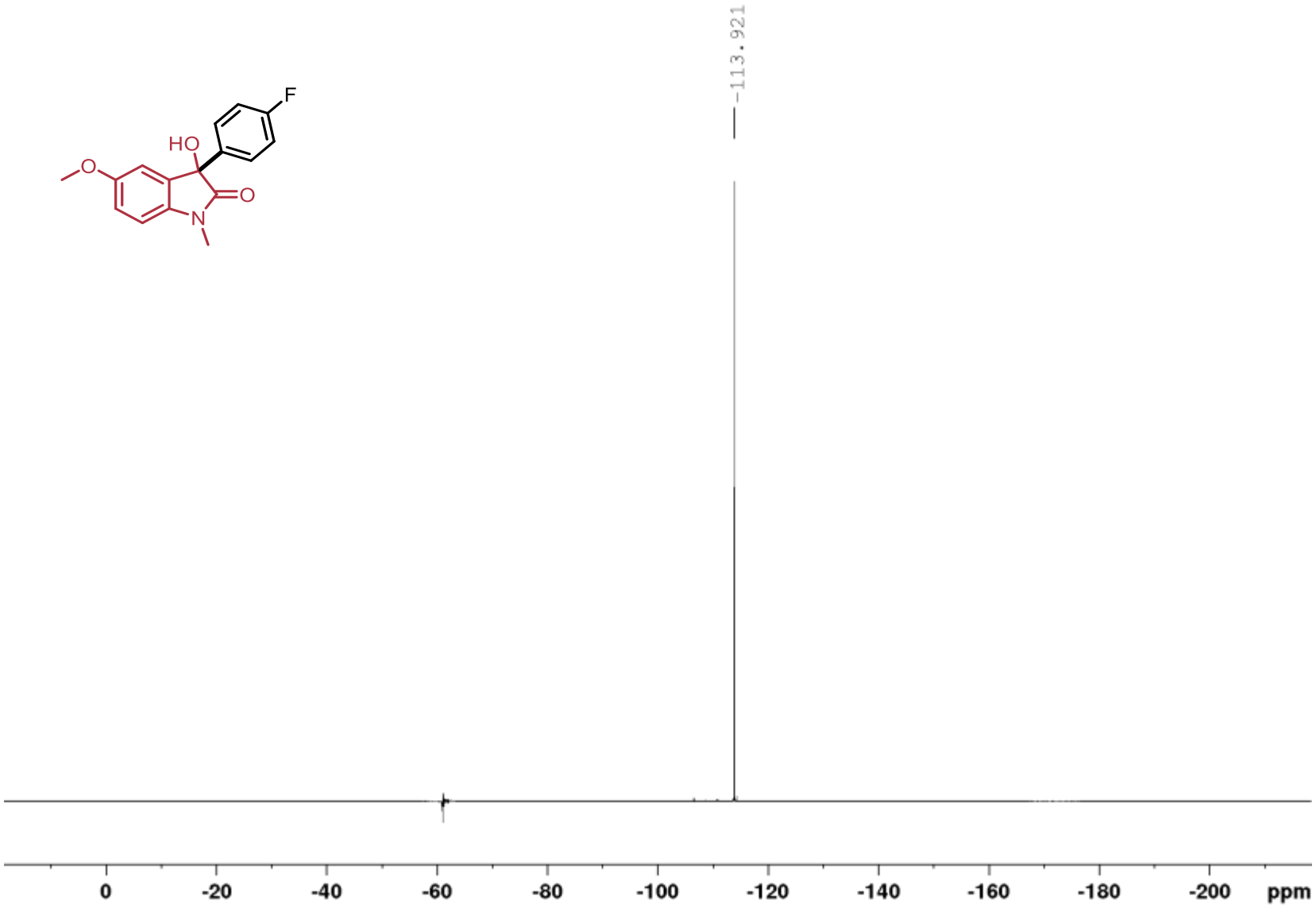

5-trifluoromethoxy-1-methyl-3-(4-fluorophenyl)-3-hydroxy-2-oxindole (3.19), ^{1}H, $CDCl_3$, 400 MHz

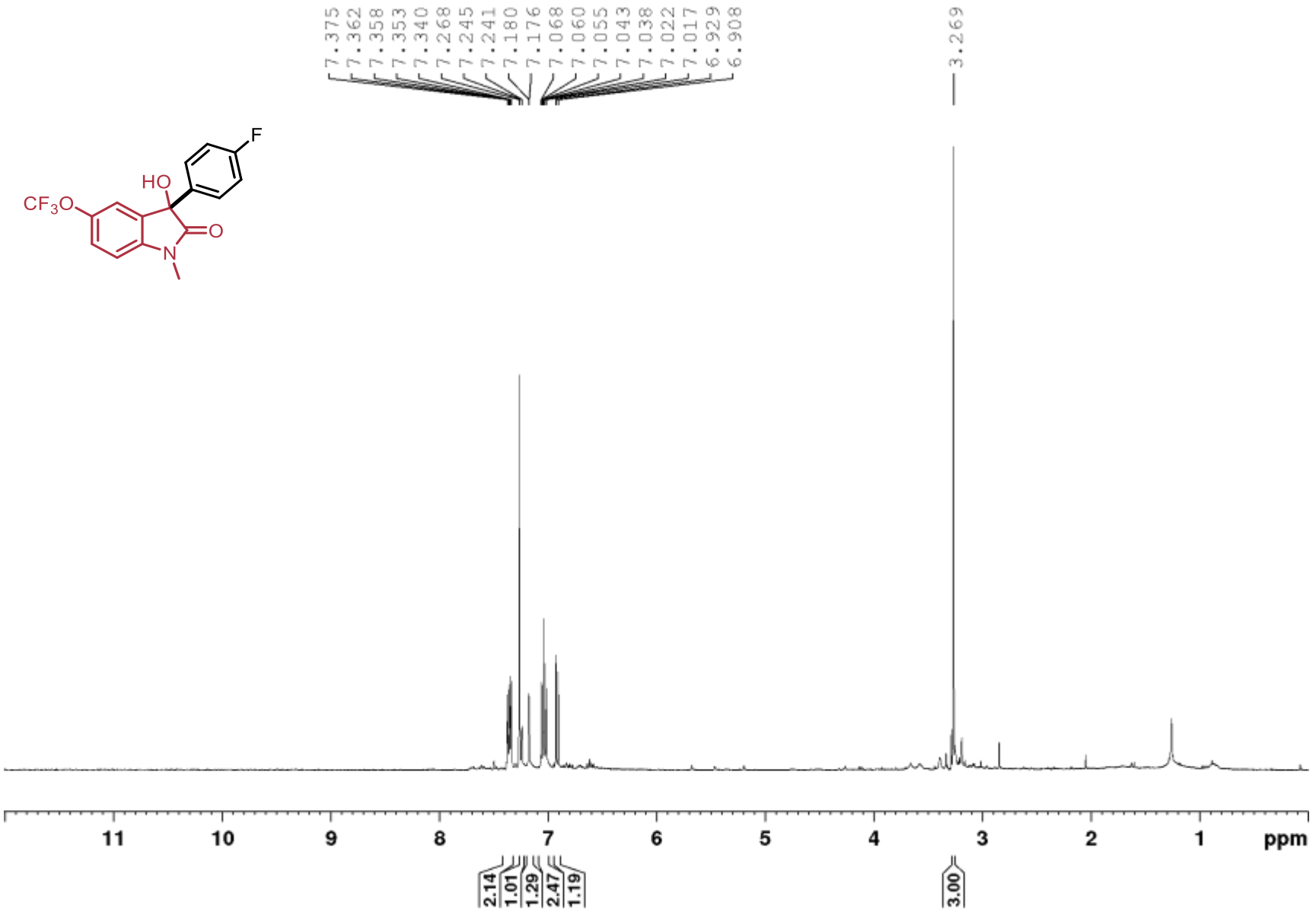

5-trifluoromethoxy-1-methyl-3-(4-fluorophenyl)-3-hydroxy-2-oxindole (3.19), ^{13}C, $CDCl_3$, 100 MHz

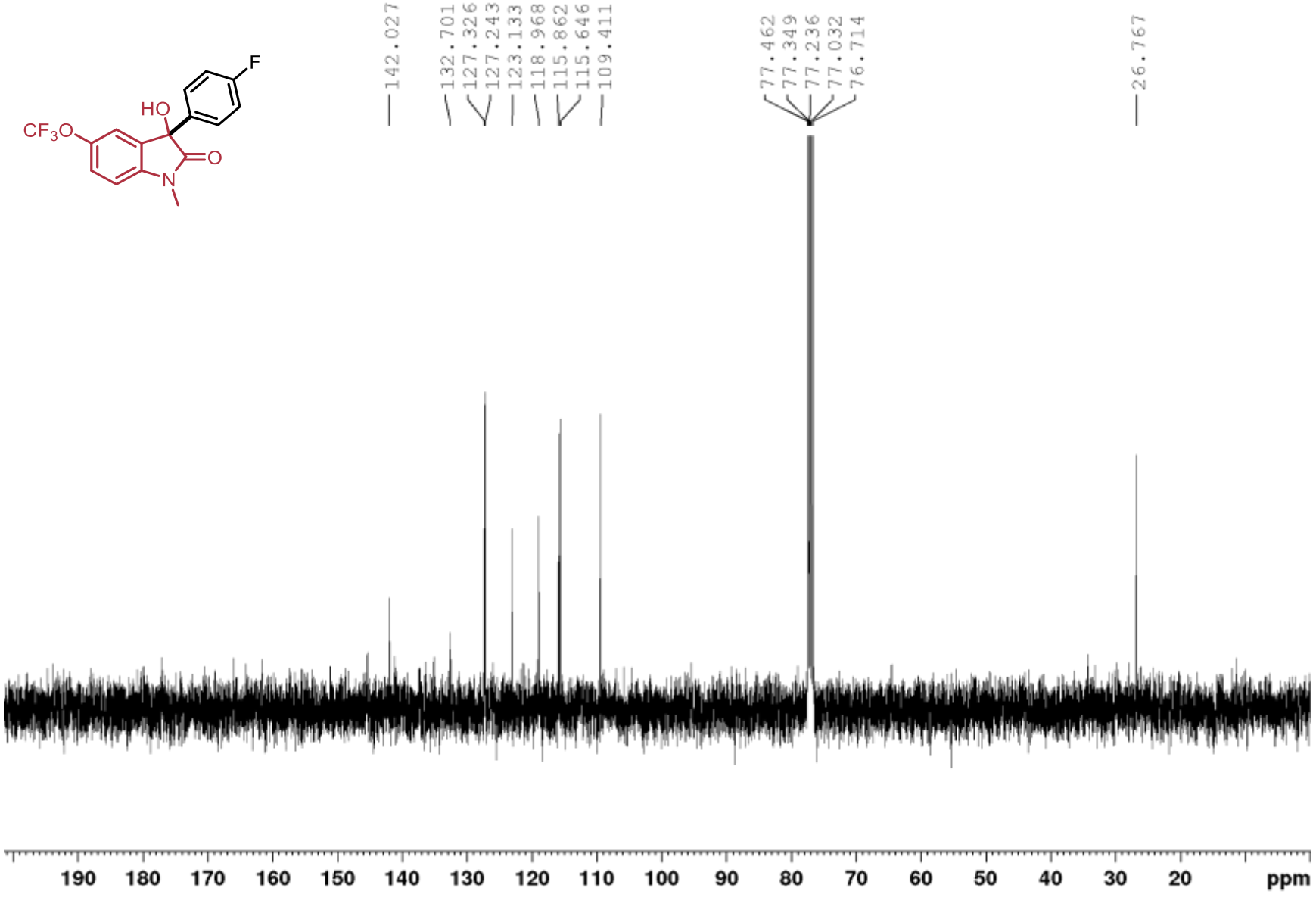

5-trifluoromethoxy-1-methyl-3-(4-fluorophenyl)-3-hydroxy-2-oxindole (3.19), ^{19}F, $CDCl_3$, 377 MHz

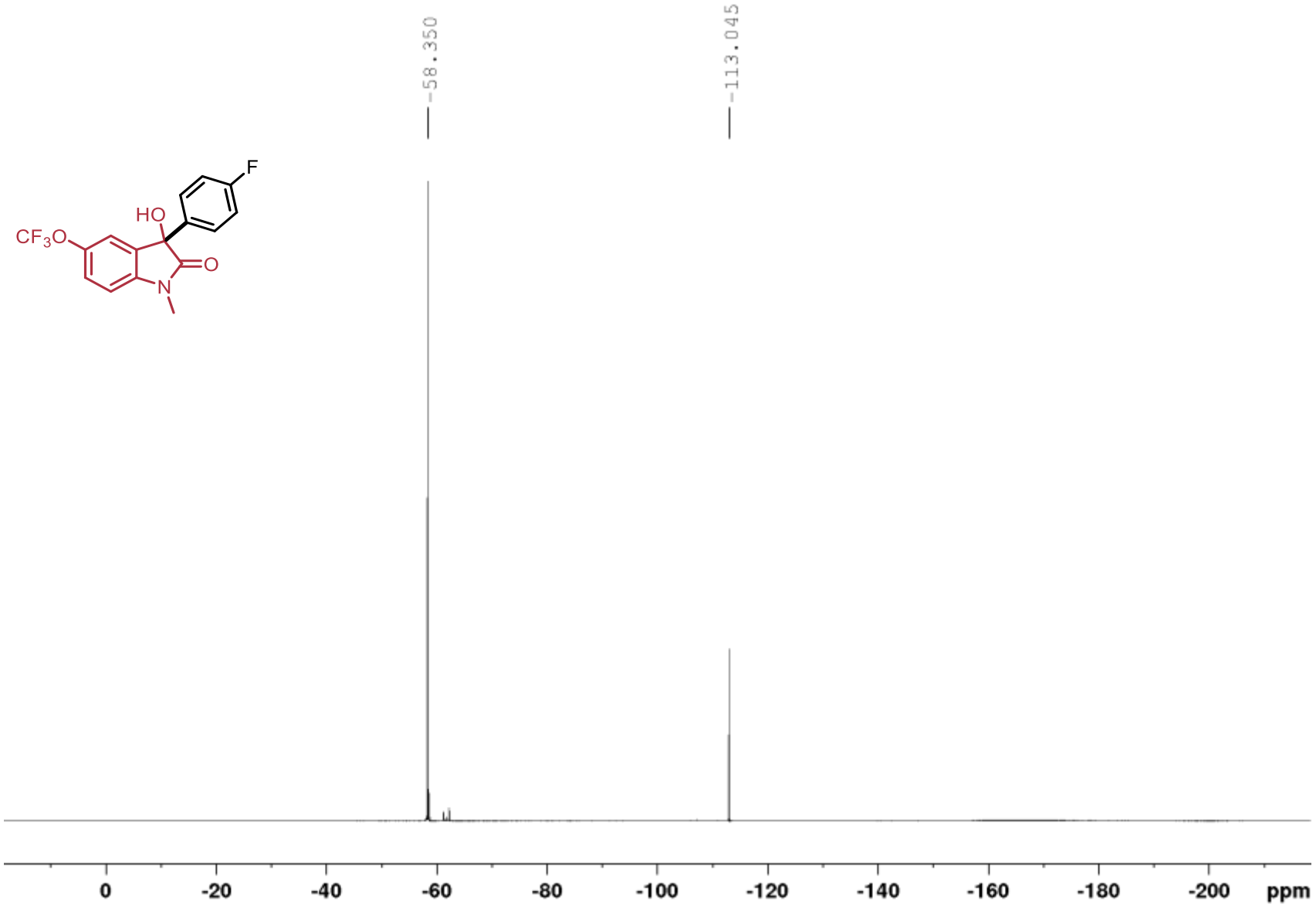

5-fluoro-1-methyl-3-(4-fluorophenyl)-3-hydroxy-2-oxindole (3.20), ^{1}H, $CDCl_3$, 400 MHz

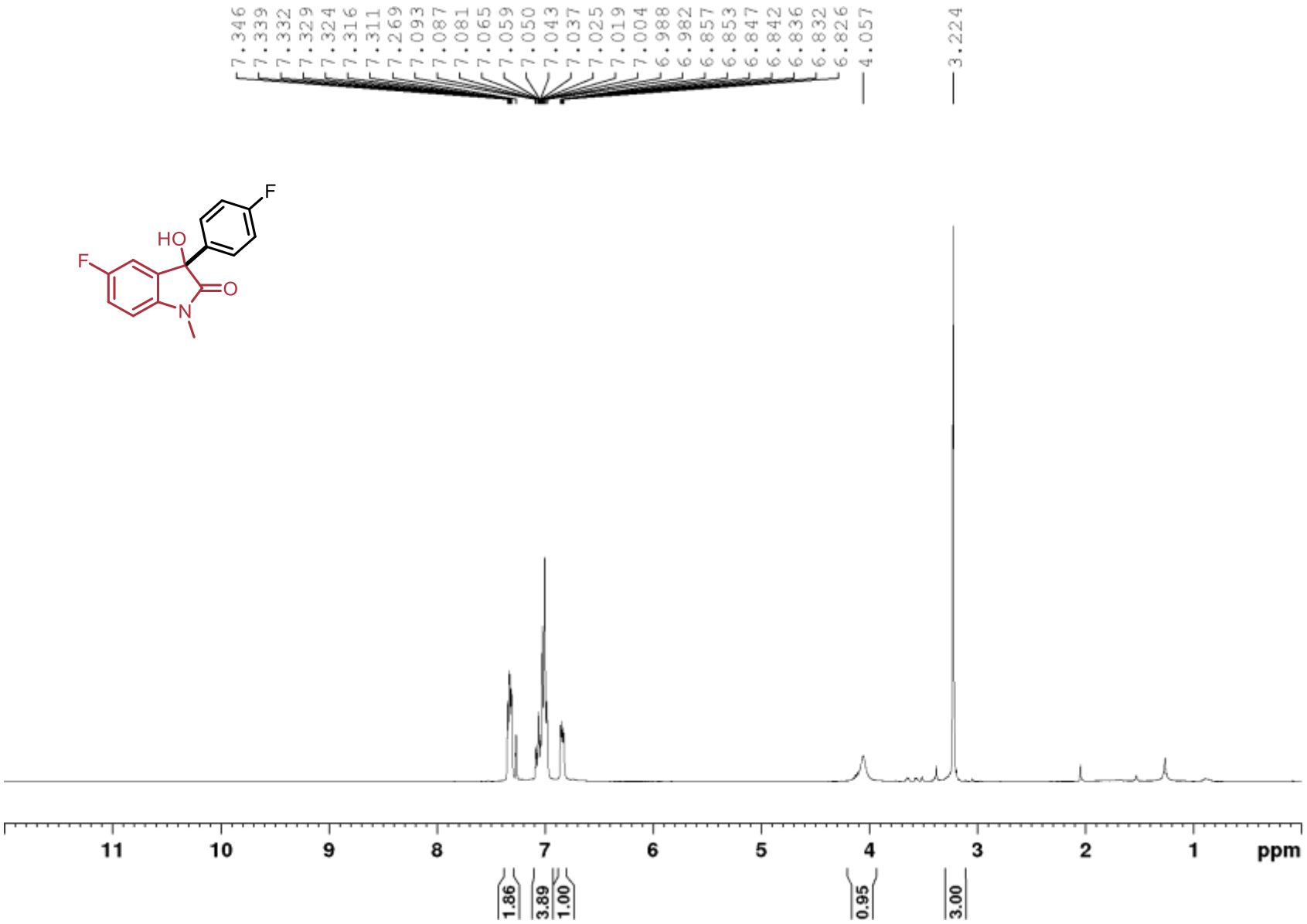

5-fluoro-1-methyl-3-(4-fluorophenyl)-3-hydroxy-2-oxindole (3.20), ^{13}C, $CDCl_3$, 100 MHz

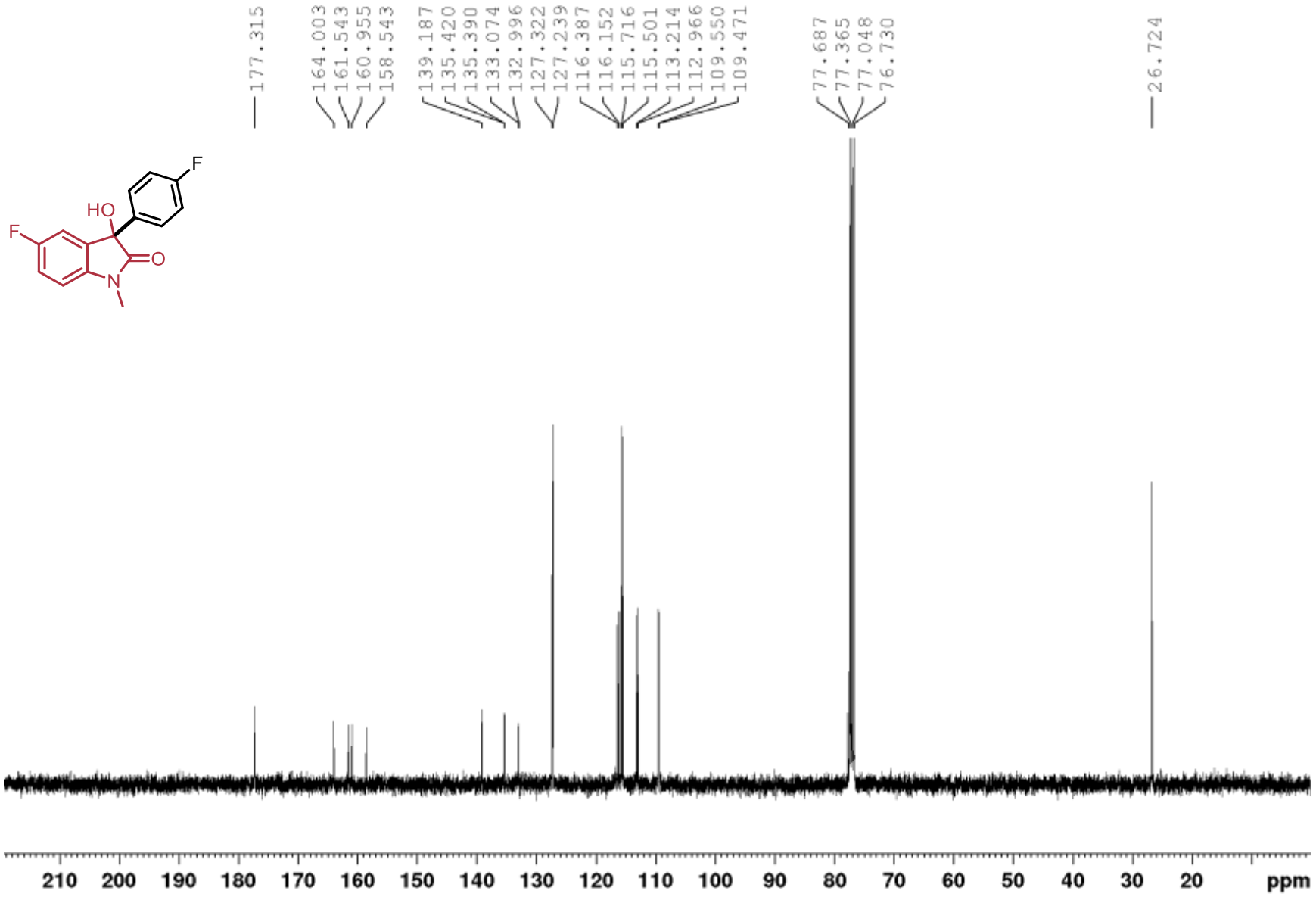

5-fluoro-1-methyl-3-(4-fluorophenyl)-3-hydroxy-2-oxindole (3.20), ^{19}F, $CDCl_3$, 377 MHz

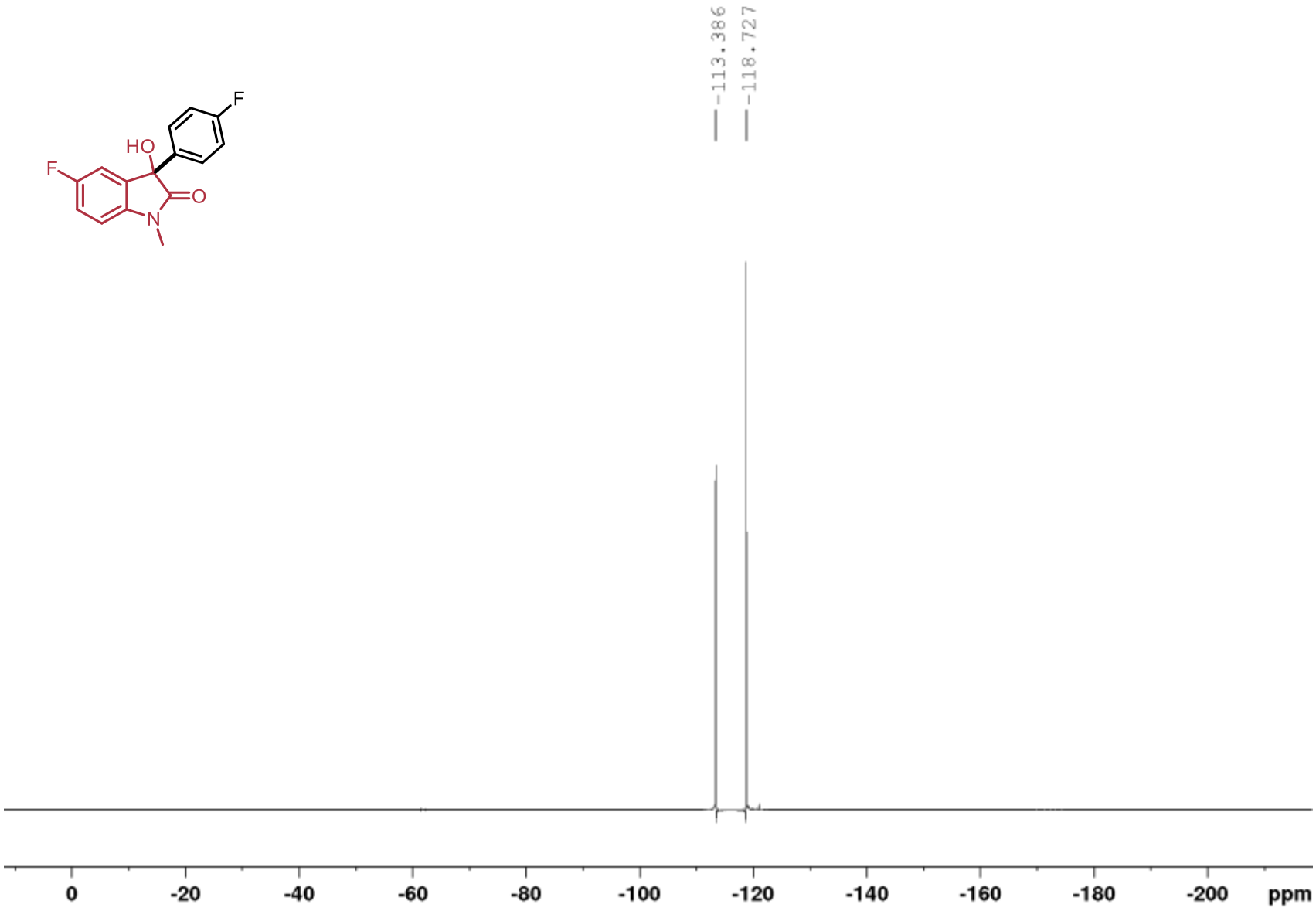

5,7-dimethyl-3-(4-fluorophenyl)-3-hydroxy-1-methyl-2-oxindole (3.21), ^{1}H, $CDCl_3$, 400 MHz

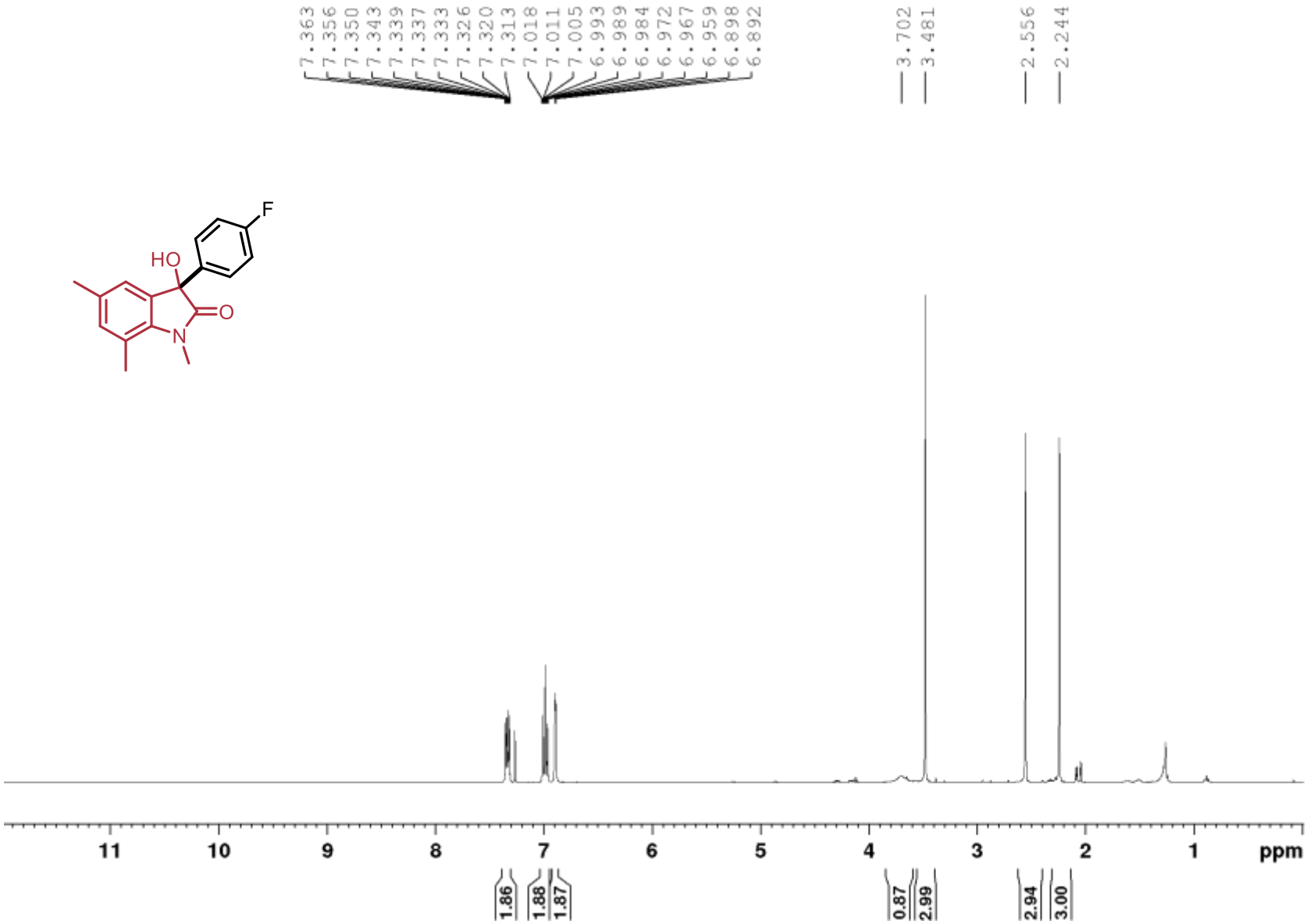

5,7-dimethyl-3-(4-fluorophenyl)-3-hydroxy-1-methyl-2-oxindole (3.21), ^{13}C, $CDCl_3$, 100 MHz

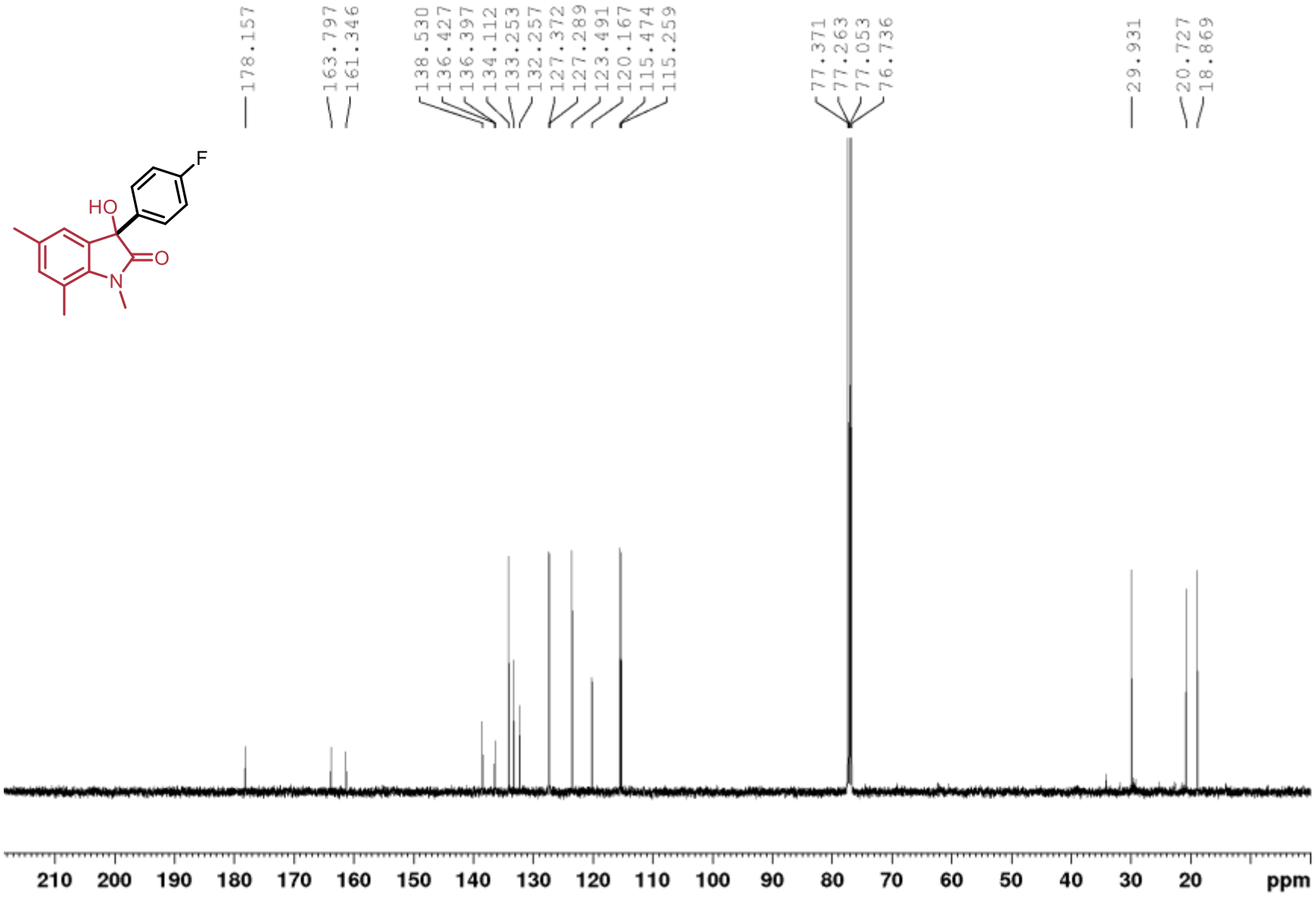

5,7-dimethyl-3-(4-fluorophenyl)-3-hydroxy-1-methyl-2-oxindole (3.21), ^{19}F, $CDCl_3$, 377 MHz

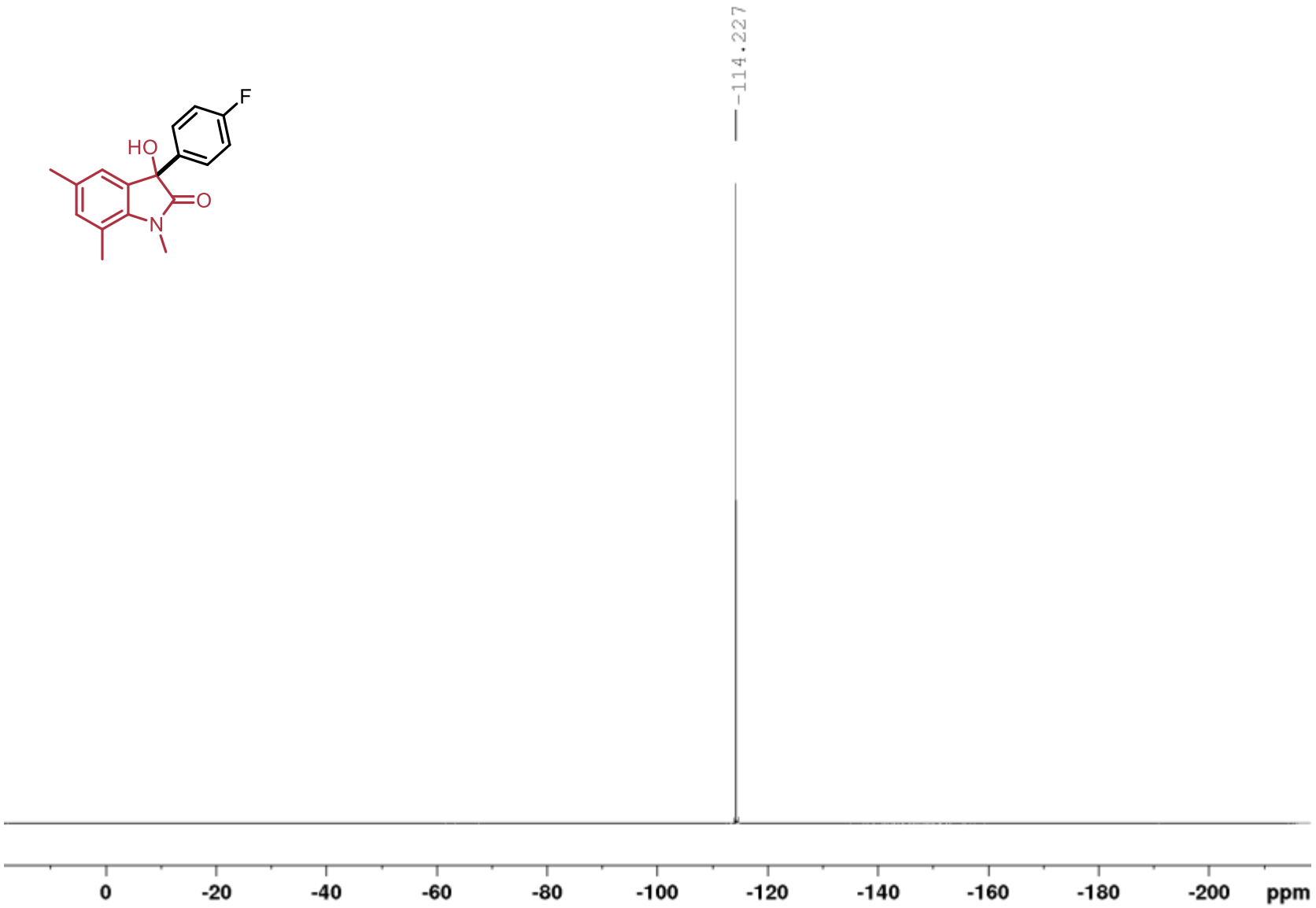

4,6-difluoro-3-(4-fluorophenyl)-3-hydroxy-1-methyl-2-oxindole (3.22), ^{1}H, $CDCl_3$, 400 MHz

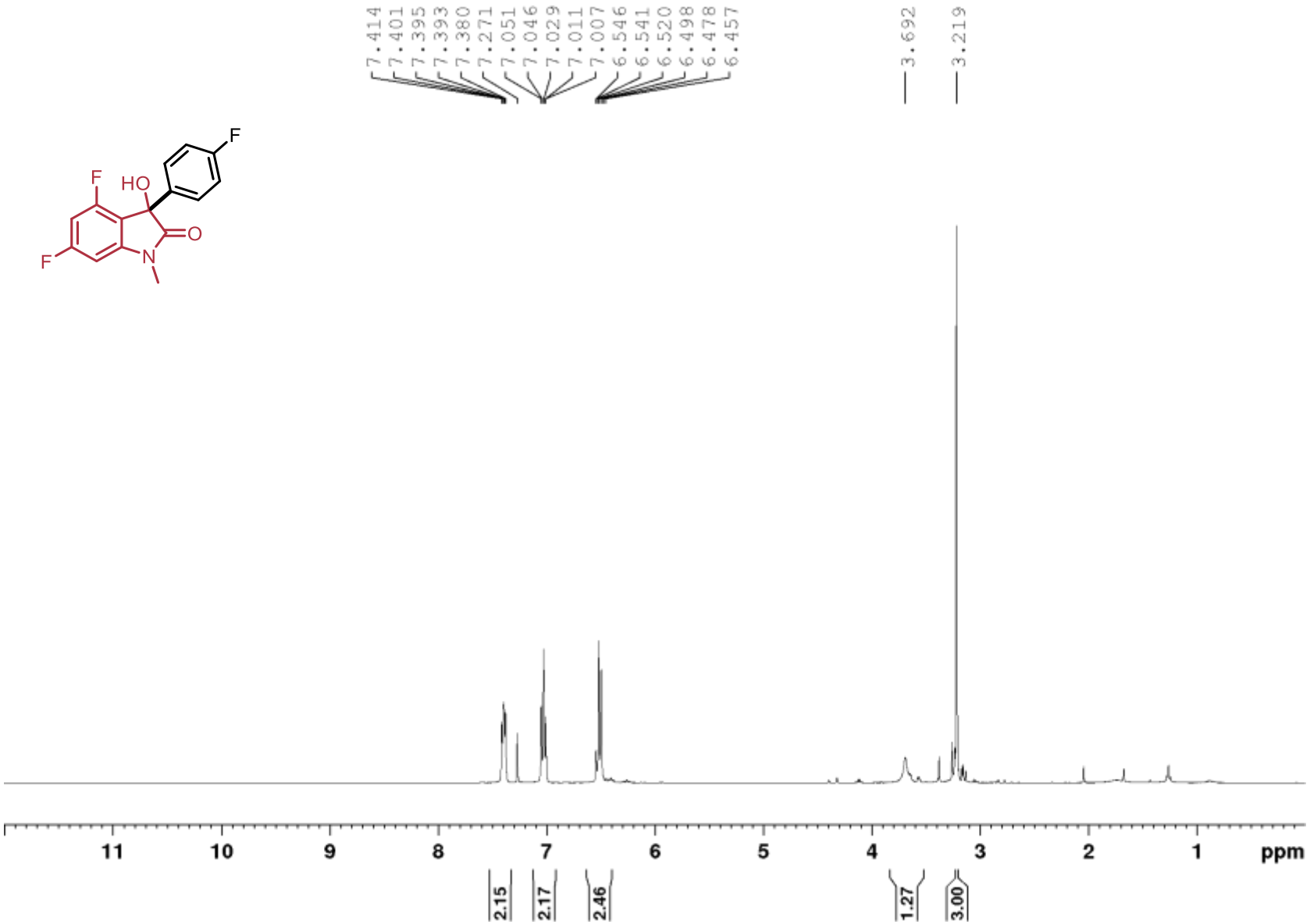

4,6-difluoro-3-(4-fluorophenyl)-3-hydroxy-1-methyl-2-oxindole (3.22), ^{13}C, $CDCl_3$, 100 MHz

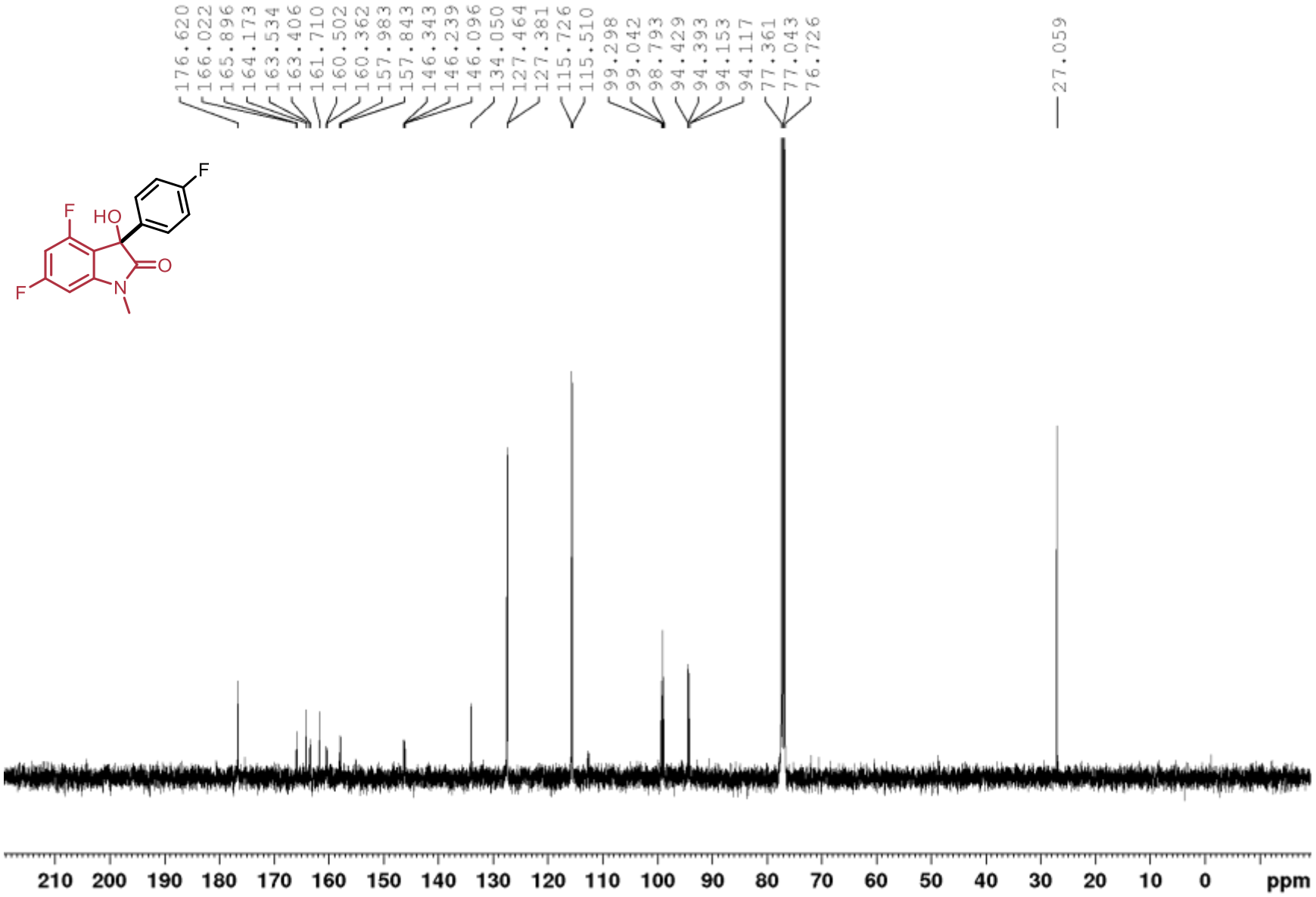

4,6-difluoro-3-(4-fluorophenyl)-3-hydroxy-1-methyl-2-oxindole (3.22), ^{19}F, $CDCl_3$, 377

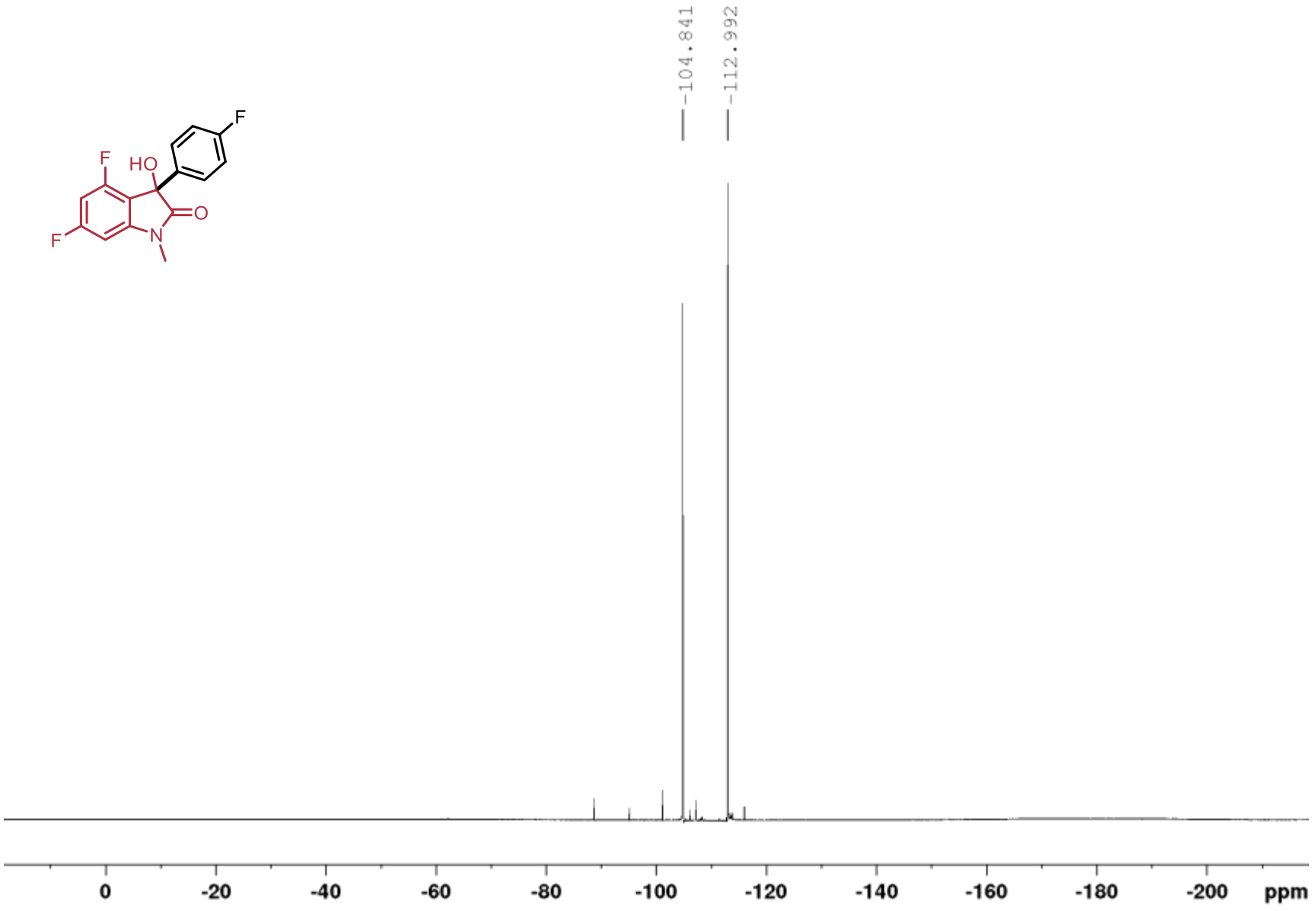

5-chloro-3-(4-fluorophenyl)-3-hydroxy-1-methyl-2-oxindole (3.23), ^{1}H, $CDCl_3$, 400 MHz

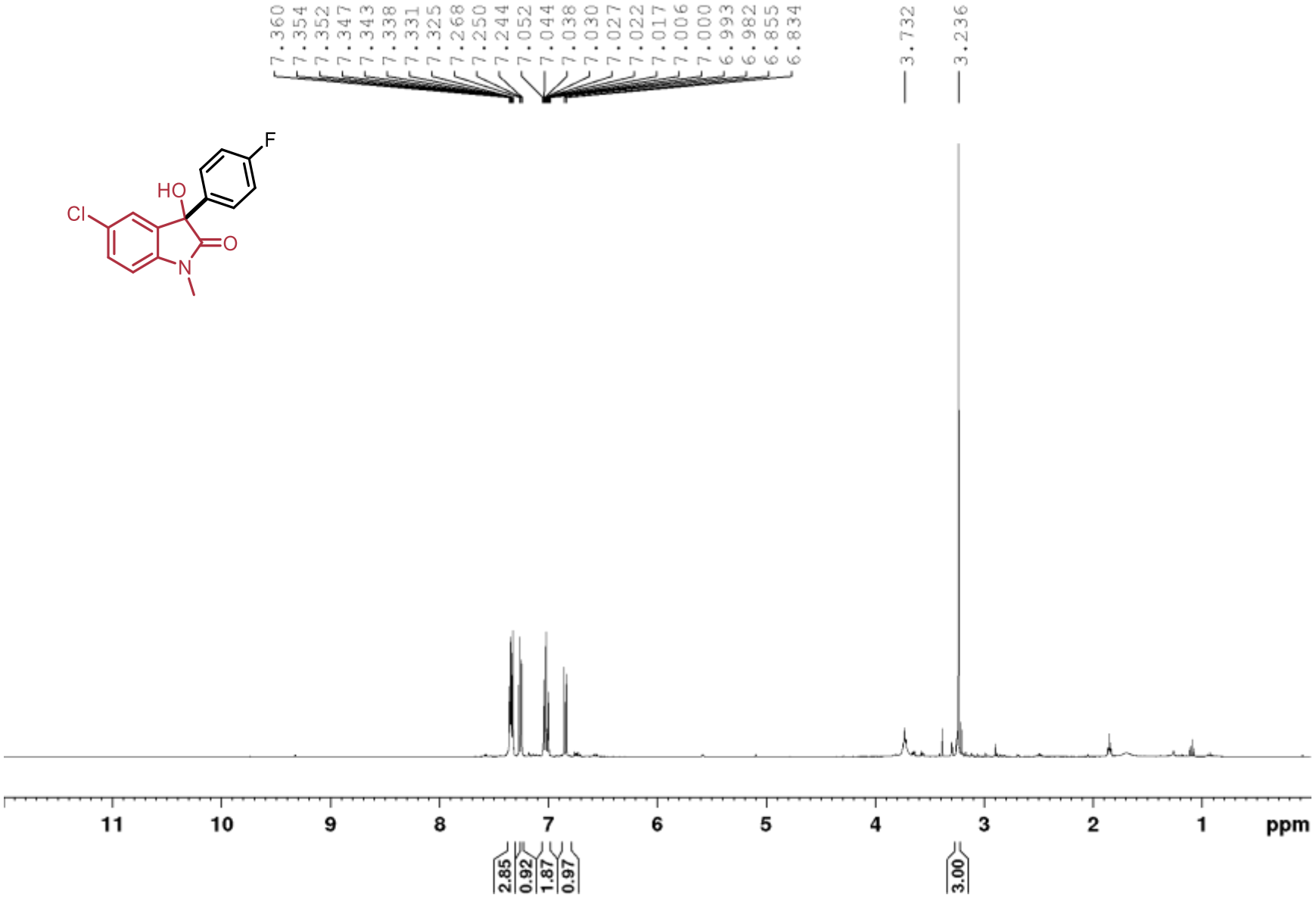

5-chloro-3-(4-fluorophenyl)-3-hydroxy-1-methyl-2-oxindole (3.23), ^{13}C, $CDCl_3$, 100 MHz

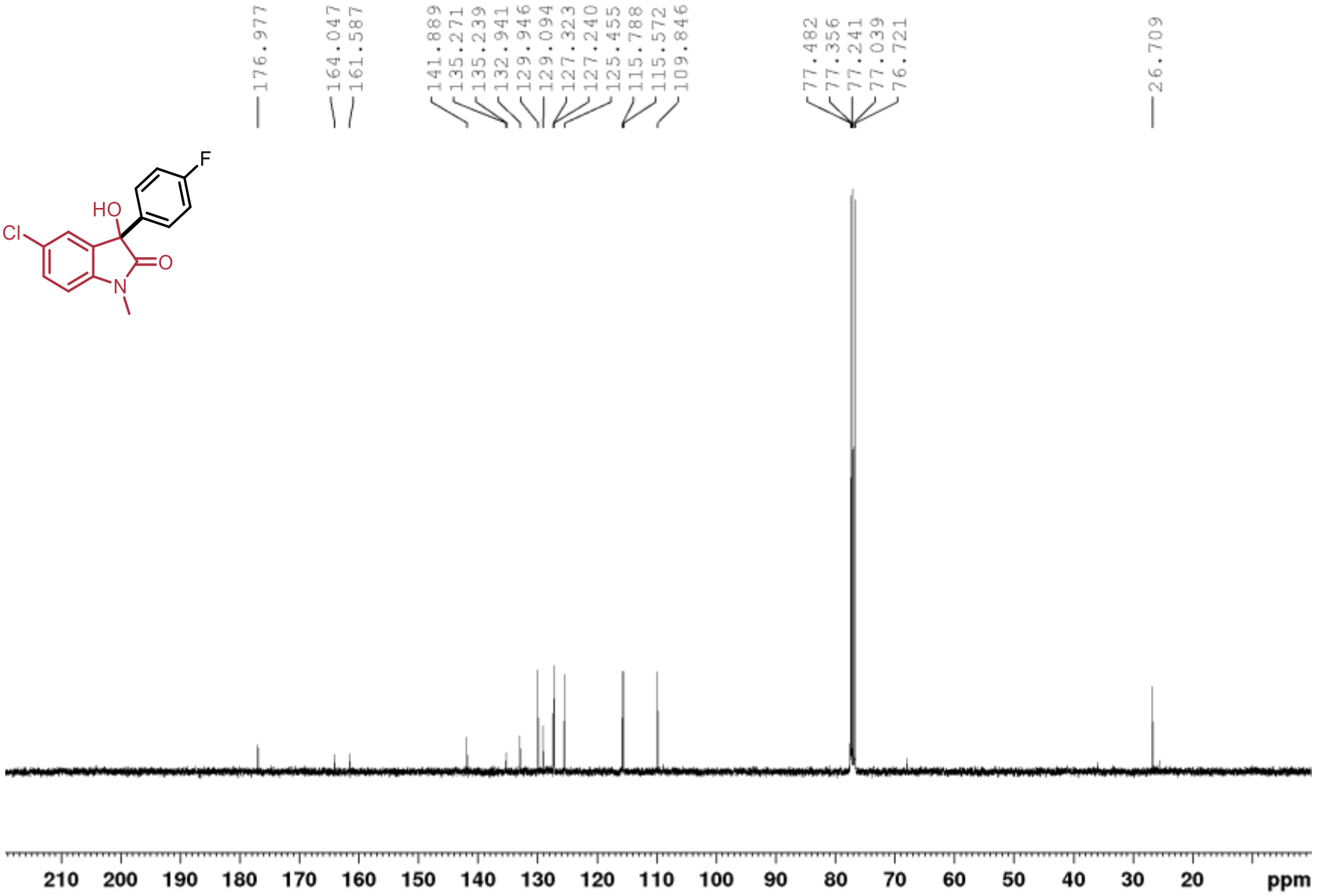

5-chloro-3-(4-fluorophenyl)-3-hydroxy-1-methyl-2-oxindole (3.23), ^{19}F, $CDCl_3$, 377 MHz

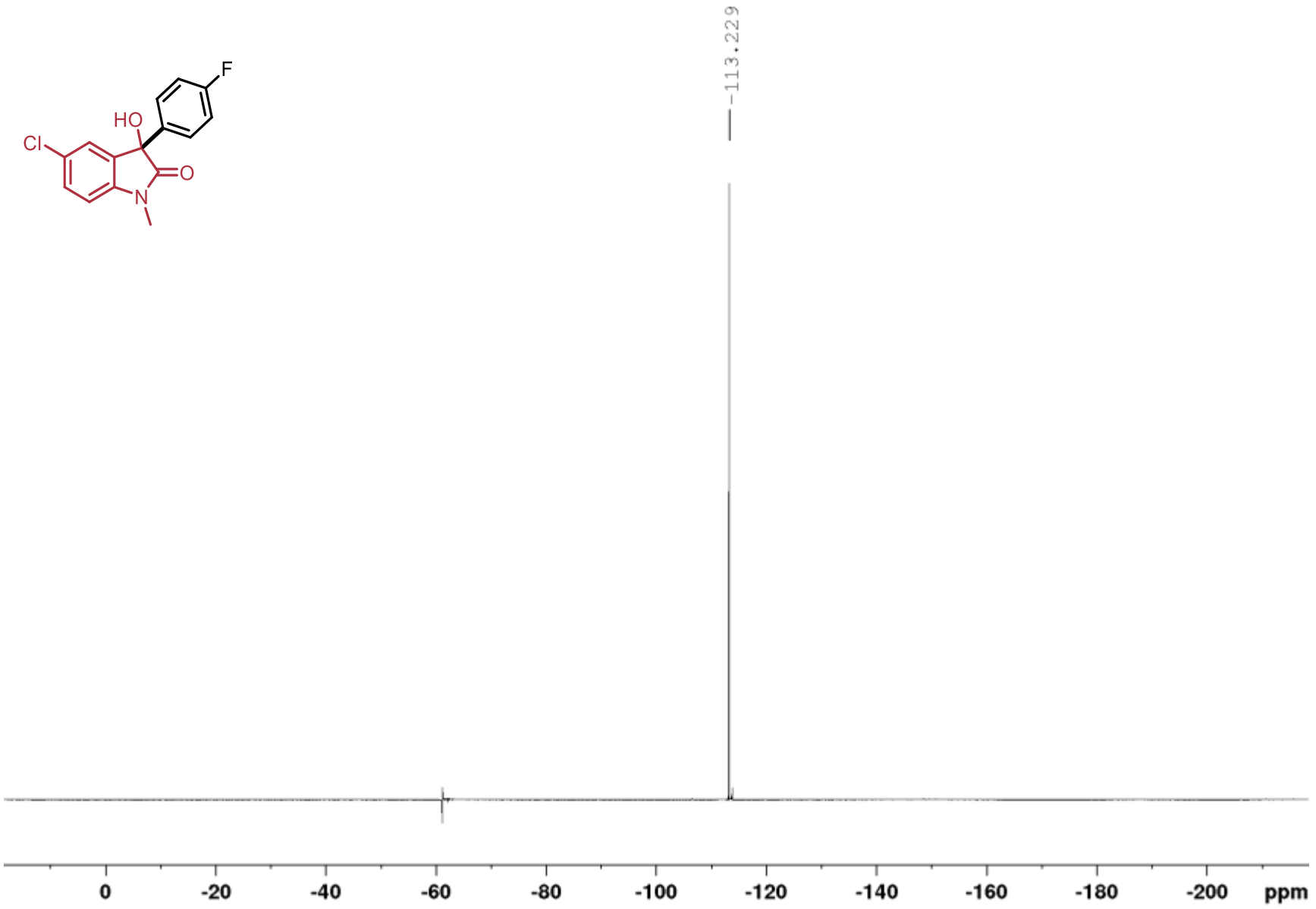

7-trifluoromethyl-3-(4-fluorophenyl)-3-hydroxy-1-methyl-2-oxindole (3.24), ^{1}H, $CDCl_3$, 400 MHz

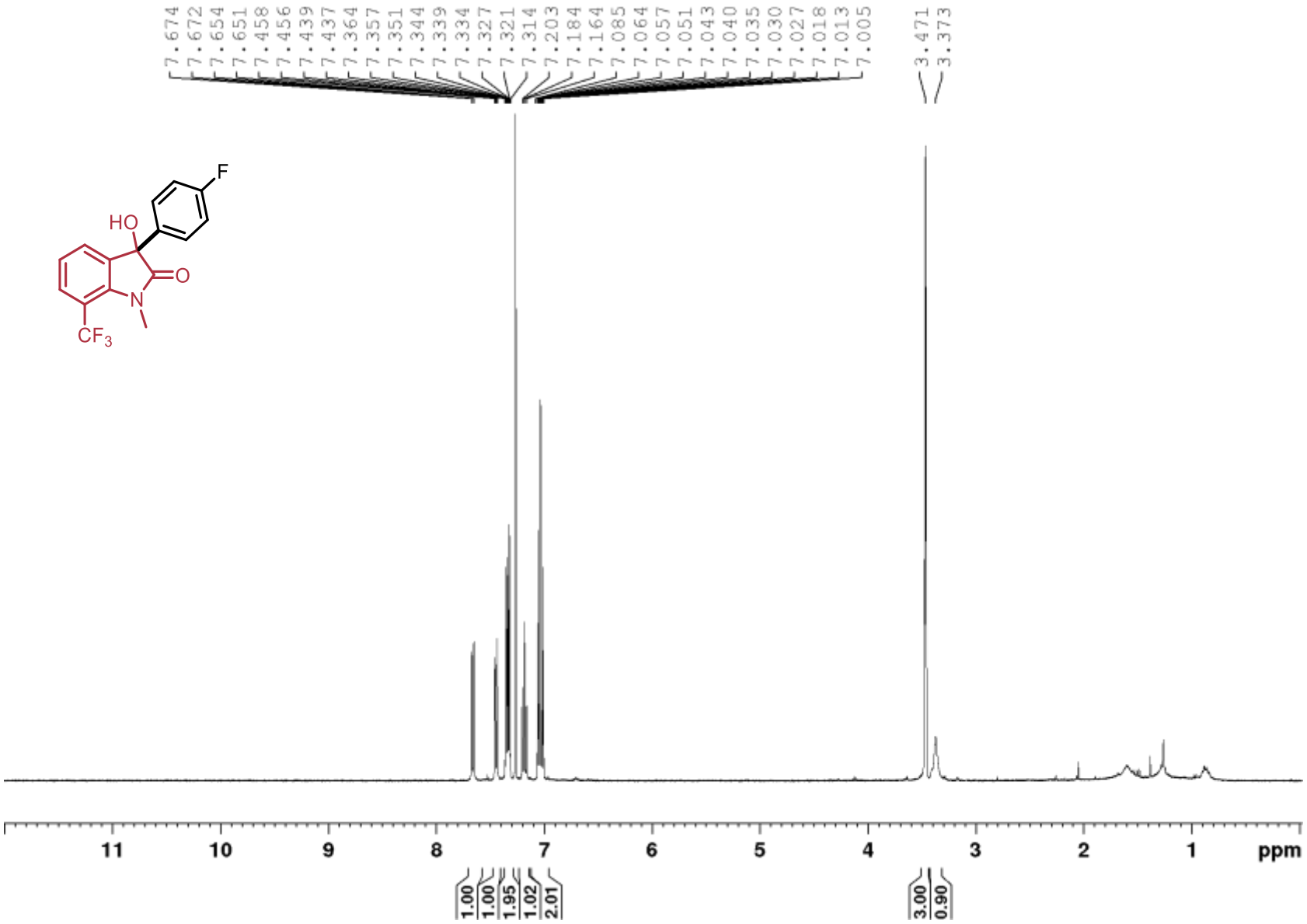

7-trifluoromethyl-3-(4-fluorophenyl)-3-hydroxy-1-methyl-2-oxindole (3.24), ^{13}C, $CDCl_3$, 100 MHz

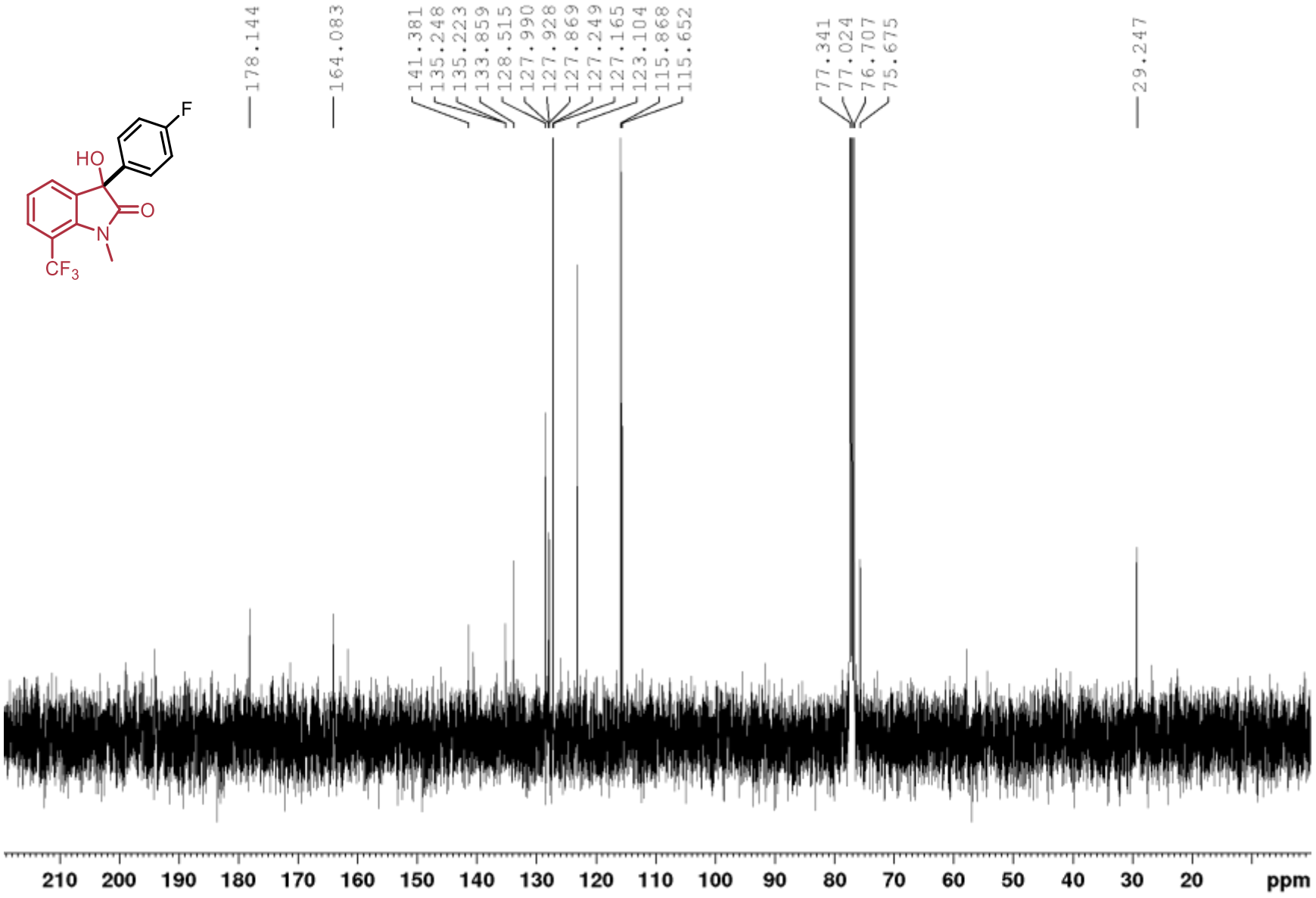

7-trifluoromethyl-3-(4-fluorophenyl)-3-hydroxy-1-methyl-2-oxindole (3.24), ^{19}F, $CDCl_3$, 377 MHz